Multi-hazard landslide dams on the global scale: distribution, characteristics, and formation

Hang Wu

Submitted in accordance with the requirements for the degree of

Doctor of Philosophy

The University of Leeds
School of Civil Engineering

September 2023

The candidate confirms that the work submitted is her own, except where work which has formed part of jointly-authored publications has been included. The contribution of the candidate and the other authors to this work has been explicitly indicated below. The candidate confirms that appropriate credit has been given within the thesis where reference has been made to the work of others.

The work in **Chapter 3** of this thesis has appeared in publication as follows:

Wu, H., Trigg, M.A., Murphy, W. Fuentes, R. A new global landslide dam database (RAGLAD) and analysis utilizing auxiliary global fluvial datasets. Landslides 19, 555–572 (2022). https://doi.org/10.1007/s10346-021-01817-z

HW designed the study, performed the major jobs of data collection and analysis, and drafting of the manuscript; MAT contribute to the majority of editing the text; MAT, WM and RF contributed to forming the research objectives, supported the data analyses and interpretations, and manuscript revisions. MAT contributed to the majority of proofreading the text. All co-authors contributed to the discussion and editing of the manuscript.

The work in **Chapter 4** of this thesis has appeared in publication as follows:

Wu, H., Trigg, M.A., Murphy, W. Fuentes, R. Are there fundamental differences between dam forming landslides and all landslides? (Undergoing revision)

HW designed the study, conducted the major jobs of data collection and analysis, and drafting of the manuscript; MT, WM and RF contributed into forming the research objectives, supporting the data analyses and interpretations, and manuscript revisions; HW, MT contributed to the proofreading.

The work in **Chapter 5** of this thesis has appeared in publication as follows:

Wu, H., Trigg, M.A., Murphy, W. Fuentes, R, Martino S., Esposito C., Marmoni G.M., Scarascia Mugnozza G. A global-scale applicable framework

of landslide dam formation susceptibility (Under review)

HW designed the study, conducted the major jobs of data collection and analysis, and drafting the manuscript; MT, WM and RF contributed to forming the research objectives, supporting the data analyses and interpretations; MT provided the Dominica catchment boundaries; HW, SM, CE, GMM and GSM conducted a field visit to Tasso River basin; HW, MT contributed to the proofreading. All the authors have contributed to the revisions of the manuscript and discussions.

Acknowledgements

Like Gatsby's pursuit of the green light, I chased my dream, crossing 6,000 miles, almost covering the distance from the east-southern corner to the west-northern corner of Eurasia. I embarked with immense excitement on the commencement of my PhD journey and life in a land enriched with diverse cultures. Here I stand, looking back towards the incredible 4-year journey of my PhD. There are many people who deserve to be mentioned here, who gave me academic and financial support, strength and love that guided me to this point, which is also an official terminal station of my ceaseless 23-year student journey (despite the lifelong learning).

My gratitude should firstly go to my supervision team: Mark Trigg, William Murphy and Raul Fuentes, who gave me endless respect, support and guidance through these 4 years. When I look back at those comments, revisions and notes from our discussions, which are really impressive and where learned a lot. Thank you for accepting my rambling ideas and guiding me back when red herrings occurred. I really enjoy and feel very lucky to have your guidance from various subject perspectives. Especially Mark, my lead supervisor, I really appreciate that you picked me up from those prospective students' emails which provided me with this opportunity to work on this topic which I am really interested in. You are always such an excellent mentor and friend to me.

My next gratitude should go to the colleagues who had inputs in my work, especially the team from Sapienza University of Rome: Salvatore Martino, Gian Marco Marmoni, Javad Rouhi, Marta Della Seta, Gabriele Scarascia Mugnozza, Carlo Esposito, and et al. Thank you for sharing your research and presenting comprehensive studies of Scanno rock avalanche, particularly with the wonderful field visit. I would also like to show my gratitude to Anja Dufresne for her insightful comments and for providing me with the data that enhanced my research. There are also quite a lot of researchers' works that inspire me and help me to stand on the shoulders of giants to explore.

My undergraduate advisors Tao Song and Xiaohao Wen deserve a special mention. They are role models showing me the potential for a first-generation university student to pursue an PhD degree, even an overseas one. Without their encouragement and guidance during my undergraduate studies, I probably won't find my real enthusiasm in natural hazard modelling and continue to pursue my

master and PhD degree.

I would like to thank my PhD funders, University of Leeds and China Scholarship Council, for funding my PhD research project with full tuition coverage and maintenance support, which allow me to have the freedom to chase my dream without considering much on economic issues. My gratitude also goes to Water@Leeds and School of Civil Engineering for providing me with travel funds for networking and field visits.

I would like to thank Amrie, probably my coolest friend, for inviting me to the parties and sharing feelings, which made me feel at home. To Lin, my longest meal pal in Leeds, thank you for everything, especially for letting me enjoy various food, which kind of helped me to escape the combination of broccoli and chicken. To Ezgi, I really enjoy the small chats in the common area of our flat.

致我读博期间，一直远程联系的朋友们：燕仪、达媛、敏仪、泽慈（得得）、培源（PeiYang）、丽君、舒婷、怡洁（五一节）。很遗憾遇上了那么多出乎意料的情况，错过了一些你们重要的时刻，让我深刻体会到什么叫做“昔我往矣，杨柳依依。今我来思，雨雪霏霏”。转眼间已经有四年没有线下见面了，但每次线上聊天的时候却总有一种似乎我们在一个地方的感觉，anyway，期待与你们再次相会，也期待着亲眼见证着你们的生活。感谢你们一直接住我的情感，也希望你们可以继续自由驰骋在自己的道路上。

To my friends that regularly remote contacted, sorry that I missed some important moments for you due to Covid travel restrictions and thank you for your support regardless of time gaps. Really miss you and can’t wait to meet you offline!

老爸老妈，因为生活环境不同，接触的事物不同，让我们产生了更多不同的想法。但是谢谢你们在如此大的差异下，甚至有时候连想法都无法互相理解的情况下，一如既往地支持与关照我，让我可以自由地遵循自己的想法，做出属于我自己人生中的一次次抉择。

The thesis is dedicated to my family, especially my parents who gave me unwavering support and love even when they did not understand my thoughts.

Life is like a combination of multiple Möbius strips. I always experience a sense of nostalgia and a temporally inconsolable feeling in a new place when I encounter similar experiences from the part that I cherish most in my memories, but such feelings and memories have become my steadfast strength to fight against the current.

Abstract

The landslide dam (LDam) is a complicated multi-hazard that can lead to enormous loss of life and properties worldwide. LDams have been frequently reported and recorded in the upstream mountainous areas, where the environment is prone to landslide occurrence and the rivers are narrow and steep. As a multi-hazard interaction between hillslope and fluvial systems, the study of landslide dams brings greater challenges compared to single hazards, especially in data collation and the integration of information from the two systems.

Previous research has focused a large amount of effort on establishing LDam datasets, identifying the characteristics related to landslide dam formation and estimating the landslide dam formation probabilities through proposing geomorphological indices or dam-formation landslide probability mapping, based on the empirical relationships among related variables. However, the applicability of outputs for other study areas, particularly for larger-scales, and the limited use and application of fluvial information remain critical gaps in current research.

This thesis proposes a new global-scale applicable framework for evaluating landslide dam formation susceptibility on river reaches. Contributing to this framework is the establishment of a global-scale LDam dataset named River Augmented Global Landslide Dams (RAGLAD) augmented by auxiliary global fluvial datasets, and a better understanding of the morphometric and spatial differences in characteristics between dam forming landslides and landslides more generally, based on multiple landslide and LDam datasets. This study expands the data collection method for enhancing the comprehensiveness of LDam records and shifts the focus from landsides to mapping the LDam formation probability on rivers instead of just the hillslopes. It also contributes a new entry point for integrating multiple data sources, such as global fluvial datasets and landslide datasets, which will enhance future LDam studies.

List of Abbreviations

2D	Two Dimensions
AD	Anno Domini
AUC	Area under the curve
B.P.	Before Present (1950 AD)
BC	Before Christ
CAFLAG	CAmpi Flegrei LAndslide Geodatabase
CEDIT	Italian Catalogue of Earthquake-Induced Ground Failures
DEM	Digital Elevation Model
DFL	Dam-forming Landslide
DMI	Dimensionless Morpho-Invasion Index
EEA	European Environment Agency
EU-Hydro	A river and drainage network dataset derived from EU-DEM
FABDEM	Forest And Buildings removed Copernicus DEM
FPR	False positive rate
FROM-GLC	Finer Resolution Observation and Monitoring of Global Land Cover
geomorpho90	A global dataset comprising different geomorphometric features based MERIT DEM
GFD	Global Fluvial Dataset
GFM	Global Flood model
GIS	Geographical Information System
GLC	Global Landslide Catalog
GloFAS	Global Flood Awareness System
GloSEM	High resolution cropland global soil erosion
GLOW	Global Long-term River Width
GPM	Global Precipitation Measurement
GRWL	Global River Widths from Landsat
GSHAP	Global Seismic Hazard Assessment Program
GWD-LR	Global Width Database for Large Rivers

H/L ratio	The ratio of the landslide drop height to landslide runout distance (landslide length)
HMSLS	High Mountain Asia Landslide Catalog
HydroAltas	A global compendium of hydro-environmental characteristics for all sub-basins of HydroBASINS
HydroBASINS	Global watershed boundaries and sub-basin delineations derived from HydroSHEDS
HydroSHEDS	Hydrological data and maps based on SHuttle Elevation Derivatives at multiple Scales
IFFI	Italian landslide inventory
LDam	Landslide dam
LHASA	Landslide Hazard Assessment for Situational Awareness
LiDAR	Light Detection and Ranging
LS	Landslides more generally
LSI	Landslide Susceptibility Index
MERIT DEM	Multi-Error-Removed Improved-Terrain DEM
MERIT Hydro	A global fluvial dataset developed based on the MERIT DEM and multiple inland water maps
MOI	Morphological Obstruction Index
NDVI	Normalized Difference Vegetation Index
NIED	National Research Institute for Earth Science and Disaster Prevention of Japan
NVE	Norwegian Water Resources and Energy Directorate
PGA	Peak Ground Acceleration
R&D	Research and development
R^2	The coefficients of determination/significance coefficients
RAGLAD	River Augmented Global Landslide Dams
RBC	River Blockage Criterion
ROC	Receiver operating characteristics
SDU	Delineated slope drainage unit
SPI	Stream Power Index
SRTM	Shuttle Radar Topography Mission

SWOT	Surface Water and Ocean Topography
TNR	True Negative Rate
TPR	True Positive Rate
USA	United Stated of America
UK	United Kingdom
UN	United Nations
UNEP	United Nations Environment Programme
UNISDR	United Nations Office for Disaster Risk Reduction
WGS1984	World Geodetic System 1984

Table of Contents

Table of Figures

Table of Tables

Chapter 1. Introduction

Landslide dams (LDams) are a natural hazard that are reported frequently around the world, especially in the mountainous upstream catchment areas of tectonically active or high intensity rainfall regions. LDams link the fluvial and hillslope system and thus can be considered as a natural multi-hazard both from a geohazard and a river hazard perspective. In this chapter, the definition of LDams is introduced first, with an introduction of its elements and types. Then, the consequences of LDam formation are illustrated based on historical LDam events, especially regarding the impacts on floods and landscape evolution. Later, a multi-hazard risk assessment framework is introduced, taking LDams as an example. After that, the focus turns to spatial scale to illustrate the requirement of global-scale landslide inventories and global fluvial datasets, and their development, as they are key components throughout the whole thesis, which make the large-scale evaluation and comparison possible. Finally, the aims, objectives and structure of this thesis are introduced in more detail. The thesis evaluates the potential impact of LDams by establishing a global-scale LDam dataset, exploring the characteristics of dam-forming landslides (DFLs) and estimating the LDam formation susceptibility for river reaches.

1.1 Definitions Related to LDams

1.1.1 LDam Definition and Classification

LDams are one of the three types of natural dams that would pose a great threat to human beings and public properties among a variety of naturally forming dams, which are quite common around the world, even though a few of them have never been breached and were utilized to build constructed dams for water supply or hydroelectric power generation (Costa and Schuster 1988; Delaney and Evans 2015). Other terms, such as landslide blockage, stream/river blockage, and lake barrier can also be applied to describe LDams (Fan et al. 2020). LDams form when landslide masses reach the main river channels or tributaries, partially or completely blocking regular river channels. A LDam typically encompasses three elements, including: landslide source, landslide toe and the LDam impounded lake, as illustrated in Figure 1-1. Some geomorphology elements of a LDam in the field are shown in Figure 1-2, using the Scanno Rock Avalanches as an

example.

The LDams have been classified into six types based on their morphological characteristics by Costa and Schuster (1988), as shown in Figure 1-1, which are frequently applied in much successive research (Perrucca, et al. 2009; Hermanns et al. 2011; Penna et al. 2013; Stefanelli et al. 2015). The six types are: I) not reaching to the other side of fluvial channels with a relatively small amount of landslide mass comparing with the river width; II) Type II, a larger dam comparing with Type I, covering the whole river width; III) not only filling the whole river width but also having a longer distance of LDam coverage from up-steam to downstream; IV) formed by the contemporary materials from both sides of the valley; V) two or more dams that are formed by multiple toes of the same landslide; and, VI) containing several failure surfaces in the same reach. There are other classification systems developed based on this classification system to further classify the LDam morphology or its stability. Hermanns et al. (2011) added four morphological types besides the six types mentioned above, which focus more on the effects of LDam on the fluvial system, especially on the changes of fluvial geomorphology, such as stream capture and changes in valley bottom due to landslide mass depositions. Fan et al. (2012) further developed this classification system with sub-types based on the dam composition material and sedimentological features from a regional-scale LDam inventory. The LDam classification results can be applied as the preliminary investigation to assess the stability of LDams (Fan et al. 2020).

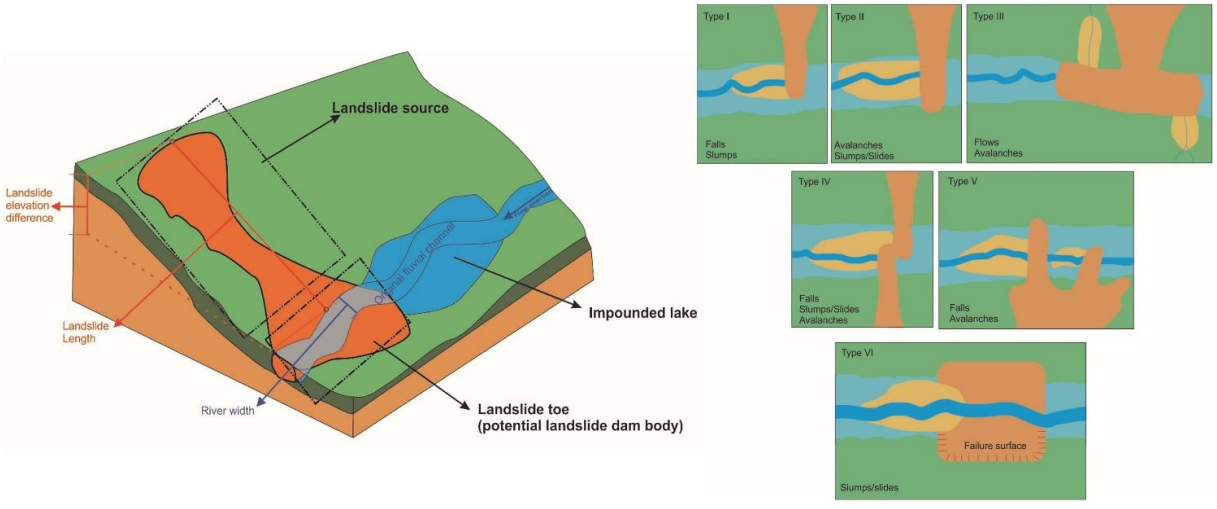

Figure 1-1 Diagrams of a LDam and its types (types were modified from Costa and

Schuster, 1988)

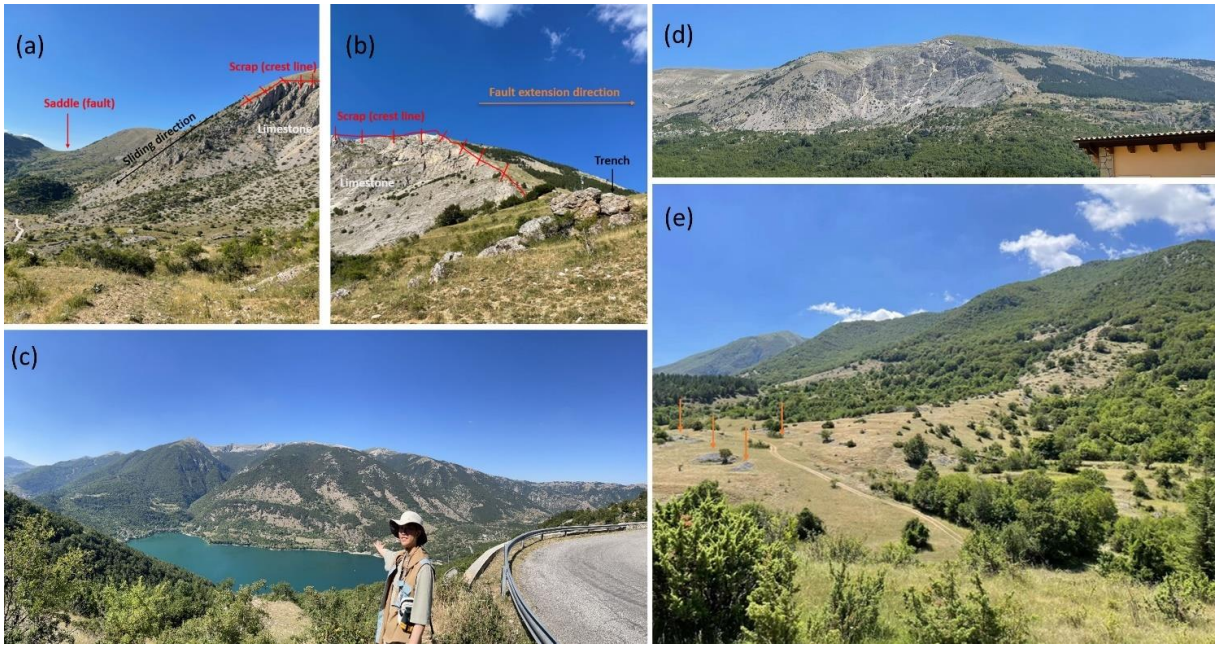

Figure 1-2 Geomorphological element examples of a LDam in the field (Scanno Rock Avalanche, Abruzzo, Italy): (a) & (b) The scarp of landslide (initial area of DFL), (c) LDam impounded lake (Lago di Scanno/Scanno Lake), (d) landslide detachment area, (e) the counter slope of landslide detachment area (extension of LDam body) with hummocky topography (orange arrow)

1.1.2 LDam as a Multi-hazard

The initial description or definition of the term "multi-hazard" within the context of risk reduction was put forth by Kappes (2011). The term “multi-hazard” had previously been used in a broader context of risk reduction by United Nations Environment Programme (UNEP 1992) and UN (2002). However, researchers had previously observed such hazard phenomenon before the terminology was defined. For instance, Hewitt and Burton (1971) referred to this concept as "all hazards-at-a-place". The Sendai Framework for Disaster Risk Reduction (United Nations Office for Disaster Risk Reduction (UNISDR) 2015) provides a clear definition for multi-hazard, encompassing two meanings: “(1) the selection of multiple major hazards that the country faces and (2) the specific contexts where hazardous events may occur simultaneously, cascadingly or cumulatively over time, and taking into account the potential interrelated effects.”

LDams can be classified as a multi-hazard due to its inherent connection between

the natural processes of the hillslope system and the fluvial system. The complete processes of a LDam hazard life cycle include: LDam formation, impounded lake storage and filling, dam failure/breach, and downstream consequences. LDam has been illustrated as a "compound hazard", "cascading hazard" or "hazard/disaster chain" in previous research (Chen et al. 2011; Fan et al. 2018; Sharma et al. 2022). These terms capture different aspects of the relationships observed in LDam events. Similar terminology is used to describe various multi-hazards where terms, such as "cascade," "domino effect," "follow-on event," "knock-on effect," or "triggering effect", are commonly employed (Kappes et al. 2012). However, these terms primarily focus on the triggering of one hazard by another, overlooking the mutual influence and interactions between hazards. Such limitation hinders their ability to fully capture the complex relationships between different hazard types within multi-hazard processes.

Regarding the relationships between floods, landslides, and LDams, it is essential to recognize that floods can arise not only from LDam breaches or failures but also directly trigger landslide occurrences, leading to the subsequent formation of LDams. At least 37 LDams were formed by dam-forming landslides, which were caused by an increment of shear stress due to the water level rise and riverbank erosion, which were recorded during the 1889 Totsukawa floods (Mizuyama et al. 2011). Kappes and Glade (2011) identified the areas showing that the relationship between landslides and floods by overlapping flood hazard analysis results and sources of shallow landslides, using LDams as evidence. Golly et al. (2017) provided a channel hillslope coupling conceptual model by observational data to illustrate how a landslide was initiated by floods and how the landslide mass was deposited into the channel (potential LDam formation). Although LDam was not mentioned in such a conceptual model, the model actually illustrates the mutual interaction between landslides and floods well (Figure 1-3). It is hard to define a clear size threshold for when an initial motion of a hillslope develops into a landslide, as the landslide area could range from tens of square meters to a couple of square kilometres for event-based landslide records (Chen and Chang 2016). LDams can also serve as a media connecting groundwater systems, which can potentially change the water supply of fluvial systems. Petitta et al. (2010) conducted isotopic measurements and found that the aquifer within the LDam, rather than the surrounding carbonate bedrock regional

aquifer connected the seepage from upstream to the springs in downstream areas.

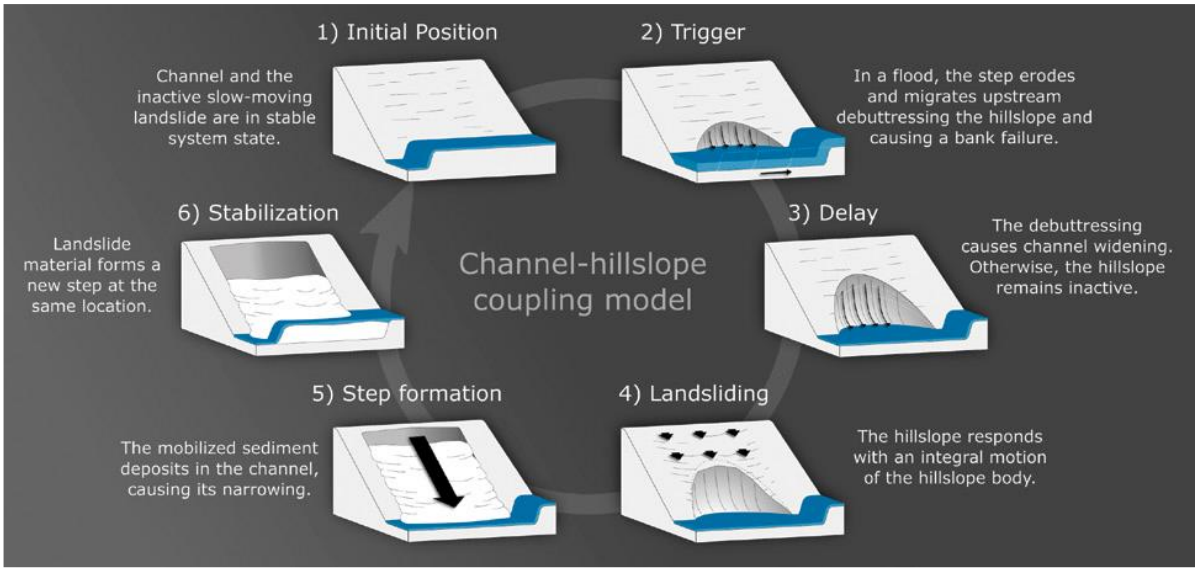

Figure 1-3 The proposed conceptual model of channel-hillslope coupling based on the observations of the event cycle in the Erlenbach catchment, central Switzerland. The cycle can be reinitiated once hillslope sediment is refilled (step 6 to 1) (Golly et al. 2017)

1.2 Consequences from LDam Formation

The LDam formation frequently occurred and reported in many areas globally, as landslides are increasingly being reported across various regions worldwide (Costa and Schuster 1988; Fan et al. 2012; 2020). LDam often results in more complex threats to people than the landslides themselves, both in space and time (Fan et al. 2020). Moreover, the consequential floods resulting from the LDam formation can potentially inflict greater losses compared to regular fluvial floods. The influx of landslide debris into river channels significantly amplifies the magnitude and risk of such floods. The combination of a landslide and subsequent LDam formation creates a heightened risk, underscoring the need for measures to mitigate the potential devastation caused by these events. The LDam formation also contributes to the impacts on landscape evolution.

1.2.1 Historical LDam Hazards and Events

Many cases of LDam formation and subsequent consequences after LDam breach or failure have been reported globally, and even a single LDam event can pose a great threat to local communities and facilities. The most devastating LDam event recorded is

the 1786 LDam formed by earthquake-triggered landslides and subsequent floods caused by LDam failure on the Dadu River, after 10 days from the LDam formation in southwestern China which probably resulted in over 100,000 deaths (Dai et al. 2005). The Kolka (Karmadon) glacier-debris flow with a total travel distance of 19 km created an impounded lake with a volume of 5 million cubic meters and directly caused approximately 140 people's deaths with the destruction of several important traffic routes, residential buildings and other infrastructures (Huggel et al. 2005; Evans et al. 2009). The Attabad rockslide that occurred in 2010 resulted in the damming of the Hunza Valley, leading to an increment in the impounded water level (Evans et al. 2009). The incident resulted in approximately 11.5 million pounds in damage and 20 casualties. (Butt et al. 2013; Chen et al. 2017).

1.2.2 Impact of LDam Events on Floods

Outburst floods resulting from the failure of either natural or artificial dams are considered as one of the most effective in producing large/extreme flood events in mountainous areas (Cenderelli 2011). The potential impacts of LDam on subsequent floods can be categorized into two distinct parts. Firstly, upstream or backwater flooding is induced by the gradual rise in water levels in the upstream area at the location of LDam. Secondly, downstream flooding primarily stems from the failure or breach of the LDam. The specific characteristics influencing the LDam stability include: the LDam's material components and their structures (texture, angle of repose, sorting), dimension and geometry of LDam (volume, size), geomorphology around the LDam location (especially the river reach being dammed and the hillslope of DFL), rates of seepage through the LDam, as well as the rates of input and outflow of LDam (Costa and Schuster 1988; Korup 2004; Tacconi Stefanelli et al. 2018; Fan et al. 2020). The longevity of the LDam can range from a couple of hours to thousand years, even millennia before their catastrophic failure (Zhang et al. 2016; Fan et al. 2020). Especially for those existing LDams that occurred in prehistoric times, normally formed by large landslides (>1 million m^3), could cause more damage given the greater volume of the impounded lake storage (0.02 to 21,000 million m^3) (Strom and Abdrakhmatov 2018). Through experimental research, Cui et al. (2013) also found that cascading LDam failures have the potential to greatly amplify the magnitude of debris flows or floods, leading to

catastrophic discharges.

There are a variety of impacts resulting from LDams that can increase the potential magnitude of floods compared to normal fluvial floods. Following the LDam formation, a series of cascading hazards, such as debris floods, can occur and result in more severe damage compared to regular floods. This heightened risk arises from the rapid release of accumulated water within LDam impounded lakes and the subsequent floods originating from upstream areas after the dam breach. The cumulative effect of these successive events amplifies the potential for extensive destruction and impact (King et al. 1989; Evans et al. 2011; Fan et al. 2018). The flow rate resulting from a LDam break or breach can increase at a much faster rate (e.g., from 100 m^3/s to 1300 m^3/s) than a normal fluvial flood within just a few hours (Perucca and Angillieri 2009). Experimental results showed that the peak flood discharge caused by sudden LDam failure can be 2–3 times when compared to that caused by overtopping (Hu et al. 2022). The landslide-induced tsunami waves, or landslide-induced sediment waves, the flood wave generated when landslide mass enters a river channel or other water body, can rise tens of meters above the mean water level (Sutherland et al. 2002; Wang et al. 2004) and directly cause damage to local communities (Duc et al. 2017).

1.2.3 Impact of LDam Events on Landscape Evolution

LDam formation plays an important role in the processes of landscape evolution, especially in the river valley evolution. By affecting the formation of knickpoints along the river longitudinal profile at the location of LDam formation, the river incision extending the fluvial networks can be thus impacted. Most of these research works were conducted from slope scale to local scale. Kroup et al. (2010) demonstrated a close association between the location, abundance, and potential longevity of large natural dams in the knickzones of the Indus and Tsangpo Rivers and changes in local topographic relief. Furthermore, their findings indicated that LDams act as a negative feedback mechanism, responding to the fluvial dissection of the Tibet plateau margins. Della Seta et al. (2017) proposed a mid-term landscape evolution model in the Tasso River Basin around the Scanno Rock Avalanche occurrence, which created the impounded Scanno Lake that still exists today. A similar landscape evolution model was also illustrated by

Delchiaro et al. (2019; 2022) with the impacts of the giant Seymareh (Saidmarreh) rock avalanche, the largest rock slope failure (44 Gm^3), which created three impounded lakes. The impacts of diverting the rivers and thus modifying the fluvial network can also occur with some large landslides (Iribar and Ábalos 2023).

1.3 LDam (Multi-hazard) Risk Management Framework

The risk management framework for a specific hazard includes several key elements, commonly defined as: hazard, exposure, and vulnerability (UNISDR 2015), even though the specific elements and definitions can vary in different contexts. Currently, for LDam hazards, there is no unified standard for their risk management framework. Some research for estimating the LDam formation probability has been directly applying the terms and definitions from landslide studies (Fan et al. 2014; Tacconi Stefanelli et al. 2020). To avoid the potential confusion brought by these different definitions in various contexts, some terminologies related to the LDam risk management framework that was applied in this thesis followed the definitions from Fell et al. (2008) and van Western et al. (2006), which are commonly applied for landslide risk assessment either by a quantitative or qualitative approaches. The definition of vulnerability and risk is the same as those in the Sendai framework (UNISDR 2015).

- Susceptibility: the assessment of landslides in a specific area involves analyzing their classification, size (or extent), and potential spatial distribution. It sometimes also includes evaluating the likelihood of landslides occurring in the area, as well as describing the speed and intensity of existing or potential landslides. Time frame is not considered in susceptibility evaluation, even though landslides are anticipated to be more frequent in highly susceptible areas. To estimate the susceptibility, an inventory of specific hazards is always required.
- Vulnerability: the extent of damage incurred by a specific element or group of elements at risk within the hazard-affected area. The elements at risk (exposure) include buildings, infrastructure, economic activities, public services, utilities, and environmental assets.
- Risk: quantification of the likelihood and severity of negative impacts on health, property, or the environment. However, risk also refers to a comparison between

the probability and consequences without actual outputs. Such a measure can be synthesized as the Eq.1-1 according to van Western et al. (2006).

$$\text{Risk} = \sum [Hazard\,(\sum Vulnerability \times Amount)] \quad \text{(Eq. 1-1)}$$

Compared to a single hazard, multi-hazards, such as LDams, can produce more challenges in quantification. Kappes et al. (2012) summarised these challenges as the comparability of hazards due to differing process characteristics and the interactions between each process. It is not just a simple summation of all the processes or outputs involved in such a multi-hazard. To further illustrate the processes and challenges of multi-hazard risk assessment, a schematic figure of a new framework, proposed as part of this thesis, for multi-hazard risk assessment taking LDams as an example is shown in Figure 1-4. The proposed framework includes four steps, including: hazard characteristics and interaction identification, susceptibility evaluation, vulnerability evaluation and risk assessment. Within this framework, the work in this thesis is focused on the hazard characteristics and interaction identification, and the susceptibility of LDam formation. Compared to single hazard risk assessment processes, such as landslide risk assessment, hazard characteristics and interaction identification is an extra process. On the step of hazard characteristics and interaction identification, the inventories of LDam, and those datasets directly relevant LDam formation were required to be collected for the exploration of the life cycle of LDams and the characteristics related to these processes, which is critical for a multi-hazard with cascading processes.

The relationships between multi-hazard triggers and processes can be complicated. Previous research summarised the relationships of multi-hazard between different hazards were summarised as independent, mutex (e.g., Hazard A and B cannot occur together), parallel and series (e.g., Hazard A induces Hazard B) relationships (Liu et al. 2016). Gill and Malamud (2016) further classified the interaction relationship of multi-hazard into triggering, increased probability, and catalysis/impedance. The relationship between landslides and floods within a LDam context extends beyond the scope of this system because they are not just interacted as triggers, but also become the components

of the cascading processes within various LDam-related processes, including LDam formation, LDam stability and flooding processes due to LDam breach or failures.

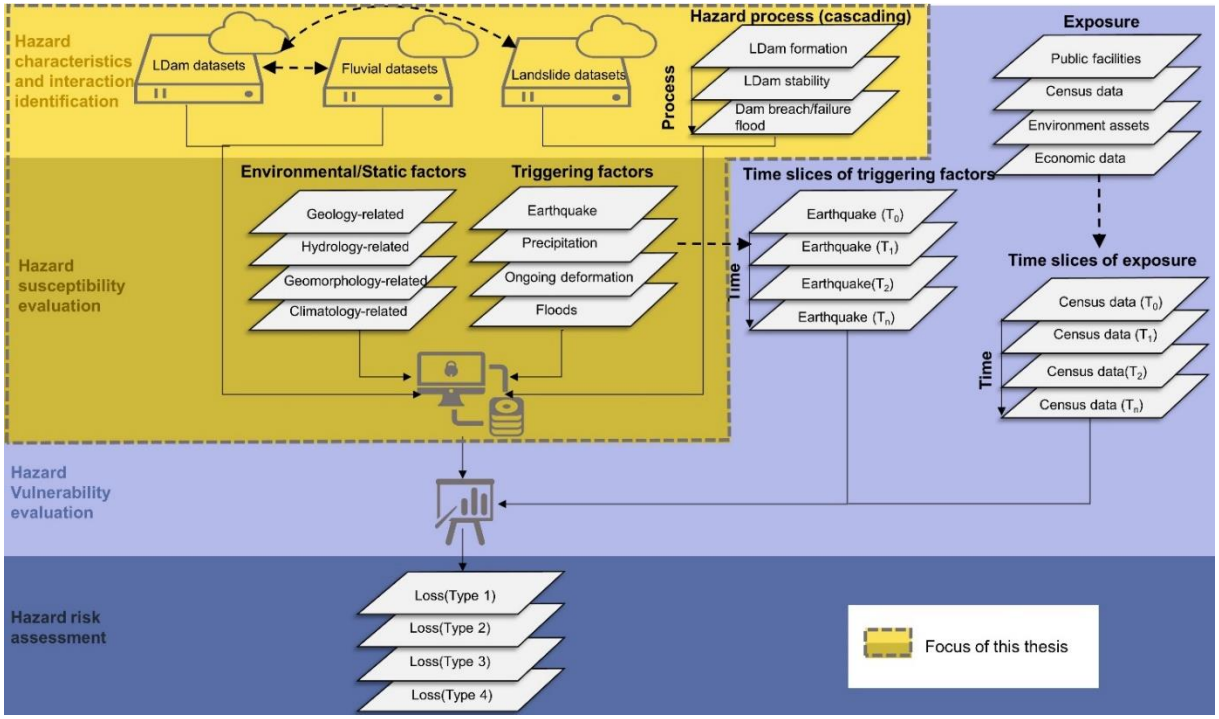

Figure 1-4 Proposed framework of multi-hazard risk assessment taking LDam as an example

As the various LDam, landslides and fluvial datasets are required in the hazard characteristics and interaction identification of LDams, the diversity of spatial distribution and comprehensiveness of these datasets from various aspects can make the assessment more challenging. The upstream mountainous regions, where LDams are more prone to form (Costa and Schuster 1988), have not received sufficient attention from a hydrological dataset's standpoint. This lack of focus can be attributed to limitations arising from data source resolution and inadequate measuring networks to represent the deep and narrow rivers in the upstream mountainous areas, especially for global-scale datasets (Yamazaki et al. 2019). Moreover, the connections between these datasets which contribute to LDam formation or other related processes can increase the difficulties of applying such datasets.

1.4 Spatial scale (Global Scale Datasets)

Exploring the spatial scale is always a critical issue in modelling. There is a strong

interest in analysing large-scale data, such as at the national or global level, for LDam risk assessment. This approach allows a variety of stakeholders to compare data using a standardized framework covering extensive areas, which is particularly helpful for those areas with limited or even no data availability. However, conducting large-scale analysis relies heavily on the availability of comprehensive datasets. Similar challenges have been encountered in other research fields in the past. In the context of global earthquake risk assessment, the mapping of global Peak Ground Acceleration (PGA) with a 10% probability of being exceeded in 50 years was accomplished by compiling maps derived from national and regional probabilistic seismic hazard models (Pagani et al. 2018). This outcome has been employed to assess changes in earthquake risk since the release of the Global Seismic Hazard Assessment Program (GSHAP) in 1999 (Shedlock et al. 2000). Similarly, for global flood risk assessment, advancements in the development of global-scale datasets for flood modelling and the formulation of efficient hydrodynamic codes have made it feasible to create global flood models (Bernhofen et al. 2021). Global-scale landslide risk assessment was also promoted based on these large-scale datasets. Stanley and Kirschbaum (2017) mapped the global landslide susceptibility map based on a global-scale rainfall triggered landslide dataset known as Global Landslide Catalog (GLC), as well as several local landslide inventories and various exploratory variables by using a heuristic fuzzy approach. Stanley et al. (2021) combined the Global Precipitation Measurement (GPM) mission and a collection of explanatory variables to develop the Landslide Hazard Assessment for Situational Awareness (LHASA) model (version 2) with the supplement of GLC. The generation and utilization of global-scale datasets as input data are essential for accurately mapping hazard risks on a global scale.

Therefore, to achieve the goal of global-scale LDam risk analysis, global-scale datasets of LDams, landslides and fluvial datasets are required. In this section, only the development of global fluvial datasets and landslide inventories are introduced while the development of LDam datasets is discussed in section 2.1 within the introduction of the development of LDam studies.

1.4.1 Global Fluvial Datasets

The Global Fluvial Datasets (GFDs) have been in rapid development in recent

decades, especially in the recent decade since more global-scale digital elevation models (DEM) have become available. The development of GFDs provides a unified standard dataset for the global-scale LDam analysis undertaken in this thesis. The timeline of GFD development is shown in Figure 1-5 with some related global-scale DEM product development. Most of the GFDs are open access. GFDs tend to represent the larger rivers relatively well due to the spatial resolution and the location of the global gauging stations for validation (Allen and Pavelsky 2018; Yamazaki et al. 2019).

The first global-coverage DEM is that from the Shuttle Radar Topography Mission (SRTM), which launched in 2000 with three major updates in the final DEM products (Farr and Kobrick 2000; Farr et al. 2007), and it could be the most applied global DEM product among research studies in the world. Based on the STRM DEM, HydroSHEDS was developed offering multiple spatial resolution hydrological-related data for hydro-environmental model development and other geographic information system (GIS) applications, such as manually adjusted basin boundaries and drainage direction derived from a hydrologically conditioned DEM (Lehner et al. 2008). Based on the elevation from SRTM Water Body Database and the HydroSHEDS flow direction, Yamazaki et al. (2014) developed an algorithm to generate the Global Width Database for Large Rivers (GWD-LR). Yamazaki et al. (2017) created a new global terrain elevation product named Multi-Error-Removed Improved-Terrain DEM (MERIT DEM) at the spatial resolution of 90m to reduce the bias, including absolute bias, stripe noise, speckle noise, and tree height bias, in such spaceborne global-scale DEM products. Based on the MERIT DEM and multiple inland water maps (Yamazaki et al. 2015), a new global-scale fluvial dataset, known as MERIT Hydro, was created containing flow direction, flow accumulation, hydrologically adjusted elevations, and river channel width (Yamazaki et al. 2019). Global flood risk assessment also provides auxiliary global fluvial datasets (Alfieri et al. 2013), such as the Global Flood Awareness System (GloFAS) from Copernicus Climate Change Service (2020). Forest And Buildings removed Copernicus DEM (FABDEM) provided a global-coverage DEM with the removal of building and tree height biases at 30 m spatial resolution (Hawker et al. 2022).

Satellite images, especially those from the long-term and global-coverage multi-temporal satellite observations, are also one of the major sources of data for developing

GFDs besides global-coverage and improved DEM development. Pekel et al. (2016) utilized 32 years of data to map the spatial and temporal variability of global surface water, along with its long-term changes by using multi-temporal orthorectified Landsat 5, 7, and 8 imageries. Allen and Pavelsky (2018) created the Global River Widths from Landsat (GRWL) Database to characterize the global coverage of rivers and streams based on the Landsat satellite images when rivers were in mean discharge validated by the data from 3693 discharge gauge stations distributed globally. Frasson et al. (2019) created spatially continuous maps of mean annual flow river width, slope, meander wavelength, sinuosity, and catchment area by using Landsat images and SRTM DEM with an analysis of these fluvial variables. Feng et al. (2022) created the dataset of Global LOng-term river Width (GLOW) based on Landsat images collected from the past 40 years to analyse the temporal variability and trends of global river width, which were supplied by GRWL and MERIT Hydro with some extra river width data derived based on the width and area relationship proposed by Frasson et al. (2019).

Auxiliary datasets combined with GFDs, and other global-scale datasets can also contribute to the development of GFDs through more extensive applications beyond the hydrological aspects. HydroALTAS was developed based on the multi-scale units derived from HydroSHED to provide hydro-environmental variables and attributes based on consistent and organized fluvial units (Linke et al. 2019). Amatulli et al. (2020) developed different geomorphological features such as the Stream power index and Terrain ruggedness index, derived from MERIT DEM.

With the continuing and future development of DEM data, satellite images and GFDs, such as NASADEM (Buckley et al. 2020), SWOT (Surface Water and Ocean Topography) mission (Feng and Glenson 2022), and HydroSHED 2.0 (Warmedinger et al. 2023), more GFDs with higher resolution and more precision can be expected in the near future.

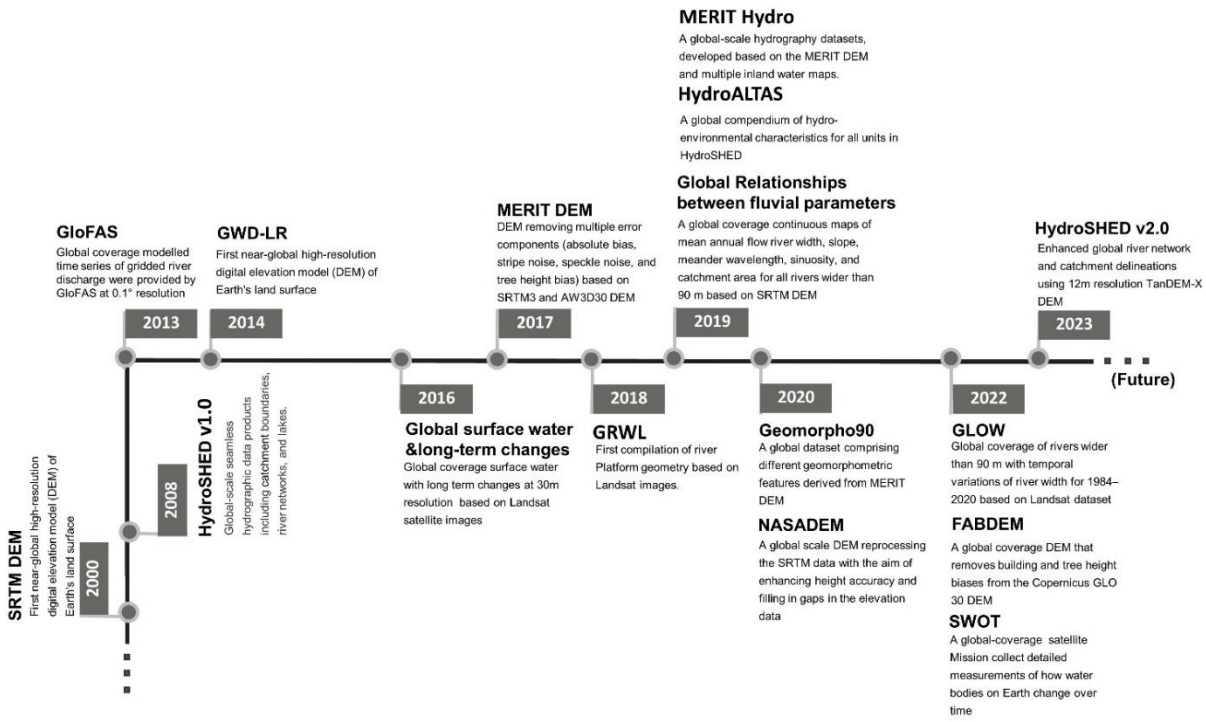

Figure 1-5 Timeline of global fluvial datasets (GFDs) development and some DEM contributed directly to GFDs (The time was set as the publication release year rather than the time of actual dataset release)

1.4.2 Large-scale Landslide Datasets

Global-scale landslide datasets were also in rapid development in the past few decades. According to the global analysis of landslide hazards (Nadim 2006; Petley 2012; Kirschbaum et al. 2015; Lin et al. 2017; Petley 2012; Schmitt et al. 2017; Tanyas et al. 2017; Froude and Petley 2018), landslide records and landslide prone areas clustered in the tectonic active and pluvial mountainous areas around the world. However, compared to the GFDs, which can be directly derived from either satellite images or global-scale DEM, global-scale landslide datasets accumulated various event-based inventories and thus the comprehensiveness of attributes within each landslide record depended on the quality of original data sources. Various landslide types and failure mechanisms link to a variety of triggers (Cruden and Varnes 1996). As a result, sometimes landslide inventories were presented with specific types. There are two global-scale landslide inventories grouped by major triggers of landslides, including Earthquake triggered landslides (Landslide Inventories from An Open Repository of Earthquake-Triggered Ground-

Failure Inventories, Schmitt et al. 2017) and rainfall-triggered landslides (Global Landslide Catalog, GLC, Kirschbaum et al. 2015).

National-scale landslide inventories face similar challenges, as they rely on the identification of landslides through various data sources rather than providing a complete and factual record of every single landslide that has occurred. Several countries, including the UK (Foster et al. 2012), USA (Jones et al. 2019), Italy (Trigila et al. 2010; Martino et al. 2022), Japan (National Research Institute for Earth Science and Disaster Prevention of Japan (NIED) 2014), and Norway (Norwegian Water Resources and Energy Directorate (NVE) 2023), have established their own national-scale landslide inventories according to their own standards.

To expand the records of landslide occurrences beyond reported events, various efforts have been made to enhance landslide databases using alternative sources such as social media or satellite images. Pennington et al. (2022) utilised live Twitter data streams to develop a large dataset of landslide images, employing a convolutional neural network. Li et al. (2016) devised a semi-automated method for mapping landslide inventories based on bitemporal aerial orthophotos. Another approach by Yang et al. (2019) involved the application of an unsupervised K-means classifier to automatically identify landslide scars in the Jinsha River valley, utilising the Normalized Difference Vegetation Index (NDVI) derived from Sentinel-2 satellite images. However, these endeavours are still in the early stages of development and require further validation. The accuracy of landslide mapping with remote sensing (LMRS) is still lower than those of general remote sensing classification because of undistinguishable characteristics, the variety of triggering impacts and completed features of landslides on satellite images (Zhong et al. 2022). Additionally, it is necessary for the revisit period of satellites to be sufficiently short to capture the formation of landslides resulting from multiple triggers.

1.5 Thesis Aims and Objectives

This thesis focuses on the key idea of quantifying where a LDam is likely to form with the inclusion of global fluvial datasets, aiming at addressing the following four scientific questions: 1) Where do the LDams occur and are clustered, and what are the characteristics of LDams and their triggers? 2) What kind of triggers and

geomorphological background means a location is prone to the LDam formation? 3) Why do only a small portion of landslides finally form a dam, and what characteristics make them more likely to form a LDam? 4) How and where is it necessary to quantify the formation of LDams, and which river reaches are more susceptible?

To address these questions, three core aims of this thesis together with specific objectives are proposed to answer these research questions:

Aim 1: Identify how significant LDams are as a multi-hazard on the global scale.

Objective 1.1. Literature-review of what we know and do not know about LDams. Identify the development of LDam studies, especially LDam datasets, characteristics of LDam and related natural systems, and LDam formation.

Objective 1.2. Collate and geolocate LDam records from different data sources to establish a global-scale database with all measurable LDam details and a united spatial reference.

Objective 1.3. Upon the establishment of a LDam database from Objective 1.2, the characteristics of LDam, including spatial distribution characteristics of LDam formation location, triggers, geomorphological characteristics of the location that formed the LDams, morphometric characteristics and triggers of DFLs are to be explored. The temporal trends of LDam records occurrence are also explored to explain any reason behind any observed trends.

Aim 2: Quantify the LDam formation areas and characteristics by identifying the interaction between hillslope and fluvial systems and their contributions to LDam formation as a multi-hazard assessment process.

Objective 2.1. Identify the connections between hillslope (landslide) and fluvial system by literature review for LDam studies, particularly LDam formation. Summarise the contributions of the datasets that relate to these two systems to LDam studies with an understanding and illustration of these datasets development.

Objective 2.2. Compare the characteristics of DFLs and landslides more generally based on the collated landslide and LDam datasets. By statistically comparing the morphometric

characteristics and spatial distribution of the locations of these records, the study will investigate whether some landslides with specific spatial characteristics are more likely to form LDams when compared to landslides generally.

Objective 2.3. Illustrate and identify the potential LDam formation area based on the findings above to highlight global LDam formation hotspots.

Aim 3: Map the susceptibility of LDam formation on river reaches.

Objective 3.1. Based on the landslide records collected from Aim 2, apply probability analysis findings through geospatial analysis (GIS modelling) to global geographical datasets, such as topography, rivers, geology and climate, to derive large-scale landslide susceptibility evaluation mapping.

Objective 3.2. Using the data derived from Aim 1 and Objective 3.1, and findings from Aim 2, a global-scale applicable framework of LDam formation susceptibility evaluation is established to provide a method to map the spatial probability of LDam formation on river reaches.

Objective 3.3. Compared the performance of the susceptibility analysis result in two different large-scale regions, Italy and Japan, to test the applicability of such a framework to different study areas.

Objective 3.4. Validate the LDam formation susceptibility evaluation maps with existing records from the LDam database achieved from Aim 1 and other local-scale LDam formation susceptibility results.

1.6 Thesis Conceptual Model and Structure

The remaining chapters of this thesis are structured as follows (Figure 1-6). In Chapter 2, a literature review of the LDam-related studies introduces the recent development of LDam studies, such as LDam dataset development and the focus of LDam formation studies, as well as the identification of current research gaps. Further, more specific literature review is also presented in each main chapter. Chapters 3 to 5 respectively introduce the global LDam formation from the perspective of data, relationship, and spatial probability estimation. A geo-located global-scale LDam

inventory named RAGLAD (River Augmented Global Landslide Dams) is created from multiple data sources with the supplement of auxiliary GFDs to see where this hazard is distributed and what characteristics it contains (Chapter 3). Given the fact that only a small portion of landslides eventually block the river, an analysis of the differences between DFLs and landslides more generally is explored with a proposal of a potential LDam formation zone based on the geomorphological and hydrological characteristics of DFLs and landslides more generally, derived from multiple landslides and LDam datasets collected globally (Chapter 4). Following this analysis, a global-scale applicable framework of LDam formation is proposed based on several open-access global-scale datasets and was tested in two large-scale tectonic active study regions, namely Italy and Japan (Chapter 5). Based on the results and key findings from Chapters 3 to 5, the contributions of this thesis are synthesised and summarised and concludes with a discussion of future research and opportunities (Chapter 6).

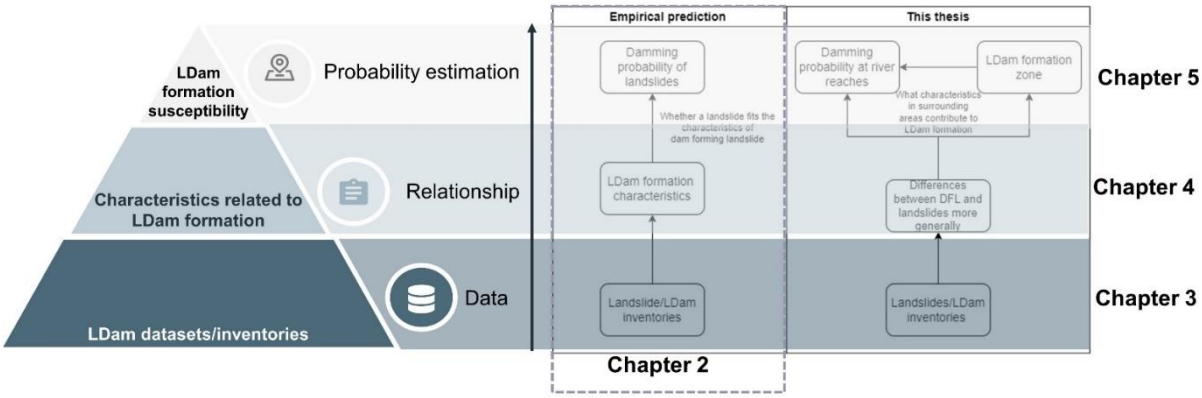

Figure 1-6 Conceptual model and structure of the thesis main contents (Chapters 2-5)

1.7 References

Allen GH, Pavelsky TM (2018) Global extent of rivers and streams. Science 361(6402):585–588

Alfieri L, Burek P, Dutra E, Krzeminski B, Muraro D, Thielen J, Pappenberger F (2013) GloFAS–global ensemble streamflow forecasting and flood early warning. Hydrol Earth Syst Sci Discuss. 17(3):1161-1175

Amatulli G, McInerney D, Sethi T, Strobl P, Domisch S (2020) Geomorpho90m, empirical evaluation and accuracy assessment of global high-resolution geomorphometric layers. Sci Data, 7(1):162

Bernhofen MV, Trigg MA, Sleigh PA, Sampson CC, Smith AM. (2021) Global flood exposure from different sized rivers. Nat Hazards Earth Syst Sci. 21(9):2829-2847

Buckley SM, Agram PS, Belz JE, Crippen EM, Gurrola EM, Hensley S, Kobrick M, Lavalle M, Martin JM, Neumann M. (2020) NASADEM: User Guide. NASA JPL: Pasadena, CA, USA

Butt MJ, Umar M, Qamar R (2013) Landslide dam and subsequent dam-break flood estimation using HEC-RAS model in Northern Pakistan. Nat Hazards 65:241-254

Casagli N, Guzzetti F, Jaboyedoff M, Nadim F, Petley DN (2017) Hydrological risk: landslides. Understanding Disaster Risk: Hazard Related Risk Issues-section II. 209-218.

Cenderelli DA (2011) Floods from natural and artificial dam failures. In: Wohl, E.E. (Ed.), Inland Flood Hazards: Human, Riparian, and Aquatic Communities. Cambridge Univ Press, New York, pp. 73–103

Chen S-C., Hsu C-L, Hu T, Chou HT, Cui P (2011) Landslide dams induced by typhoon Morakot and risk assesment. Ital J Eng Geol Environ 653–660

Chen X, Cui P, You Y, Cheng Z, Khan A, Ye C (2017) Zhang S. Dam-break risk analysis of the Attabad landslide dam in Pakistan and emergency countermeasures. Landslides 14:675-683

Copernicus Climate Change Service (C3S) (2020): River discharge and related forecasted data from the Global Flood Awareness System. Copernicus Climate Change Service (C3S) Climate Data Store (CDS). DOI: 10.24381/cds.ff1aef77 (Accessed on May 2023)

Costa JE, Schuster RL (1988) The Formation and Failure of Natural Dams. Geol Soc Am Bull 100(7): 1054-1068

Cruden DM, Varnes DJ (1996) Landslide Types and Processes, Transportation Research Board, U.S. National Academy of Sciences, Special Report, 247: 36-75.

Cui P, Zhou GG, Zhu XH, Zhang JQ (2013) Scale amplification of natural debris flows caused by cascading landslide dam failures. Geomorphology182:173-189

Dai FC, Lee CF, Deng JH, Tham LG (2005) The 1786 earthquake-triggered landslide dam and subsequent dam-break flood on the Dadu River, southwestern China. Geomorphology. 2005 65(3-4): 205-221

Delaney KB, Evans SG (2015) The 2000 Yigong landslide (Tibetan Plateau), rockslide-dammed lake and outburst flood: Review, remote sensing analysis, and process modelling. Geomorphology 246: 377-393

Delchiaro M, Della Seta M, Martino S, Dehbozorgi Nozaem MR, Nozaem R (2019). Reconstruction of River valley Evolution before and after the Emplacement of the Giant Seymareh Rock Avalanche (Zagros Mts., Iran). Earth Surf Dynam 7:929–947

Delchiaro M, Iacobucci G, Troiani F, Della Seta M, Ballato P, Aldega L(2022) Morphoevolution of the Seymareh landslide-dam lake system (Zagros Mountains, Iran): Implications for Holocene climate and environmental changes. Geomorphology 413:108367

Della Seta M, Esposito C, Marmoni GM, Martino S, Scarascia Mugnozza G, Troiani F (2017) Morpho-structural evolution of the valley-slope systems and related implications on slope-scale gravitational processes: New results from the Mt. Genzana case history (Central Apennines, Italy). Geomorphology 289: 60-77

Duc DM, Khang DQ, Duc DM, Ngoc DM, Quynh DT, Thuy DT, Giang NK, Van Tien P, Ha NH (2020) Analysis and modeling of a landslide-induced tsunami-like wave across the Truong river in Quang Nam province, Vietnam. Landslides. 17:2329-2341.

Evans SG, Tutubalina OV, Drobyshev VN, Chernomorets SS, McDougall S, Petrakov DA, Hungr O (2009) Catastrophic detachment and high-velocity long-runout flow of Kolka Glacier, Caucasus Mountains, Russia in 2002. Geomorphology, 105(3-4):314-321

Fan X, Xu Q, van Westen CJ, Huang R, Tang R (2017) Characteristics and classification of landslide dams associated with the 2008 Wenchuan earthquake. Geoenviron Disasters 4(1):1-15

Fan X, Dufresne A, Siva Subramanian S, Strom A, Hermanns R, Tacconi Stefanelli C, Hewitt K, Yunus AP, Dunning S, Capra L, Geertsema M, Miller B, Casagli N, Jansen JD, Xu Q (2020). The formation and impact of landslide dams – State of the art. Earth-Sci Rev 203

Farr TG, Rosen PA, Caro E, Crippen R, Duren R, Hensley S, Kobrick M, Paller M, Rodriguez E, Roth L, Seal D (2007) The shuttle radar topography mission. Rev Geophys 45(2)

Farr TG, Kobrick M (2000). Shuttle Radar Topography Mission Produces a Wealth of Data. Eos, Transactions, American Geophysical Union, 81:583-585

Feng D, Gleason CJ (2022) An updated understanding of global rivers from a new global river discharge reanalysis product: implications for SWOT mission. In: AGU Fall Meeting Abstracts 2022 Dec (Vol. 2022, pp. OS25C-04).

Feng D, Gleason CJ, Yang X, Allen GH, Pavelsky TM (2022) How have global river widths changed over time? Water Resour Res 8(8):e2021WR031712.

Foster C, Pennington CVL, Culshaw MG, Lawrie K (2012) The National Landslide Database of Great Britain: development, evolution and applications. Environ Earth Sci 66 (3):941-953. https://doi.org/10.1007/s12665-011-1304-5

Golly A, Turowski JM, Badoux A, Hovius N (2017) Controls and feedbacks in the coupling of mountain channels and hillslopes. Geology 45(4):307-310

Hawker L, Uhe P, Paulo L, Sosa J, Savage J, Sampson C, Neal J (2022) A 30 m global map of elevation with forests and buildings removed. Environ. Res. Lett 17(2): 024016

Hermanns, RL, Hewitt K, Strom A, Evans SG, Dunning SA, Scarascia-Mugnozza G (2011) The classification of rockslide dams, Natural and artificial rockslide dams. Springer, pp. 581-593

Hu W, Li Y, Fan Y, Xiong M, Luo H, McSaveney M, Zheng Y, Tang M (2022) Flow amplification from cascading landslide dam failures: Insights from flume experiments. Eng Geol 297:106483

Huggel C, Zgraggen-Oswald S, Haeberli W, Kääb A, Polkvoj A, Galushkin I, Evans SG (2005) The 2002 rock/ice avalanche at Kolka/Karmadon, Russian Caucasus: assessment of extraordinary avalanche formation and mobility, and application of QuickBird satellite imagery. Nat Hazards Earth Syst Sci 5(2):173-187

Iribar V, Ábalos B (2023) Pleistocene river diversions caused by large landslides in the western Pyrenees (Oria River drainage basin, N Spain). Basin Res

Jones ES, Mirus BB, Schmitt RG, Baum RL, Burns WJ, Crawford M, Godt JW, Kirschbaum DB, Lancaster JT, Lindsey KO, McCoy KE, Slaughter S, Stanley TA (2019) Summary Metadata – Landslide Inventories across the United States, U.S. Geological Survey data release, https://doi.org/10.5066/P9E2A37P. Accessed 20 Feb 2022

Kappes MS (2011) Multi-hazard risk analyses: a concept and its implementation. PhD thesis, University of Vienna

Kappes MS, Glade T (2013) Landslides in a multi-hazard context. In: Margottini C, Canuti P, Sassa K (eds). Landslide Science and Practice: Volume 7: Social and Economic Impact and Policies. Berlin: Springer pp83-90

Kappes MS, Keiler M, von Elverfeldt K, Glade T (2012) Challenges of analyzing multi-hazard risk: a review. Nat hazard 64:1925-1958

Kirschbaum DB, Stanley T, Zhou Y (2015) Spatial and Temporal Analysis of a Global Landslide Catalog. Geomorphology. doi:10.1016/j.geomorph.2015.03.016.

Korup O, Montgomery DR, Hewitt K (2010) Glacier and landslide feedbacks to topographic relief in the Himalayan syntaxes. PNAS 107(12):5317-5322

Lehner B, Verdin K, Jarvis A (2008) New global hydrography derived from spaceborne elevation data. Eos, Transactions, American Geophysical Union, 89(10): 93–94. https://doi.org/10.1029/2008eo100001

Li Z, Shi W, Myint SW, Lu P, Wang Q (2016) Semi-automated landslide inventory mapping from bitemporal aerial photographs using change detection and level set method. Remote Sens Environ 175:215-230

Liu B, Siu YL, Mitchell G (2016) Hazard interaction analysis for multi-hazard risk assessment: a systematic classification based on hazard-forming environment. Nat Hazards Earth Syst Sci 16(2):629-642

Linke S, Lehner B, Ouellet Dallaire C, Ariwi J, Grill G, Anand M, Beames P, Burchard-Levine V, Maxwell S, Moidu H, Tan F, Thieme M (2019) Global hydro-environmental sub-basin and river reach characteristics at high spatial resolution. Sci Data 6(1): 1-15

National Research Institute for Earth Science and Disaster Prevention of Japan (NIED) (2014) Digital archive for Landslide Distribution Maps. National Research Institute for Earth Science and Disaster Prevention of Japan. https://dil-opac.bosai.go.jp/publication/nied_tech_note/landslidemap/index.html Accessed 23 Feb 2022 (in Japanese)

Norwegian Water Resources and Energy Directorate (NVE) (2023) Norwegian landslide database, https://nve.no/map-services/ Accessed June 2023

Pagani M, Garcia-Pelaez J, Gee R, Johnson K, Poggi V, Styron R, Weatherill G, Simionato M, Vigano D, Danciu L, Monelli D (2018). Global Earthquake Model (GEM) Seismic Hazard Map (version 2018.1 - December 2018), DOI: https://doi.org/10.13117/GEM-GLOBAL-SEISMIC-HAZARD-MAP-2018.1

Pekel JF, Cottam A, Gorelick N, Belward AS (2016) High-resolution mapping of global surface water and its long-term changes. Nature 540(7633):418-422

Pennington CV, Bossu R, Ofli F, Imran M, Qazi U, Roch J, Banks VJ (2022) A near-real-time global landslide incident reporting tool demonstrator using social media and artificial intelligence. Int J Disaster Risk Reduct 77:103089

Perucca LP, Esper Angillieri MY (2009) Evolution of a debris-rock slide causing a natural dam: the flash flood of Río Santa Cruz, Province of San Juan—November 12, 2005. Nat hazards 50:305-320

Petitta M, Scarascia Mugnozza G, Barbieri M, Bianchi Fasani G, Esposito C (2010) Hydrodynamic and isotopic investigations for evaluating the mechanisms and amount of groundwater seepage through a rockslide dam. Hydrol Processes 24(24):3510-3520

Schmitt RG, Tanyas H, Nowicki Jessee MA, Zhu J, Biegel KM, Allstadt KE, Jibson RW, Thompson EM, van Westen CJ, Sato HP, Wald DJ, Godt JW, Gorum T, Xu C, Rathje EM, Knudsen KL (2017). An open repository of earthquake-triggered ground-failure inventories. U.S. Geological Survey data release collection, https://doi.org/10.5066/F7H70DB4. Accessed 23 Feb 2022

Sharma S, Talchabhadel R, Nepal S, Ghimire GR, Rakhal B, Panthi J, Adhikari BR, Pradhanang SM, Maskey S, Kumar S (2022) Increasing risk of cascading hazards in the central Himalayas. Nat Hazard 1-10

Shedlock KM, Giardini D, Grunthal G, Zhang P (2000) The GSHAP global seismic hazard map. Seismol Res Lett 71(6):679-686

Stanley TA, Kirschbaum DB, Benz G, Emberson RA, Amatya PM, Medwedeff W, Clark MK (2021) Data-driven landslide nowcasting at the global scale. Front Earth Sci 9:640043

Sutherland DG, Ball MH, Hilton SJ, Lisle TE (2002) Evolution of a landslide-induced sediment wave in the Navarro River, California. Geol Soc Am Bull 114(8):1036-1048

Tanyaş H, van Westen CJ, Allstadt KE, Anna Nowicki Jessee M, Görüm T, Jibson RW, Godt JW, Sato HP, Schmitt RG, Marc O, Hovius N. (2017) Presentation and analysis of a worldwide database of earthquake-induced landslide inventories. J Geophys Res: Earth Surf. 122(10):1991-2015

Trigila A, Iadanza C, Spizzichino D (2010) Quality assessment of the Italian Landslide Inventory using GIS processing. Landslides 7:455–470

United Nations Office for Disaster Risk Reduction (UNISDR) (2015) Sendai Framework for Disaster Risk Reduction 2015-2030. United Nations - Headquarters (UN).

United Nations Environment Programme (UNEP) (1992) Agenda 21. Tech. rep., United Nations Environment Programme, http://www.un.org/esa/dsd/agenda21/res_agenda21_07.shtml, Accessed in June, 2023

van Westen CJ, van Asch TW, Soeters R (2006) Landslide hazard and risk zonation—why is it still so difficult? Bull Eng Geol Environ 65:167-184

Warmedinger L, Huber M, Walper C, Anand M, Lehner B, Thieme M, Roth A (2023) Improved hydrologic conditioning of the TanDEM-X dataset for HydroSHEDS v2 (No. EGU23-15182). Copernicus Meetings.

Yamazaki D, Ikeshima D, Sosa J, Bates PD, Allen GH, Pavelsky TM (2019) MERIT Hydro: A High-Resolution Global Hydrography Map Based on Latest Topography Dataset. Water Resour Res 55(6): 5053-5073

Yamazaki D, Ikeshima D, Tawatari R, Yamaguchi T, O'Loughlin F, Neal JC, Sampson CC, Kanae S, Bates PD.(2017) A high-accuracy map of global terrain elevations. Geophys Res Lett 44(11):5844-5853

Yamazaki D, Trigg MA, Ikeshima D (2015) Development of a global~ 90 m water body map using multi-temporal Landsat images. Remote Sens Environ 171:337-351

Zhong C, Liu Y, Gao P, Chen W, Li H, Hou Y, Nuremanguli T, Ma H (2020) Landslide mapping with remote sensing: challenges and opportunities. Int J Remote Sens 41(4):1555-1581

Chapter 2. The Development of LDam Formation Studies

Compared to single hazards, such as floods and landslides, the study of LDams as a multi-hazard has received relatively less attention in the past until the 1980s (Schuster 1986; Costa and Schuster 1988). The objective of this literature review aims to summarise some key developments and issues within the research field, especially related to LDam formation. This section commences with an introduction of the development of LDam datasets, followed by a summary of characteristics related to LDam formation, as typically compiled from these datasets. Subsequently, the review delves into the current research focus on LDam formation, particularly on LDam formation susceptibility evaluation. Lastly, the review culminates in an overview of the prevailing gaps that persist within the realm of these LDam studies. Note that there is further literature exploration in each of the main chapters (Chapter 3 to 5), specific to those chapters, due to their paper format.

2.1 Development of LDam Datasets

The establishment of a dataset forms the fundamental basis for conducting further analyses of specific hazards, such as risk assessment, hazard mapping, and the development of mitigation strategies. LDam records are well documented in historical records. The physical processes of LDam formation are very hard to measure as LDams occur unexpectedly as they are difficult to precisely forecast currently, especially when they occur in remote areas, which likely escape being reported. Physics-based model for landslide damming probability estimation are often established on a single event and validated with field measurements, which can be difficult to directly apply to estimate the LDam formation probability for a wider area after a short time of LDam occurrence (Dal Sasso et al. 2014; Nian et al. 2020). These reasons may explain the LDam physical processes research gap identified, as evidenced by no significant process-based publications describing LDam observations since the first global-scale LDam dataset was published (Costa and Schuster 1991). As a result, empirical studies are more popular than physical-based studies for LDam. Fan et al. (2020) encouraged more detailed study cases of by different types of landslides and new field measurement methods in their review.

The earliest recorded LDam event dates back to 586 BC, as documented in the Spring and Autumn Annals (Liu et al. 2019). Another significant event was a LDam occurrence in 1786, commemorated by a stone monument created by residents and presented in the research of Dai et al. (2005). Sekiya and Kikuchi (1889) recorded several floods that resulted from the breach of LDams on Nagase River. However, such records were either recorded in the floods resulting from the breach of LDam and impounded lake, or landslide events. It was not until 1991 that the first global-scale LDam dataset was established (Costa and Schuster 1991). Table 2-1 presents relevant information on various LDam datasets from the past decades, including their data sources, temporal and spatial coverage, as well as the recorded attributes. LDam datasets can categorize and structure the LDam record based on various attributes, including landslide types (of DFLs), triggers, time, and locations. These datasets ensure the collected LDam records adhere to a unified data collation standard and maintain consistent data formatting. In both regional and global-scale LDam datasets, certain attributes are commonly included, such as spatial information presented through either approximate locations or precise coordinates. Additionally, dimension parameters of LDam elements, including DFLs (whether separated into landslide source and dam body) and impounded lakes, are recorded, along with consequences such as general losses or detailed parameters related to subsequent floods. It is also noted that a majority of these LDam datasets are stored as tables rather than geospatial data formats, such as vector or raster file formats, primarily due to the unavailability of precise location data for LDam events. Nonetheless, despite the format used, LDam datasets serve as valuable resources for understanding and managing LDam hazards across different regions and scales.

Table 2-1 Review of LDam datasets around the world (mainly global-scale and regional-scale)

Reference	Numbers	Data Source	Area coverage	Time coverage	Milestones	Attributes recorded
Costa and Schuster 1991	463	Literature and some unpublished data	Worldwide	From historical times to the 1980s	The first completed global landslide dam dataset	Approximate spatial location, dimension data of LDams and impounded lakes; dam

Reference	Numbers	Data Source	Area coverage	Time coverage	Milestones	Attributes recorded
						failure time and mechanism; consequence
Clague and Evans 1994	21	Literature	Canada	1880-1984	Natural dam inventory in Canada Cordillera	Approximate location, time and dam material
Chai et al. 1995	147	Literature including historical records	China	From the early quaternary to the early 1990s	First LDam dataset in China	Approximate location; time of occurrence; volumes of landslides; triggers; consequence
Evans et al. 2011	18	Literature	Worldwide	1840-2010	Records of rockslide dams which impounded lake volume larger than 100 Mm^3	Approximate location, volume of landslide and impounded lake, triggers
Hermanns et al. 2011	61	Literature	Argentina	Not mentioned	LDams larger than 100 Mm^3 in northwest Argentina and northern Patagonia	Approximate location, catchment area, dam status and dimension data
Mizuyama et al. 2011	164	Literature including historical records	Japan	714-2008	The most completed LDam dataset in Japan	Precise location with coordinates, catchment area, triggers, dimension data of landslides and LDams, geological background, hazard duration time, hazard status

Reference	Numbers	Data Source	Area coverage	Time coverage	Milestones	Attributes recorded
Fan et al. 2012	828	Satellite images and field survey	China	2008	Largest LDam inventory for a single regional-scale triggering event (2008 Wenchuan Earthquake)	Geomorphometric properties of LDams and impounded lakes; conditions of the lakes and dams
Stefanelli et al. 2015	300	Literature and field survey	Italy	Prehistorical period to 2015	The most completed LDam dataset in Italy	Precise location; consequences; movement type; trigger; dimension data of landslides, LDams, upstream areas, damming rivers and impounded lakes
Zhang et al. 2016	1044	Literature	Worldwide	20,000 BP to 2008	One of the most completed worldwide LDam datasets by bibliographic work	Hazard occurrence countries and time; dimension data of landslides, LDams and impounded lakes; consequence
Stefanelli et al. 2018	51	Field survey	Peru	Historical	First database of LDams in the Cordillera Blanca Mountains, Peru	Precise location; dimension data of landslides, LDams, upstream areas; lake and LDam conditions
Strom and Abdrakhmatov (2018)	549	Literature and field survey	Central Asia	Mainly prehistoric	The most completed LDam inventories	Precise location; dimension data of landslides (detachment area

Reference	Numbers	Data Source	Area coverage	Time coverage	Milestones	Attributes recorded
					formed by rockslides and rock avalanches in Central Asia	and main landslide body); presence and parameters of river damming
Fan et al. 2020	410	Literature	Worldwide	Since 1900	Global-scale LDam dataset focuses on landslides with a volume larger than 10^6 m^3	Locations, triggers; landslide type; dimension of impounded lake and LDam; presence and parameters related to river damming and breach floods; consequences

The process of collecting records to establish LDam datasets closely resembles that of compiling landslide datasets. It involves gathering numerous records from various data sources, such as literature or data directly collected through field surveys during or after hazard events. At times, an LDam dataset is created as a subset from the landslide dataset in the same area (Fan et al. 2012; Oppikofer et al. 2020), which means it relies on the comprehensiveness and quality of the original landslide datasets. Consequently, the accessibility and availability of the LDam dataset depend on the willingness of researchers to share their findings and contribute to collective knowledge in this field. Cross-referencing with multiple dataset sources can enhance the accuracy and reliability of local-scale or regional-scale LDam datasets. Fan et al. (2012) extracted the LDam records based on satellite images with validations through field survey for the LDam records that occurred in the 2008 Wenchuan Earthquake. This illustrates the importance of combining different data sources to improve the overall quality of LDam datasets and enrich our understanding of these hazardous events.

Developing and maintaining a comprehensive LDam dataset is crucial for effective LDam risk management in the landslide prone areas. Updating LDam record

entries in datasets can provide more comprehensive and precise information about the locations and characteristics, which leads to better identification of LDam hazard-prone areas and enables the implementation of targeted measures to reduce potential impacts brought by LDam in such areas. Therefore, it is critical to have a comprehensive LDam dataset to study the characteristics of landslides with LDam formation.

2.2 Characteristics Related to LDam Formation

Even though the factors of LDam formation and stability, including the LDam material composition, dam geometry, upstream catchment area at the point of river blockage, lake volume, and water inflow rates, maybe clearly identified, a clear mechanism for most LDams often remains unknown (Fan et al. 2020). Laboratory works are helpful to study the mechanism of LDam formation, especially by controlling some key factors related to LDam formation. Nian et al. (2020) found that the LDam formation is related to the ratio of the landslide discharge to the water flow rate by a laboratory-scale experimental investigation. The experimental study performed by Liao et al. (2019) reveals a clear positive correlation between LDam deposit height and rockslide volume. However, the applicability of laboratory-scale research to large-scale research remains to be validated, especially when some hydrodynamic parameters are hard to be recorded for most large-scale LDam datasets at the current stage. Therefore, statistical analysis based on LDam records is more common for studying the characteristics of LDam and its DFL, especially using their geomorphological characteristics.

Maintaining and updating a global-scale LDam dataset with a larger number of data entries by encompassing diverse case studies forms a robust statistical foundation for studying DFL and LDam characteristics, especially for LDam formation, failure mechanisms and longevity (Fan et al. 2020). The most applied characteristics to study LDam formation are the dimension data of DFLs or LDams, and the geomorphological characteristics related to the local fluvial system, including the upstream catchment at the point of river blockage, impounded lake and the dammed river. Korup (2004) used a new LDam dataset in New Zealand using several parameters, including LDam height, impounded lake volume, catchment area and upstream relief to evaluate LDam formation. Tacconi Stefanelli et al. (2016) applied the river width and the landslide volume to

estimate the LDam formation while applying the slope and upstream area to access the stability of the LDams in Italy based on an Italian LDam dataset (Tacconi Stefanelli et al. 2015). Studying these characteristics could lead to the advancement of the LDam classification system, enabling its application as an initial assessment tool to determine the formation and stability of LDams. Based on the LDam records in the 2008 Wenchuan Earthquake (Fan et al. 2012), Fan et al. (2017) analysed the characteristics of LDams and proposed a refined classification system for LDams by the dam deposition elements, which further developed the classification proposed by Costa and Schuster (1988), which can be applied as the preliminary result for evaluating the LDam stability.

Some characteristics related to elements of LDam formation processes, such as the dimension data and geomorphological characteristics of DFLs and fluvial system, are found to be correlated in some areas. Consequently, certain parameters that are difficult to directly obtain from the LDam dataset are instead derived based on these established relationships. For example, the volume of the impounded lake resulting from LDam formation increases linearly with the volume of its DFL (Argentin et al. 2021). Another example is drainage area, serving as an indicator of discharge, is linked to various fluvial parameters including river flow length (Hack 1957), stream gradient (Flint 1974), and river width (Finnegan et al. 2005; May et al. 2013).

However, such relationships can depend on the local environment and thus may not be suitable for generalising in a unified equation to represent the relationship between various parameters. Frasson et al. (2019) aimed to investigate the correlation between catchment area and river width. The researchers derived the catchment area from the Landsat dataset using the method introduced by Allen and Pavelsky (2015; 2018), while the river width data was sourced from the HydroSHED dataset (Lehner et al. 2008). However, despite their comprehensive analysis on a global scale, the results revealed a relatively weak significance for this relationship, with an r-squared value of only 0.25. Moreover, achieving precise characteristics for LDams or DFLs can be particularly challenging, which can be summarised into two aspects. The first is that achieving accurate LDam and DFL geometry can be challenging in reality, as the pre- and post-landslide topography and hydrological parameters are often unknown (Dong et al. 2014). The rapid formation and failure of most LDams, occurring within a short period ranging

from a couple of hours to a few days (Costa and Schuster 1988), contribute to this difficulty. The second challenge is that the uncertainty in data entries for LDam inventories is inevitably influenced by measurement uncertainties resulting from initial data acquisition and calculation, inconsistent terminology application, and systematic underrepresentation of small LDams (Kourp 2004; Argentin et al. 2021).

2.3 Development of Current LDam Formation Studies

The primary objective of LDam formation studies is to determine the likelihood of LDam formation at specific locations or identify areas prone to their occurrence. Current research on LDam formation probability spatial estimation mainly focuses on evaluating the damming probability of landslides, or the occurrence probabilities of DFLs. Even though the numerical stimulation of LDam formation processes can stimulate the processes at various times and also show the results with different scenarios (Braun et al. 2018), this section only focuses on the review of statistical methods to evaluate the LDam formation susceptibilities, such as proposing the river blockage index of landslides and LDam formation susceptibility evaluation.

Based on the geomorphological characteristics and differences of non-LDam formation landslides and DFLs, multiple geomorphological indexes were explored as to whether or not a landslide can form a LDam. Most of the geomorphological indices for estimating the LDam formation are established based on the LDam inventories and statistical analysis. Tacconi Stefanelli et al. (2016) designed the Morphological Obstruction Index (MOI) based on the relationship between valley width and landslide volume based on an Italian LDam dataset. The MOI was also applied to LDam records in Peru (Tacconi Stefanelli et al. 2018). Dal Sasso et al. (2014) proposed the Dimensionless Morpho-Invasion Index (DMI) by combining the landslide and river momentum. The acceptability of such geomorphological indexes to estimate the LDam formation varied in different regions as they were established based on local datasets. Argentin et al. (2021) compared six river obstruction and LDam stability indices from previous research for the LDam records in the Austrian Alps and found their results are not consistent when compared to previous research, which is similar to the results from the research conducted in Eastern European Alps (Dufresne et al. 2018). Cencetti et al. (2020) and Struble et al.

(2021) also found that such a geomorphological index cannot fit with their LDam records, which are located in different study regions from where such indexes were established. One of the reasons behind this could be the LDam formation indexes are relatively dimensional compared to the LDam stability indexes, which gives less consistent results across different scales (Argentin et al. 2021). Experimental research has been used to propose a dimensionless River Blockage Criterion (RBC) determined by landslide discharge and water flow rate of the LDam formation (Nian et al. 2020). However, similar to the geomorphological index based on statistical analysis, such an index was validated with the experimental investigation and a few cases and thus the capability for large-scale research application requires further validated.

More details of the LDam formation indexes mentioned above are shown in Table 2-2. Geomorphological LDam formation indexes, such as MOI (Tacconi Stefanelli et al. 2016; Tacconi Stefanelli et al. 2018), allow evaluation of the stability of a LDam in near real-time. Such an index is efficient for application for large-scale areas and its variable data are easy to get. However, the capability of this index for other regions requires further validation as they were established based on local geomorphological data. In contrast, the experimental-based LDam formation index can be applied to various case studies with similar conditions but the data collation for modelling is very complex and can hinder the large-scale application of such model within a short time when the hazard occurred.

Table 2-3. Detailed explanation of LDam formation index

Index	**DMI**	**MOI**	**RBC**
Equation	$\frac{2 \cdot \rho_S \cdot {U_s}^2 \cdot V_s}{\rho_w \cdot g \cdot h^2 \cdot B_w \cdot W}$	$\log \frac{V_l}{W_v}$	$\frac{Q_1}{Q_w}$
Simplified deriving reason	Momentum of both landslides and rivers	Correlation between landslide volume and valley width (Fan et al. 2012)	Experiment results
Parameters	ρ_S:material density of the landslide U_s: landslide average velocity V_s:landslide volume ρ_w: water density	V_l: landslide volume W_v: river width	Q_1: landslide discharge ($\times 10^{-3}$ m3/s) Q_w: water flow rate of a river valley (L/s).

	g: gravity acceleration h :hydraulic level B_w: river width W: landslide width		
Adoption scale	Zillona landslide (Single event)	Regional scale (Italy and Peru)	Baige River-blocking event (Single event)
Reference	Dal Sasso et al. (2014)	Tacconi Stefanelli et al. 2016; Tacconi Stefanelli et al. 2018	Nian et al. 2020

Establishing an empirical relationship for estimating the LDam formation probability by combining all LDam formation related parameters as input variables based on LDam datasets has also been popular. It can either directly predict the probability of LDams or generalize some parameters related to LDam geometry. Chen and Chang (2016) explored 13 parameters, mainly related to local geomorphology and river characteristics, and found that the logistic regression function fits best to estimate the probability of LDam formation compared to Fisher's discriminant analysis for the LDams in Taiwan island. Oppikofer et al. (2020) established a semi-empirical relation to predict the LDam height by linking the maximum height, area and volume of LDam, and valley width based on the rock slope failures in southwestern Norway. Moreover, modelling the LDam formation probability of DFL can be conducted by combining the effects or probabilities in LDam formation-related processes, such as landslide occurrence, landslide mass run-out and damming processes (Fan et al. 2014; Tacconi Stefanelli et al. 2020).

2.4 Research Gaps

Integrating the fluvial and hillslope systems is a crucial challenge for LDam studies. Based on the literature review above, researchers have attempted to address this issue by recording parameters from both environments and utilizing them as input variables to establish empirical relationships or estimate LDam formation probability. However, it is important to highlight that parameters from the fluvial aspect were predominantly used as direct inputs, without adequately considering other characteristics, such as the spatial proximities to the river or conducting further analysis to enhance their relevance and significance among LDam studies. The spatial distribution of LDams was

conceptually described as upstream hillslope mountainous areas without further quantitative analysis unless the LDam formation probability is mapped. Conversely, more extensive analyses have been conducted from the landslide perspective, such as predicting potential landslide volume and run-out distance to estimate the damming probability for landslides based on the empirical relationships established from LDam or landslide inventories (Fan et al. 2014; Tacconi Stefanelli et al. 2020). Therefore, such LDam formation probability estimation is constrained to the locations where multiple LDam and landslide records are located.

Another crucial issue pertains to the applicability of research outputs in different study areas, particularly concerning large-scale regions. Both the data sources and methods employed to predict LDam formation or to explore the characteristics between DFL and landslides more generally can directly influence their applicability, especially when relying on methodologies established using local-scale datasets and environments. To ensure a consistent global-scale LDam formation research, the utilization of global-scale datasets becomes necessary for establishing an approach that can be applied consistently to large-scale regions. One of the challenges behind this could be the potential underrepresentation of LDam records within the LDam database. The fact that the number of recorded landslide events can be underestimated ranging from 1400% to 2000% have been mentioned in the global-scale fatal landslide studies by Petley (2012), Kirschbaum et al. (2015) and Froude and Petley (2018), as certain regions prone to landslide occurrences documented only a few of the total events that have happened. Tanyas et al. (2017) demonstrated a power relationship for the number of earthquakes, indicating that records of most earthquakes did not report landslide events. Similarly, LDams may not be reported in most landslide inventories, despite being a multi-hazard that frequently occurs worldwide. This highlights the necessity for a comprehensive dataset and approach in collecting and incorporating LDam data to ensure a more accurate and globally representative understanding of LDam formation.

Changes to climate, especially the changes in precipitation and temperature, influence the landslide magnitude and frequency, particularly the largest mass movements (Korup et al. 2012). Various climatic conditions can impact the different types of landslide occurrence. Heavy precipitation, snow melt events and longer periods

with humid and cool climate conditions are linked to debris flow occurrence, for example, around the study area of Lake Lago di Braies, northeast Italy (Schneider et al. 2010). Changes of temperature are also connected to rock fall occurrence in Mittlerer Burgstall, central Austria, by influencing the glacial retreat, erosion, slope oversteepening, permafrost degradation and weathering (Kellerer-pirklbauer et al. 2012). Long-term permafrost degradation could be a potential trigger of rockslides and rock avalanches in the Central Andes of Argentina (Tapia Baldis and Trombotto 2019). The climate also influences some geomorphological changes and thus can also lead to LDam formation. Some of knickpoints, created by change in climate-related river discharge, were reportedly associated with LDam formation across different regions, including the Himalayas, Tibetan Mountains, Central Asia, and the Southern Alps of New Zealand (Fan et al. 2020). Climate changes can also lead to high LDam formation risk. Li et al. (2022) reported several LDam records located in eastern Tibet formed in recent decades with environmental records showing increasing average temperatures, cumulated rainfalls and strong earthquakes. However, such effects were not reflected in the current dataset establishment or modelling processes given the spectrum of climate data and landslide or LDam processes were not consistent.

2.5 References

Allen GH, Pavelsky TM (2018) Global extent of rivers and streams. Science 361(6402):585–588

Allen GH, Pavelsky TM (2015) Patterns of river width and surface area revealed by the satellite-derived North American River Width data set. Geophys Res Lett 42(2):395-402

Argentin AL, Robl J, Prasicek G, Hergarten S, Hölbling D, Abad L, Dabiri Z (2021) Controls on the formation and size of potential landslide dams and dammed lakes in the Austrian Alps. Nat Hazards Earth Syst Sci 21(5):1615-1637

Braun A, Cuomo S, Petrosino S, Wang X, Zhang L (2018) Numerical SPH analysis of debris flow run-out and related river damming scenarios for a local case study in SW China. Landslides 15:535-550

Cencetti C, De Rosa P, Fredduzzi A (2020) Characterization of landslide dams in a sector of the central-northern Apennines (Central Italy). Heliyon, 6(6): e03799.

Chai HJ, Liu HC, Zhang ZY (1995) The catalog of Chinese landslide dam events. Journal of Geological Hazards and Environment Preservation. 6(4): 1-9 (In Chinese)

Clague JJ, Evans SG (1994) Formation and failure of natural dams in the Canadian Cordillera. Geological Survey of Canada Bulletin

Costa JE, Schuster RL (1988) The formation and failure of natural dams. Geol Soc Am Bull 100(7):1054–1068

Costa JE, Schuster RL (1991) Documented historical landslide dams from around the world (No. 91–239), https:// pubs. usgs. gov/ of/ 1991/ 0239/report. pdf. Accessed 10th Jan 2021

Dai FC, Lee CF, Deng JH, Tham LG (2005) The 1786 earthquake-triggered landslide dam and subsequent dam-break flood on the Dadu River, southwestern China. Geomorphology. 65(3-4):205-221

Dal Sasso SF, Sole A, Pascale S, Sdao F, Bateman Pinzón A, Medina V (2014) Assessment methodology for the prediction of landslide dam hazard. Nat Hazards Earth Syst Sci 14(3):557-567

Dong JJ, Lai PJ, Chang CP, Yang SH, Yeh KC, Liao JJ, Pan YW (2014) Deriving landslide dam geometry from remote sensing images for the rapid assessment of critical parameters related to dam-breach hazards. Landslides 11:93-105

Dufresne A, Ostermann M, Preusser F (2018) River-damming, late-Quaternary rockslides in the Ötz Valley region (Tyrol, Austria). Geomorphology 310:153-167

Evans SG, Hermanns RL, Strom A, Scarascia-Mugnozza G (2011) Natural and artificial rockslide dams. Springer Science & Business Media.

Fan X, Dufresne A, Siva Subramanian S, Strom A, Hermanns R, Tacconi Stefanelli C, Hewitt K, Yunus AP, Dunning S, Capra L, Geertsema M, Miller B, Casagli N, Jansen JD, Xu Q (2020). The formation and impact of landslide dams – State of the art. Earth-Sci

Rev 203

Fan XM, Rossiter DG, van Westen CJ, Xu Q, Gorum T (2014) Empirical prediction of coseismic landslide dam formation. Earth Surf Proc Land 39(14):1913–1926

Fan X, van Westen CJ, Xu Q, Gorum T, Dai F (2012) Analysis of landslide dams induced by the 2008 Wenchuan earthquake. J Asian Earth Sci 57:25-37

Fan X, Xu Q, van Westen CJ, Huang R, Tang R (2017) Characteristics and classification of landslide dams associated with the 2008 Wenchuan earthquake. Geoenviron Disasters 4(1):1-15

Finnegan NJ, Roe G, Montgomery DR, Hallet B (2005) Controls on the channel width of rivers: Implications for modeling fluvial incision of bedrock, Geology 33:229–232

Flint JJ (1974) Stream gradient as a function of order, magnitude, and discharge, Water Resour Res 10:969–973

Frasson RPD, Pavelsky TM, Fonstad MA, Durand MT, Allen GH, Schumann G, Lion C, Beighley RE, Yang X (2019) Global relationships between river width, slope, catchment area, meander wavelength, sinuosity, and discharge. Geophys Res Lett 46(6):3252–3262

Froude MJ, Petley DN (2018) Global fatal landslide occurrence from 2004 to 2016. Nat Hazards Earth Syst Sci 18(8):2161-2181

Hack JT (1957) Studies of longitudinal stream profiles in Virginia and Maryland, in: vol. 294, US Government Printing Office, Washington, DC.

Hermanns RL, Folguera A, Penna I, Fauqué L, Niedermann S (2011) Landslide dams in the Central Andes of Argentina (northern Patagonia and the Argentine northwest), In: Evans SG, Hermanns RL, Strom A, Scarascia-Mugnozza G(eds), Natural and artificial rockslide dams. Springer, pp147-176

Li W, Zhao B, Xu Q, Scaringi G, Lu H, Huang R. (2022) More frequent glacier-rock avalanches in Sedongpu gully are blocking the Yarlung Zangbo River in eastern Tibet. Landslides. 1:1-13

Liao HM, Yang XG, Tao J, Zhou JW (2019) Experimental study on the river blockage

and landslide dam formation induced by rock slides. Eng Geol 261:105269

Liu W, Carling PA, Hu K, Wang H, Zhou Z, Zhou L, Liu D, Lai Z, Zhang X. (2019) Outburst floods in China: A review. Earth Sci Rev 197:102895

Kellerer-pirklbauer A, Lieb GK, Avian M, Carrivick J. (2012) Climate change and rock fall events in high mountain areas: Numerous and extensive rock falls in 2007 at Mittlerer Burgstall, Central Austria. Geogr Ann Ser A Phys Geogr. 94(1):59-78.

Korup O, Görüm T, Hayakawa Y. (2012) Without power? Landslide inventories in the face of climate change. Earth Surf Processes Landforms. 37(1):92-99

May C, Roering J, Eaton LS, Burnett KM (2013) Controls on valley width in mountainous landscapes: The role of landsliding and implications for salmonid habitat. Geology 41:503–506

Mizuyama T, Mori T, Sakaguchi T, Inoue K. (2011) Landslide dams and countermeasure method in Japan, Kokon Shoin, (in Japanese).

Nian TK, Wu H, Li DY, Zhao W, Takara K, Zheng DF (2020) Experimental investigation on the formation process of landslide dams and a criterion of river blockage. Landslides 17:2547-2562

Oppikofer T, Hermanns RL, Jakobsen VU, Böhme M, Nicolet P, Penna I (2020) Semi-empirical prediction of dam height and stability of dams formed by rock slope failures in Norway. Nat Hazards Earth Syst Sci 20(11):3179-3196

Petley D (2012) Global patterns of loss of life from landslides. Geology 40(10):927-930

Schneider H, Höfer D, Irmler R, Daut G, Mäusbacher R. (2010) Correlation between climate, man and debris flow events—a palynological approach. Geomorphology. 120(1-2):48-55.

Schuster RL (1986) Landslide dams: processes, risk, and mitigation. Proceedings of a Session in Conjunction with the ASCE Convention, American Society of Civil Engineers (ASCE)

Sekiya S, Kikuchi Y (1889) The eruption of Bandai-san. Journal of College of Science,

Imperial University. Japan 111part II 91-172

Strom A, Abdrakhmatov K (2018). Rockslides and Rock Avalanches of Central Asia - Distribution, Morphology, and Internal Structure. Elsevier

Struble WT, Roering JJ, Burns WJ, Calhoun NC, Wetherell LR, Black BA (2021) The Preservation of Climate-Driven Landslide Dams in Western Oregon. J Geophys Res.: Earth Surf 126(4): e2020JF005908.

Tacconi Stefanelli C, Segoni S, Casagli N, Catani F (2016) Geomorphic indexing of landslide dams evolution. Eng Geol. 208:1-10

Tacconi Stefanelli C, Catani F, Casagli N. (2015) Geomorphological investigations on landslide dams. Geoenviron Disasters. 2(1):1-15

Tacconi Stefanelli C, Vilímek V, Emmer A, Catani F (2018) Morphological analysis and features of the landslide dams in the Cordillera Blanca, Peru. Landslides 15(3):507–521

Tanyaş H, van Westen CJ, Allstadt KE, Anna Nowicki Jessee M, Görüm T, Jibson RW, Godt JW, Sato HP, Schmitt RG, Marc O, Hovius N. (2017) Presentation and analysis of a worldwide database of earthquake-induced landslide inventories. J Geophys Res: Earth Surf. 122(10):1991-2015

Tapia Baldis C, Trombotto Liaudat D. (2019) Rockslides and rock avalanches in the Central Andes of Argentina and their possible association with permafrost degradation. Permafrost and Periglacial Processes. 30(4):330-347.

Zhang L, Peng M, Chang D, Xu Y (2016). Database of 1044 Cases of Failures of Landslide Dams, John Wiley & Sons

Chapter 3. A New Global Landslide Dam Database (RAGLAD) and Analysis Utilizing Auxiliary Global Fluvial Datasets

To address the current data and understanding knowledge gap in landslide dam inventories related to geomorphological parameters, a new global-scale landslide dam dataset named River Augmented Global Landslide Dams (RAGLAD) was created. RAGLAD is a collection of landslide dam records from multiple data sources published in various languages and many of these records we have been able to precisely geolocate. In total 779 landslide dam records were compiled from 34 countries/regions. The spatial distribution, time trend, triggers, and geomorphological characteristics of the landslides and catchments where landslide dams formed are summarised. The relationships between geomorphological characteristics for landslides that form river dams are discussed and compared with those of landslides more generally. Additionally, a potential threshold for landslide dam formation is proposed, based on the relationship of landslide volume to river width. Our findings from our analysis of the value of the use of additional fluvial datasets to augment the database parameters indicate that they can be applied as a reliable supplemental data source, when the landslide dam records were accurately and precisely geolocated, although location precision in smaller river catchment areas can result in some uncertainty at this scale. This newly collected and supplemented dataset will allow the analysis and development of new relationships between landslides located near rivers and their actual propensity to block those particular rivers based on their geomorphology. (Appendix A is the supplementary material for providing more details and data access related to this chapter.)

Keywords: Landslide dam, Global fluvial data, Global-scale, Database

3.1 Introduction

The damming of rivers due to landslides and the following consequences pose great threats to people and facilities locally as well as in downstream areas. These landslide dams, which are effectively a subset of landslides that happen to block rivers, are reported in many areas around the world, almost exclusively in mountainous areas (e.g., Costa and Schuster 1988; Fan et al. 2020). The landslide dam (LDam) is an event

that forms when the mass of a landslide or multiple landslides from the adjacent hillslopes, partially, or completely blocks the normal fluvial channels (e.g., Costa and Schuster 1988; George et al. 2019). Hundreds of LDams have occurred among the thousands of landslides generated in each triggering event, such as from earthquake or intense rainfall (e.g., Fan et al. 2012). Additionally, the economic and life loss of global LDam can accumulate into a considerable amount, as each event can cause the loss of millions of US dollars and many casualties (Dai et al. 2005; Tacconi Stefanelli et al. 2016; Fan et al. 2017). Moreover, LDams play an important role as an interface connecting hillslope and fluvial channel systems in geomorphology (e.g., Korup 2002).

The primary consequence of LDams is the subsequent flood hazard resulting from the formation of a LDam. The potential impacts of LDams on ongoing floods can be divided into two parts: (1) upstream consequences, backwater floods, induced by rise of water level in the upstream area at the point of the LDam; (2) downstream consequences, downstream floods, mostly caused by the LDam failure, either by overtopping or breaching within short timescales (hours to days) (Zhang et al. 2016), depending on their dam material components (volume, texture, angle of repose, sorting), rates of seepage through the dam, and rates of LDam lake input and outflow (Costa and Schuster 1988; Korup 2004; Tacconi Stefanelli et al. 2018). In contrast to river flooding, which normally occurs after intense or prolonged precipitation or increasing snowmelt, the floods caused by LDam failures are more complicated to predict due to the rapid water release from the impounded lake when the dam fails, and the complexity of the LDam stability. The flowrate of dam-breach floods can increase river flows to many times typical flood flows experienced in a river system and can even reach a rate much larger than the flowrates of recorded flash floods (Perucca and Angillieri 2009). The impacts of dam-breach flooding can extend to broad areas since the distances of dam-breach floods can vary from 1 to more than 1000 km (Geertsema 2008; Evans et al. 2011; Macias et al. 2004). The flood wave generated when the landslide debris enters the fluvial channel can have a significant impact, such as a water level tens of meters above the mean water level (Wang et al. 2004), or a large peak discharge flood wave (e.g., 5900 m^3/s reported by Dunning et al. 2006). These can have the potential to kill thousands of people in the downstream areas (Barla and Paronuzzi 2013).

The typical approach to study LDams currently is to establish a dataset of case studies and undertake analyses of the hazard prone conditions of LDam formation from the empirical relationships using geomorphological parameters from the LDam and geomorphological records (e.g., Fan et al. 2012; Tacconi Stefanelli et al. 2016, 2018). The physical processes are very hard to capture accurately due to the lack of observational data. The formation of LDams is difficult to forecast, which makes systematic monitoring difficult. Even though LDam events are not uncommon, the records and datasets for this specific hazard are relatively sparse compared with its frequency of occurrence, especially on a global scale. The establishment of local, regional, or global LDam datasets has begun in earnest in the last few decades by collecting records from literature, field investigations, or remote sensing data (e.g., Costa and Schuster 1991; Fan et al. 2012, 2020; Tacconi Stefanelli et al. 2016, 2018; Zhang et al. 2016). These previous studies have explored and proposed frameworks for data fields to be recorded in the LDam datasets, which are easy to use and update, even for non-experts, and have discussed LDam classifications, processes, origins, distributions, and stability on both a regional and global scale. Most of the records collected in these datasets were triggered by single events, mainly earthquakes (e.g., the 2008 Sichuan earthquake). These events result in a more comprehensive area coverage and data accessibility than single a LDam that may occur due an isolated landslide. There are some studies on the formation, stability, and short-term impacts of LDam that use these datasets (Ermini and Casagli 2003; Korup 2002; Fan et al. 2014), and most of them focus on studying the geomorphologic features of hillslopes, landslides, and the LDams.

However, the systematic understanding of the quantitative relationships between LDam formation and related geomorphological parameters on the global scale are still unclear due to the limited accessibility of valid records and parameters and the large variety of the local conditions. Most global LDam formation studies rely on descriptive analysis of case studies or quantitative relationships based on regional LDam studies or global landslide studies (Larsen et al. 2010; Tacconi Stefanelli et al. 2016, 2018). In previous LDam datasets, some of the geomorphological parameters of the landslides and blocked river valley came from empirical statistical relationships based on hydrological, geomorphological, or landslide studies (Evans et al. 2011), while others came from

records or other accessible data sources (Tacconi Stefanelli et al. 2016, 2018; Fan et al. 2020).

To fill these gaps, in this paper, we develop a new global scale dataset of LDams, abbreviated as RAGLAD (River Augmented Global Landslide Dams), using a united spatial reference system and measurement units to allow a better understanding of the spatial distribution and characteristics of LDams and geomorphological conditions that might affect their formation on the global scale in relation to fluvial information. The records are collated from a wide range of data sources in multiple languages and geolocated with precise and accurate spatial information, where possible. The parameters of these records are then extended by linking the locations with recently available global fluvial datasets. This study is the first time that the combination of landslide databases with fluvial datasets has been presented. RAGLAD focusses on a global scale and allows us to explore and better understand the spatial distribution and geomorphological characteristics of LDams. For example, the relationships between geomorphological parameters, such as landslide volume and river width, are developed to explore the connection between geomorphological parameters and further reveal potential parameter thresholds for LDam formation from a global perspective.

3.2 Methods

3.2.1 Global Landslide Dam Record Collection

For a more comprehensive coverage in this dataset, the records in RAGLAD were collected from a wide range of sources: academic journal articles, government and institution reports, social media,and other available datasets in multiple languages (for more details, please see the supplementary materials in Appendix A1 and A3). The languages that were used most systematically for searching for relevant records were English, Chinese, and Japanese, although other languages related to the location of collected LDam records were also used, where available. A particularly careful focus of our data collection was in developing countries, where there was a distinct lack of records in previous studies. The measurement of geomorphological data is obtained directly from publications or extracted from published figures. An added difficulty is that current LDam records may include several events in one record. In order to create a unique LDam record

for a particular location, where a LDam reference consists of multiple separate events and contain information that comes from different data sources, we need to precisely geolocated each LDam when its approximate location is available. During data entry, when conflicting data from various sources is presented for one record, data from field investigations and those records reported most recently to the LDam formation time are prioritized. We focused on more recent LDam events (in the last 1000 years) due to the sparsity of records and data from times before this, and because the reliability of the data is much less clear.

Previous LDam databases consist of similar geomorphologic parameters to landslides records, as well as parameters related to the LDam body, river valley and fluvial channel, impounded lakes, and the general information of LDam events which were helpful in building our database and locating original sources of information (Costa and Schuster 1991; Fan et al. 2012, 2020; Tacconi Stefanelli et al. 2016, 2018; Zhang et al. 2016; Zheng et al. 2021). The records in RAGLAD dataset contain information on the spatial and temporal information from dam formation to dam breach, dam materials, geomorphological characteristics, and dimension data of upstream catchments at the point of blockage, landslides and impounded lakes, and hydrographic characteristics of subsequent flood events and their consequences, including casualties and economic losses, as shown in Table 3-1. For a better understanding of the relationships between landslide types and the geomorphological characteristics of LDam formation, we applied the landslide definitions established by Hungr et al. (2014), including fall, topple, slide, spread, and flow, to recategorize the original landslide types from LDam record. Some descriptive and supplement information of the LDam events is also included to allow easier updating of the spatial location and geomorphological parameters in the future, if necessary.

On the global scale, 84% of valley blockage resulting from LDams were reported as being caused by rainfall and earthquakes (Schuster and Costa 1986). Similar results can be also found in the study by Zheng et al. (2021) with 50.4% cases induced by earthquakes and 39.3% by rainfall. Considering the triggering mechanism of landslides with large volume, the result is slightly different as 44.4% landslides were caused by rainfall, and 20.5% caused by earthquakes (Fan et al. 2020), so a smaller percentage. At

that scale, localized effects that are also important cannot be considered. However, on a local scale, the fluvial erosion of channel beds/banks and erosion processes that change the condition of hillslopes are known to influence the hillslope stability (Golly et al. 2017). Based on RAGLAD, triggering processes of landslides that have formed dams can be summarized into three major categories: (1) meteorological triggering processes, including meteorological events, such as storm, snowmelt, and intense precipitation, and the alternation of the seasons, when the temperature and humidity change sufficiently; (2) geological precondition and triggering processes, including the geological background that is prone to LDam occurrences, such as layers and lithological characteristic of the bedrocks on the hillslopes and long-term tectonic movement, infiltration towards potential or current landslide bodies that could alter the shear strengths of surface materials and induce potential landslides, and geological hazards such as earthquake, volcano eruption, and landslide reactivation; and (3) geomorphological triggering processes, such as the fluvial geomorphology changes caused by fluvial erosion processes at the base of a hillslope, alluviation, or flood hazards.

Table 3-1 The information field of LDam records (for more details, check with supplemental materials).

Criteria	Information/Parameters	Format	Unit/Category	Description
Basic information and location	ID	Number	-	The unique recording index of events in this dataset
	Name	Text	-	The local name of LDam in English
	Name in the original language	Text	-	The local name of LDam in their original language
	y	Number	-	Location - Latitude (WGS1984)
	x	Number	-	Location - Longitude (WGS1984)
	Location	Text	-	Location description of where the LDam event occurred
	Country/Region	Text	-	Country or region of origin
Time	Formed time	Time/Text	yyyy/mm/dd	Time of formation

Criteria	Information/Parameters	Format	Unit/Category	Description
	Dam failure time	Text	-	Time of Dam collapse
	LDam status	Text	Failed/Existing/Unknown	Status of LDam
	Failure mechanism	Text	-	Mechanism of dam collapse if known.
	Overflow/flood Time	Time	-	Time of collapse or overtopping of an existing dam which causes subsequent flood
	Duration from formation to flood (lake life)	Text	-	The time from dam formation to failure or time when the impounded lake disappeared
Catchment	Drainage area	Number	km^2	The upstream drainage area of the river channel at point of the LDam
	River width	Number	m	The width of the river channel where the LDam occurred
Landslide	Landslide Subcategories	Text	-	Landslide classification in original pieces of literature
	Type of movement	Text	Uncategorised/ slide/fall/flow/ topple/complex	Landslide movement categories (Hungr et al. 2014)
	Landslide area	Number	m^2	The surface area of the landslide
	Landslide-elevation difference	Number	m	The elevation difference between the crown and toe of the landslide
	Landslide length	Number	m	The main body length of the landslide that formed the dam
	H/L Ratio	Number	-	The ratio of landslide height divided by length for measuring the mobility of landslides debris (Iverson et al. 1997)
	Landslide volume	Number	10^6 m^3	The volume of

Criteria	Information/Parameters	Format	Unit/Category	Description
				landslide that forms the LDam
LDam	LDam-type	Text	-	Classification of LDam (Costa and Schuster 1988)
	Dam materials	Text	-	Grain size and lithology of LDam materials
	Reported cause	Text	-	Landslide triggering processes described in original works of literature
	Interpreted cause	Text	Meteorological/ geological / hydrographical triggering processes (with detailed categories)	Categories of landslide triggering processes summarised in this study
	Dam height	Number	m	Height of Landslide deposit forming the dam
	Dam length	Number	m	Length of LDam (across the valley)
	Dam width	Number	m	Width of LDam (along the valley)
Impounded lake	Impounded lake length	Number	km	Length of an impounded lake dammed by a landslide
	Impounded lake volume	Number	10^6 m^3	The volume of an impounded lake dammed by a landslide
Subsequent flood	Mean flow velocity	Number	m^3/s	Mean flow velocity of river under normal flow conditions
	Peak flow velocity	Number	m^3/s	The peak flow velocity of flood related to LDam formation and failure processes
Consequence	Casualties	Text	-	Number of deaths/injuries
	Economic loss	Text	-	Economic losses including properties and infrastructure
References	-	Text	-	References used for recording LDam

Criteria	Information/Parameters	Format	Unit/Category	Description
				events (Sources of information)
More details	-	Text	-	Related details that were not mentioned above

3.2.2 Geolocating LDam records

The precise and accurate spatial location of LDam records is crucial for further geospatial or geomorphological analysis and to allow linking of parameters from other data sources (Fan et al. 2020). However, most of the spatial information in the records in current global datasets was recorded as approximate location descriptions, without precise spatial coordinates. Hence, these datasets cannot be used to link records with other geolocated data. There are three key challenges in recording the precise spatial coordinates of records: (1) LDam can form and fail in a very short time and thus its precise location can escape being recorded; (2) older LDam events were not recorded with very precise locations because the locations were derived from the geomorphological or sedimentary relics, which may not be clearly presented in modern terrain (Tacconi Stefanelli et al. 2016); and (3) collating data recorded in different data formats, inconsistent units with vague and patchy spatial information impedes the process of assigning precise coordinates and can result in the imprecision of spatial information.

In this study, the records were geolocated individually by georeferencing, projection transformation, or based on the geomorphological information and location description provided in the original data sources. To improve the spatial precision of the records, we visually scanned the target area using Google Earth to find the geomorphological signature of the landslides that had created the dams. These signatures include landslide scarps, the extreme colour differences on the ground caused by surface vegetation changes or the loss of soil cover, hazard mitigation infrastructures, and existing LDam bodies and impounded lakes, and then matched the approximate location with the description and images reported on social media or local reports to pin down the precise spatial location of LDam records (for more details, check with Appendix A2).

3.2.3 Appending the Data from the Global Fluvial Dataset to Landslide Dam Records

Even though the number of LDam records increased during the past decades, some of the data, especially the geomorphological data, such as river width and drainage area at the point of the LDam, is not valid in every information field for each record. The LDam body and its deposits may be removed by erosion, in some cases even within a few hours after its formation and thus sometimes it is impossible to record their dimension by field investigations. When most records are geolocated, linking accessible parameters from other data sources by spatial proximity becomes possible. This allows us to complete some records that lack valid data on the fluvial system parameters, such as upstream drainage area and river width. In parallel, with the development of digital elevation models (DEM) in recent decades, the geomorphological parameters can be easily obtained. Therefore, linking the geomorphological data from the validated global fluvial dataset can be a valuable approach.

Global fluvial datasets (GFDs) have made significant progress in recent decades. Lehner et al. (2006) released HydroSHEDS (Hydrological data and maps based on SHuttle Elevation Derivatives at multiple Scales) derived primarily from elevation data from the Shuttle Radar Topography Mission (SRTM) at the spatial resolution ranging from 3 arc-second (~ 90 m) to 5 min (~ 10 km). Yamazaki et al. (2014) developed a new global river width database to provide fluvial data sources with global coverage for data supplemented with river widths. Allen and Pavelsky (2018) completed the first global compilation of river planform geometry based on the Landsat images. Linke et al. (2019) published the HydroATLAS database providing the descriptive hydro-environmental information for worldwide watersheds and rivers at 15 arc-second (~ 500 m) resolution. In the same year, the first global dataset including mean annual flow, river width, slope, meander wavelength, sinuosity, and catchment area was created from river centrelines derived from Landsat images and Shuttle Radar Topography Mission DEM (Frasson et al. 2019). Yamazaki et al. (2019) published MERIT Hydro, a new global flow direction map at the resolution of 3 arc-second (90 m) derived from the latest elevation and waterbody data. Among all these GFDs, we selected the raster-based MERIT Hydro dataset for data assembling of drainage area and river width data because it reduced the

vegetation biases from the elevations of satellite-derived DEMs, which can lead to an imprecise water body representation in forest areas, and includes the correction of many other DEM errors (Yamazaki et al. 2019). The global empirical relationship between river width (W) and drainage area (A) achieved from the study of Frasson et al. (2019) was also selected for calculating the river width for further comparison (Eq. 3-1), because the MERIT Hydro does not cover all the smaller catchments. We compare the fluvial data from original records with that derived from GFDs by retaining the data from original records and appending all the valid data from the GFDs to evaluate the assembled performance of these different sources.

$$W = 9.68A^{0.32} \quad \text{(Eq. 3-1)}$$

3.3 Results

3.3.1 Observed Trends in the Landslide Dam Database

In total, 779 LDam records were compiled from 34 countries/regions. The locations of the records are clustered in the mountainous areas around the world, especially in the areas including European Alps (Tacconi Stefanelli et al. 2016), Rocky Mountains (Costa and Schuster 1988; Clague and Evans 1994), Andes Mountains (Hermanns et al. 2011; Tacconi Stefanelli et al. 2018), Pamir Mountains (Storm 2010), Himalayas (Evans et al. 2011), the eastern edge of Tibet Plateau (Yin et al. 2009; Xu et al. 2009; Fan et al. 2012), and some mountainous areas on islands (Nash et al. 2008) (Figure 3-1). In terms of spatial information of the new database, 85% of the records (666 out of 779 records) contain location information with a precision of approximately 0.01 degree (~ 1 km) and 583 records (~ 75%) have a precision better than or equal to 0.001 degree (~ 100 m) after geolocating processes. The influence of geolocating in the data completeness is shown in Table 3-2 (for all parameters, see more details in Appendix A4). The diversity of data availability in different countries due to funding, expertise availability, and disaster management policies strongly affects the spatial data distribution. For instance, most of the current LDams are recorded in developed countries, such as the USA, Canada, Italy, and Japan, and some developing countries with plenty of researchers in this study topic (e.g., China and Argentina).

Table 3- 2 Data entry completeness of specific critical parameters. Bold values are improvements after geolocating and adding Global Fluvial Datasets.

Parameters	Completeness	Completeness after geolocating and adding GFD
Name	47.1%	47.1%
y(latitude)	68.1%	**85.5%**
x(longitude)	68.1%	**85.5%**
Country/region	100%	100%
Location (text)	89.6%	89.6%
Formation time	90.2%	90.2%
Type of landslide movement	76.7%	76.7%
Drainage area	71.7%	**85.5%**
River width	38.3%	**85.5%**
Landslide area	39.0%	39.0%
H/L Ratio	51.0%	51.0%
Landslide volume	70.3%	70.3%

The recorded date of LDam formation shows a clear increasing trend in the number of records during the past 1000 years, with the highest number in the last 20 years (Figure 3-2). This increase is probably due to the greater amount of landslide research and the growing interdisciplinary interest in multi-hazard research, particularly in mountainous areas, rather than an actual increase in events. LDams that occurred in the past may have only been recorded occasionally, and this leads to the under-representation of LDam numbers in the past (Tacconi Stefanelli et al. 2016). Extreme hazard events such as the 1783 Calabria earthquake in Italy, the 1889 Totsugawa Flood in Japan, the 2008 Sichuan earthquake in China, and Typhoon Morakot in 2008 have contributed to the notable peaks in the LDam formation time trends.

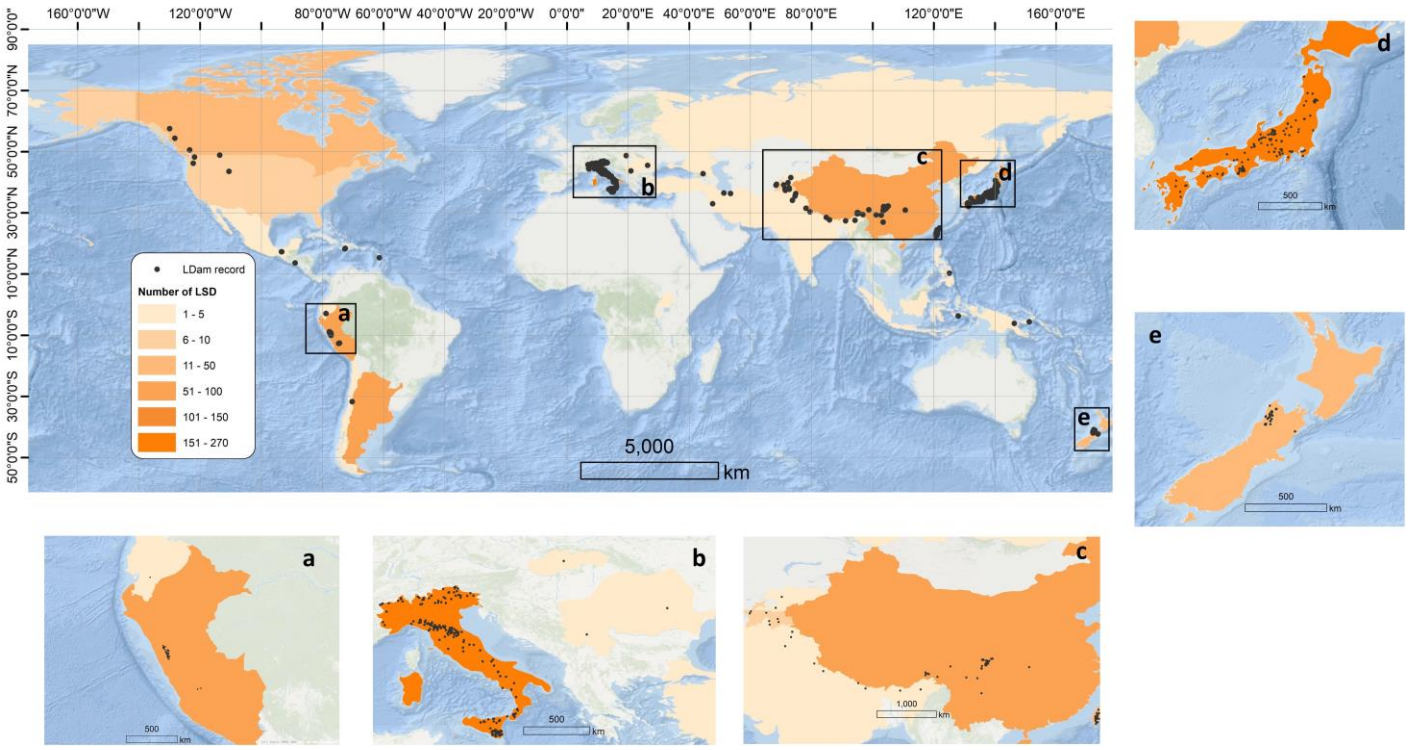

Figure 3-1 Spatial distribution of LDam records with precise geospatial locations in RAGLAD (a. Peru; b. Italy and southern Europe; c. Himalaya areas; d. Japan; e. New Zealand)

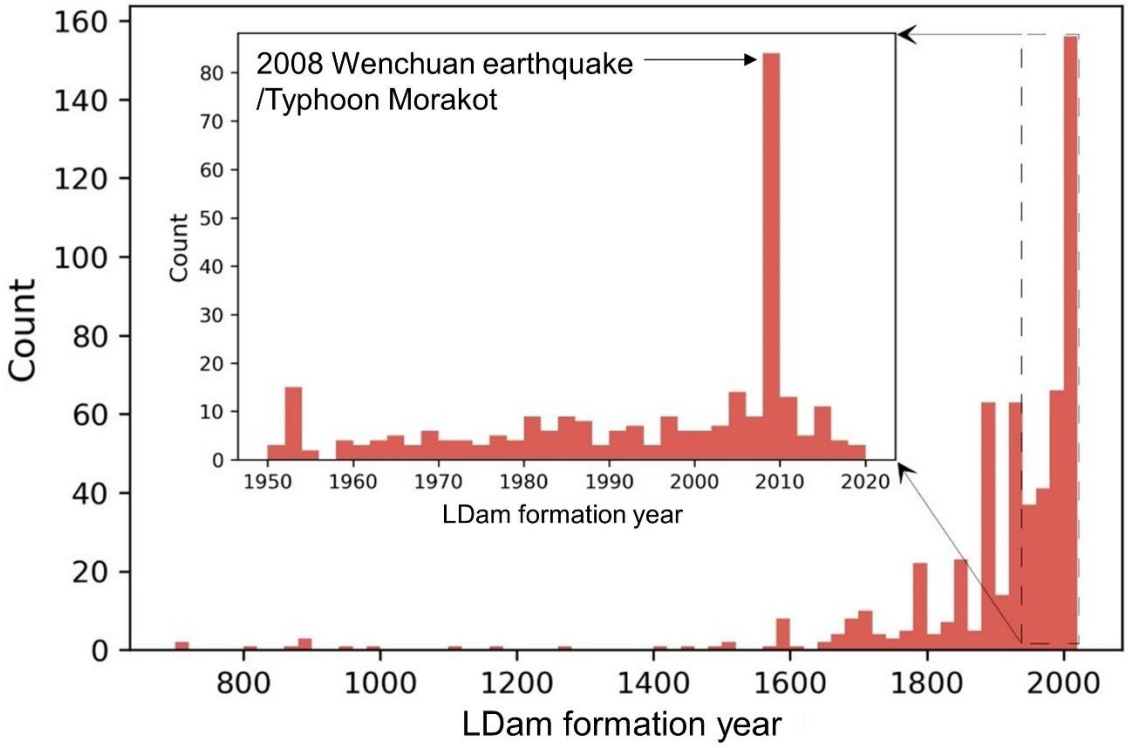

Figure 3-2 Formation time trend of LDam event, inset shows the last 70 years in more

detail

3.3.2 Landslide Dam Triggering Processes

The database records show that the LDams were triggered by multiple factors. Among the 506 LDams with the recorded categories of landslide triggering processes (Figure 3-3), 314 were induced by extreme geological events, 151 were triggered by weather events, and 65 were directly caused by fluvial landform system changes. It must be noted that a single LDam record may have more than one triggering factor. The results indicate that the triggering processes of geology and meteorology dominantly control the formation of LDam around the world as 62% of LDam s are induced by geological triggers, 30% of LDam records caused by meteorological triggers, and 13% LDams are caused by geomorphological triggers. This finding is similar to that by Schuster and Costa (1986), who that found more than 84% of global natural dams were triggered by factors related to earthquakes and precipitation and Zheng et al. (2021) with 50.4% of landslide triggered by earthquakes and 39.3% induced by rainfall. A slight difference can be found for long run-out distance landslides according to Fan et al. (2020), who found that 20.5% of landslides were triggered by earthquakes and 44.4% were induced by rainfall. However, it is not clear that the LDam triggering processes result is due to the actual hazard occurrence or some of these triggers happen to attract more research attention. Additionally, these triggering processes can place a strong bias on the dataset by producing a lot of landslides and landslide dams at once.

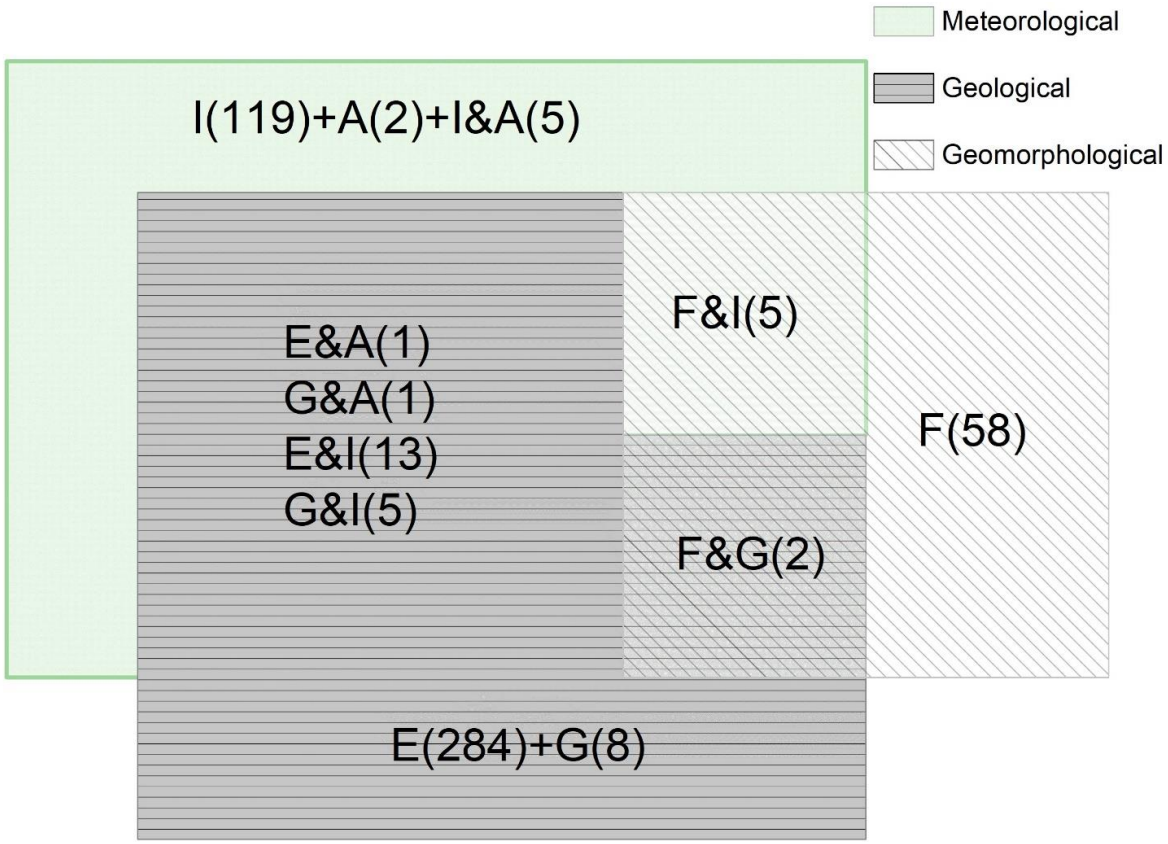

Figure 3-3 Venn diagram of landslide triggering processes categories (A: Alternation of season; I: Instant weather event; E: Extreme geological hazard; G: Geological background; number followed the categories is the number of records with specified landslide triggering processes categories)

3.3.3 Geomorphological Characteristics of Landslide Dam Records

As observational data of the LDam formation processes in action are rarely available, summarizing the geomorphological characteristics of upstream catchments, and the landslides from records can be helpful when considering the geomorphological conditions prone to LDam formation. We consider here the 4 geomorphological characteristics of LDams in the RAGLAD database, including drainage area (at the point of LDam), river width (at the point of LDam), the ratio of the landslide drop height to landslide runout distance (H/L ratio), and landslide volume (Figure 3-4), which can include the geomorphological conditions from the blocked river channel and its triggered landslide from the adjacent hillslopes. This allows us to study two specific factors: (1) where LDams occur along the course of a river, and (2) what kind of landslides are likely

to dam a river.

Based on the geomorphological data of the blocked river channel, the LDam records occurred more frequently in the upstream areas of river systems where the slopes tend to be steeper and therefore, more likely to fail. The geomorphological characteristics of the drainage area at the point of valley blockage shows an exponential distribution, with most records having a drainage area less than 500 km^2 (Figure 3-4(a)). Strahler stream order is used in river morphology as a measure of the stream network connectivity. The most upstream reaches of a river are classed as order 1 and when these join another stream of order 1, then the reach becomes an order of 2, and this continues downstream with ever increasing stream orders (Geological Survey 1965). The range of stream orders for the records vary from 1^{st} to 5^{th} order. This large number of low stream orders, as well as the smaller catchment areas, confirms that LDams usually occur in upper river catchment areas. The data distribution of river width suggests that the LDam is more likely to occur in smaller rivers from the range of 0 to 300 m width, as expected, which is similar to the result shown for the drainage area distribution (Figure 3-4(b)).

The geomorphological data distributions of landslide dimension parameters indicate that a larger volume and longer run-out distance of a landslide can contribute to the LDam formation prone conditions. However, the condition depends on specific landslide types and LDam locations. The H/L ratio is a popular parameter for measuring the mobility of a landslide, even though it is still under discussion within long-runout landslide literature (Iverson 1997; Legros 2002; Shanmugam and Wang 2015), and its mechanical meaningfulness as a description of friction has been refuted several times (Hsü 1975; Davies 1982; Dufresne and Geertsema 2020). The result of the landslide H/L ratio shows a Weibull distribution with most H/L ratios concentrated in the range from 0.12 to 0.6 and this indicates the contribution of relatively long run-out landslides to LDam formation. Typical landslides have a H/L ratio smaller than 0.5, with some well-studied examples reaching a value of 0.1 to 0.2 (Iverson 2015); this work on debris flows demonstrates that the run-out distance can be considerable. For example, the debris flows, debris avalanches, and rock slides in west central British Columbia have an H/L value between 0.1 and 0.5 (Geertsema et al. 2009). Scheidegger (1973) described a general trend of a reducing H/L ratio with an increase in volume and suggested that some

obstructed mudslides and earth flows will have a lower H/L ratio than other landslides. The fact that the majority of landslide movement types that formed LDams include slide (> 28%), complex (> 24%), and flow (19%) can affect this data distribution because the H/L ratio is highly influenced by the landslide type.

The data distribution of landslide volume from landslides that block the valley reveals an exponential distribution, with 68% data concentrated in a volume of less than 10 million cubic meters. Among all the data, it is interesting to note that for more than 17% of LDam records (132 out of 779 records), landslides with a small volume (< 1 million m^3, as a volume threshold of long run-out rock avalanches/slides defined and applied by Glastonbury and Fell 2008; Evans et al. 2011; Davies and McSaveney 2012; Robinson et al. 2015; Chunyuk et al. 2020; Fan et al. 2020) also plays an important role in contributing to the total amount of records.

The data distribution of landslide geomorphological characteristics could be the result of various reasons:

1) the proportion of larger landslides is relatively small in LDam studies. However, compared with those in general landslides studies, the landslides causing LDams with a volume larger than 1 million cubic meters account for a larger proportion of the total (75%). In the study of Guzzetti et al. (2009), the landslides with a large volume took up approximately 29% of 667 landslides in Umbria, central Italy. In the national scale landslide dataset of Slovenia, the large volume landslides account for approximately 0.4% of the total (Komac and Hribernik 2015);

2) the result is affected by both the river width and H/L ratio distribution result, because to block a larger river width requires a larger volume of landslide material, which may require a longer landslide runout distance from a lower H/L ratio. However, from previous studies, the increase in L/H (opposite to H/L ratio) with increasing volume of landslides was not observed for both small and large landslides (Roback et al. et al. 2018) and Okura et al. (2003) reported that there is no correlation between the volume and H/L ratio for shallow landslides under the volume of 10^3–10^4 m^3;

3) The result could be affected by landslide types and the actual volume of the

LDam blocking the river. For some landslide types, the volume that actually blocks the river is much smaller than the total landslide volume (~ 10% for the cases covered in Miller et al. 2018).

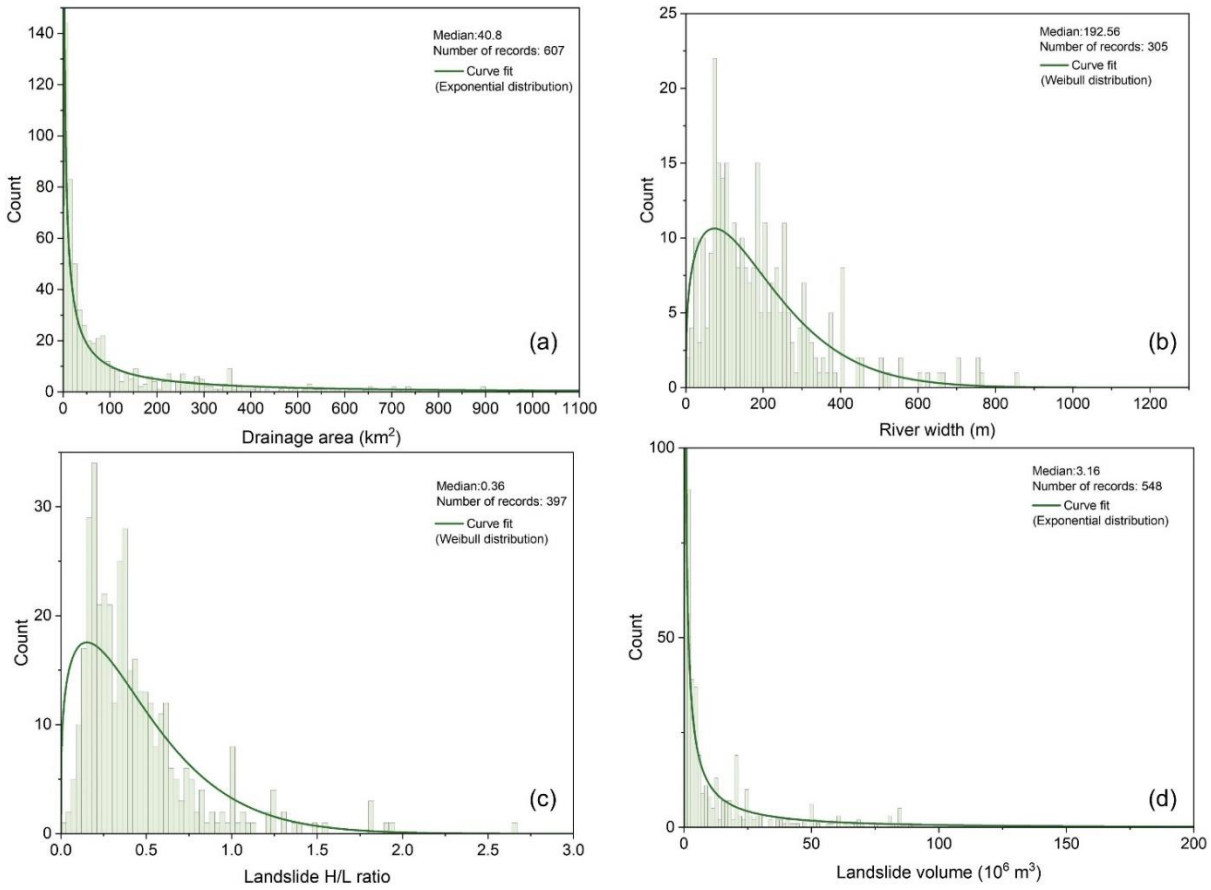

Figure 3-4 Data distribution of geomorphological parameters of LDam records: (a) drainage area; (b) river width; (c) landslide H/L ratio; (d) landslide volume.

3.3.4 Empirical Relationships Between Parameters

The relationship between landslide volume and landslide area, based on the LDam records collected in this research, is shown in Figure 3-5. As landslide type is a principal factor for determining the relationships between landslide runout and volume (Legros 2002), we have measured the relationships grouped by different landslide movement types. As shown in Eq. 3-2, the relationship between landslide area and volume is presented as a scaling relationship. Previous studies (Guzzetti et al. 2009; Larsen et al. 2010; Fan et al. 2012, 2014) have shown its applicability to a broad range of landslide types.

$$V = \alpha A^{\Upsilon} \qquad \text{(Eq. 3-2)}$$

where V is the landslide volume (m^3), α is the intercept, A is the landslide area (m^2), and ϒ is the scaling exponent. A previous study by Larsen et al. (2010) established a global prediction equation of the exponential relationship between landslide volume and landslide area that was based on more than 4,000 landslides in both soil and rock types collected globally. The value of ϒ derived for landslides in soil is 1.1-1.3. For landslides which occurred in rock masses the range of values is 1.3-1.6. This relationship has been directly applied to both landslide and LDam studies on the regional scale for calculating landslide volumes (Fan et al. 2014; Tacconi Stefanelli et al. 2018). The smaller scaling exponent of landslides that dam the river, with a range from 0.66 to 0.97, indicates that these landslides typically have smaller volumes compared to landslides more generally (i.e. including those that do not cause LDams). This situation could be due to the erosion depth of landslides that dam rivers being shallower or having steeper slopes comparing with the general landslides. However, as the scaling exponent varied with slope materials in the V-A scaling exponent study in global landslides (Larsen et al. 2010), it is common to expect that most of the coefficients of determination (r^2) in these relationships are relatively low (<0.5) because of the vast combinations of landslide mass materials, patchy data sources, and different triggering mechanisms of landslides.

To determine whether a landslide can actually form a LDam, it is vital to know the empirical relationship between landslide volume and river width from current records. The empirical relationships within the geomorphological parameters, especially the relationships between landslide volume and area, were applied in establishing geomorphology indexes for evaluating the LDam formation probability and stability (Tacconi Stefanelli et al. 2018). The correlation between landslide volume and river width revealed similar relationships within the categorized landslides that formed the LDam, but the relationships are not clear, with a lot of data noise (Figure 3-6). LDam formation index from previous research, such as Morphological Obstruction Index (MOI), also applied the relationship between valley width and landslide volume (Tacconi Stefanelli et al. 2016). However, we have to point out that there is a difference between valley width

and river width. River (channel) width is based on the mean annual flow (Frasson et al. 2019), while the valley width derived from the valley morphology system rather than just the river, so valley width is always wider than river channel width. One of the reasons for the data noise may came from the uncertainties resulting from the original records. Nonetheless, although a correlation between landslide volume and river width is not possible, it still reveals a potential threshold for LDam formation (Figure 3-7). Only one outlier from the dataset in Italy (Tacconi Stefanelli et al. 2016) is above this threshold line, and it dammed a valley of 400 m width with 9000m^3 debris. No further information was found regarding this outlier. The threshold can be applied to explore the LDam formation prone areas where landslides can generate sufficient volume of mass to block the river: i.e. the minimum landslide volume that forms a LDam can be calculated from a given river width.

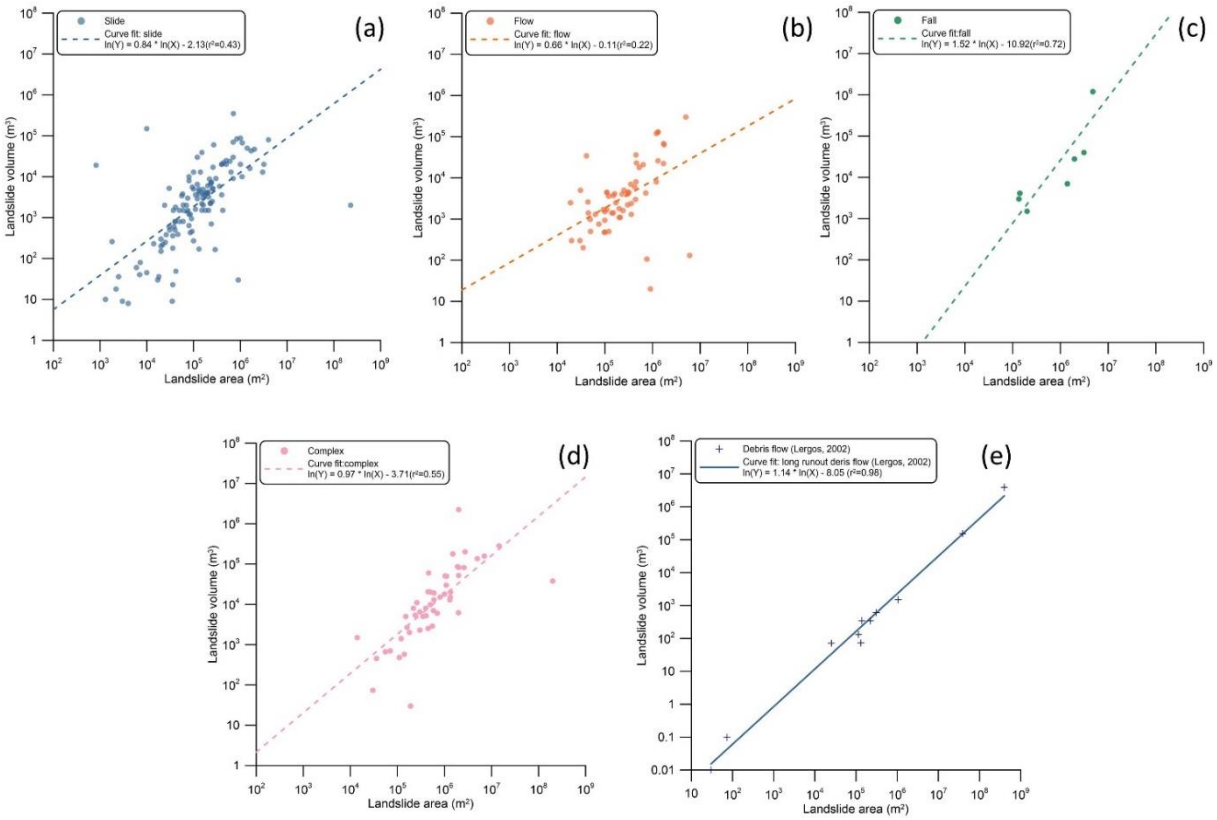

Figure 3-5 Correlation between landslide volume and landslide area for 260 records with valid data, categorised by landslide types: (a)Slide; (b) Flow; (c) Fall; (d) Complex; (e) Long run-out debris flow (Legros 2002).

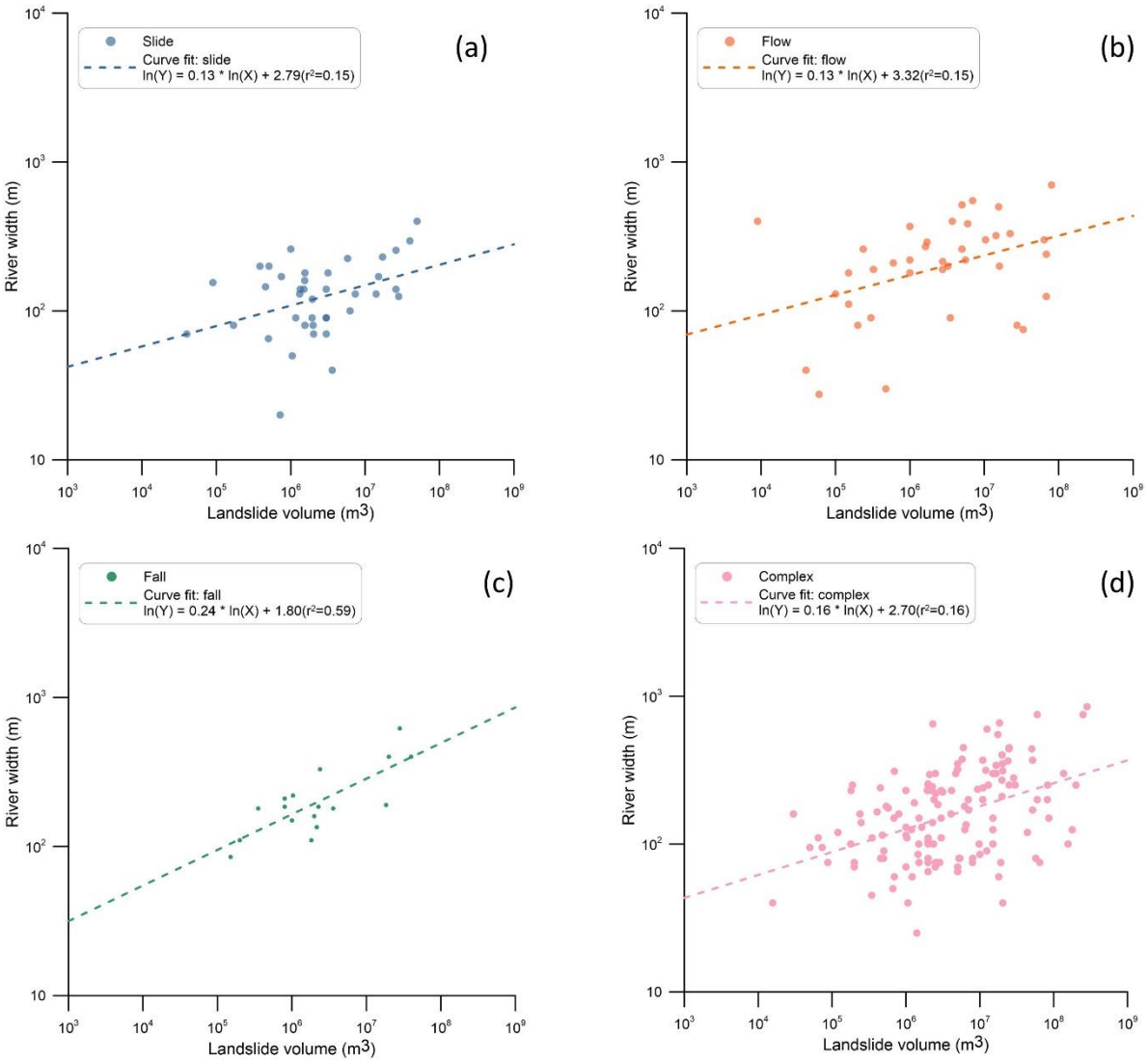

Figure 3-6 Correlation between landslide volume and river width (as defined in Table 3-1) for 250 records with valid data, categorised by landslide types: (a) Slide; (b) Flow; (c) Fall; (d) Complex.

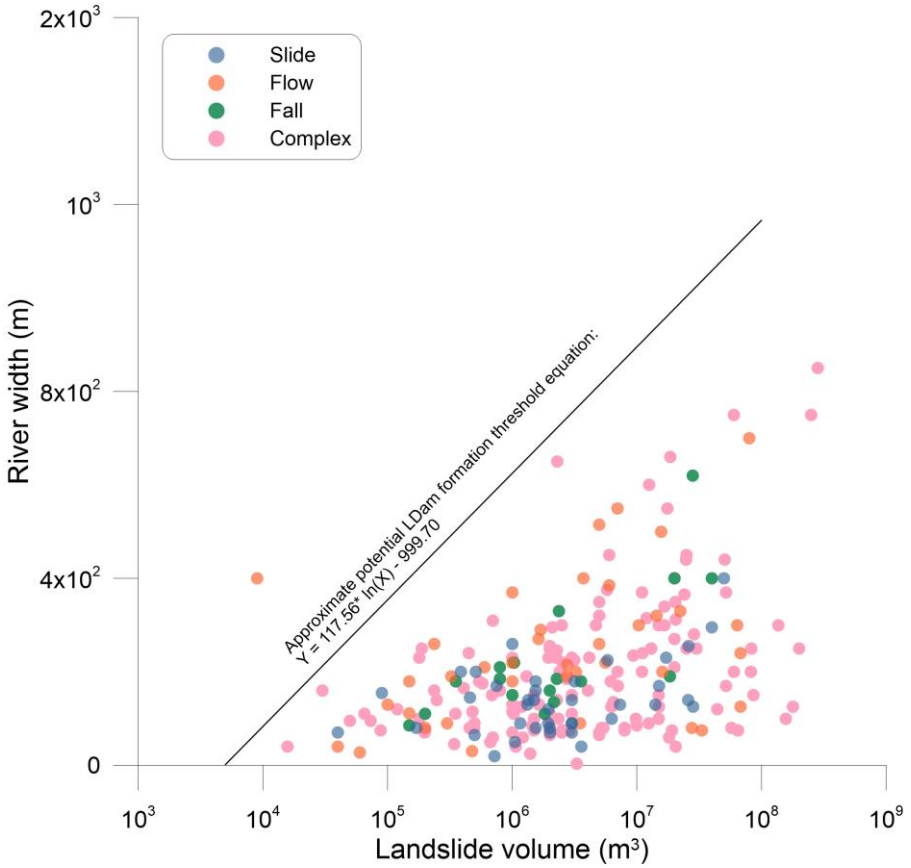

Figure 3-7 The potential threshold of LDam formation by the relationships of landslide volume and river width

3.3.5 Global Fluvial Datasets Parameter Results

The data distribution results of the drainage area when combined with the global fluvial datasets (GFD) reveals three similar Weibull data distributions of drainage area developed from: (1) the original LDam records only; (2) GFD data only; and (3) RAGLAD dataset combined with the GFD data (Figure 3-8). The drainage area data collected from the GFDs contain more values for the areas less than 20 km^2, which are lacking in the original LDam records. When zooming into these upstream catchments with smaller areas, we can also see the data gathered from GFD only shows as integer values (due to the GFD format) and this could lead to a larger data value difference and distribution in narrower rivers (drainage area < 20 km^2). In contrast to the very similar distributions for the drainage area, the distributions of river width from various data sources are more diverse (Figure 3-9). The data difference exists mainly in the rivers with

a width less than 50 metres, whose width data were mainly collected from the GFDs. Therefore, one of the most significant reasons for the difference between drainage area and river width is the amount of valid data between these 2 parameters; there are 627 records containing valid data on drainage area while there are only 303 records that have a valid river width values from the original records.

Both the data supplement of river width from the GFDs and the empirical relationship between river width and drainage area fill a significant data gap in the current LDam datasets, particularly in the range of river widths less than 100 metres (Figure 3-9). The data distribution is slightly different after data combination, but is still very similar, but with differences concentrated at the smaller river scales where there is the most difference in the data. The data gap between LDam records and GFDs is concentrated in small rivers and catchments, which also raises the need to improve the GFD performance in smaller catchments. We also compared the data extracted from different data sources in each record (Figure 3-10). For those LDam records with a valid river width value, the GFD data gathered from MERIT hydro performs better than river width data estimated by drainage area simply using the empirical relationship of drainage area and river width (Frasson et al. 2019).

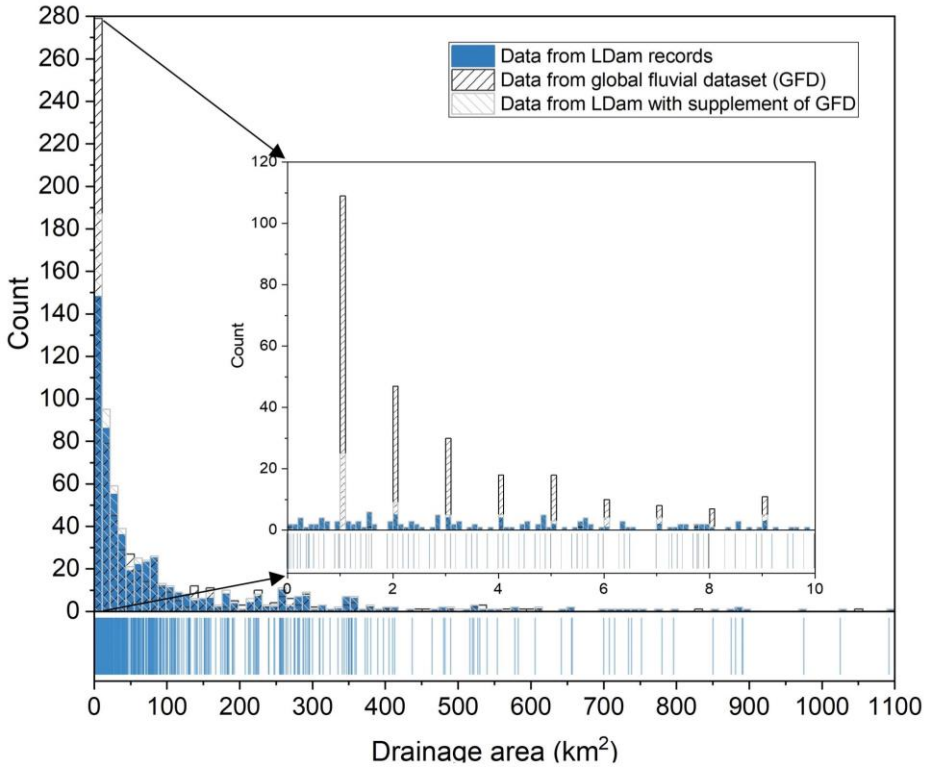

Figure 3-8 Data distribution of drainage area from RAGLAD, GFD, and RAGLAD with the supplement of the GFD (bin interval of 10), inset shows the data distribution in the first bar in more detail (bin interval of 1)

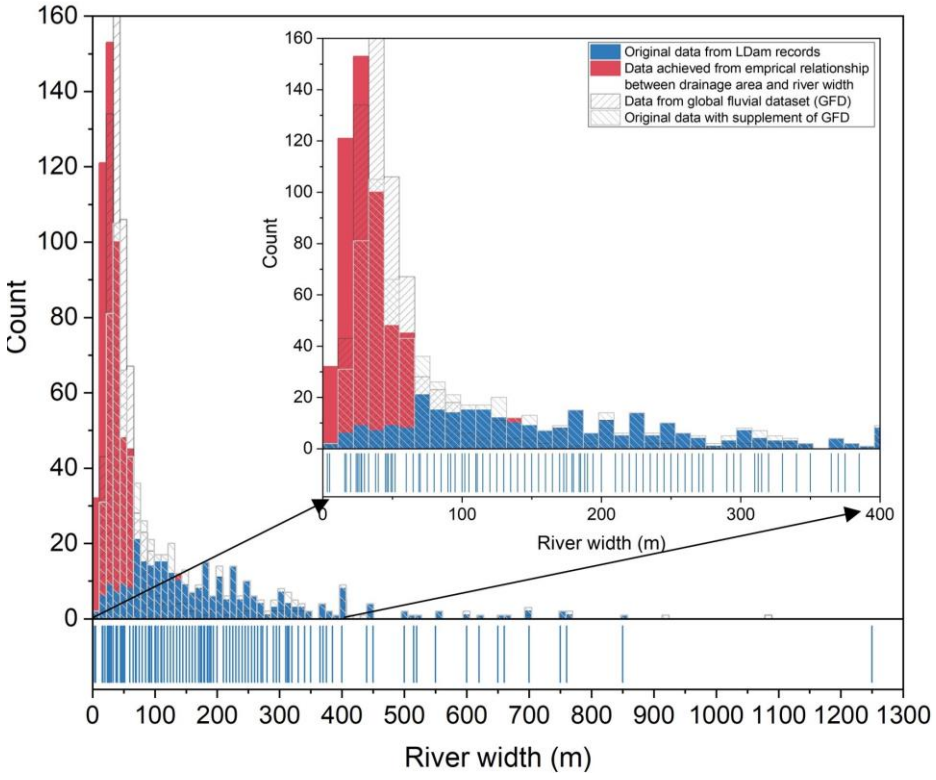

Figure 3-9 Data distribution of river width from RAGLAD, GFD, RAGLAD with the supplement of GFD and data derived from empirical relationship to drainage area, inset shows the data distribution of river width from 0 to 400m)

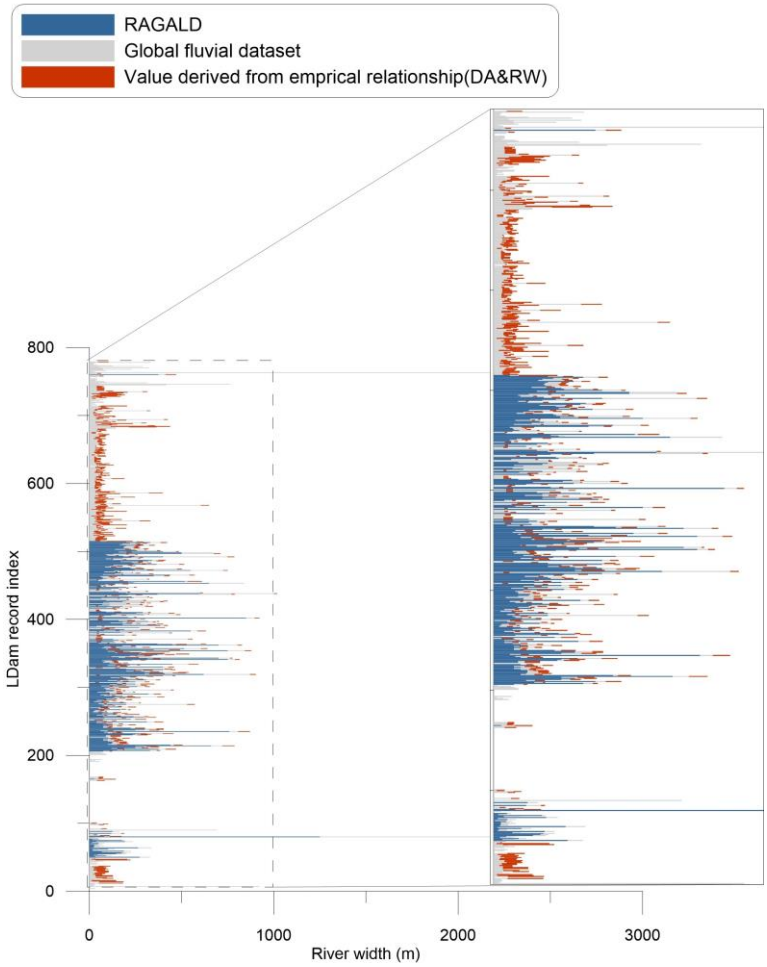

Figure 3-10 River width data comparison among LDam records, GFD and data achieved from the global W-A empirical relationship (Eq. 3-1 from Frasson et al. (2019))

3.4 Discussion

We have presented the data distribution and parameter correlation results achieved from our new-established RAGLAD dataset. Record gaps of river morphology parameters have been filled, where possible, with values derived from global fluvial datasets. There is some obvious data noise when correlating geomorphological parameters based on original LDam records. The results also showed that obtaining data

based on data combination with GFD results in better performance, comparing with calculating a specific parameter value based on established generalised global empirical relationships. However, it is also notable that the data combination results can affect the data distribution when the valid data in original records are limited (less than 50% of records with valid data). Our result indicates that although the GFD can be a better supplement source for current records than supplying data based on empirical relationships from other geomorphological parameters, there are also some uncertainties that exist that affect the data combination result, and this can reduce the accuracy of resulting data.

A possible reason for inaccuracies could be the potential data recording bias and uncertainties caused by original LDam records, including the inaccuracy and imprecision of spatial information or geomorphological data occurring during the recording process. Depending on the quality of data sampling and age of the event, the spatial inaccuracy and imprecision of the records can become one of the most important sources of uncertainty in the data when recording dimension data from other data sources, because it can link inaccurate data to the record (Tacconi Stefanelli et al. 2016). Some of the geomorphological parameters from the records, such as landslide volume and landslide area, were estimated based on the empirical relationships or achieved from remote sensing data, because the data cannot be obtained before the LDam disappears (Costa and Schuster 1988; Fan et al. 2020). The records from RAGLAD came from various landslide types and sizes and this can also lead to uncertainty in the mechanism of LDam, if it is a result of more complex combined processes. Since a lot of records from the RAGLAD dataset are clustered in the smaller catchments and the fact that smaller catchments have less persistent river flow fluctuations (Hirpa et al. 2010), it is possible to speculate that there may be a larger data difference between obtained data from the literature and actual event investigation data because of the temporal gap. Inconsistency in the terminology used during the data acquisition of LDams and landslides from different works of literature can lead to some confusion. For instance, the volume of the landslide may refer to either the volume of the landslide or the total landslide excluding the LDam body (Korup 2004) , and the length and width of a LDam body from different studies could be used interchangeably (Costa and Schuster, 1988). Additionally, the data collected from

the various data sources or recorded in different data formats, inconsistent units and spatial references can increase the uncertainties of data collation.

As the GFD datasets contain global-coverage hydro-morphological data, they can provide a reliable source for supplementing the original records. Therefore, another possible reason that can cause inaccuracy of data entries can also come from the GFD datasets themselves. Although GFDs have been developed over the past decade with a more precise representation of river networks, there remain some limitations within the current GFDs: (1) GFDs generally apply single flow direction methods, such as the D8 algorithm, for generating the flow direction map and thus they contain no channel bifurcations because the flows in the upstream areas tend to become concentrated to a distinct single flow direction (Tarboton 1997; Seibert et al. 2007); (2) most of the geomorphological characteristics or relationships between fluvial parameters from GFDs were recorded with mean annual values, and there may exist a temporal gap between the time of LDam formation and the time of data collection and thus result in the data difference between GFD and actual LDam events; (3) small rivers are still poorly represented due to the limitation of horizontal spatial resolution of the DEMs that these GFDs are derived from (pixel size of raster grids) (Yamazaki et al. 2014). These limitations of current GFDs can lead to the underestimation or overestimation of related fluvial parameters. For example, Figure 3-11 (a) shows an example of the situation when the GFD data did not contain river channels where some records were located. Figure 3-11 (b) shows the landslides in Peilong valley that reoccurred in the same place several times in the 1980s (Li et al. 2020), which actually blocked a tributary nearby instead of the mainstream presented in the GFD data, so the data of fluvial related parameters could be inaccurately linked to the mainstream instead of the tributary, if using automated geolocation methods.

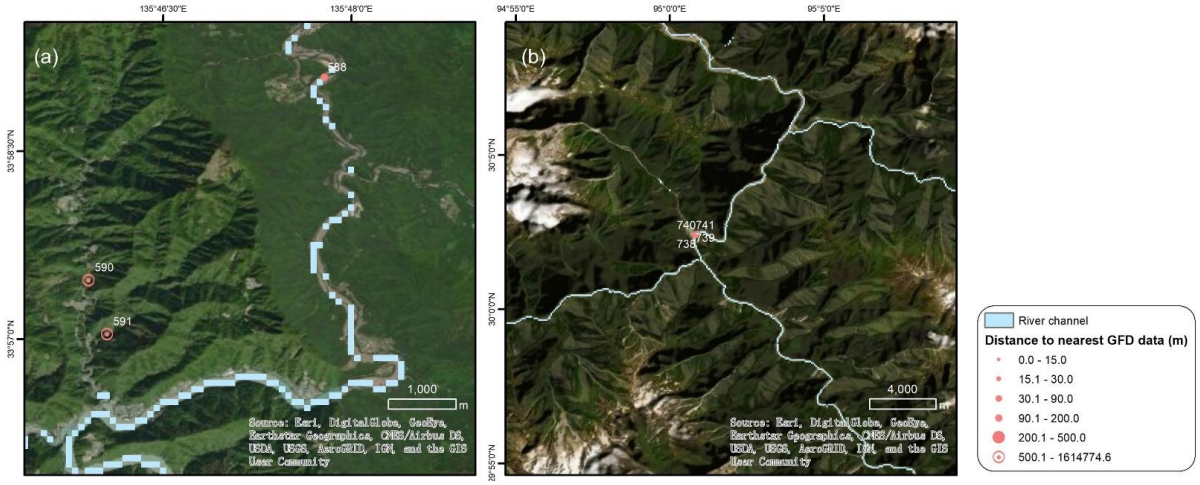

Figure 3-11 Examples of uncertainty due to the limitations of GFDs: missing representation of features and inaccurate assembling result due to imprecise location: (a) missing fluvial channel representation in small catchments; (b) inaccurate data assembling result at the channel junctions due to the imprecision of spatial information

In summary, the uncertainty of data from LDam records assembling with GFDs can be summarized into two aspects: (1) the limitations of GFDs; (2) uncertainty caused by geolocated error in the records. To further address which aspect accounts more for the data assembling uncertainties, we apply a measurement called relative error for measuring the data difference between these two datasets. The relative error (δx) is defined as Eq. 3-3:

$$\delta x = \frac{x - x_0}{x} \qquad \text{(Eq. 3-3)}$$

where x is the data value from original LDam records, x_0 is the estimated value (data from GFDs). The distance from the LDam record to the nearest data point does not proportionally increase with the relative error of drainage area and river width (Figure 3-12). The noise observed on the plot suggests that the spatial precision of records may not be the major cause of the data difference.

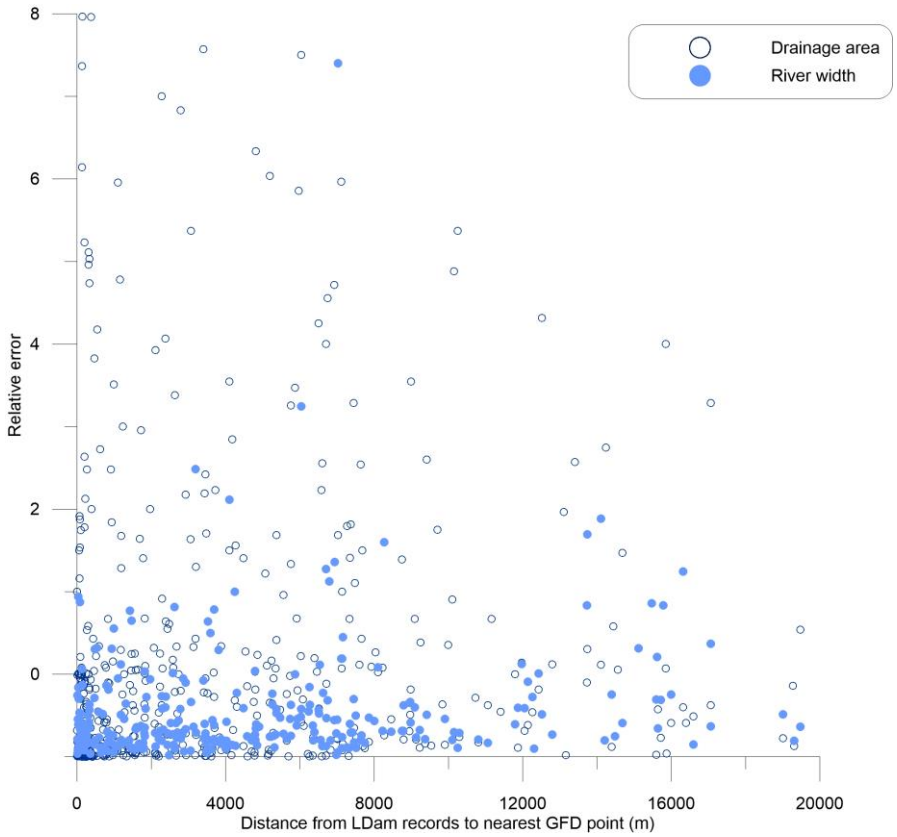

Figure 3-12 Correlation between the relative errors of drainage area and river width, and the distance from LDam records to the nearest GFD point

3.5 Conclusions

Linking other additional supplemental data to geolocated LDam datasets was highly recommended in previous LDam research (e.g. Tacconi Stefanelli et al. 2016; Tacconi Stefanelli et al. 2018; Fan et al. 2020). We have successfully created a geolocated landslide dam inventory and linking the records with other available fluvial data sources to supplement the parameters in the data. Our new global LDam dataset is called RAGLAD and contains 779 records. The records contain spatial coordinates, time information, dam materials, geomorphological characteristics of catchments, landslides and impounded lakes dimensions, and hydrographic characteristics of subsequent flood events and their consequent damage. The data were compiled from literature in mainly 3 languages. The geospatial accuracy of the records in RAGLAD was enhanced to reduce the uncertainty when linking with global fluvial datasets. RAGLAD can be useful for

researchers and global communities to further explore and discuss the LDam formation and risks, and the data are openly available through the authors.

For the first time, we supplied LDam records with auxiliary data from GFDs. The result shows that GFDs can be applied as an acceptable supplement data source for presenting a more comprehensive data distribution of geomorphological parameters. By exploring the limitations, we found that the data difference between actual data and combined data is caused by the poor fluvial channel presentation in small catchments of the GFDs and the uncertainties caused by original records in the data combination. The data combination results can be expected to improve when global datasets improve in the future.

Analysis of the resulting database reveals LDam records are clustered in the mountainous areas, which is similar to those of general landslides (Nadim 2006; Petley, 2012; Froude and Petley, 2018). The geomorphological parameter relationships show that the scale exponent difference based on landslide volume and landslide area compared well with those identified in the previous landslide research. We have also discovered a potential threshold based on the relationship of landslide volume and river width, which could be useful for exploratory LDam formation risk estimation.

This study is the first attempt to publish a global geolocated LDam dataset and link it with global fluvial datasets as a supplement for data gaps in fluvial parameters. Our research also recommends considering the LDam as an independent hazard type, as the landslides that formed LDam have different geomorphological characteristic, such as H/L ratio and landslide volume, compared with general landslides. More efforts are required to study the specific LDam formation triggers and the geomorphological background that shows susceptibility to LDam formation. Additionally, further analysis such as the evaluation of landslide dam formation susceptibility can be carried out based on this dataset.

3.6 References

Allen GH, Pavelsky TM (2018) Global extent of rivers and streams. Science 361(6402):585–588

Barla G, Paronuzzi P (2013) The 1963 Vajont Landslide: 50th Anniversary. Rock Mech Rock Eng 46(6):1267–1270

Chunyuk D, Selviyan S, Selviyan A (2020) Possible methods analysis and optimization of the landslide slope stabilization in the reconstruction area of the escalator gallery on the Moscow River shore. IOP Conference Series: Mater Sci Eng 883

Costa JE, Schuster RL (1988) The formation and failure of natural dams. Geol Soc Am Bull 100(7):1054–1068

Costa JE, Schuster RL (1991) Documented historical landslide dams from around the world (No. 91–239), https:// pubs. usgs. gov/ of/ 1991/ 0239/ report. pdf. Accessed 10th Jan 2021

Clague JJ, Evans SG (1994) Formation and failure of natural dams in the Canadian Cordillera. Geol Surv Canada Bull 404

Dai FC, Lee CF, Deng JH, Tham LG (2005) The 1786 earthquake-triggered landslide dam and subsequent dam-break flood on the Dadu River, southwestern China. Geomorphology 65(3–4):205–221

Davies TR (1982) Spreading of rock avalanche debris by mechanical fluidization. Rock Mech 15:9–24

Davies TR, McSaveney MJ (2012) Mobility of long-runout rock avalanches. Landslides–types, mechanisms and modeling. Clague JJ and Stead D (Eds). Cambridge University Press 50–58

Dufresne A, Geertsema M (2020) Rock slide–debris avalanches: flow transformation and hummock formation, examples from British Columbia. Landslides, 17(1):15–32. https:// doi. org/ 10. 1007/s10346- 019- 01280-x

Dunning S. A., Rosser N. J., Petley D. N., Massey C. R. (2006) Formation and failure of the Tsatichhu landslide dam, Bhutan. Landslides 3(2):107–113. https:// doi. org/ 10. 1007/ s10346- 005- 0032-x

Ermini L, Casagli N (2003) Prediction of the behaviour of landslide dams using a

geomorphological dimensionless index. Earth Surf Proc Land 28(1):31–47

Evans SG, Delaney KB, Hermanns RL, Strom A, Scarascia-Mugnozza G (2011) The formation and behaviour of natural and artificial rockslide dams; implications for engineering performance and hazard management. Natural and artificial rockslide dams. Springer, Berlin, Heidelberg, pp 1–75

Fan X, Dufresne A, Siva Subramanian S, Strom A, Hermanns R, Tacconi Stefanelli C, Hewitt K, Yunus AP, Dunning S, Capra L, Geertsema M, Miller B, Casagli N, Jansen JD, Xu Q (2020). The formation and impact of landslide dams – State of the art. Earth-Sci Rev 203

Fan X, Xu Q, Scaringi G, Dai L, Li W, Dong X, Zhu X, Pei X, Dai K, Havenith H-B (2017) Failure mechanism and kinematics of the deadly June 24th 2017 Xinmo landslide, Maoxian, Sichuan. China Landslides 14(6):2129–2146

Fan XM, Rossiter DG, Van Westen CJ, Xu Q, Gorum T (2014) Empirical prediction of coseismic landslide dam formation. Earth Surf Proc Land 39(14):1913–1926

Fan XM, Van Westen CJ, Xu Q, Gorum T, Dai FC (2012) Analysis of landslide dams induced by the 2008 Wenchuan earthquake. J Asian Earth Sci 57:25–37

Froude MJ, Petley DN (2018) Global fatal landslide occurrence from 2004 to 2016. Nat Hazards Earth Syst Sci 18(8):2161–2181

Frasson RPD, Pavelsky TM, Fonstad MA, Durand MT, Allen GH, Schumann G, Lion C, Beighley RE, Yang X (2019) Global relationships between river width, slope, catchment area, meander wavelength, sinuosity, and discharge. Geophys Res Lett 46(6):3252–3262

Geertsema M (2008) Natural dams, temporary lakes, and outburst floods in Western Canada, The first World Landslide Forum UN/ISDR Tokyo, Japan 211–214

Geertsema M, Schwab JW, Blais-Stevens A, Sakals ME (2009) Landslides impacting linear infrastructure in west central British Columbia. Nat Hazard 48(1):59–72

Geological Survey (1965) Geological Survey Research 1965. U.S. Government Printing

Office, Washington, D.C.

George DL, Iverson RM, Cannon CM (2019) Seamless numerical simulation of a hazard cascade in which a landslide triggers a dam-breach flood and consequent debris flow, in Debris-Flow Hazards Mitigation: Mechanics, Monitoring, Modeling, and Assessment, Proceedings of the Seventh International Conference on Debris-flow Hazards Mitigation, Association of Engineering and Environmental Geologists Special Publication 28, In: Kean J W, Coe JA, Santi PM, Guillen B. K(ed):287–293

Glastonbury J, Fell R (2008) Geotechnical characteristics of large slow, very slow, and extremely slow landslides. Can Geotech J 45(7):984–1005

Golly A, Turowski JM, Badoux A, Hovius N (2017) Controls and feedbacks in the coupling of mountain channels and hillslopes. Geology 45(4):307–310

Guzzetti F, Ardizzone F, Cardinali M, Rossi M, Valigi D (2009) Landslide volumes and landslide mobilization rates in Umbria, central Italy. Earth Planet Sci Lett 279(3–4):222–229

Hermanns RL, Folguera A, Penna I, Fauqué L, Niedermann S (2011) Landslide dams in the Central Andes of Argentina (Northern Patagonia and the Argentine Northwest), natural and artificial rockslide dams. Lect Notes Earth Sci 147–176

Hirpa FA, Gebremichael M, Over TM (2010) River flow fluctuation analysis: effect of watershed area. Water Resour Res 46(12)

Hsü KJ (1975) Catastrophic debris streams (Sturzstroms) generated by rockfalls. Geol Soc Am Bull 86:129–140

Hungr O, Leroueil S, Picarelli L (2014) The Varnes classification of landslide types, an update. Landslides 11(2):167–194

Iverson RM (1997) The physics of debris flows. Rev Geophys 35(3):245–296

Iverson RM, George DL, Allstadt K, Reid ME, Collins BD, Vallance JW, Schilling SP, Godt JW, Cannon CM, Magirl CS, Baum RL, Coe JA, Schulz WH, Bower JB (2015) Landslide mobility and hazards: implications of the 2014 Oso disaster. Earth and

Planetary Science Letters, 412: 197–208

Komac M, Hribernik K (2015) Slovenian national landslide database as a basis for statistical assessment of landslide phenomena in Slovenia. Geomorphology 249:94–102

Korup O (2002) Recent research on landslide dams - a literature review with special attention to New Zealand. Prog Phys Geog 26(2):206–235

Korup O (2004) Geomorphometric characteristics of New Zealand landslide dams. Eng Geol 73(1):13–35

Larsen IJ, Montgomery DR, Korup O (2010) Landslide erosion controlled by hillslope material. Nat Geosci 3(4):247–251

Legros F (2002) The mobility of long-runout landslides. Eng Geol 63(3–4):301–331

Lehner B, Verdin K, Jarvis A (2006) HydroSHEDS technical documentation. World Wildlife Fund US, Washington, DC, pp 1–27

Li Z, Tang T, Yuan X, Yu G (2020) Impacts of barrier dams blocking the river on morphological processes of upper alluvial channel in Yarlung Tsangpo Grand Canyon Zone. J Yangtze River Sci Res Inst 37(8):16–21 (In Chinese, with English title and abstract)

Linke S, Lehner B, Ouellet Dallaire C, Ariwi J, Grill G, Anand M, Beames P, Burchard-Levine V, Maxwell S, Moidu H, Tan F, Thieme M (2019) Global hydro-environmental sub-basin and river reach characteristics at high spatial resolution. Sci Data 6(1):1–15

Macias JL, Capra L, Scott KM, Espindola JM, Garcia-Palomo A, Costa JE (2004) The 26 May 1982 breakout flows derived from failure of a volcanic dam at El Chichon, Chiapas. Mexico Geol Soc Am Bull 116(1–2):233–246

Miller B, Dufresne A, Geertsema M, Atkinson N, Evensen H, Cruden D (2018) Longevity of dams from landslides with sub-channel rupture surfaces, Peace River region, Canada. Geoenviron Disasters 5(1)

Nadim F, Kjekstad O, Peduzzi P, Herold C, Jaedicke C (2006) Global landslide and avalanche hotspots. Landslides 3(2):159–173

Nash T, Bell D, Davies T, Nathan S (2008) Analysis of the formation and failure of Ram Creek landslide dam, South Island, New Zealand. N Z J Geol Geophys 51(3):187–193

Okura Y, Kitahara H, Kawanami A, Kurokawa U (2003) Topography and volume effects on travel distance of surface failure. Eng Geol 67(3–4):243–254

Perucca LP, Angillieri MYE (2009) Evolution of a debris-rock slide causing a natural dam: the flash flood of Rio Santa Cruz, Province of San Juan-November 12. Nat Hazards 50(2):305–320

Petley D (2012) Global patterns of loss of life from landslides. Geology 40(10):927–930

Roback K, Clark MK, West AJ, Zekkos D, Li G, Gallen SF, Chamlagain D, Godt JW (2018) The size, distribution, and mobility of landslides caused by the 2015 Mw7.8 Gorkha earthquake. Nepal Geomorphology 301:121–138

Robinson TR, Davies TRH, Wilson TM, Orchiston C, Barth N (2015) Evaluation of coseismic landslide hazard on the proposed Haast-Hollyford Highway, South Island, New Zealand. Georisk: Assessment and Management of Risk for Engineered Systems and Geohazards 10(2):146–163

Scheidegger AE (1973) On the prediction of the reach and velocity of catastrophic landslides. Rock Mech 5:231–236

Schuster RL, Costa JE (1986) Perspective on landslide dams. In Landslide Dams: Processes, Risk, and Mitigation. Proceedings of a Session in Conjunction with the ASCE Convention, pp 1–20

Seibert J, McGlynn BL (2007) A new triangular multiple flow direction algorithm for computing upslope areas from gridded digital elevation models. Water Resour Res 43(4)

Shanmugam G, Wang Y (2015) The Landslide Problem J Palaeogeogr 4(2):109–166

Strom A (2010) Landslide dams in Central Asia region. Journal of the Japan Landslide Society, 47(6): 309-324

Tacconi Stefanelli C, Segoni S, Casagli N, Catani F (2016) Geomorphic indexing of landslide dams evolution. Eng Geol 208:1–10

Tacconi Stefanelli C, Vilímek V, Emmer A, Catani F (2018) Morphological analysis and features of the landslide dams in the Cordillera Blanca. Peru Landslides 15(3):507–521

Tarboton DG (1997) A new method for the determination of flow directions and upslope areas in grid digital elevation models. Water Resour Res 33(2):309–319

Wang FW, Zhang YM, Huo ZT, Matsumoto T, Huang BL (2004) The July 14, 2003 Qianjiangping landslide, Three Gorges Reservoir. China Landslides 1(2):157–162

Yamazaki D, Ikeshima D, Sosa J, Bates PD, Allen GH, Pavelsky TM (2019) MERIT hydro: a high-resolution global hydrography map based on latest topography dataset. Water Resour Res 55(6):5053–5073

Yamazaki D, O'Loughlin F, Trigg MA, Miller ZF, Pavelsky TM, Bates PD (2014) Development of the global width database for large rivers. Water Resour Res 50(4):3467–3480

Yin Y, Wang F, Sun P (2009) Landslide hazards triggered by the 2008 Wenchuan earthquake, Sichuan. China Landslides 6(2):139–152

Xu Q, Fan XM, Huang RQ, Westen CV (2009) Landslide dams triggered by the Wenchuan Earthquake, Sichuan Province, south west China. Bull Eng Geol Environ 68(3):373–386

Zhang L, Peng M, Chang D, Xu Y (2016) Dam failure mechanisms and risk assessment. John Wiley & Sons, Singapore

Zheng H, Shi Z, Shen D, Peng M, Hanley KJ, Ma C, Zhang L (2021) Recent advances in stability and failure mechanisms of landslide dams. Front Earth Sci 9

Chapter 4. Are There Fundamental Differences Between Dam Forming Landslides and all Landslides?

The characteristics of dam forming landslides are intriguing for researchers, as only ~1% or fewer landslides eventually block the river and subsequently result in severe flooding following collapse than when compared with normal fluvial flooding. Differences in dimension data or landslide dam formation index have been identified for landslides that have gone on to dam rivers and those landslides that do not, in regional-scale studies. However, a quantitative comparison on a global-scale between these two hazards has not been conducted before. Using open-access datasets of landslides and landslide dams collected globally at different spatial scales, we implemented a statistical comparison of the distribution of their morphometric and spatial characteristics, such as: landslide volume, height/length ratio, and spatial positions in specific catchments, to investigate whether some landslides are more likely to form dams than others. The results suggest that the dam forming landslides are a special subset of all landslides: dam forming landslides occur in relatively upstream areas with larger stream power index values when compared to landslides more generally; dam forming landslides have lower mobility as they may be spatially confined in the upstream area with steeper slopes and less hillslope length; shallower landslides with large area coverage are also more likely to form a dam. Even with some quality and completeness limitations in the data sources used, this global-scale comparison study provides some directions for quantifying a landslide dam formation index on a global scale and identifying those areas prone to landslide dam formation.

Keywords: landslides, landslide dams, global-scale, hazard zonation, fluvial datasets, river hazards

4.1 Introduction

Landslides and landslide dams (LDams) are frequently reported worldwide, with significant consequential damage to both public facilities and citizens (Costa and Schuster 1988; Petley 2012; Froude and Petley 2018; Fan et al. 2020; Wu et al. 2022). Landslides that form dams are a special subset of landslides, referring to the mass movement when

it partially, or completely blocks the fluvial channels (rivers and streams). Among all landslides, only a small portion actually form LDams and block rivers. In Norway, at least 181 historical landslides forming LDams were recorded out of more than 33,000 registered landslides in the national landslide database of Norway (Oppikofer et al. 2020). A total of 828 LDams were reported among more than 600,000 landslides caused by the 2008 Wenchuan Earthquake, constituting approximately 1.4% of the total number of landslide records (Fan et al. 2012). Even though a small proportion of landslides cause river blockages, the impacts of LDams on upstream and downstream floods can be more significant than normal flash floods (Perucca and Angillieri 2009). One of the most dangerous LDams triggered by the 2008 Wenchuan earthquake, Tangjiashan LDam, caused a flood wave to reach an estimated peak discharge of 15,474 m^3/s (Xu et al. 2009), ten times the flood warning discharge of 1,500 m^3/s reported by the Chengdu Water Authority (2020). Very recently, in May of 2023, torrential rains triggered around 280 landslides and caused devastating floods in Emilia-Romagna (Ghiglione and Bettiza 2023), Italy, which could potentially have been caused or exacerbated by LDam formation.

To examine whether a landslide could form an LDam, Korup (2002) suggested quantifying the 'scaling threshold' for river blockage based on the geomorphology variables of valley/river and landslide, and hydrologic variables. The divisions of characteristics of landslides and dam forming landslides (DFLs) in specific regions have been studied by Tacconi Stefanelli et al. (2015; 2018). Their research indicated differences in landslide dimension data and valley-related or fluvial-related parameters between landslides and DFLs where there are differences in the relationship of valley width and landslide volume, as well as the data distribution of LDam formation index, combining landslide volume and valley width. However, the LDam formation thresholds calculated on a regional scale may not be reliable when applied to other datasets or regions. Cencetti et al. (2020) showed that such an index is hard to generalize as it was generated from specific geomorphological and hydrological conditions. Struble et al. (2021) also found that the dam stability index did not fit with their LDam record in Western Oregon and the scaling relationship between the upstream catchment area and landslide dam size did not match the Oregon dataset.

Currently, the LDam formation index, or 'scaling threshold' for river blockage, for global-scale research still awaits identification because the relative variables that finally differentiate a river blockage event from a non-blockage one are still unclear. Based on an earlier study on the global-scale LDam dataset, RAGLAD (River Augmented Global LAndslide Dams), DFLs have shown some physical/geomorphological differences compared to landslides, especially in the geomorphological characteristics (Wu et al. 2022). In the RAGLAD dataset, the DFLs with a volume larger than 1 million cubic meters account for a larger proportion of records compared with that of the general landslide volumes. The power law scaling exponent of DFLs achieved from the relationship of landslide volume and landslide area is smaller than those of landslides more generally, regardless of landslide mass materials: the scaling exponent of global soil-slope landslides ranged from 1.1 to1.3 and the exponent in rock-based landslides in the range of 1.3-1.6 (Larsen 2010), comparing with the scaling exponent of DFLs from RAGLAD dataset, ranging from 0.66 to 0.97 (except for falls, which had a scaling exponent of 1.52).

Previous research leads to questions regarding the fundamental differences between landslides and DFLs. What are the properties of DFLs that need to be identified as unique compared to landslides more generally? Do the DFLs have different mobility or size that makes it easier to block rivers compared to landslides more generally? Are there differences in the spatial distribution of DFLs and all landslides? To answer these questions, we collected landslide records and LDam records from 12 datasets globally and assembled them as two subsets, one for the records of general landslides, and another for DFLs (landslide dimension data recorded in LDam records). After data compilation, the differences between DFLs and landslides are systematically explored in two main sections: (i) the landslide morphometric data differences, mainly mobility and size, between all landslides and DFLs; and (ii) the spatial distribution differences of their locations, especially their locations in river reaches. The findings may help identify the required conditions for LDam formation that need to be considered, both in the context of landslides as well as the hydrological and geomorphological factors of rivers. This study could provide directions for establishing a global-scale LDam formation index or global-scale LDam formation susceptibility evaluation. The study will help in identifying

characteristics of regions prone to LDam formation globally.

4.2 Data and Methods

4.2.1 Data Sources of Landslides and Dam Forming Landslides

The dimensional data of DFLs or landslides more generally show differences between data recorded in different regions. For example, the average impounded lake size of LDam records from New Zealand is smaller than the average value from the worldwide dataset (Costa and Schuster 1991; Korup 2004). Another example is the differences in river blockage index combining landslide volume and valley width between LDam records in Italy and Peru, as shown by Tacconi Stefanelli et al. (2016; 2018). The spatial distribution of landslides and LDams in different locations around the world highlights the differences in geomorphological parameters. Jibson and Harp (2012) found that the maximum epicentral distance limits for landslide occurrence were different between those landslides located in continental interiors as opposed to plate boundaries, and the differences are also related to geologic structures and ground motion attenuation in diverse regions. The varied qualities of the dataset also affect the data comparison. Korup (2002) demonstrated that the impacts of the multivariate geomorphic characteristics inherent in LDam records are restricted for the quantification of data comparison. Therefore, global consistent datasets are needed to compare the differences between general landslides and DFLs globally.

However, currently, both landslides or LDams (or DFLs) barely have a well-established inventory with comprehensive and consistent data attributes, such as landslide size, on a global scale. We tried to collect more consistent data from landslide records to cover landslide inventories from different scales and trigging mechanisms to avoid the issues caused by the scarcity of data on the specific type of landslides. For LDam/DFL records, the data is derived from the global-scale geolocated LDam dataset RAGLAD (Wu et al. 2022). In the analysis of landslide/DFL records, different classification schemes have been employed, while global-scale datasets consistently adopted the primary landslide classification type derived from the Varnes scheme (Varnes et al. 1984) or its subsequent revisions (Hungr et al. 2014).

There were 12 databases collected from local to global scale, including one mosaic database consisting of multiple event-based landslide datasets from seismically triggered landslides (Table 4-1). These records were either from an open-access online database or obtained with permission from the original authors or institutions. The most ideal scenario for a global-scale inventory establishment of landslides would be to collect all the event-based inventories, aiming at mapping all landslides within a single landslide-triggering episode. Schmitt et al. (2017) attempted to collect event-based seismically triggered landslides from various events, but they also found several limitations: (i) obtaining permissions from all known datasets was challenging; (ii) the diversity of methods, objectives and priorities for establishing the inventories results in inventories with variable quality, completeness, and presentation. There are several attempts for establishing global-scale geolocated inventories directly for landslides and LDam records (Kirschbaum et al. 2019; Dufresne et al. 2021; Wu et al. 2022). From these datasets, it is difficult to balance the number of records against a consistent and complete dataset.

Table 4-1 Landslide datasets and LDam datasets that were used for this study

Index	Name	Time coverage	Scale (Area)	Database format	Data coverage	Number of landslide records /events	Contributors
1	Landslide Inventories from An Open Repository of Earthquake-Triggered Ground-Failure Inventories	since 1900	Global (event-based)	Shapefile	Earthquake-triggered landslides	356,497 geolocated data	Schmitt et al. 2017
2	Landslide Inventories across the United States	1900-2019	National (U.S.A.)	Shapefile	Landslides-Not specific	64,433	Jones et al. 2019
3	Dufresne (unpublished inventory)	From 270,000 B.P. (Before present)	Global	Excel	Landslides-Not specific triggers/specific types of landslides	179	Dufresne et al. 2021
4	Rockslides and Rock Avalanches	-	Regional (Middle Asia)	Excel	Landslides and LDams-Not specific triggers/speci	1016	Strom and Abdrakhmatov 2018

Index	Name	Time coverage	Scale (Area)	Database format	Data coverage	Number of landslide records /events	Contributors
	of Central Asia				fic types of landslides		
5	Global Landslide Catalog (GLC)	2007-2019	Global	Shapefile	Rainfall-triggered landslides	14,532	Kirschbaum et al. 2015
6	FraneItalia	From January 2010 to 2017	National (Italy)	SQL database	Landslides-not specific	5438(single)+1787(areal)	Calvello and Pecoraro 2018
7	High Mountain Asia Landslide Catalog V001(HMS_LS)	1956-2018	Regional (Asia)	Shapefile	Rainfall-triggered landslides	12,755	Kirschbaum et al. 2019
8	Landslides in Dominica	-	National (Dominica)	Shapefile	Landslides-not specific	10,551	van Westen and Zhang (2018)
9	CAmpi Flegrei LAndslide Geodatabase (CAFLAG)	1828-2017	Local (Campi Flegrei caldera, Italy)	Shapefile	Landslides-not specific	2302	Italian National Research Council (CNR) (Esposito and Matano 2021)
10	Digital Archive for Landslide Distribution Maps	1981-2014	National (Japan)	Shapefile	Landslides-not specific	359,387 mass movement polygons	National Research Institute for Earth Science and Disaster Prevention of Japan (2014)
11	CEDIT-updated 2019	1169-2019	National (Italy)	Excel	Earthquake-triggered landslides	2077	Sapienza University of Rome (Caprari et al. 2018)
12	RAGLAD	Since 8 century	Global	shapefile	LDam-not specific	779	Wu et al. 2022

We first categorise the data by quality. Figure 4-1 is a schematic figure to illustrate dividing the data quality into 5 different levels for landslide and LDam records: level 1 -

records with landslide existence reported without any reliable qualitative, quantitative, or spatial information being recorded; level 2 - geolocated records without further information; level 3 - geolocated records reported with some qualitative information such as effects or quantified data recorded qualitatively; level 4 - geolocated records reported with qualitative information and some quantitative attributes; level 5 - geolocated records with comprehensive quantitative attributes, especially the dimension data of landslides/LDams. As the completeness of records increases, the number of records is expected to reduce. The records in the final datasets that were used for this study were assigned a level based on the comprehensiveness of each dataset's attributes as shown in Figure 4-1. Most of the records in the datasets are geolocated and at least have some qualitative information recorded.

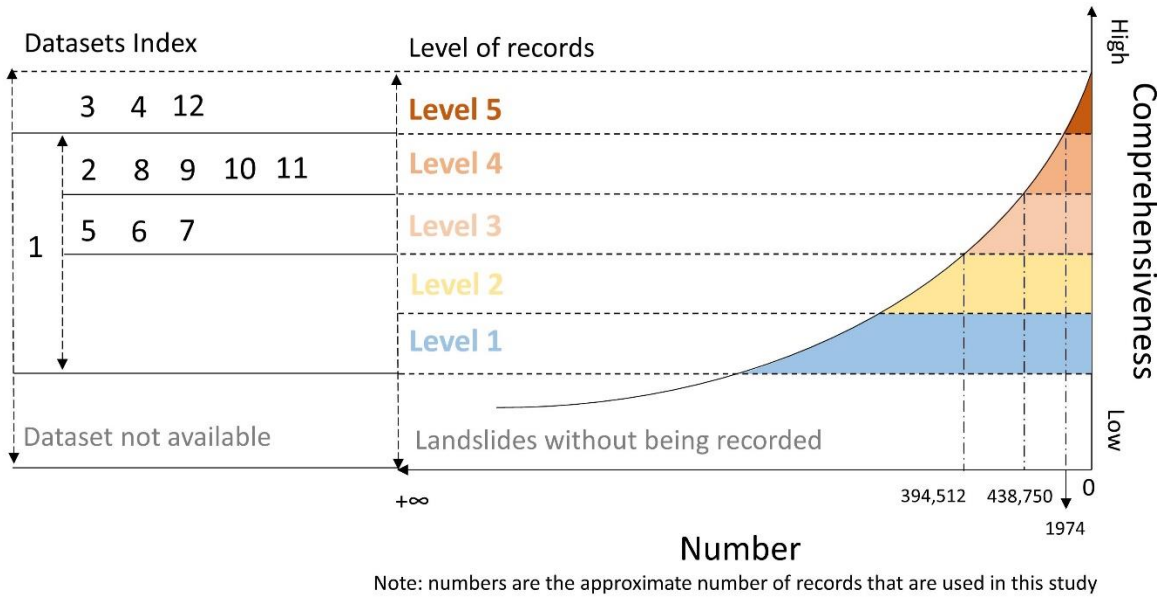

Figure 4-1 Schematic graph showing the different levels of data quality of datasets for the landslide and LDam records used in this study (Level 1 to 5 reveals the 5 different levels of data comprehensiveness; data index on the left is the datasets number from Table 4-1)

After assembling the records of all the separate datasets their data fields were unifying, specifically: the geospatial references to WGS 1984 as well as units and data format. There are more than 800,000 landslide records in total (more than 90% of landslide records contained coordinates). We kept one landslide record if they had duplicated from various data sources with the same spatial coordinates (~1000 records

were found duplicated, less than 0.1% of all records). Figure 4-2 illustrates the spatial distribution of mapped landslide records and LDam records from the geolocated records in the databases shown in Table 4-1. The landslides are geographically concentrated in the tectonic-activate areas, especially along the convergent plate boundaries, such as the Circum-Pacific Belt (Andes Mountains, Rocky Mountains, mountainous areas on the islands along the eastern Pacific coast, etc.) and Alpine-Himalayan orogenic belt (European Alps, Pamir Mountains, Himalayas, etc.). The landslides are also concentrated in those countries that have more well-established national-scale landslide inventories or more landslide research, such as Norway, Italy, Japan, China, India, New Zealand, and the USA. LDam records are distributed in similar locations, but as they have fewer records from currently available datasets, the areas of specific researchers' focus may play an important role in the LDam record clusters.

Figure 4- 2 Spatial distribution of landslide records from various datasets and LDam records with precise geospatial locations in RAGLAD

4.2.2 Method for Data Comparison

4.2.2.1 Morphometric Differences

To explore the differences between landslides and DFLs, we first compared the morphometric data, including the mobility and size, of landslides by comparing their data distribution from the globally collected records. The H/L ratio is a parameter calculated

by landslide fall height (H) divided by travel length (L) (Figure 4-3) and is popular for measuring the mobility of landslide debris (Corominas 1996; Iverson 1997). Landslide size, especially landslide volume significantly contributes to LDam formation. Fan et al. (2012) found that the correlation between landslide volume and river width played a key role in LDam formation for the landslides triggered by the 2008 Wenchuan Earthquake. The LDam records from the global-scale dataset RAGLAD also showed a clear potential threshold for LDam formation, based on the relationship between landslide volume and river width (Wu et al. 2022). Therefore, the morphometric parameters including landslide H/L ratio and landslide volume were applied to the landslide morphometric data comparison in landslide mass mobility and landslide size.

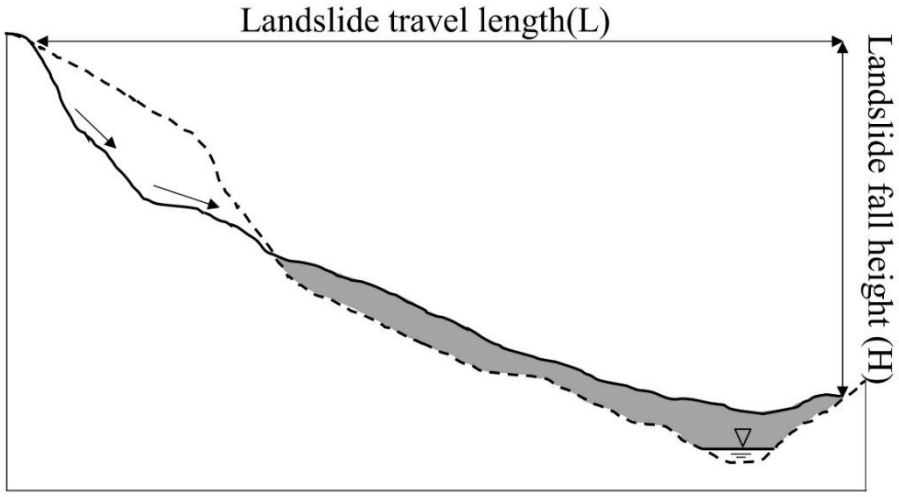

Figure 4-3 Illustration of landslide fall height and travel length in H/L ratio, simplified from Fan et al. (2014)

It is noted that the dimension data of landslides significantly relies on the landslide types, so it would be better to compare the morphometric data within landslide types where possible (Corominas 1996). As the records in rock avalanches and rockslides have the largest numbers and completeness, we used the H/L ratio and landslide volume data from these types of landslides in three different landslide/LDam datasets for comparison. The three datasets in data quality level 5 included one global-scale rockslide/rock avalanche dataset (Dufresne et al. 2021, 179 records), a combined dataset of DFLs and landslides in regional scale (the landslide type of the record is mainly rockslide/rock avalanche, at least 19% of landslides were DFLs; Strom and Abdrakhmatov 2018, 1016

records), and one global-scale LDam /DFL dataset (Wu et al. 2022, 779 records). If the landslide volume from the data source is a range of values rather than a single value, the average value of the highest and lowest value of the range is applied, without further classification. The data comparison of landslide height was also included to check whether the landslide height affects the H/L ratio distribution for landslides. For the landslide volume comparison, those records dated before the end of the Younger Dryas era (11,500 B.P.) were excluded since the land surface has been modified substantially and thus changed the landslide volume value.

Compared with landslide volume, more records with valid landslide area data are available. There are several methods for estimating the initial landslide failure depth and volume (Jaboyedoff et al. 2020). However, for a global-scale study where it is hard to collect valid data for other parameters, such as thickness and surface profile shapes, the empirical relationships between landslide horizontal surface area and volume are an efficient method to estimate volume because the data for landslide area is relatively easier to quantify on aerial and satellite images from GIS geometry calculation. Such a relationship was first applied by Simonett (1967), then followed by many expert-based approaches to get the landslide volume based on the different datasets (Hovius et al. 1997; Guzzetti et al. 2009). The empirical relationship between landslide volume and landslide area from a global-scale shallow landslide study was established and found the hillslope material controls the landslide volume (Larsen et al. 2010). Fan et al. (2014) also used this relationship and adjusted it based on the data from the inventory of landslides that occurred in the 2008 Wenchuan earthquake to estimate the volume of landslides that dammed the rivers. Some empirical relationships between landslide volume and area were presented in RAGLAD based on landslide type (Wu et al. 2022). However, as the datasets are different, the scaling exponent and intercept could have different values and thus lead to different results for estimating the landslide volume. The difference between general landslides and LDam landslides of landslide area is an alternative parameter of landslide volume. We only compare the landslide area data from the records in Japan because Japan contains 359,387 records from the Digital Archive for Landslide Distribution Maps, a national-scale landslide inventory of Japan, with valid landslide area data, and 171 geolocated LDam records from RAGLAD are located there.

4.2.2.2 Spatial distribution differences (Italy example)

Besides landslide morphometric data differences, whether there is any difference in spatial distribution between landslides and DFLs was also explored. There is considerable evidence showing that LDams tend to form in tributary and headwater basins, which have small upstream areas, either from global-scale studies (Costa and Schuster 1988; Fan et al. 2020; Wu et al. 2022) or regional scale studies (Korup 2002), from the spatial distribution of LDam records of regional or global-scale datasets. There are also some spatial distribution studies on global-scale landslides resulting in fatalities (Petley 2012; Froude and Petley 2018), and regional-scale landslide hazards occurring within a single landslide-triggering episode (Borgomeo et al. 2014; Dai et al. 2011). However, our study is the first attempt to quantitively compare the spatial distribution of landslide records and data on landslides that form dams on a large spatial scale.

In comparison to landslides generally, DFLs are a small subset of the overall total. To avoid the bias caused by data scarcity of LDam records in some areas, Italy was selected as the area for studying the spatial distribution differences, because Italy has relatively more records in both landslide records and LDam records, which are spatially distributed in this region. Based on the Italian landslide inventory (IFFI, Trigila et al. 2010), the national and official database on landslides in Italy, and other landslide/LDam datasets from different spatial scales (Table 4-1), there are more than 1 million landslide records and 257 LDam records from RAGLAD located in Italy, as shown in Figure 4-4. Italy can be considered as a miniature of the global scope, it has multiple lithology types and landforms through its territory, including mountain areas dominated by limestones in Alps and Apennines, metamorphic form the Calabrian mountains, volcanic terrains occur in some places; its precipitation covers a wide range, similar areas globally, with a mean annual rainfall from lower than 800mm (Sicily, Melillo et al. 2016) to over 3000mm (European alps, Palladino et al. 2018); it is also a tectonic active area with compressional tectonics dominating in the alpine regions and with extensional tectonics dominating the south of Italy.

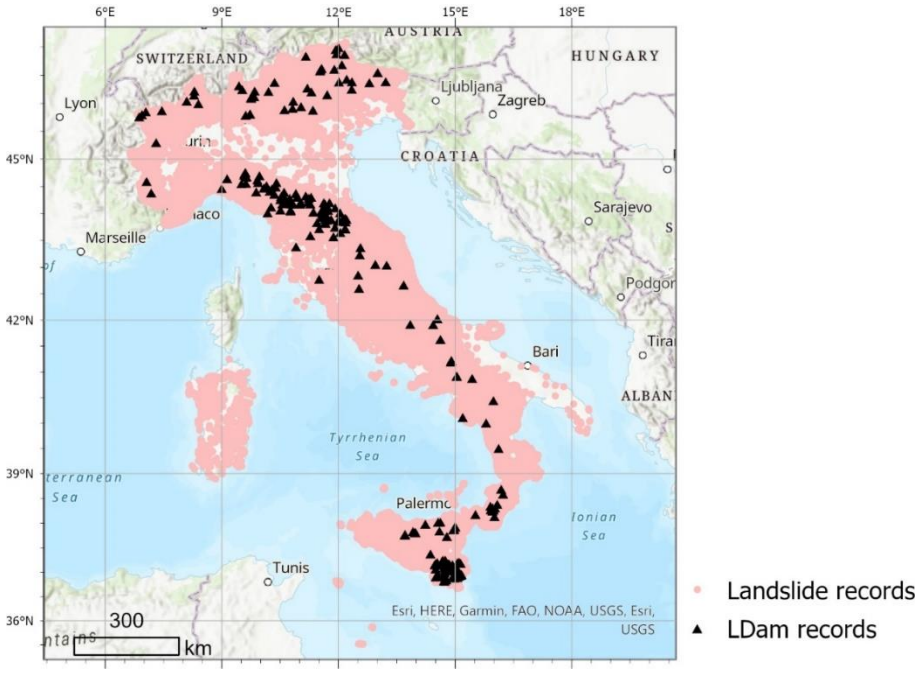

Figure 4-4 LDam and landslide records in Italy that were used for the spatial distribution comparison

Firstly, we explore the spatial distribution of their locations in the catchment, including the elevations, and upstream catchment area at the location of records. The development of global fluvial datasets and geolocated inventories of landslides and LDams make this spatial distribution comparison possible. Global fluvial datasets have had rapid development during the past decade (Yamazaki et al. 2014; Allen and Pavelsky 2018; Linke et al. 2019; Yamazaki et al. 2019; Frasson et al. 2019; Feng et al. 2022). Even though the global fluvial datasets still have limitations in depicting upstream tributaries where the river width is relatively small, they are a more consistent and reliable data source of river width compared with estimating river width directly from a simple empirical relationship of the drainage area and river width (Wu et al. 2022). MERIT Hydro, a global fluvial dataset (Yamazaki et al. 2019), was applied to obtain drainage area and river width for this comparison. MERIT hydro contains flow direction, river width, drainage area and other hydrological characteristics of the river channel, at a resolution of 90 m derived from the latest elevation and waterbody data.

Besides the spatial distribution difference of landslides in catchment locations, the differences in river reach characteristics are also worth exploring. The stream power index (SPI) is a parameter commonly used for describing the potential flow erosion power at a

given point of the topographic surface (Moore et al. 1991). The SPI data we used came from geomorpho90, a global dataset comprising different geomorphometric features derived from the MERIT-Digital Elevation Model (DEM) (Amatulli et al. 2020). The SPI can be calculated with the following Eq. 4-1 using slope gradient (G) and upstream catchment area (CA):

$$SPI = ln(CA \times tanG) \quad \text{(Eq. 4-1)}$$

To prevent the uncertainties caused by the variations of catchment area size, we created a subset with similar upstream catchment areas to LDams by extracting those landslides located in the areas with an upstream catchment area of less than 627 km^2, which is the upstream catchment area where 87% LDam record are located (upstream catchment threshold calculated from records in RAGLAD, Wu et al. 2022). To keep the consistency with the SPI data calculation of geomorpho90 and to prevent uncertainties by using other DEM sources, we used the upstream catchment area derived from MERIT hydro.

To explore the reasons behind the spatial distribution difference between DFLs and a wider group of landslides, we identify the proximity of landslides/DFLs to the river reaches. The travel distance of a long run-out landslide that dammed the river could be long if we consider defining a specific runout distance threshold for DFLs. The longest distance of a DFL is 19 km from RAGLAD (Wu et al. 2022), specifically the Kolka glacier-debris flow (Evans et al. 2009), and the mean landslide length for the LDam records in RAGLAD is 3 km. These numbers are far beyond what might be typically considered "close". Therefore, instead of directly exploring what proportion of landslides/DFLs are located close to the rivers, we analysed the landslide proximities to rivers by using global fluvial datasets, and the river network from EU-Hydro, a dataset with all EEA39 countries providing photo-interpreted river networks consisting of surface interpretation of water bodies and a drainage model derived from the EU-DEM (European Environment Agency 2020). Because the representation of fluvial channels from various datasets could also affect the comparison result, a combination of global fluvial datasets (GFD), including Global River Widths from Landsat (GRWL, Allen and Pavelsky 2018),

MERIT Hydro (Yamazaki et al. 2019), and the river channel section points from Global Long-term River Width (GLOW, Feng et al. 2022), were also applied to show the river proximities of DFLs and general landslides to compare with the result derived from EU-Hydro. We converted all the GFD data into points and merged them to present the total river channels derived from GFD. However, none of these open-access datasets perfectly depict the river and tributaries as seen in reality. Figure 4-5 presents an example of the differences between these two datasets for the river channels around Scanno, Italy. The EU-hydro includes more tributaries by deriving from DEM directly, while the combination of GFDs only represents the main channel of the River Tasso and River Sagittario compared to the rivers and tributaries in the basin of River Tasso and River Sagittario mapped in the geomorphological study around Scanno by Della Seta et al. (2017).

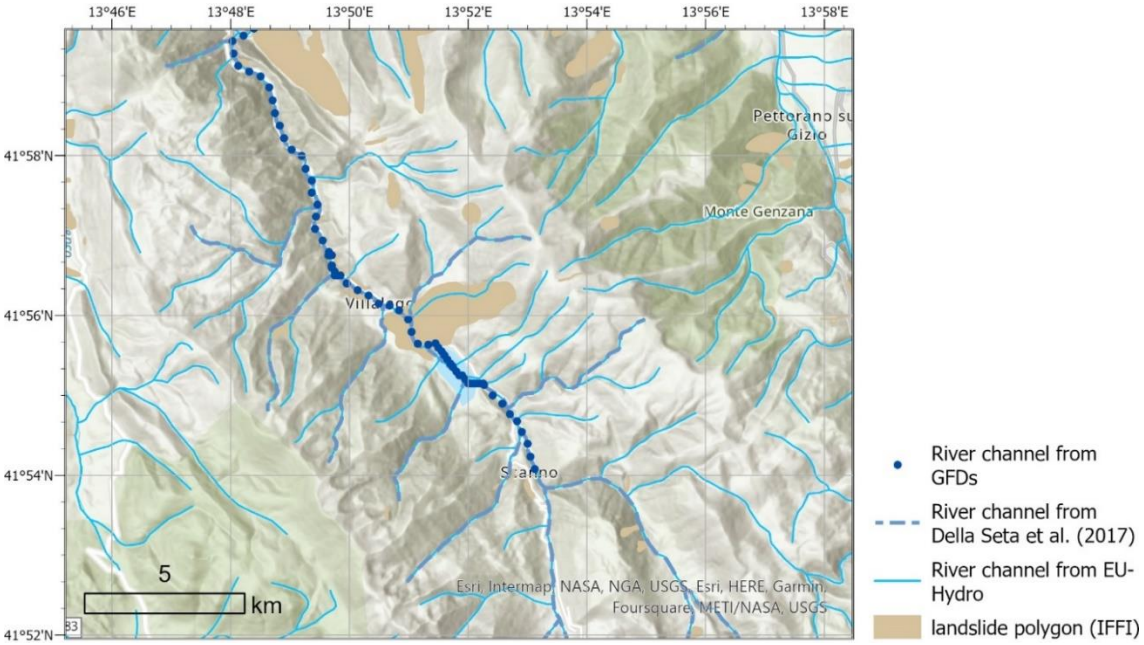

Figure 4-5 The river channels presented by EU-hydro, the combination of GFDs and previous research by Della Seta et al. (2017) around Lake Scanno. GFD: global fluvial datasets, including Global River Widths from Landsat (GRWL, Allen and Pavelsky 2018), MERIT Hydro (Yamazaki et al. 2019), and the river channel section points from Global Long-term River Width (GLOW, Feng et al. 2022); IFFI: Italian landslide inventory (Trigila et al. 2010); EU-Hydro: EU-Hydro is a river and drainage network dataset derived from EU-DEM (European Environment Agency 2020)

4.3 Results

4.3.1 Mobility and Landslide Size

Using the methodology described above we sought to answer 3 questions related to the mobility and size of landslides and DFLs: 1) do DFLs show higher mobility than a wider group of landslides? 2) do DFLs show higher volumes than landslides as a whole? 3) do DFLs cover larger areas than landslides more generally? The first question relates to the reach of the landslide and whether DFLs need to have higher mobilities to reach waterbodies in sufficient volume to allow dam formation. Questions 2 and 3 seek to identify whether a smaller, deeper slide mass (almost certainly some form of block movement) is more efficient at forming dams than a larger shallower landslide (more likely to be disrupted/fragmented).

Corominas (1996) was able to extract data for the mobility of landslides by landslide type. In broad terms it was observed that rockfalls (of which some were rock avalanches) were the most mobile followed by debris flows (strongly influenced by channelized debris flows), then earthflows and finally translational landslides. The dataset described by Dufresne et al. (2021) showed that the rockfall/rock avalanche group shows the smallest H/L ratio, mainly concentrated in the range of less than 0.3. The landslide dataset including DFLs (Strom and Abdrakhmatov 2018) showed a H/L ratio slightly larger but generally smaller than 0.5. The LDam dataset (Wu et al. 2022), contained more records with H/L ratios in excess of 0.5 (Figure 4-6). The H/L ratios from landslides and a combination of landslides and DFLs have a value of less than 0.5, which is similar to the value achieved from landslides more generally (Iverson et al. 2015). It is also noted that the rock avalanche/slide records from RAGLAD (DFLs) have more data with larger H/L ratio values, which implies that the rock avalanches/slides that dammed the river have travelled short distances before damning rivers and that those rock avalanches/slides with lower H/L ratios tend not to block rivers, possibly because of loss of debris prior to the furthest reach of the slide mass. To make this mobility comparison in more landslide types, we also collected H/L ratio data from other literature beside the three datasets used for this comparison (Table 4-2). Most of the H/L ratios of DFLs are generally larger or close to (median H/L ratio difference: ~±0.1) that of landslides in a wider group. Among

different landslide types of landslides and DFLs, DFLs show lower mobility than a wider group of landslides.

Table 4-2 H/L ratio comparison based on different landslide types in DFLs and landslides more generally, coloured by type.

	Landslide type	Number of records	Min H/L ratio	Max H/L ratio	Median H/L ratio	Database/Reference (Spatial scale)
Landslides more generally	Rockslide/rock avalanche	122	0.020	0.858	0.235	Dufresne et al. 2021 (Global)
		N/A	0.083	0.929	0.641	Fan et al. 2014 (Regional)
	DFL/LS combination – Rockslide/rock avalanche	538	0.091	0.982	0.376	Strom and Abdrakhmatov 2018 (Regional)
	Translational/rotational slide	36	0.089	0.919	0.406	Devoli et al. 2009 (Local)
		14	0.258	0.485	0.398	Sun et al. 2021 (Local)
		N/A	0.275	1.090	0.624	Fan et al. 2014 (Regional)
	Debris flow/avalanches	65	0.052	0.739	0.467	Corominas 1996 (Global)
		12	0.009	0.153	0.021	Capra et al. 2002 (Local)
		17	0.240	0.410	0.340	Toyos et al. 2007 (Local)
		N/A	0.205	1.025	0.528	Fan et al. 2014 (Regional)
	Earth flow	17	0.041	0.800	0.257	Corominas 1996 (Global)
	Rockfall	45	0.117	1.087	0.664	Corominas 1996 (Global)
		N/A	0.288	0.942	0.733	Fan et al. 2014 (Regional)
DFL	Rockslide/avalanche	21	0.150	1.930	0.804	RAGLAD (Wu et al. 2022; Global)
		N/A	0.253	0.876	0.519	Fan et al 2014 (Regional)
	Translational/rotational slide	229	0.040	1.400	0.375	RAGLAD (Wu et al. 2022; Global)
		N/A	0.323	1.578	0.859	Fan et al 2014 (Regional)
	Debris flow/avalanches	15	0.132	0.700	0.407	RAGLAD (Wu et al. 2022; Global)
		N/A	0.170	0.837	0.488	Fan et al. 2014 (Regional)
	Earth flow	1	0.163	-	-	RAGLAD (Wu et al. 2022; Global)
	Rockfall	14	0.011	1.534	0.443	RAGLAD (Wu et al. 2022; Global)
		N/A	0.859	1.766	1.108	Fan et al. 2014 (Regional)

The height of the landslide is one of the critical factors that affects the H/L ratio and landslide dynamics, such as the motion and the barycentre of sliding mass (Li et al.

2021), so it was used to explore whether it affects the H/L ratio comparison result. The landslide fall height of DFLs is slightly smaller than those of landslides more generally as the median landslide height value of DFLs is 580 m, with nearly 50% of DFLs with a fall height of less than 500 m, while the median value from other two datasets is respectively 685 m (Dufresne et al. 2021) and 970 m (Strom and Abdrakhmatov 2018) (Figure 4-7). Combining Figure 4-6 and Figure 4-7, the decreasing landslide runout distance could be the main factor that leads to the higher H/L ratio of DFLs, given the landslide fall height of DFLs is even smaller than landslides more generally. This result implies that the spatial distribution of landslide could be the main reason for LDam formation as the hillslopes in the upstream area are steeper and thus confined the travel distance of hillslope mass when a landslide occurs.

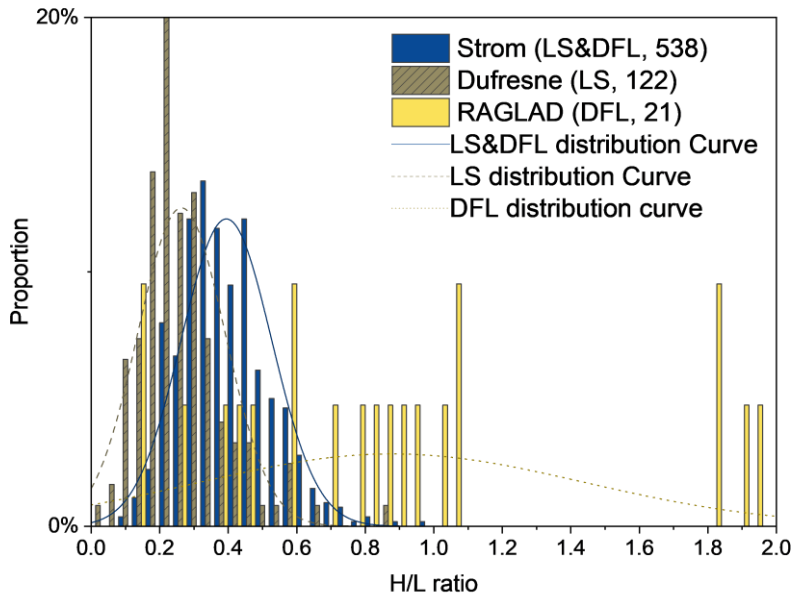

Figure 4-6 H/L ratio data distribution from different landslide datasets (Landslide type: rock avalanches and rockslide; LS: landslides; Strom: a dataset from Rockslides and Rock Avalanches of Central Asia (dataset Index 4 as presented in Table 4-1, Strom and Abdrakhmatov 2018); Dufresne: an unpublished dataset (dataset index 3, Dufresne et al. 2021); RAGLAD: River Augmented Global LAndslide Dams dataset (dataset index 12, Wu et al. 2022; numbers are the sample sizes)

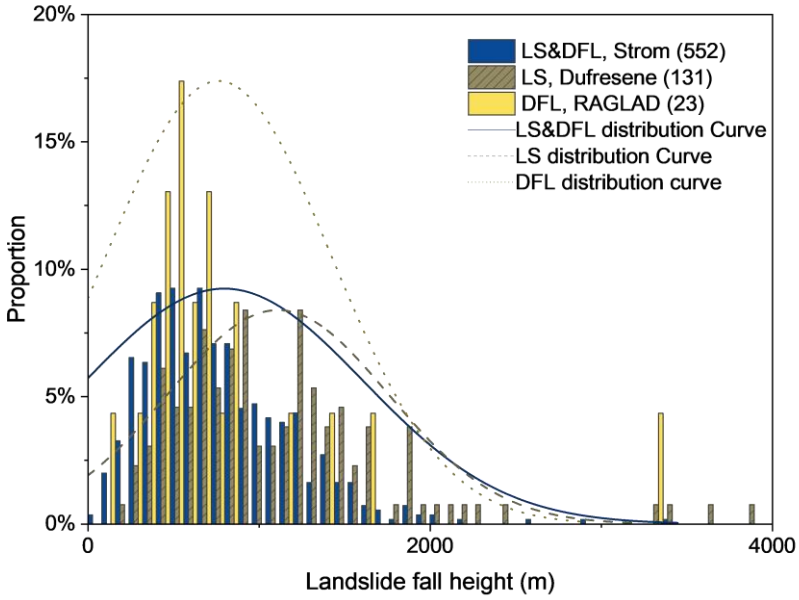

Figure 4-7 Landslide fall height data distribution from different landslide datasets (Landslide type: rock avalanches and rockslides; LS: landslides; Strom: a dataset from Rockslides and Rock Avalanches of Central Asia (dataset Index 4 as presented in Table 4-1, Strom and Abdrakhmatov 2018); Dufresne: an unpublished dataset (dataset index 3, Dufresne et al. 2021); RAGLAD: River Augmented Global LAndslide Dams dataset (dataset index 12, Wu et al. 2022; numbers are the sample sizes)

For the landslide volume, landslides contained in the database have a more even distribution while the landslide volume from DFLs is mostly concentrated in the volume of less than 250 million cubic meters (Figure 4-8). The distributions of these three datasets are similar, especially with the landslide volume less than 100 million cubic meters. A slight difference occurred on those landslides with large volumes exceeding 1000 million cubic meters, probably due to the data collection focus: the dataset collected by Dufresne et al. (2021) and Strom and Abdrakhmatov (2018) focused on those with more than one million cubic meter in volume, while RAGLAD included a broader volume range. However, if the landslide volume loss caused by erosion were considered (Malamud et al. 2004), the volume from the dataset collected by Dufresne et al. (2021) and Strom and Abdrakhmatov (2018) could be larger as they contain more historical landslides compared to RAGLAD (Wu et al. 2022). We also explored the relationship between landslide area and frequency density of rockslides and rock avalanches to explore the landslide size distribution (Figure 4-9). When DFLs are smaller at around 10^5 m^2 in area

(roll-over point), they didn't show a similar distribution with the data from rockslides and rock avalanches in Central Asia (Strom and Abdrakhmatov 2018). The potential reasons behind this could be either the insufficient sample size in the DFL dataset or landslides with smaller areas tend not to form the dam.

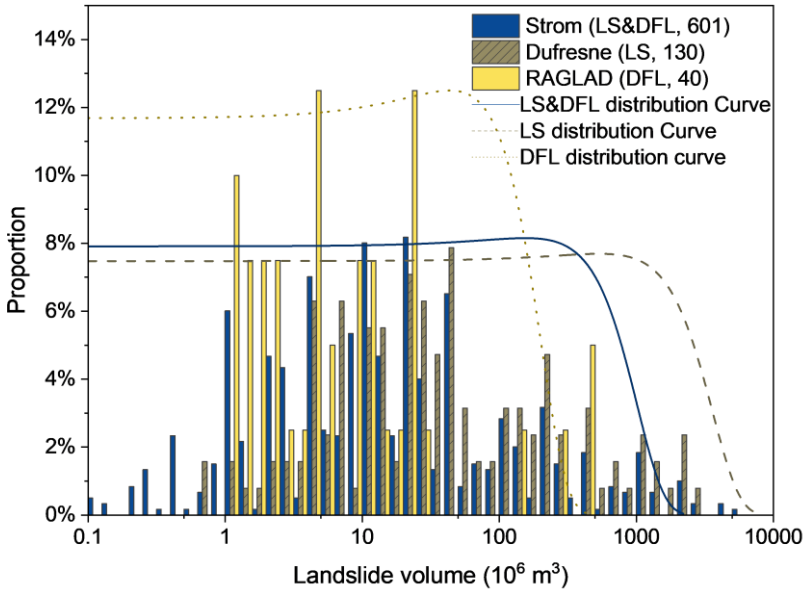

Figure 4-8 Landslide volume data distribution for landslides and DFLs (Landslide type: rock avalanches and rockslides; LS: landslides; LDam: DFLs; Strom: a dataset from Rockslides and Rock Avalanches of Central Asia (dataset Index 4 as presented in Table 4-1, Strom and Abdrakhmatov 2018); Dufresne: an unpublished dataset (dataset index 3, Dufresne et al. 2021); RAGLAD: River Augmented Global LAndslide Dams dataset (dataset index 12, Wu et al. 2022); numbers are the sample sizes)

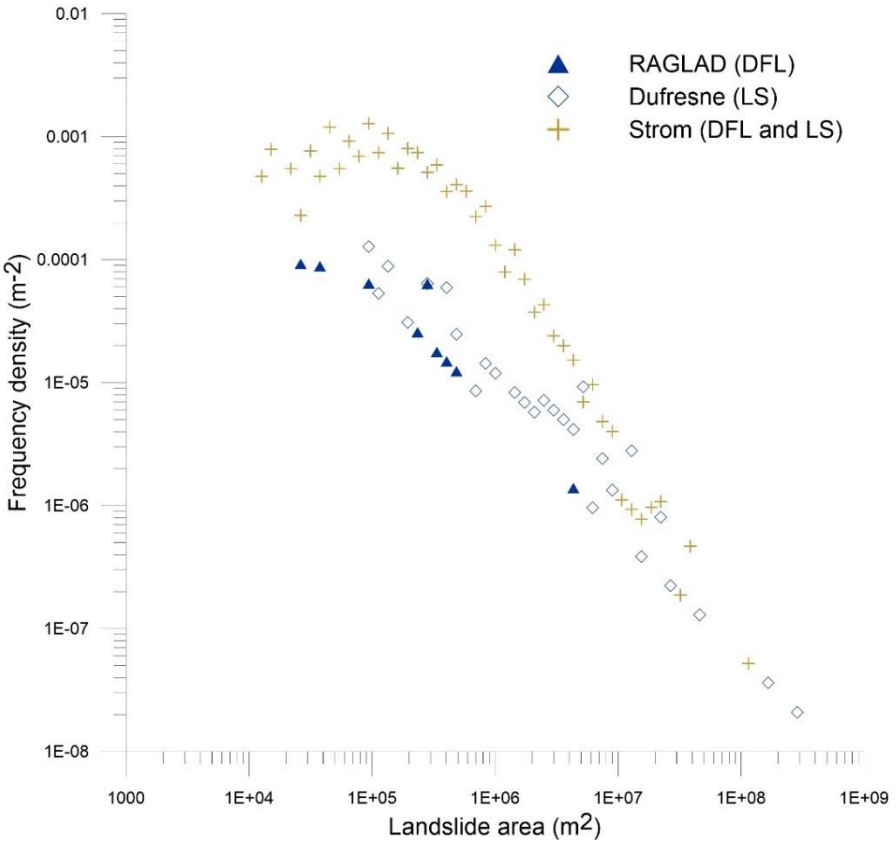

Figure 4-9 Relationship of landslide frequency densities and landslide area, for three landslide datasets (Landslide type: rock avalanches and rockslides): LS: landslides; DFLs: Dam forming landslides; Strom: a dataset from Rockslides and Rock Avalanches of Central Asia (dataset Index 4 as presented in Table 4-1, Strom and Abdrakhmatov 2018); Dufresne: an unpublished dataset (dataset index 3, Dufresne et al. 2021); RAGLAD: River Augmented Global LAndslide Dams dataset (dataset index 12, Wu et al. 2022); Frequency density calculated using the same method from Tanyas et al. 2018

The landslide area distribution for the DFLs and landslides in Japan showed that the planar area from the more than 90% of landslides that occurred in Japan is found in the range of less than 10^5 m^2, while area data from DFLs also have more data with a larger area, even with an area exceeding 1 km^2 (Figure 4-10). The landslide area distribution difference result is contrary to the landslide volume comparison of rock avalanches and rockslides given the positive correlation between landslide area and volume. This contrast may be caused by the spatial distribution of landslides if more landslides are located in the upstream area where the confined hillslopes hinder the landslide mass to travel longer and developing more surface area.

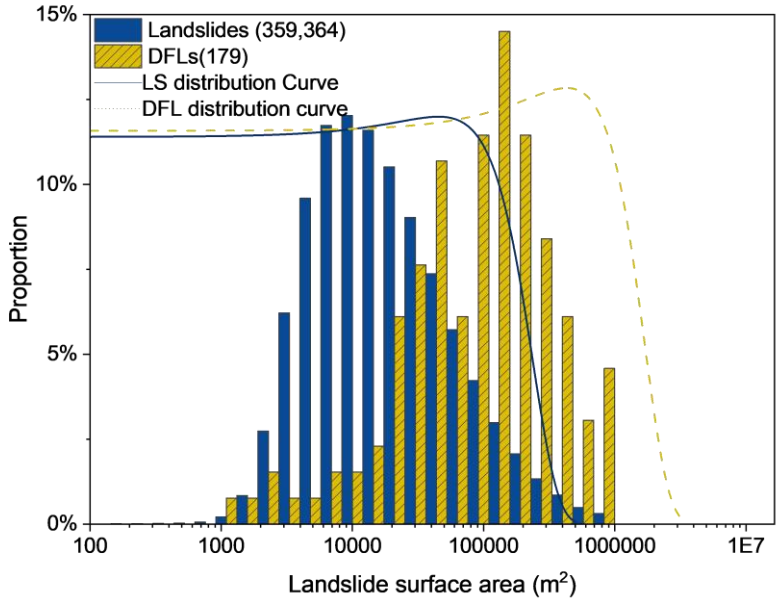

Figure 4-10 Landslide surface area distribution for landslides and DFLs from data records in Japan (Landslide type unclassified; Landslide data from Digital archive for Landslide Distribution Maps (dataset index 10, National Research Institute for Earth Science and Disaster Prevention of Japan, accessed in 2022); DFL data from RAGLAD: River Augmented Global LAndslide Dams dataset (dataset index 12, Wu et al. 2022); numbers are the sample sizes)

Based on the landslide size differences of DFLs and landslides, we further explore the relationship between landslide volume and landslide runout length (horizontal travel distance). The relationship between landslide runout distance and volume of landslides and DFLs presented differently at 2000 m (Figure 4-11): when the runout length is less than 2000 m, a greater volume of the landslide was required to block the river; however, the landslide volume could be less than average volume of landslides in a wider group to form a dam. Moreover, there is a clear division on the fitted curve with a 95% confidence band between landslides and DFLs. The significance coefficients (R^2) are strong for the relationship of landslide length and volume established based on the records from Rockslides and Rock Avalanches of Central Asia (Strom and Abdrakhmatov 2018) and RAGLAD (Wu et al. 2022), but the strong coefficient was not revealed in the rockslides and rock avalanches more generally (Dufresne et al. 2021, $R^2 < 0.2$). The division indicates that the relationship of landslide length and volume could be a good landslide dimension indicator to determine whether a landslide could form a LDam if other

conditions for LDam formation are also met. However, the relationship would require further exploration of other types of landslides besides rockslides/rock avalanches, if data were available.

In summary, the shallow landslides could be more likely to form LDam, this is also consistent with the descriptions of dam materials in RAGLAD (Wu et al. 2022): descriptions related to fragmented material, such as debris (26.6% of all records) and clay (10.8%), is more than those in descriptions related to obstacles, such as boulders (0.03%) and blocks (4.2%).

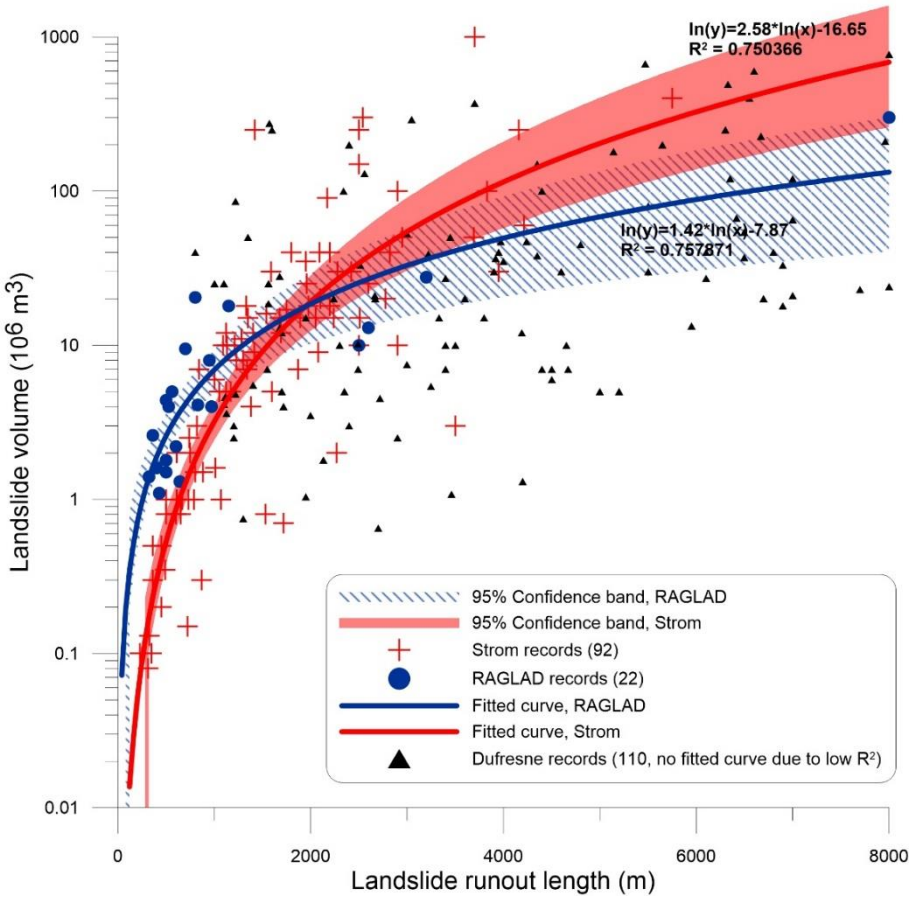

Figure 4- 11 Fitted curves of different landslide datasets based on the power relationship of landslide length and landslide volume (Landslide type: rock avalanches and rockslides; Strom: a dataset from Rockslides and Rock Avalanches of Central Asia (dataset Index 4 as presented in Table 4-1, Strom and Abdrakhmatov 2018); Dufresne: an unpublished dataset (dataset index 3, Dufresne et al. 2021); RAGLAD: River Augmented Global LAndslide Dams dataset (dataset index 12, Wu et al. 2022); numbers are the sample sizes)

4.3.2 Spatial Distribution Differences

The spatial distribution comparison showed that the DFLs are concentrated in the relatively upstream areas of the river systems compared with landslides more generally. More than 82% of DFLs were located at the catchment with an upstream catchment area of less than 500 km^2, while only 69% of landslides in the wider group are located in these areas (Figure 4-12). The rivers located in the upstream catchment at such scale were defined as "streams or small rivers" according to Bernhofen et al. (2021)'s classification. The landslides have more records (~20%) located in large catchments (> 1000 km^2) compared to DFLs (<6%). The median values of the upstream catchment area of DFLs and landslides are 230 km^2 and 289 km^2 respectively This catchment area difference of 59km^2 could lead to a river width difference of ~36 m based on the relationship between river width and catchment area by the global-scale study from Frasson et al. (2019) even with the large uncertainties of presenting such a single relationship for the catchments in different regions.

We also compared the elevation distribution based on the locations of records to see whether the difference also exists in the elevation distribution of DFLs and landslides (Figure 4-13). To avoid the problem that most locations of LDam records may be collected at the bottom of the valley (where the river is blocked) rather than on the uphill slope, the landslide height from RAGLAD was added to the original elevation extracted from MERIT DEM to adjust the elevation. Taking the upstream catchment area and elevation distribution comparison in combination, it is interesting that even though DFLs are located in the relatively upstream area, the elevation distribution did not show they are concentrated in the areas with a narrower range of elevation regardless of elevation adjustment. The spatial distribution of the LDam record is unique as the elevation distribution of DFL records is not similar to the elevation distribution of either all landslides or all the territory in Italy.

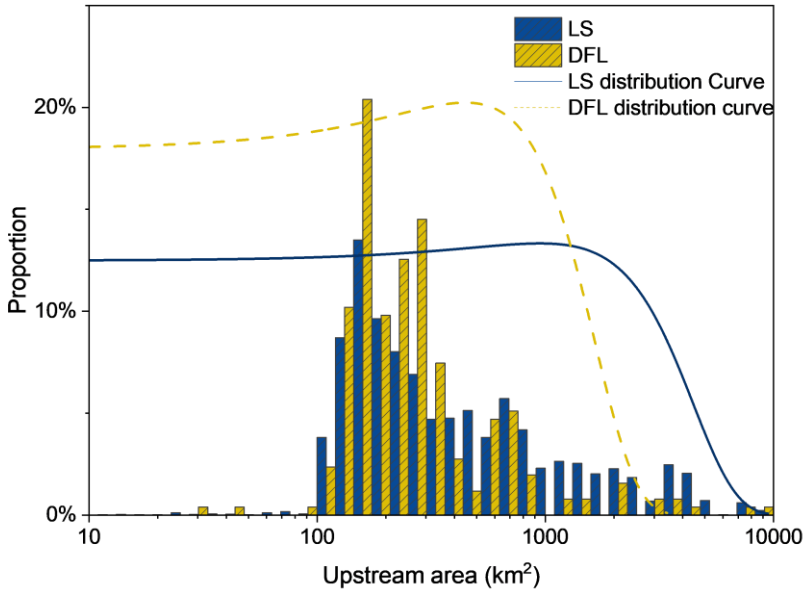

Figure 4-12 Upstream catchment area distribution of landslides and DFLs in Italy (Landslide type unclassified; LS: landslides more generally)

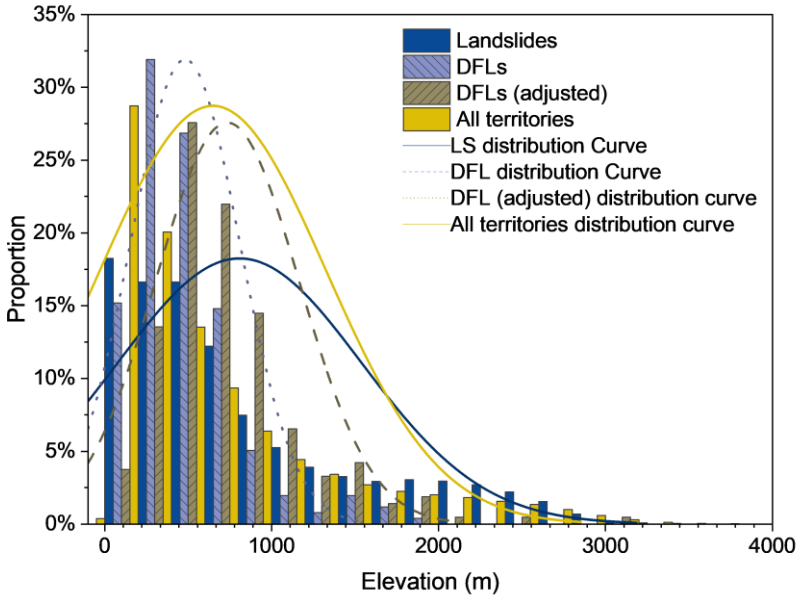

Figure 4-13 Elevation distribution of landslides, DFLs and spatially balanced samples from all territories in Italy with and without adjusted elevation (Landslide type: unclassified; adjusted elevation: landslide height was added to the original elevation; LS: landslides more generally; DFL: landslides that blocked the river)

It is expected that DFLs have a larger SPI (stream power index calculated from slope gradient (G) and upstream catchment area (CA), see Eq. 4-1) value compared to those of general landslides (Figure 4-14). The data distribution of SPI in the upstream subset of general landslides is similar to those including all of the landslide records in Italy but with higher SPI values. This SPI distribution result can be supported by the fact that LDam records have relatively smaller upstream catchments (Wu et al. 2022). The river knickpoint occurrence, where the channel slope in the river's long profile sharply changes, coincident with the LDam formation could also explain the high SPI, whilst the mechanism behind this connection is still under discussion (Fan et al. 2020). Steep narrow valleys require relatively small volumes of material to form dams; thus, even small mass movements present a potential for forming LDams in these locations.

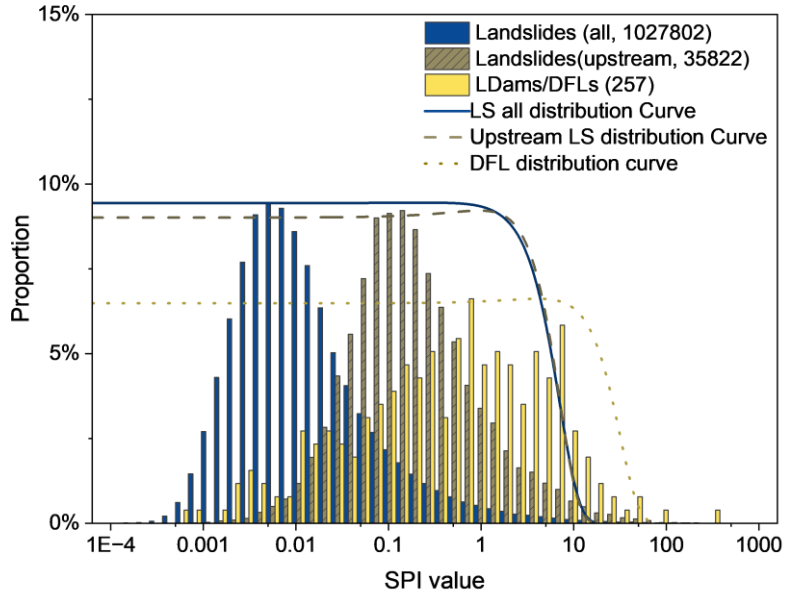

Figure 4-14 Stream power index (SPI) distribution of landslides and landslides that form LDams in Italy (Landslide type unclassified; numbers: sample size; Landslide all: all landslide records collected in Italy; Landslide upstream: landslides located in the upstream catchment area (upstream catchment area < 627 km^2)).

4.4 Discussion

4.4.1 Right-skewed Distribution of Landslide and Fluvial Characteristics

From the results above, it is clear that the landslide size (volume and area) of a wider group of landslides and DFLs both have a right-skewed distribution, although the overall size of the DFLs is smaller when compared to landslides more generally. One of the reasons behind this distribution is that landslides contain more records with smaller sizes. The landslide area and landslide volume of landslides followed the right-skewed distribution, which shows a large number of landslides clustered in the relatively small landslide size, despite the fact that large variations exist in general landslide types, spatial distribution patterns and triggering mechanisms. Two examples are: (i) Stark and Hovius (2001) indicated these distributions based on two regional-scale landslide databases with rollovers are probably caused by undersampled in small landslides due to spatial resolution; (ii) Malamud et al. (2004) examined and found that the frequency–area (or volume) statistics are in similar inverse-gamma distribution regardless of the magnitudes and mechanisms of triggers.

Even though DFLs are more likely to be formed in the relatively upstream area, the data of fluvial characteristics, such as the upstream area or river width around the points the landslide occurred, of both general landslides and DFLs, also illustrated the right-skewed distribution. Frasson et al. (2019) demonstrated a similar right-skewed distribution of several global river properties, including river width, sinuosity, meander wavelength, water surface slope, the ratio between meander wavelength and width, and upstream catchment area. The river width was also reported to follow similar log-normal distributions across the fluvial networks in headwater basins (Allen et al. 2018), which contributed to approximately 89% of the global fluvial network length (Downing et al. 2012). In other words, narrow rivers are much more common compared to wider rivers in the river system.

Therefore, the fact that landslides tend to cluster in the upstream areas with small catchment sizes can be supported by the distributions of landslide and fluvial characteristics which are all right-skewed, either from previous studies or from the spatial data distribution results in this study. Compared with the previous landslide studies, it is

clearly shown that most DFLs are of smaller volume, even though landslides in that range of small volume/area are likely to be undersampled due to spatial resolution, erosion, vegetation and human activities (Stark and Hovius 2001; Malamud et al. 2004). There are two assumptions to be considered behind this spatial distribution characteristics: (i) DFL tends to occur at the locations coinciding with landslide occurrence, i.e., LDam are more likely to form when more landslides are clustered nearby (higher landslide occurrence density), and landslides tend to form in upstream areas; (ii) LDam form because of the proximity to the river. Therefore, we did some further analysis on the relationship between LDam formation and landslide density/river proximity in the following section.

4.4.2 The Relationships Between LDam formation, and Landslide Occurrence/River Proximity

LDam may form in areas with higher landslide occurrence density. Fan et al. (2012) found that the landslide occurrence density directly affects LDam occurrence density along four cross-sections of Min River, China. However, we did not find the LDam occurrence and landslide density value show a strong relationship. We mapped the landslide density based on the landslide records (more than 1 million records in total) in Italy and extracted the landslide density value at the locations of the LDam records to explore whether this relationship occurs (Figure 4-15). A lot of LDams are located within low landslide density areas and most of them are located in areas with only a single landslide recorded location nearby (Figure 4-16). That is to say, when we extracted the landslide density value based on the location of the DFLs, we could not find them located in areas of high landslide density.

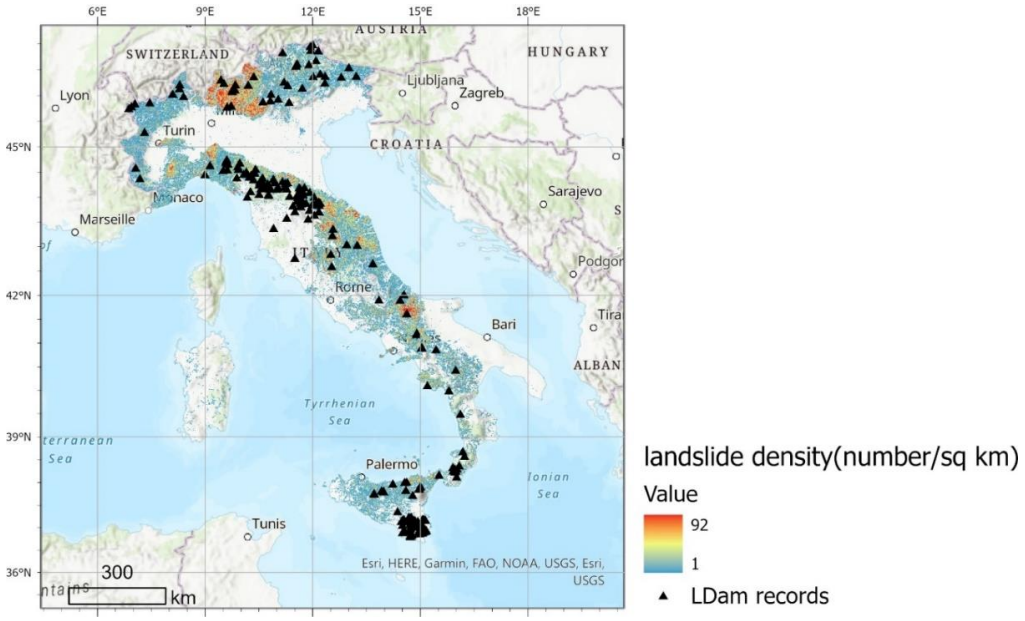

Figure 4-15 LDam records and landslide density map of Italy

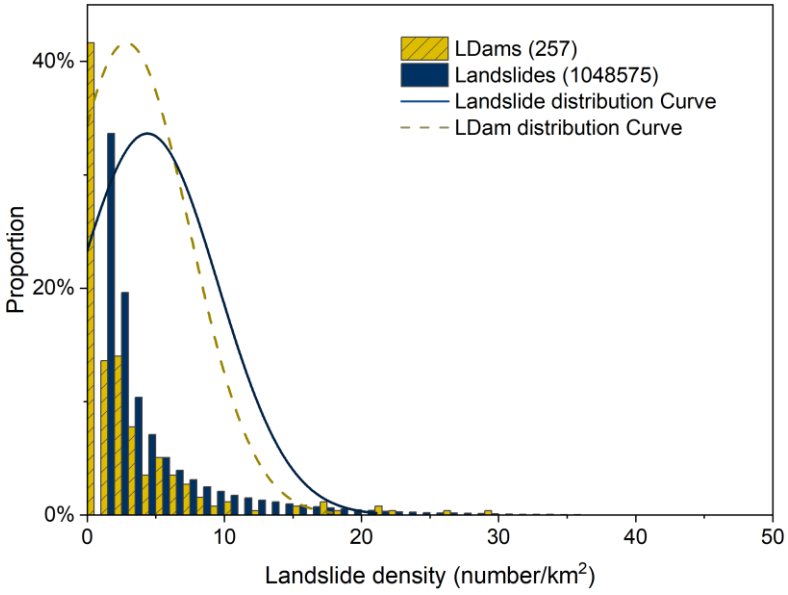

Figure 4-16 Landslide density distribution at the locations of landslide records and LDam records in Italy

In order to measure whether river proximity is related to LDam formation, we explored the data distribution of the landslide and LDam (or DFL) records to river channels from various fluvial datasets. Similar to how we adjusted the elevation of LDam records previously, we adjusted the distance to the river channels for the fact that most

LDam records were located at the bottom of the valley instead of the slope. The landslide length (horizontal distance of landslide body) from RAGLAD was added to the extracted distance to the river from various datasets. The DFLs either before or after the distance adjustment were located at locations with a shorter distance to river channels (Figure 4-17). The distribution of distance to GFD channel points from either the DFL (regardless of adjustment of distance) or landslides presented a similar distribution of distance to the river. The distribution of distance to the EU-Hydro river channels shows a shorter distance of LDam records compared to general landslides. However, the median value of adjusted distance to rivers from EU-Hydro and GFD is respectively 848 m and 6654 m, which shows a slightly higher value compared to other results of DFLs (56 m and 5274 m, respectively), but the median value is much smaller compared with those from the general landslide records. This result shows the effects of the locations of LDam records and landslide records as we have modified the distance of LDam records, but there is no further information for all the general landslide records, either the landslide crown, centre point of landslide body or landslide toe could represent landslide records in various landslide datasets. Despite these effects of record locations, the proximity to the river is an important factor for LDam formation as the differences existed between DFLs and general landslides with the fluvial datasets revealing more details.

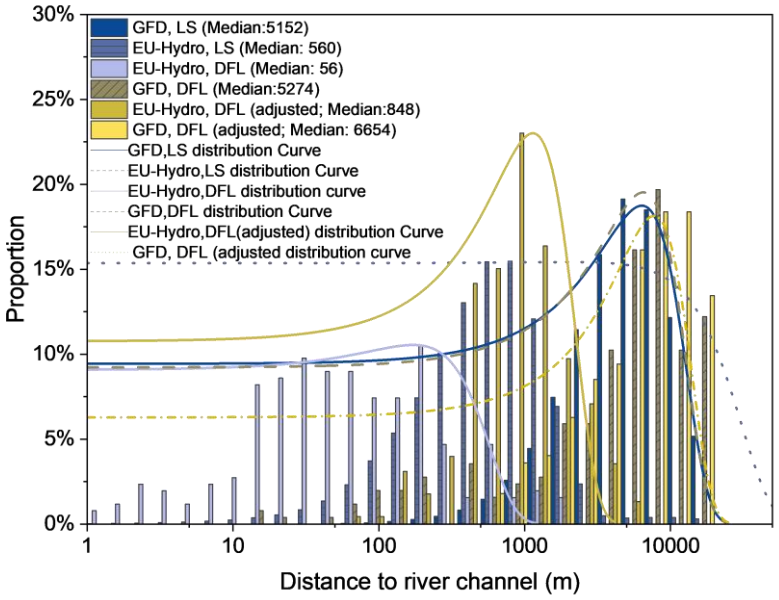

Figure 4-17 Distribution of distance to river channel, from either EU-hydro or a combination of GFDs, of DFLs and landslides (LS). (GFD: combined global fluvial datasets, including GRWL (Allen and Pavelsky 2018), MERIT Hydro (Yamazaki et al. 2019), and GLOW (Feng et al. 2022); EU-Hydro: a river and drainage network dataset derived from EU-DEM (European Environment Agency 2020))

4.4.3 Limitations

The scarcity of records of landslides, especially for DFLs, in some areas is an inevitable issue for data collection of global scale research because not all the areas have sufficient investment in research and development (R&D). Even though 12 datasets of landslides and LDams were collected from all over the world, most datasets did not contain quantified landslide morphometric data. Therefore, most morphometric comparisons in this research are carried out based on the specific types of landslides, rock avalanches and rockslides, which contain the most valid data in both landslides and DFLs. Additionally, the fact that current landslide records were exclusively recorded as point features reflect the difficulties of calculating the dimension data of landslide based on a GIS geometry calculation or some empirical relationships by using geomorphological parameters, such as the relationship between landslide volume and area (Larsen 2010; Fan et al. 2014). We did not do more analysis of differences based on the current datasets, because they would not change the result that LDam is located in the more confined areas of the upstream area compared to general landslides. These data source limitations for complete data comparison are inevitable at the current stage due to insufficient R&D investment and thus raise the significance of global fluvial dataset development and open access geolocated inventories of landslides with more completeness, especially the morphometric data and landslide types. If more data could be accessible for global-scale research, a LDam formation index could be proposed as they would present a clearer distribution difference in landslide dimensions and spatial distribution.

4.4.4 LDam Formation Zone

Even though the current global-scale LDam and landslide datasets are not perfect, we can still learn some lessons from the differences between them by illustrating the LDam formation zone with more details. The spatial distribution could potentially affect the landslide morphometric. For instance, DFLs tend to form in the upper reaches of

drainage systems with smaller catchment areas, where valleys are narrower and therefore they hit the other side of the valley in shorter runout distances and thus result in mobility and size differences. Moreover, the focus of landslides and LDam formation are also different, and thus the LDam formation zone will need to be quantified specifically. For the mechanism of general landslides formation, researchers focus more on the development of slope conditions, such as increment of shear stresses, low strength of slope materials and reduction of strength (Cruden and Varnes 1996). For LDam formation studies, it is more interesting to know why the dams formed on specific river reaches and thus not only the DFLs themselves but also require an understanding of the geomorphological and hydrological characteristics at the point of river blockage (Korup 2004; Fan et al. 2020).

According to the differences in landslide morphometric data and spatial distribution of DFLs and general landslides, DFLs tend to form in the upstream areas. We use a simplified schematic figure (Figure 4-18) to illustrate where these locations are along the river's longitudinal profile. The figure shows that the LDam formation zone, where DFL are prone to occur, falls in the areas between headwater areas and sediment transfer zones, where the slopes are steeper but within the smaller range compared to general landslides. The steeper slopes with shorter hillslope lengths in the upstream area may be one of the reasons that confine a landslide to develop into a larger one with a longer travel distance because the hillslope length increases along with the decreasing distance the length of the subsequent drainage path through the streams down to the watershed outlet (D'Odorico and Rigon 2003). As the river flow magnitude and slope gradient are the two major factors that determine stream power (Church 2002), the flow magnitude increases while the gradient decreases with increasing distance towards the river sources from headwaters. According to the SPI distribution difference (Figure 4-13), the LDam formed in those areas with much higher SPI values compared to general landslides, so LDam probably tends to form in those areas with the highest SPI value among all the river reaches.

For LDam formation zone identification, the prerequisites of these areas include landslide occurrence and river presence. River proximity could be an important factor that affects the probability of LDam formation. However, the area is not necessarily the

area with a high density of landslide occurrence, as the LDam record occurrence did not show a strong correlation with the density of landslide occurrence. Based on this schematic figure, we can propose some geomorphological aspects that may help identify the areas of LDam formation in the river channels with complete development, which include headwater sediment source zones (V-shaped valley), sediment transfer zones (U-shaped valley) and sediment depositional zone (flat-shaped valley), besides proximity to river and landslide occurrence:

1) Elevation limitation: either those elevations above the headwater or those below the elevation of the depositional area are excluded for LDam formation;

2) River width or upstream area limitation: only those located in the upstream area will need more focus because a large volume of landslide to dam the river will be more uncommon if the river width at specific reach is large;

3) Coastal area exclusion: the area along the coasts can be ignored for LDam formation, as most of them can be divided as depositional areas in the river system or the slide mass of a landslide occurring in the coastal zone cause displacement waves. However, the coastal areas on the mountainous islands may need to be included as smaller river systems.

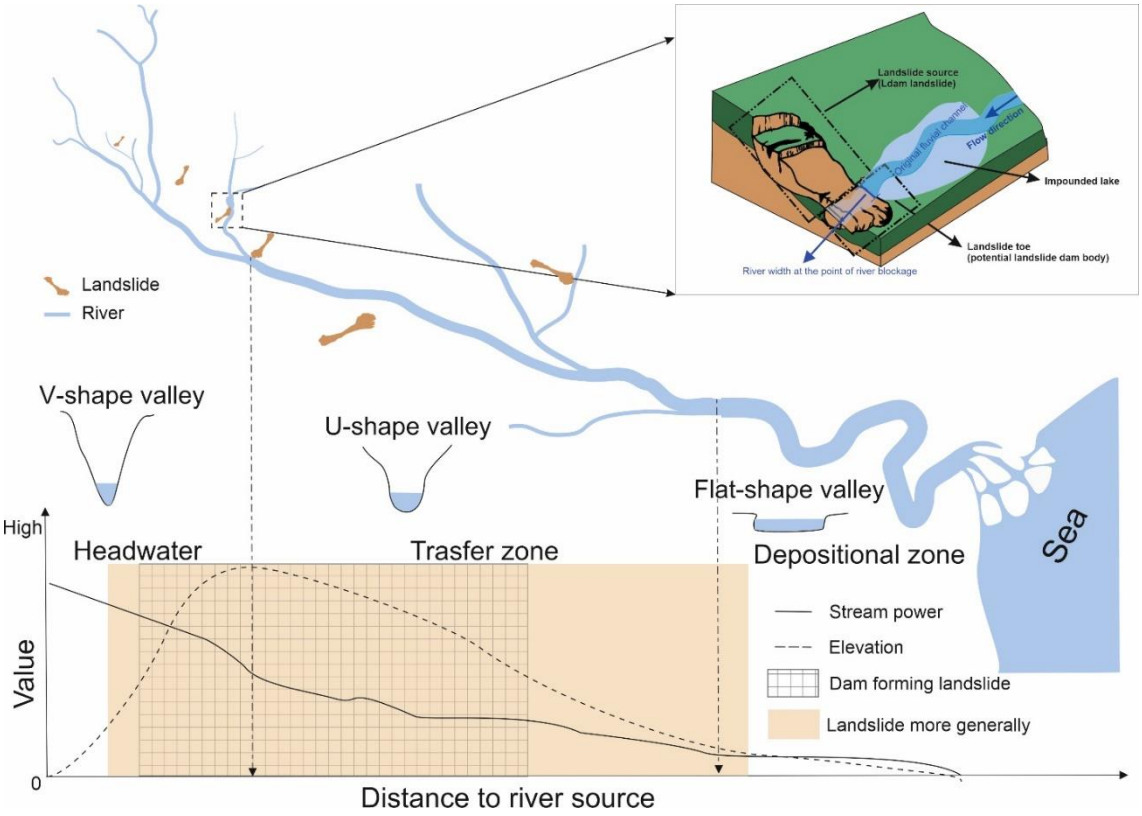

Figure 4-18 Schematic figure of the LDam formation zone (stream power modified from Church, 2002)

4.5 Conclusions

To identify the specific characteristics of landslides when they form river dams, we collected 12 open-access datasets of landslides and LDam records to compare the data distribution differences of dimension data, mainly landslide mobility and landslide size, and spatial distribution of landslides and DFLs. The landslide morphometric data was mainly compared within the landslide type of rock avalanches/rockslides by using the records from datasets with the most completeness in dimension data. To compare the spatial distribution, we explored the locations at the river system, such as the elevation and upstream catchment area, and the fluvial characteristics, such as stream power index, for the LDam and landslide records in Italy. We used global fluvial datasets, such as MERIT Hydro, and derived global-scale geomorphological datasets, such as geomorpho90, to extract the relative fluvial or geomorphological characteristics for special distribution comparison. It is the first time that the landslide spatial distribution in the river system has been compared to the spatial distribution of LDam records on a large

scale.

Upon the landslide morphometric data comparison of landslides and DFLs, DFLs are a special subset of all landslides. DFLs tend to form with a larger H/L ratio compared with landslides as a whole, which implies that LDams can be more easily formed with landslides with less mobility. According to the landslide volume and area comparison, larger shallower landslides are more efficient at forming LDams compared to deeper landslides. There is a clear division shown at the relationships between landslide runout distance and landslide volume derived from the landslide and DFL records. The morphometric data distribution still followed the nature of landslide size and fluvial characteristics, which is right-skewed.

For the spatial location distribution comparison, the LDam formation location is also unique based on the elevation distribution. The DFLs are concentrated on the upstream area of the river system but located in a more confined area where the SPI value is larger compared to landslides more generally. The result could explain the smaller landslide volume in dimension data comparison as the hillslope is steeper and thus confine the landslides preventing them developing with a larger volume. We explored the reasons behind spatial distribution differences by exploring the landslide occurrence density and river proximity. We found that the river proximity could be the reason that leads to this difference while the high landslide occurrence density will not be a necessary condition for LDam formation.

Based on the result of the data distribution comparison, a schematic zone to show those areas prone to LDam formation was proposed along the river longitude profile besides considering several aspects, including the presence of landslides and river channels, river proximity, fluvial and geomorphology characteristics. The research also provided some ideas on selecting the variables for differentiating a river blockage event and a non-blockage one by presenting differences between DFLs and landslides, most of which did not block the rivers.

4.6 References

Allen GH, Pavelsky TM (2018) Global extent of rivers and streams. Science 361(6402):585–588

Allen GH, Pavelsky TM, Barefoot EA, Lamb MP, Butman D, Tashie A, Gleason CJ (2018) Similarity of stream width distributions across headwater systems. Nat Commun 9(1), 610

Amatulli G, McInerney D, Sethi T, Strobl P, Domisch S (2020) Geomorpho90m, empirical evaluation and accuracy assessment of global high-resolution geomorphometric layers. Sci Data, 7(1), 162.

Bernhofen MV, Trigg MA, Sleigh PA, Sampson CC, Smith AM (2021) Global flood exposure from different sized rivers. Nat Hazards Earth Syst Sci 21(9):2829-2847

Borgomeo E, Hebditch KV, Whittaker AC, Lonergan L (2014) Characterising the spatial distribution, frequency and geomorphic controls on landslide occurrence, Molise, Italy. Geomorphology 226:148-161

Calvello M, Pecoraro G (2018) FraneItalia: a catalog of recent Italian landslides. Geoenviron Disasters 5(13):1-16

Capra L, Macías JL, Scott KM, Abrams M, Garduño-Monroy VH (2002) Debris avalanches and debris flows transformed from collapses in the Trans-Mexican Volcanic Belt, Mexico - behavior, and implications for hazard assessment. J Volcanol Geotherm Res 113:81–110

Caprari P, Della Seta M, Martino S, Fantini A, Fiorucci M, Priore T (2018) Upgrade of the cedit database of earthquake-induced ground effects in Italy. Ital J Eng Geol Environ 2:23-39

Cencetti C, De Rosa P, Fredduzzi A (2020) Characterization of landslide dams in a sector of the central-northern Apennines (Central Italy). Heliyon 6(6):e03799

Chengdu Water Authority (2020) Analysis of flood control situation in September 2020. Chengdu Water Authority. http://cdwater.chengdu.gov.cn/cdsswj/c109454/2020-

09/18/content_a00cf189c76b4188941ee3cacb815abd.shtml. Accessed 13 Nov 2022. (In Chinese)

Church M (2002) Geomorphic thresholds in riverine landscapes. Freshwater Biol 47(4):541-557

Corominas J (1996) The angle of reach as a mobility index for small and large landslides. Can Geotech J 33(2): 260-271

Costa JE, Schuster RL (1988) The formation and failure of natural dams. Geol Soc Am Bull 100(7):1054–1068

Costa JE, Schuster RL (1991) Documented historical landslide dams from around the world (No. 91–239), https:// pubs.usgs. gov/ of/ 1991/ 0239/report. pdf. Accessed 10 Jan 2021

Cruden DM, Varnes DJ (1996) Landslide types and processes, Transportation Research Board, U.S. National Academy of Sciences, Special Report. 247:36-75

D'Odorico P, Rigon R (2003) Hillslope and channel contributions to the hydrologic response. Water Resour Res 39(5)

Dai FC, Xu C, Yao X, Xu L, Tu XB, Gong QM (2011) Spatial distribution of landslides triggered by the 2008 Ms 8.0 Wenchuan earthquake, China. J Asian Earth Sci 40(4):883-895

Della Seta M, Esposito C, Marmoni GM, Martino S, Scarascia Mugnozza G, Troiani F (2017) Morpho-structural evolution of the valley-slope systems and related implications on slope-scale gravitational processes: New results from the Mt. Genzana case history (Central Apennines, Italy). Geomorphology 289:60-77

Devoli G, De Blasio FV, Elverhøi A, Høeg K (2009) Statistical analysis of landslide events in Central America and their run-out distance. Geotech Geol Eng 27:23-42

Downing J (2012) Global abundance and size distribution of streams and rivers. Inland Waters 2(4): 229-236

Dufresne A, Siebert L, Bernard B (2021) Distribution and geometric parameters of

volcanic debris avalanches. In: Roverato M, Dufresne A, Procter J. (eds) Volcanic Debris Avalanches - From Collapse to Hazards. Advances in Volcanology, Springer Heidelberg, pp75-90

Esposito G, Matano F (2021) CAmpi Flegrei LAndslide Geodatabase (CAFLAG). 4TU.ResearchData. Dataset. https://doi.org/10.4121/14440757.v2. Accessed 20 Feb 2022

European Environment Agency (2020) EU-Hydro - River Network Database, Copernicus Land Monitoring Service. https://land.copernicus.eu/imagery-in-situ/eu-hydro/eu-hydro-river-network-database?tab=metadata. Accessed 25 May 2022

Evans SG, Tutubalina OV, Drobyshev VN, Chernomorets SS, McDougall S, Petrakov DA, Hungr O (2009) Catastrophic detachment and high-velocity long-runout flow of Kolka Glacier, Caucasus Mountains, Russia in 2002. Geomorphology 105(3-4):314-321

Fan X, Dufresne A, Siva Subramanian S, Strom A, Hermanns R, Tacconi Stefanelli C, Hewitt K, Yunus AP, Dunning S, Capra L, Geertsema M, Miller B, Casagli N, Jansen JD, Xu Q (2020). The formation and impact of landslide dams – State of the art. Earth-Sci Rev 203

Fan XM, Rossiter DG, van Westen CJ, Xu Q, Gorum T (2014) Empirical prediction of coseismic landslide dam formation. Earth Surf Proc Land 39(14):1913–1926

Fan XM, van Westen CJ, Xu Q, Gorum T, Dai FC (2012) Analysis of landslide dams induced by the 2008 Wenchuan earthquake. J Asian Earth Sci 57:25-37

Feng D, Gleason CJ, Yang X, Allen GH, Pavelsky TM (2022) How Have Global River Widths Changed Over Time? Water Resour Res 58(8):e2021WR031712.

Frasson RPD, Pavelsky TM, Fonstad MA, Durand MT, Allen GH, Schumann G, Lion C, Beighley RE, Yang X (2019) Global relationships between river width, slope, catchment area, meander wavelength, sinuosity, and discharge. Geophys Res Lett 46(6):3252–3262

Froude MJ, Petley DN (2018) Global fatal landslide occurrence from 2004 to 2016. Nat Hazards Earth Syst Sci 18(8):2161–2181

Ghiglione D, Bettiza S (2023) Italy floods leave 13 dead and force 13,000 from their homes. BBC News. https://www.bbc.co.uk/news/world-europe-65632655. Accessed 20 May 2023

Guzzetti F, Ardizzone F, Cardinali M, Rossi M, Valigi D (2009) Landslide volumes and landslide mobilization rates in Umbria, central Italy. Earth Planet Sci Lett 279(3–4):222–229

Hovius N, Stark CP, Allen PA (1997). Sediment flux from a mountain belt derived by landslide mapping. Geology 25(3): 231-234

Hungr O, Leroueil S, Picarelli L (2014) The Varnes classification of landslide types, an update. Landslides 11(2):167–194

Iverson RM (1997) The physics of debris flows. Rev Geophys 35(3):245–296

Iverson RM, George DL, Allstadt K, Reid ME, Collins BD, Vallance JW, Schilling SP, Godt JW, Cannon CM, Magirl CS, Baum RL, Coe JA, Schulz WH, Bower JB (2015) Landslide mobility and hazards: implications of the 2014 Oso disaster. Earth Planet Sci Lett 412:197–208

Jaboyedoff M., Carrea D, Derron M H., Oppikofer T, Penna IM, Rudaz B (2020) A review of methods used to estimate initial landslide failure surface depths and volumes. Eng Geol 267, 105478

Jibson RW, Harp EL (2012). Extraordinary Distance Limits of Landslides Triggered by the 2011 Mineral, Virginia, Earthquake. Bull Seismol Soc Am 102(6):2368-2377

Jones ES, Mirus BB, Schmitt RG, Baum RL, Burns WJ, Crawford M, Godt JW, Kirschbaum DB, Lancaster JT, Lindsey KO, McCoy KE, Slaughter S, Stanley TA (2019) Summary Metadata – Landslide Inventories across the United States, U.S. Geological Survey data release, https://doi.org/10.5066/P9E2A37P. Accessed 20 Feb 2022

Kirschbaum DB (2019) High Mountain Asia Landslide Catalog, Version 1. Boulder, Colorado USA. NASA National Snow and Ice Data Center Distributed Active Archive Center. https://doi.org/10.5067/5ST0TZCD9RQ3. Accessed 23 Feb 2022

Kirschbaum DB, Stanley T, Zhou Y (2015) Spatial and Temporal Analysis of a Global Landslide Catalog. Geomorphology. doi:10.1016/j.geomorph.2015.03.016.

Korup O (2002) Recent research on landslide dams - a literature review with special attention to New Zealand. Prog Phys Geog 26(2):206–235

Korup O (2004) Geomorphometric characteristics of New Zealand landslide dams. Eng Geol 73(1):13–35

Larsen IJ, Montgomery DR, Korup O (2010) Landslide erosion controlled by hillslope material. Nat Geosci 3(4):247–251

Li H, Duan Z, Wu Y, Dong C, Zhao F (2021) The Motion and Range of Landslides According to Their Height. Front Earth Sci, 9, 736280

Linke S, Lehner B, Ouellet Dallaire C, Ariwi J, Grill G, Anand M, Beames P, Burchard-Levine V, Maxwell S, Moidu H, Tan F, Thieme M (2019) Global hydro-environmental sub-basin and river reach characteristics at high spatial resolution. Sci Data 6(1): 1-15

Malamud BD, Turcotte DL, Guzzetti F, Reichenbach P (2004) Landslide inventories and their statistical properties. Earth Surf Processes Landforms 29(6):687-711

Melillo M, Brunetti MT, Peruccacci S, Gariano SL, Guzzetti F (2016) Rainfall thresholds for the possible landslide occurrence in Sicily (Southern Italy) based on the automatic reconstruction of rainfall events. Landslides 13:165-172

Moore ID, Grayson RB, Ladson AR (1991) Digital terrain modelling: A review of hydrological, geomorphological and biological applications. Hydrol Processes 5: 3–30

National Research Institute for Earth Science and Disaster Prevention of Japan (2014) Digital archive for Landslide Distribution Maps. National Research Institute for Earth Science and Disaster Prevention of Japan. https://dil-opac.bosai.go.jp/publication/nied_tech_note/landslidemap/index.html Accessed 23 Feb 2022 (in Japanese)

Oppikofer T, Hermanns RL, Jakobsen VU, Böhme M, Nicolet P, Penna I (2020) Semi-empirical prediction of dam height and stability of dams formed by rock slope failures in

Norway Nat Hazards Earth Syst Sci 20(11):3179-3196

Palladino MR, Viero A, Turconi L, Brunetti MT, Peruccacci S, Melillo M, Luino F, Deganutti AM, Guzzetti F (2018) Rainfall thresholds for the activation of shallow landslides in the Italian Alps: The role of environmental conditioning factors. Geomorphology 303:53-67

Petley D (2012) Global patterns of loss of life from landslides. Geology 40(10):927–930

Perucca LP, Angillieri MYE (2009) Evolution of a debris-rock slide causing a natural dam: the flash flood of Rio Santa Cruz, Province of San Juan-November 12. Nat Hazards 50(2):305–320

Schmitt RG, Tanyas H, Nowicki Jessee MA, Zhu J, Biegel KM, Allstadt KE, Jibson RW, Thompson EM, van Westen CJ, Sato HP, Wald DJ, Godt JW, Gorum T, Xu C, Rathje EM, Knudsen KL (2017). An open repository of earthquake-triggered ground-failure inventories. U.S. Geological Survey data release collection, https://doi.org/10.5066/F7H70DB4. Accessed 23 Feb 2022

Simonett DS (1967) Landslide distribution and earthquakes in the Bewani and Torricelli Mountains, New Guinea, statistical analysis. In: Jennings JN, Mabbutt JA (eds), Landform Studies from Australia and New Guinea, Cambridge University Press, Cambridge, pp64-84

Stark CP, Hovius N (2001) The characterization of landslide size distributions. Geophys Res Lett 28(6):1091-1094

Strom A, Abdrakhmatov K (2018). Rockslides and Rock Avalanches of Central Asia - Distribution, Morphology, and Internal Structure. Elsevier.

Struble WT, Roering JJ, Burns WJ, Calhoun NC, Wetherell LR, Black BA (2021) The Preservation of Climate-Driven Landslide Dams in Western Oregon. J Geophys Res.: Earth Surf 126(4): e2020JF005908.

Sun J, Wang X, Liu H, Yuan H (2021). Effects of the attitude of dominant joints on the mobility of translational landslides. Landslides 18:2483-2498

Tacconi Stefanelli C, Catani F, Casagli N (2015) Geomorphological investigations on landslide dams. Geoenviron Disasters 2(1): 1-15

Tacconi Stefanelli C, Segoni S, Casagli N, Catani F (2016) Geomorphic indexing of landslide dams evolution. Eng Geol 208:1–10

Tacconi Stefanelli C, Vilímek V, Emmer A, Catani F (2018) Morphological analysis and features of the landslide dams in the Cordillera Blanca. Peru. Landslides 15(3):507–521

Tanyas H, Allstadt KE, van Westen CJ (2018) An updated method for estimating landslide-event magnitude, Earth Surf Processes Landforms 43(9):1836-1847

Toyos G, Dorta DO, Oppenheimer C, Pareschi MT, Sulpizio R, Zanchetta G (2007) GIS-assisted modelling for debris flow hazard assessment based on the events of May 1998 in the area of Sarno, Southern Italy: Part I. Maximum run-out. Earth Surf Processes Landforms 32(10):1491-1502

Trigila A, Iadanza C, Spizzichino D (2010) Quality assessment of the Italian Landslide Inventory using GIS processing. Landslides 7:455–470

van Westen C J, Zhang J (2018). Landslides and floods triggered by Huricane Maria (18 September, 2017) in Dominica. Digital or Visual Products, UNITAR-UNOSAT. http://www.unitar.org/unosat/node/44/2762 Accessed 23 May 2021

Varnes D J (1984) Landslide Hazard Zonation: A Review of Principles and Practice, Natural Hazards. UNESCO, Paris.

Wu H, Trigg MA, Murphy W, Fuentes R (2022) A new global landslide dam database (RAGLAD) and analysis utilizing auxiliary global fluvial datasets. Landslides, 19(3):555-572

Xu Q, Fan XM, Huang RQ, Westen CV (2009) Landslide dams triggered by the Wenchuan Earthquake, Sichuan Province, south west China. Bull Eng Geol Environ 68(3):373–386

Yamazaki D, Ikeshima D, Sosa J, Bates PD, Allen GH, Pavelsky TM (2019) MERIT Hydro: A High-Resolution Global Hydrography Map Based on Latest Topography

Dataset. Water Resour Res 55(6): 5053-5073

Yamazaki D, O'Loughlin F, Trigg MA, Miller ZF, Pavelsky TM, Bates PD (2014) Development of the Global Width Database for Large Rivers. Water Resour Res 50(4): 3467-3480

Chapter 5. A Global-scale Applicable Framework of Landslide Dam Formation Susceptibility

The formation and failure of landslide dams is an important and understudied, multi-hazard topic. A framework of landslide dam formation susceptibility evaluation was designed for large-scale studies to avoid the traditional dependence on landslide volume calculations based on empirical relationships, which requires comprehensive local landslide and landslide dam inventories. The framework combines logistic regression landslide susceptibility models and global fluvial datasets and was tested in Italy and Japan based on landslide and landslide dam inventories collected globally. The final landslide dam formation susceptibility index identifies which river reach is most prone to landslide dam formation, based on the river width and the landslide susceptibility in the adjacent delineated slope drainage areas. The logistic regression models showed good performances with area under the receiver operating characteristics curve values of 0.89 in Italy and 0.74 in Japan. The index effectively identifies the probability of landslide dam formation for specific river reaches, as demonstrated by the higher index values for river reaches with past landslide dam records. The framework is designed to be applied globally or for other large-scale study regions, especially for less studied data scarce regions. It also provides a preliminary evaluation result for smaller catchments and has the potential to be applied at a more detailed scale with local datasets. (Appendix B is the supplementary material for providing more details and data access related to this chapter.)

Keywords: landslides, landslide dams, global-scale, susceptibility, fluvial datasets, river hazards

5.1 Introduction

Landslide dams (LDams) represent a river blockage hazard caused by landslides obstructing river channels; LDams are frequently reported in international literature, particularly in mountainous regions with narrow river channels and steep hillsides in upstream catchment areas (Costa and Schuster 1988; Scarascia Mugnozza et al. 2006; Della Seta et al. 2017; Fan et al. 2020; Wu et al. 2022). Most LDams can form and

collapse within a short period, ranging from a few hours to a month, potentially causing significant flooding consequences. These floods result from upstream backwater floods above the blockage, and/or the breach or failure of the LDams, as well as the long-term effects on local geomorphological and hydrological conditions as a result of interactions between the hillslopes and fluvial systems (Costa and Schuster 1988; Korup 2002; Korup 2004; Scarascia Mugnozza et al. 2006; Fan et al. 2012; Della Seta et al. 2017; Fan et al. 2020; Wu et al. 2022). To predict and manage the risks posed by LDam formation, it is therefore imperative to be able to predict which specific river reaches are most likely to experience these events.

Evaluating the statistical probability of LDam formation on a local to regional scale has been the focus of many studies, which can be summarised into three major approaches: 1) Damming probability classification based on expert experience; 2) river blockage index establishment based on the empirical relationships of the landslide (deposit) volume and other related parameters; 3) the combination of probabilities related to LDam formation processes (source–pathway–receptor), including slope failure processes, landslide mass movement and mass deposition in the channel.

The first approach, damming probability classification, identifies the final probability of LDam formation as qualitative measurements, and it relies on the subjective experience of experts. For example, van Westen et al. (2020) established several standards for classifying landslide damming potential in Dominica, including the evidence of LDam records, potential LDam occurrence based on the calculated results from the empirical estimation of landslide volume, and other relevant geomorphological criteria of LDam formation.

The second approach, the river blockage indexes is a measurement of LDam formation probability or stability directly estimated from parameters related to LDam formation or stability, such as landslide volume, valley width, landslide velocity, catchment area, and dam height (see Table 5-1). Examples of these indexes are summarised in Table 5-1. Among all the parameters, we see that landslide (or LDam) volume is always used to establish such an index, alongside various other parameters also listed in the table. From Table 1, fluvial characteristics such as drainage area and river

width, are also identified as important variables when establishing a river blockage index.

Table 5-1 River blockage indexes for estimating the probability of LDam formation or stability

River blockage index name	Geomorphological parameters used other than landslide or LDam volume	Reference
Annual Constriction Ratio	Landslide velocity, valley width	Swanson et al. 1986
Dimensionless Blockage Index	Catchment area, dam height	Ermini and Casagli 2003
Blockage Index	Catchment area	Canuti et al. 1998; Casagli and Ermini 1999
Morphological Obstruction Index	Valley width	Tacconi Stefanelli et al. 2016; 2018
Backstow Index	Landslide height (maximum crest height of the LDam)	Korup 2004
Catchment ruggedness-based indices (CRBI)	Catchment area, mean slope of the catchment, Melton ruggedness number, the mean height of the dam, the width of the dammed valley, run-out distance	Shafieiganjeh et al. 2022

Finally, the LDam formation probabilities approach attempts to generate a final probability by combining the effects of LDam formation-related processes. Fan et al. (2014) estimated the LDam formation susceptibility using three combined steps, including evaluating landslide occurrence probability (traditional landslide susceptibility), and estimating landslide run-out distance and landslide volume by frequency–size assessments based on the empirical relationships and local datasets. In other words, they calculated the Dam Formation Landslide (DFL) susceptibility from three specific LDam formation-related processes: i) whether the slope is prone to slope failures; (ii) whether the landslide mass can travel far enough to reach the fluvial channel; and (iii) whether the landslide volume is sufficient to form a LDam. Another method is proposed by Tacconi Stefanelli et al. (2020), who proposed using damming predisposition and damming probability to estimate the probability of LDam formation. This method combined the separate processes of LDam formation into a single susceptibility index for evaluating the LDam formation probability of landslides.

However, these efforts exploring the probability of LDam formation require either comprehensive records with landslide dimension data or rely heavily on empirical formulas based on local conditions and expert knowledge, making it challenging to

prepare in advance for future landslide event occurrences, especially for application at large-scales, for which detailed inventories of landslides/LDams are usually unavailable. Moreover, it is noted that most previous research has focused predominantly on the surrounding hillslopes to predict the damming probability of potential landslides or current landslide reactivation, rather than identifying the LDam formation probability for the prone river reaches based on the joint information of landslide occurrence and the river characteristics. Most current LDam and landslide records are only recorded as point locations which makes it difficult to calculate the landslide dimension data for large-scale research that is needed to identify which river reach is most prone to having LDams form. Besides, the river blockage index derived from regional scale studies may not apply to other datasets and its application accuracy may not be reliable. Dufresne et al. (2018) found that the previous landslide dam stability thresholds were applicable to some large rockslide dams in the European Alps among their LDam records. Cencetti et al. (2020) showed that such an index is hard to generalize as it was generated from specific local geomorphological and hydrological conditions. Struble et al. (2021) also found that the dam stability index from another study didn't fit with their LDam records in Western Oregon and the scaling relationship between the upstream catchment area and landslide dam size was also not present in this area, which was contradictory to the previous studies.

We therefore develop a framework of LDam formation susceptibility evaluation based on slope drainage units that can be applied globally by combining a landslide susceptibility evaluation with global fluvial datasets to address the gaps identified above. The output of the framework is the LDam formation susceptibility for river reaches themselves. To test the effectiveness of this framework, we use the comprehensive data available from Italy and Japan to develop the framework given the limited numbers of robust datasets. These two countries are chosen as they are well-studied and their national-scale landslide records are available as open access to the public. The similarity of land areas, climate, geomorphology, geology and tectonic conditions, partially contribute to the control of certain large-scale constraints (Table 5-2). We also validate the susceptibility evaluation results using collected landslide and LDam records. The developed framework uses global-scale climate, geomorphological and fluvial datasets and therefore can be applied in the traditionally data-scarce areas to understand which

river reaches globally are most prone to LDam formation.

Table 5-2. Environmental parameters of Italy and Japan

	Italy	**Japan**
Land Area (km^2)	302073	377973
Mean annual rainfall (mma^{-1})	More than 3000 (European Alps, Palladino et al. 2018), to lower than 800 (Sicily, Melillo et al. 2016)	1000-4500 (Saito et al. 2015)
Mean annual temperature (°C)	13.5	12.36
Geology and landforms	Mountain areas dominated by metamorphic and sedimentary rocks in the Alps, marly-limestones and flysch in the Apennines. Volcanic and metamorphic rocks mainly outcrop in Sardinia and Calabrian mountains.	Mountain areas dominated by recent volcanics with Neogene sedimentary rocks forming lower ground
Tectonics	Compressional tectonics are represented in some parts of the alpine regions while extensional tectonics dominate the middle to southern Apennines.	Compressional tectonics

5.2 Data Sources

5.2.1 Landslide and LDam Datasets

A total of more than 1 million landslide records and 779 LDam records, most of which are geolocated, were collected globally from datasets covering different spatial scales. The details of the datasets used are provided in Table 5-3. These records were utilised to identify the appropriate input variables for a landslide susceptibility evaluation model applied in different regions, creating training datasets for establishing the model and validating the susceptibility results.

Table 5-3 Datasets of landslide and LDam records

Name	Time coverage	Scale (Area)	Number of landslide records /events	Contributors
Landslide Inventories from An Open Repository of Earthquake-Triggered Ground-Failure Inventories	Since 1900	Global (event-based)	356,497 geolocated data	Schmitt et al. 2017
Landslide Inventories across the United States	1900-2019	National (U.S.A.)	64,433	Jones et al. 2019
Dufresne (unpublished inventory)	-	Global	179	Dufresne et al. 2021
Rockslides and Rock Avalanches of Central Asia	-	Regional (Middle Asia)	1016	Strom and Abdrakhmatov 2018
Global Landslide Catalog (GLC)	2007-2019	Global	14,532	Kirschbaum et al. 2015
FraneItalia	From January 2010 to 2017	National (Italy)	5438(single)+1787(areal)	Calvello and Pecoraro (2018)
High Mountain Asia Landslide Catalog V001(HMS_LS)	1956-2018	Regional (Asia)	12,755	Kirschbaum et al. 2019
Landslides in Dominica	-	National (Dominica)	10,551	van Westen and Zhang (2018)
CAmpi Flegrei LAndslide Geodatabase (CAFLAG)	1828-2017	Local (Campi Flegrei caldera, Italy)	2302	Italian National Research Council (CNR) (Esposito and Matano, 2021)
Digital Archive for Landslide Distribution Maps	1981-2014	National (Japan)	359,387 mass movement polygons	National Research Institute for Earth Science and Disaster Prevention of Japan (Accessed in 2022)
Italian Catalogue of Earthquake-Induced Ground Failures (CEDIT)	1169-2019	National (Italy)	2077	Martino et al. 2022
River Augmented Global Landslide Dams (RAGLAD)	Since 8 century	Global	779	Wu et al. 2022
IFFI project (Italian Landslide Inventory)	1116-2017	National (Italy)	620,808	Trigila et al. 2010

5.2.2 Global Fluvial Datasets

Global fluvial datasets have been developing rapidly in the past decade (Lehner and Gill 2013; Yamazaki et al. 2014; Allen and Pavelsky 2018; Linke et al. 2019; Yamazaki et al. 2019; Frasson et al. 2019; Feng et al. 2022). According to the previous global-scale LDam dataset research by Wu et al. (2022), global fluvial datasets provide a more reliable and consistent data source for determining river width compared to

estimating it through a simple empirical relationship between drainage area and river width. This was demonstrated by Frasson et al. (2019), who showed significant variations in results between catchments across different regions when compared to directly applying a single relationship.

Multiple global fluvial datasets were included in several stages in this research: MERIT Hydro, a global fluvial dataset containing the data of river width at a resolution of 90 m (Yamazaki et al. 2019), was used for the river width data for the LDam formation susceptibility evaluation model establishment; HydroBASINS, the catchment boundaries and sub-basin delineations derived from HydroSHEDS data with twelve scales/levels (Lehner and Gill 2013), was utilised to further delineated the slope drainage area; HydroATLAS, a global compendium of hydro-environmental characteristics for all sub-basins of HydroBASINS (Linke et al. 2019), was used to explore related basin characteristic variables for the landslide susceptibility evaluation model establishment.

5.3 Methods

The LDam formation susceptibility framework consists of four main stages, as shown in Figure 5-1 and introduced here, and followed below by a more detailed description for each stage, and even further detail in the supplementary (Appendix B1). Firstly, all necessary data was collected, and the study areas were prefiltered to identify locations susceptible to LDam formation, specifically where local conditions are prone to LDam formation, and a previous landslide record exists within the catchment. Secondly, there are two processing steps that proceed in parallel: 1) further delineating slope drainage units as the main calculation unit, based on the current HydroBASIN sub-catchments and the Forest And Buildings removed Copernicus Digital Elevation Model (FABDEM, Hawker et al. 2022); 2) performing a landslide susceptibility evaluation based on the collected landslide records. Thirdly, the delineated slope drainage units are then categorized based on their locations and the median landslide susceptibility index extracted from each slope drainage unit to represent the landslide occurrence probability of each delineated slope drainage unit. Fourthly and finally, the Landslide Susceptibility Index (LSI) around a specific river reach was derived by first accumulating the landslide

occurrence probability on all adjacent slope drainage units around the reach, which was further combined with the river width data from global fluvial datasets to calculate the spatial probability of LDam formation on each river reach.

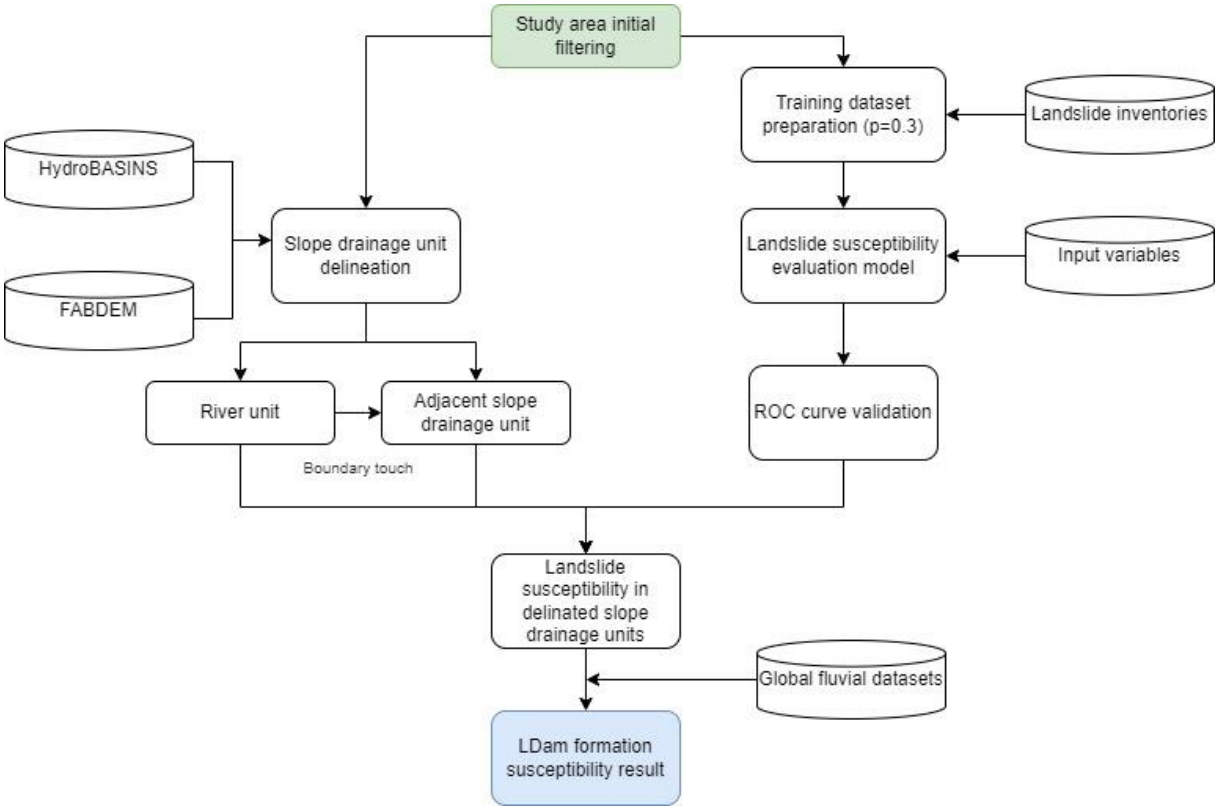

Figure 5-1 Schematic figure of research methods for establishing the LDam formation susceptibility framework by combining the landslide susceptibility model and global fluvial datasets (the visualisation of this framework with more details is shown in Appendix B1)

5.3.1 Initial Area Prefiltering for LDam Formation Study

Prefiltering the study area for the LDam formation susceptibility evaluation beforehand is crucial to avoid the burden of significant unnecessary computational workload for a large-scale modelling application. An example of a rainfall threshold for landslide susceptibility in the Bhutan Himalayas was proposed by Dikshit et al. (2019), suggesting that a 30-day antecedent precipitation of 350 mm serves as a threshold. As geomorphological data differences were observed when the landslides or LDam records were located in different regions (Jibson and Harp 2012; Tacconi Stefanelli et al. 2018), we prefiltered those areas with current landslide and LDam records located nearby to

reduce the potential data bias caused by the regional differences. Moreover, according to previous global-scale LDam dataset research (Wu et al. 2022), the DFLs present some distinctive dimensional and geomorphological characteristics when compared with landslides more generally, such as landslide height/length ratio (a parameter to show the mobility of landslide). A potential threshold for LDam formation was proposed by Wu et al. (2022), based on the relationship between river width and landslide volume, which means that some wider river reaches have little probability to be dammed due to the limited landslide size relative to the river scale.

Therefore, the LDam formation zone has the prerequisites of (i) potential landslide occurrence and (ii) the presence of a river with blockable width in the surrounding area. The condition for prefiltering the LDam formation zones mainly included the presence of landslides and LDam records within a 19 km searching radius (a likely maximum envelope for DFL travel, Wu et al. 2022), proper climate conditions, such as sufficient rainfall and appropriate temperature to form active/perennial rivers or to trigger landslides, in which landslides located in the river reaches with a width that landslides can be dammed, and the exclusion of river reaches along the continental coastline to avoid the underrepresentation of river width of anabranching river reaches in global fluvial datasets (Yamazaki et al. 2019). The schematic figure of the prefiltering method and the results are shown in Figure 5-2 with more details of the prefiltering procedures illustrated in Appendix B2. The prefiltered methods were performed based on the level-12 HydroBASINS sub-catchments products, which have an average area of 130.5 km^2 because the level-12 sub-catchments are the highest resolution.

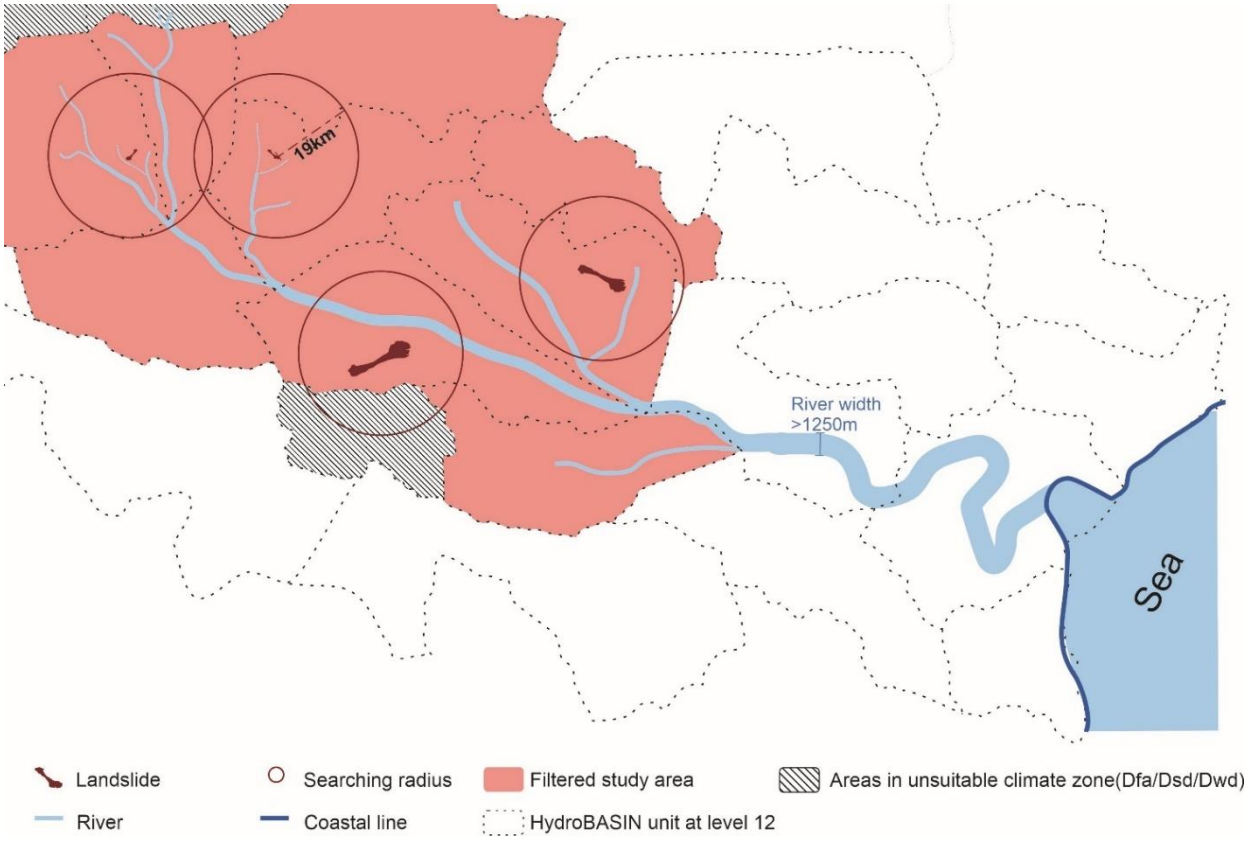

Figure 5-2 Schematic figure of the prefiltering of the LDam formation study area: the areas near landslides and rivers with blockable width, excluding coastal areas and areas in unsuitable climate zones

5.3.2 Slope Drainage Unit Delineation by Pfafstetter

Selecting a proper mapping unit (or "terrain unit") is crucial to map the spatial probability of a specific hazard in susceptibility modelling (Guzzetti et al. 2005). Reichenbach et al. (2018) summarised the mapping units from previous landslide susceptibility evaluation research into seven groups and found that the most common mapping units are grid units (86.4% of the articles), slope units (5.1%), and unique condition units (4.6%). However, the relative performances and comparisons of the grid unit, slope unit, and subbasin unit are still under discussion. Compared with grid units-based mapping which is the most common approach being applied in the statistical-based hazard susceptibility evaluation modelling, slope mapping units are still in exploration although they have already been found to be a powerful tool for regional hazard susceptibility mapping and consistently exploiting heterogeneous information (Jacobs et al. 2020). Erener and Duzgun (2012) found that a susceptibility evaluation model mapped

with slope units had a better performance compared to those models based on grid cells. Martinello et al. (2021) compared the three different slope unit delineation methods and found that all methods maintained a great predictive performance compared with a pixel-based model. Palau et al. (2020) found that the quality of gridded landslide susceptibility mapping decreased with resolution while the subbasin method had a better performance compared with the grid unit at 100 m resolution. The transferability of some automatic unit delineation methods for mapping susceptibility requires further validation, as van Westen et al. (2020) found that the results when directly applying the slope unit delineation method from Alvioli et al. (2020) were not suitable for landslides in Dominica, because they contained many inconsistencies. All mapping units have their pros and cons, so the selection of mapping units relies on multiple factors, such as the study's purpose, computation cost and model performance.

For this study, we chose to use the classic hydro-morphological unit, named as a slope drainage unit, based on an automatic subbasin coding method, Pfafstetter (Verdin and Verdin 1999). Slope drainage unit is a further delineated drainage unit of the geomorphological gully from FABDEM based on the most detailed HydroBASIN drainage unit. A unit encompassing hillslope processes and river processes is required for this study, as our framework for LDam formation combines both these processes. All the sediment and flow accumulate within each slope drainage unit at the same outlet. Although the subcatchments are available in the HydroBASINS product, some small river reaches/subcatchments were underrepresented as they were delineated based on a 90 m resolution digital elevation model (DEM) (Lehner and Gill 2013). With the higher resolution data, we carried out further delineation jobs based on the FABDEM at a resolution of 30m (Hawker et al. 2022). This improves the resolution of the delineated slope drainage units to resolve smaller river reaches. The refined delineation was implemented in the open-source Python pyflwdir package (Eilander 2020). To validate whether the resulting delineated slope drainage areas were reliable, the FABDEM derived slope drainage units were compared to high resolution LiDAR (Light Detection And Ranging) derived catchments in Dominica (see Figure 5-3) (Trigg et al. 2023). The FABDEM delineated boundaries have a high similarity with the LiDAR catchments with an 81.3% area overlap. The locations with the largest differences are mainly located along

the coast, which is generally not important for LDam formation susceptibility modelling.

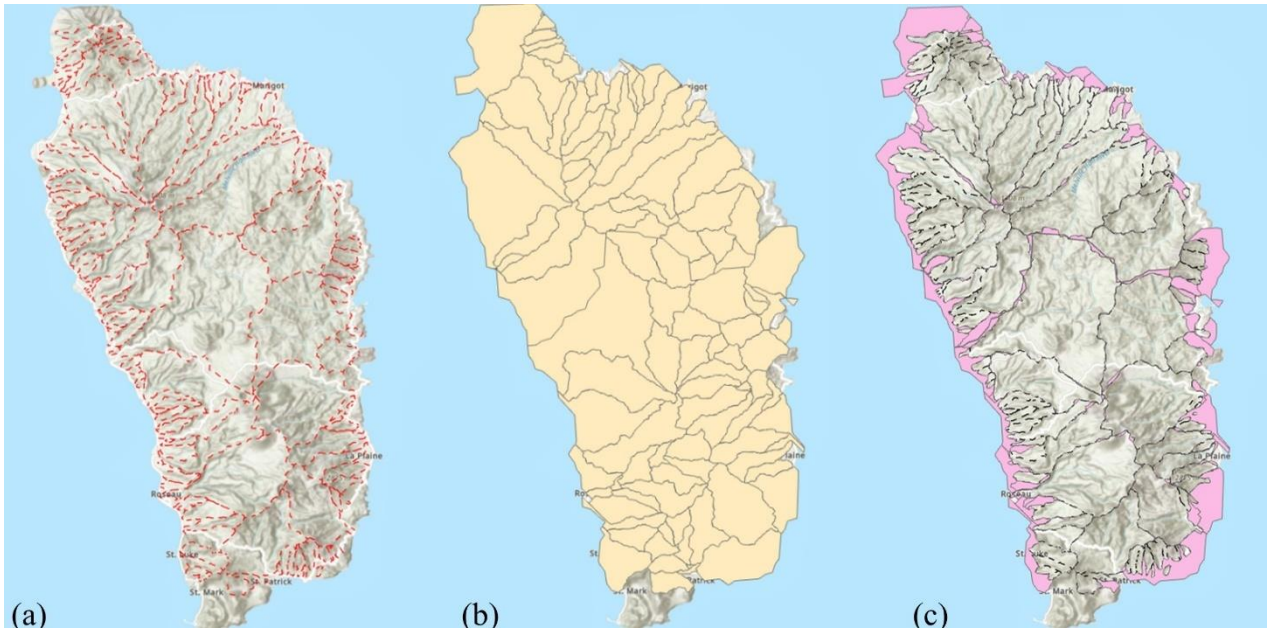

Figure 5-3 Validation of FABDEM delineated slope drainage units against catchments derived from Dominica: (a) river catchment delineation result based on LiDAR data (Trigg et al. 2023); (b) slope drainage unit delineation result by Pfafstetter method based on FABDEM data; (c). Boundary difference areas of the two datasets are highlighted in pink.

Once the slope drainage unit delineation results had been validated, those units were further separated into river units and adjacent slope drainage units for further LDam formation susceptibility calculations. The river units are those slope drainage units that intersect with river reaches from the global fluvial datasets and the adjacent slope units are those units that sit immediately adjacent to the boundaries of the river units (see Figure 5-4). The delineated slope drainage unit can provide a geomorphology-based buffer zone instead of a distance-based buffer zone to define the "adjacent areas" that are prone to LDam formation (Data access to the delineated slope drainage can be found at Appendix B3).

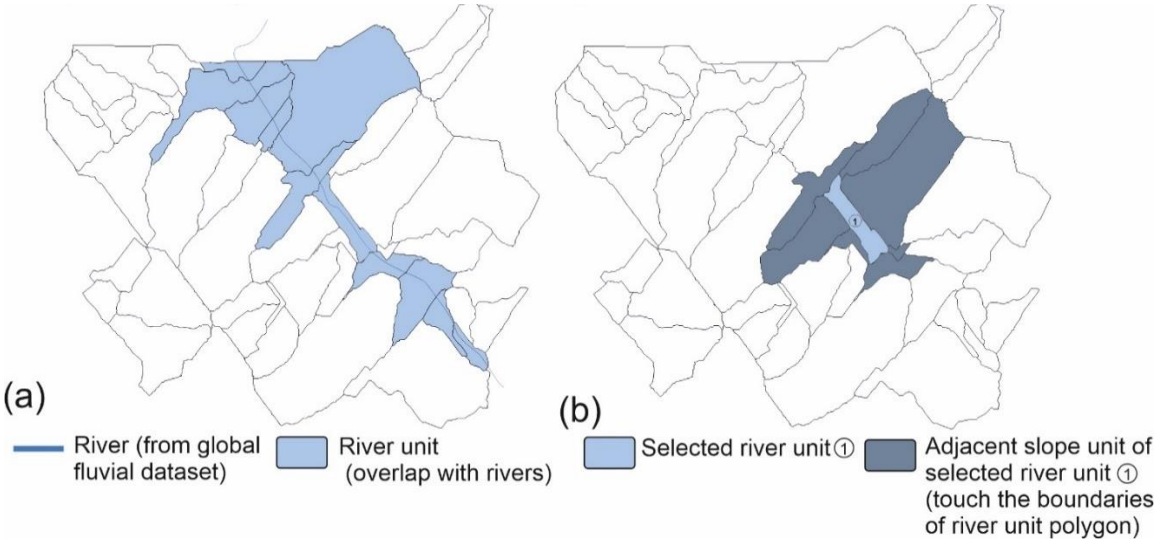

Figure 5-4 Example figure showing the identification of the river unit and adjacent slope drainage units from the delineated slope drainage units: (a) river reach and intersected river units. (b) adjacent slope units to a single river unit.

5.3.3 Landslide Susceptibility Evaluation Model

Landslide susceptibility describes the spatial probability of landslide occurrence in a given location based on a set of specific geomorphological and environmental conditions (Guzzetti et al. 2005). Because input data and calibration for these physically based models are not practical for large-scale regional studies, especially global-scale, statistical-based methods are more widely applied in the large-scale landslide susceptibility evaluation (Nadim et al. 2006; Stanley and Kirschbaum 2017; Lin et al. 2017).

The logistic regression model is commonly applied in previous landslide susceptibility evaluation studies and was demonstrated to be efficient at various spatial scales from local to global scale (Ayalew and Yamagishi 2005; Rossi et al. 2010; Dou et al. 2015; Budimir et al. 2015; Lin et al. 2017; Raja et al. 2017). For large-scale landslide susceptibility modelling, the further delineation of landslide types and triggers is normally not considered during the modelling methods (Nadim et al. 2006; Lin et al. 2017). The logistic regression model predicts the probability of a landslide occurrence at specific locations based on the relationship between landslide occurrences and related variables. The general formulas of the logistic regression model for landslide susceptibility evaluation, based on grid cell units, are described in Eq. 5-1 and 5-2:

$$P(landslide\ occurrence\ ) = \frac{1}{1 + e^{-z}} \quad \text{(Eq. 5-1)}$$

$$z = \beta_0 + \beta_1 \times x_1 + \beta_2 \times x_2 \ldots \ldots \beta_n \times x_n \quad \text{(Eq. 5-2)}$$

Before inputting into logistic regression model, all the categorical variables were changed into dummy variables, which is a bivariate variable (0 or 1) of each attribute of specific variables. As a result, each categorical variable layer was transferred as multiple dummy variable layers, whose total number is equal to n-1 where n is the number of different attribute numbers of a specific categorical variable. The output value P (landslide occurrence) in Eq. 5-1 of a logistic model ranges from 0 to 1, typically described as the landslide susceptibility index (LSI), which shows the spatial probability of future landslide occurrence at a given location. If the LSI value approaches 1, it means that the given location is more likely to have a landslide occurrence; if the LSI is close to 0, it means that the given location has much less probability of landslide occurrence. z is a dependent variable that reflects landslide occurrence based on all input variable x_n. β_n is the coefficient of a specific variable measuring the importance of the final evaluation result based on the past landslide records (the coefficient is the constant when n=0).

According to Martinello et al. (2020), grid-cell units appear to be the more suitable measurement unit for modelling, while dimensionally appropriate slope units seem to be the most effective way to generate accurate landslide susceptibility maps. Therefore, a few studies have combined these two unit types together to achieve the final landslide susceptibility evaluation result (Domènech et al. 2020; Martinello et al. 2020). In our study, the final LSI evaluation result is modelled and assessed based on the grid cell first. The result of the grid cell approach was then aggregated to identify the LSI based on the delineated slope drainage unit by assigning the median LSI value within each slope drainage area to present the spatial probability for the whole unit.

5.3.3.1 Variables exploration for landslide susceptibility evaluation

Previous research can provide a foundation for selecting appropriate variables to evaluate landslide susceptibility by identifying potentially useful characteristics. Variables that were applied in previous landslide susceptibility studies mainly came from

the fields related to the conditions required for landslide occurrence, such as geology, hydrology, land cover, and geomorphology (Reichenbach et al. 2018).

We first selected those variables related to landslide occurrence from HydroATLAS, a global-scale compendium of hydro-environmental characteristics for all sub-basins of HydroBASINS (Linke et al. 2019). We use these to explore the relationship of variables to landslide occurrence, based on the landslide records collected from the datasets in Table 5-2. HydroATLAS contains 56 variables, partitioned into 281 individual attributes. A subset of 23 variables in HydroATLAS was selected after excluding anthropogenic variables and other non-related natural variables. The data distribution of all selected variables was assessed. If the data distribution of a specific variable is a uniform distribution, the variable would be removed because the variable is not helpful to the predictive model if any value of the variable contributes equally to landslide occurrence. For each variable, the priority was on selecting the attributes of annual average values (for average conditions) and those focused on river reaches (segments). For the statistical susceptibility evaluation model application, the dependence between input variables is an inevitable issue to be addressed. The selected attributes were further assessed for correlation by using the Pearson matrix (Table 5-4). When two attributes have a strong correlation ($p > 0.5$), only one was kept. The one that was kept was the one which is from a more easily accessible data source and process and also has no strong correlations with other attributes. Even though their correlation is strong, slope angle and elevation were both kept for the landslide susceptibility model to make our research more comparable to previous research, which also use both variables, mainly because they are two significant controlling factors of landslide occurrence and have different impacts on the susceptibility mapping (Alkhasawneh et al. 2013; Dou et al. 2015).

The final 11 selected variables for landslide susceptibility evaluation are: river area, elevation, slope, curvature, air temperature, precipitation, landcover classes, potential natural vegetation classes, clay fraction in soil, lithological classes, and soil erosion rate. All the numerical variables were transformed with a quantile transformer to make them dimensionless and to improve the performance of the predictive models, as this data transformation is a robust pre-processing scheme and makes the variables measured at different scales more directly comparable (Pedregosa et al. 2011).

Table 5-4 Correlation matrix for exploratory research of input variables for landslide susceptibility evaluation (those highlighted with red colour are the attributes with a strong correlation, p>0.5)

Variable name	Natural discharge (dis)	Surface Runoff (run)	River Area (ria)	River Volume (riv)	Elevation (ele)	Terrain slope (slp)	Stream gradient (sgr)	Air temperature (tmp)	Precipitation (pre)	Climate moisture index (cmi)	Clay fraction in soil (cly)	Silt fraction in soil (slt)	Sand fraction in soil (snd)	Soil water content (swc)
Attributes	pyr	cyr	rsu	rsu		cav	cav	cyr	cyr	cyr	cav	cav	cav	cyr
dis	1.00	0.04	**0.73**	**0.91**	0.04	0.02	0.05	0.00	-0.03	-0.03	0.01	0.00	0.00	-0.04
run		1.00	0.18	0.04	-0.18	-0.11	0.05	0.04	**0.76**	**0.72**	-0.07	0.21	-0.08	**0.51**
ria			1.00	**0.86**	0.07	0.09	0.11	-0.01	0.02	0.02	0.01	0.03	0.02	-0.01
riv				1.00	0.04	0.03	0.05	0.00	-0.04	-0.05	0.01	0.00	0.00	-0.05
ele					1.00	**0.83**	**0.86**	-0.28	-0.37	-0.41	0.00	-0.15	0.21	-0.32
slp						1.00	**0.77**	-0.21	-0.21	-0.22	0.04	-0.07	0.13	-0.13
sgr							1.00	-0.20	-0.15	-0.18	0.01	-0.12	0.22	-0.17
tmp								1.00	0.41	-0.12	0.36	-0.24	-0.03	-0.12
pre									1.00	**0.78**	0.09	0.17	-0.17	**0.60**
cmi										1.00	-0.12	0.35	-0.22	**0.86**
cly											1.00	**0.56**	**0.61**	-0.08
slt												1.00	0.49	0.41
snd													1.00	-0.16
swc														1.00
ero														

Notes: pry--annual average at reach pour point; cyr-annual average in reach catchment; rsu--sum along reach segment; cav: average in reach catchment.

5.3.3.2 Data sources of landslide susceptibility evaluation variables

The data sources for the selected variables mainly kept on the same data sources as HydroALTAS or the updated version of original datasets after the HydroALTAS released (Linke et al. 2019). The data sources of DEM and land cover variables were replaced with higher resolution data sources, including the 30m resolution FABDEM (Hawker et al. 2022), 30m resolution FROM-GLC (Finer Resolution Observation and Monitoring of Global Land Cover, Gong et al. 2013) and 1km resolution Global Maps of Potential Natural Vegetation (Hengl et al. 2018). All these data sources are open-access, and their information were provided in Table 5-5.

Spatial resolution for landslide susceptibility evaluation modelling process is determined by considering the detailed degree of the mapping details of landslide and LDam records, and the collected data. We selected the 30m as the resolution for grid-cell based landslide susceptibility evaluation modelling because the resolution keeps a good

balance on presenting the potential probability of landslide occurrence and the data source resolution. More than 50% landslides that blocked the river have an area less than 175,000 m^2 (Wu et al. 2022), this is approximately 20 grids at 30m resolution.

Table 5-5 Data sources information of input variables for landslide susceptibility

Index	Category	Variable	Special resolution	Data source (reference)	Updated from HydroALTAS data sources
1	Hydrology	River Area	500 m	HydroALTAS (Linke et al. 2019)	N
2	Geomorphology	Elevation	30 m	FABDEM (Hawker et al. 2022)	Y
3		Slope	30 m	FABDEM (Hawker et al. 2022)	Y
4		Curvature	30 m	FABDEM (Hawker et al. 2022)	Y
5	Climate	Air Temperature	30 arc-second (1km)	WorldClim 2.1 (Fick and Hijmans 2017)	Y-version updated of the same data source
6		Precipitation	30 arc-second	WorldClim 2.1 (Fick and Hijmans 2017)	Y-version updated of the same data source
7	Landcover	Land Cover Classes	30 m	FROM-GLC (updated version in 2017) (Gong et al. 2013)	Y
8		Potential Natural Vegetation Classes	1 km	Global Maps of Potential Natural Vegetation at 1 km resolution (Hengl et al. 2018)	Y
9	Soil and geology	Clay Fraction in Soil	1 km	Soilgrid1km (Hengl et al. 2014)	N
10		Lithological Classes	30 arc-second	GLiM – Global Lithological Map (Hartmann and Moosdorf 2012)	N
11		Soil Erosion	100m	High resolution cropland global soil erosion (GloSEM 1.3) (Borrelli et al. 2022)	Y-version updated of the same data source

5.3.3.3 Training dataset preparation

The first assumptions of statistical-based methods for susceptibility evaluation are that the past is the key to the future (Guzzeti et al. 2005), so a training dataset based on landslide records needs to be prepared for modelling. We took all the landslide records from collected datasets as the landslide samples for two detailed study regions, Italy and Japan. There were more than 1 million landslide records in Italy, with 300 thousand landslide records in Japan.

Only a few researchers focused on exploring the sampling method of landslide susceptibility evaluation (Kornejady et al. 2017; Shao et al. 2020). The ratios of non-landslide/landslide sample greatly affect the occurrence probability of landslides. Shao et al. (2020) found that the landslide susceptibility model prediction is almost consistent with the actual ratio of landslide area based on the seismic landslides that occurred in the 2013 Lushan earthquake when the ratio is 1, which means the number of non-landslides is equal to the number of landslides. Therefore, we kept the non-landslide sample with the same number as the landslide samples. The non-landslide sample was selected by the spatially balanced sampling method on the area within the initial filtered area but excluded the landslide areas.

5.3.3.4 Validation and optimal threshold extraction

The ROC (Receiver operating characteristics) curve was applied to validate the model performance of logistic regression model for the modelling result in Italy and Japan respectively. The ROC curve is a quantitative measure to evaluate the performance of the evaluation model by calculating the value of the area under the curve (AUC) and has been shown as a reliable tool for the landslide susceptibility evaluation model (Vakhshoori and Zare 2018). The ROC curve provides an analysis based on true positive rate (TPR) and false positive rate (FPR) at any classification threshold of the delineated result. The ROC curve has been widely applied in the validation of landslide susceptibility models and measurement of model applicability (Lin et al. 2017; Raja et al. 2017). If the area under the ROC curve (AUC) value is above the value of 0.5, which is the value of the random classifier, it shows that the model has better performance than the random classifier. A higher AUC value indicates that the evaluation model is more reliable. The most ideal AUC value of ROC curve would be 1, which means in any given threshold, all the TPR is 1 while the FPR is 0.

Not all the LSI values indicated landslide occurrence. However, it is hard to determine a unified threshold to define which value means a landslide potential occurrence simply based on the LSI value for the landslide susceptibility result, because the landslide inventories that are applied as training datasets cannot include all the landslide events that have actually occurred. Therefore, selecting a proper threshold based

on ROC analysis depends on the study's purposes (Cantarino et al. 2018). An optimal threshold for LSI activation value, calculated by finding the balanced point between true positive rate and true negative rate (TNR), was applied as the threshold to extract the activated mask, those areas with an activated LSI value that means landslide occurrence. In other words, the minimum value of the difference between TPR and TNR (TNR is equal to the value of 1-FPR, False Positive Rate), was calculated as the optimal threshold.

5.3.4 Model for LDam Formation Susceptibility

Assessing the LDam formation susceptibility evaluation is to predict the LDam occurrence probability on specific river reaches. For LDam formation, landslide volume is a significant variable that contributes to the damming probability, while its accuracy is hard to measure (Tacconi Stefanelli et al. 2020). Previous LDam formation susceptibility research applied the empirical relationship between landslide area and landslide volume based on the local landslide inventories to achieve the landslide volume (Fan et al. 2014; Tacconi Stefanelli et al. 2020). Such a power law correlation between landslide area and landslide volume has been widely acknowledged although the coefficients of the empirical relationship depended on regions, landslide types or slope materials (Simonett, 1967; Hovius et al. 1997; Guzzetti et al. 2009; Larsen et al. 2010).

Many LDam formation indexes have used landslide volume and river/valley width as important components (Swanson et al. 1986; Tacconi Stefanelli et al. 2016; Tacconi Stefanelli et al. 2018). A relationship between landslide volume and river width also showed a potential threshold for LDam formation according to a global-scale LDam dataset (Wu et al. 2022). Therefore, we estimate the LDam formation susceptibility at specific river reaches by combining the LSI, landslide area and river width, as shown in Eq. 5-3. Most of LDam formation index used logarithmic transform (Chen and Chang 2016; Tacconi Stefanelli et al. 2016; Tacconi Stefanelli et al. 2018). Eq. 5-3, originated from trial and error, showed the LSI result of the areas near specific river reach was achieved by combining all the LSI value from the slope drainage unit nearby.

$$P(LDam\ formation) = \frac{\log \sum_{i=1}^{n} LSI_n \times SA_n}{\log RW} \quad \text{(Eq. 5-3)}$$

The LSI_n is the median landslide susceptibility index of the adjacent delineated slope drainage unit n, SA_n is the surface area of the slope drainage unit n, RW is the river width at specific river reach, which can be directly accessed on MERIT Hydro (Yamazaki et al. 2019). The method did not rely on any specific empirical relationships, such as the relationship between landslide volume and landslide area. By combining all the delineated slope drainage units that are near the specific river reach, it is likely that these areas encompass all the regions where an adjacent potential landslide occurrence could potentially block the river. This is because over 94% of landslides that have dammed rivers from a global-scale LDam dataset have had a length of less than 3 km (Wu et al. 2022), while the delineated slope drainage unit in this study has a mean length of 3 km and a mean width 1.5 km.

5.4 Results

5.4.1 Landslide susceptibility Evaluation Results and Validations

The input variables for landslide susceptibility showed different relative contributions in the different study areas. Table 5-6 shows the importance of variables contributing to landslide susceptibility results in Italy and Japan. The top three variables in Italy are topographical slope degree, soil erosion, and clay fraction of soil, whilst those for Japan were the specific type of lithology, landcover and potential natural vegetation classes. Some variables, such as temperature, precipitation, clay fraction in soil, and lithology, have contrary contributions to the final landslide susceptibility evaluation result in Japan and Italy. The varying results in variable contribution imply that local landslide inventories are crucial for accurately assessing landslide susceptibility and capturing localized contributions of variables, even when utilizing the same input variables.

Both of the landslide susceptibility evaluation result in Italy and Japan were also validated by AUC value under the ROC curve. The fact that the logistic regression model of Italy landslide susceptibility evaluation presents an AUC value of 0.89 indicates the

model has a great performance (Figure 5-5(a)). The AUC value of logistic model performance in Japan is 0.74, which is lower, but still an acceptable value for a model performance (Figure 5-5(b)).

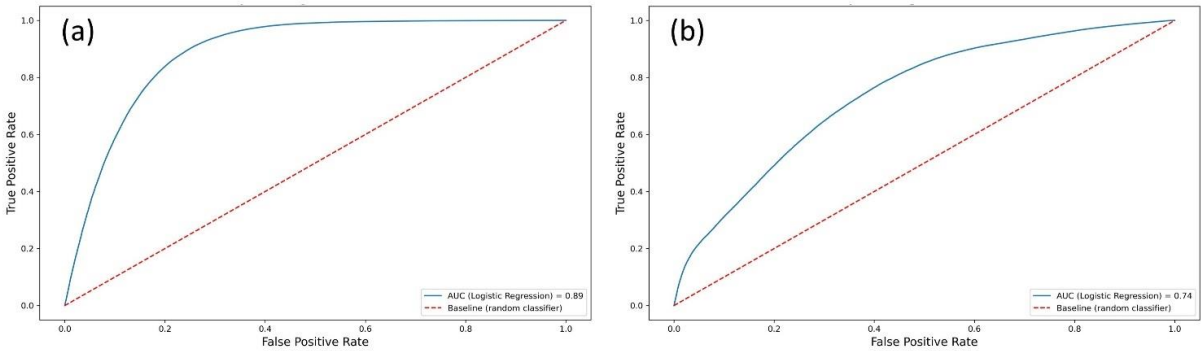

Figure 5-5 The ROC curve of logistic regression model for landslide susceptibility evaluation in Italy (a) and Japan (b)

Table 5-6 Coefficients for variables of logistic regression model to evaluate landslide susceptibility in Italy and Japan

Variable	Sub-categories (for categorized data)	Coefficient (Italy)	Coefficient (Japan)
Constant (β_0)	-	-5.7501	-1.8699
River Area	-	0.7812	0.5560
Elevation	-	0.5212	0.2674
Slope	-	3.3264	0.0336
Curvature	-	-0.4516	-0.3091
Air Temperature	-	0.4834	-0.7604
Precipitation	-	-0.7287	0.8281
Land Cover Classes	Cropland	1.4880	0.8853
	Forest	0.8660	1.3087
	Grassland	1.3700	1.5579
	Impervious surface	1.4876	-
	Shrubland	1.2335	2.1241
	Wetland	-0.4929	-
Potential Natural Vegetation Classes	Cool.mixed.forest	0.4718	-
	Warm temperate evergreen and mixed forest	-1.1116	-
	Xerophytic.woods.scrub	-1.6595	-
	Cool-temperate rainforest	-	-2.0414
Clay Fraction in Soil	-	2.0425	-0.2902
Lithology	Acid Plutonic Rocks	-1.1782	-1.7111
	Carbonate Sedimentary Rocks	0.6074	-1.5354
	Siliciclastic Sedimentary Rocks	0.8585	-0.5162
	Unconsolidated Sediments	-0.7271	-
	Acid Volcanic Rocks	-0.6466	-
	Basic Volcanic Rocks	-1.4378	-1.3939
	Intermediate Volcanic Rocks	-0.6715	-1.1064
	Metamorphic Rocks	-	0.6604

	Basic Plutonic Rocks	-	-0.6779
	Pyroclastics	-	-2.0740
Soil erosion	-	2.7336	0.2486

After the ROC curve validation, the landslide susceptibility result can be used to identify where a landslide is more likely to occur given the LSI value. The mountainous regions along the European Alps and Apennine in Italy exhibit the highest susceptibility to landslides, as indicated in Figure 5-6 (a). This observation aligns with the most landslide-susceptible classification area in Italy from the continental-scale landslide susceptibility evaluation result reported by Günther et al. (2014). Similarly, In Japan, the mountains areas in the Hida Mountains, northern Shikoku, Kyoshu, Ōu Mountains and Hokkaido are the areas prone to landslide occurrences (Figure 5-6 (b)), which correspond to area with the highest landslide density from a national-scale study in Japan by Paudel et al. (2016).

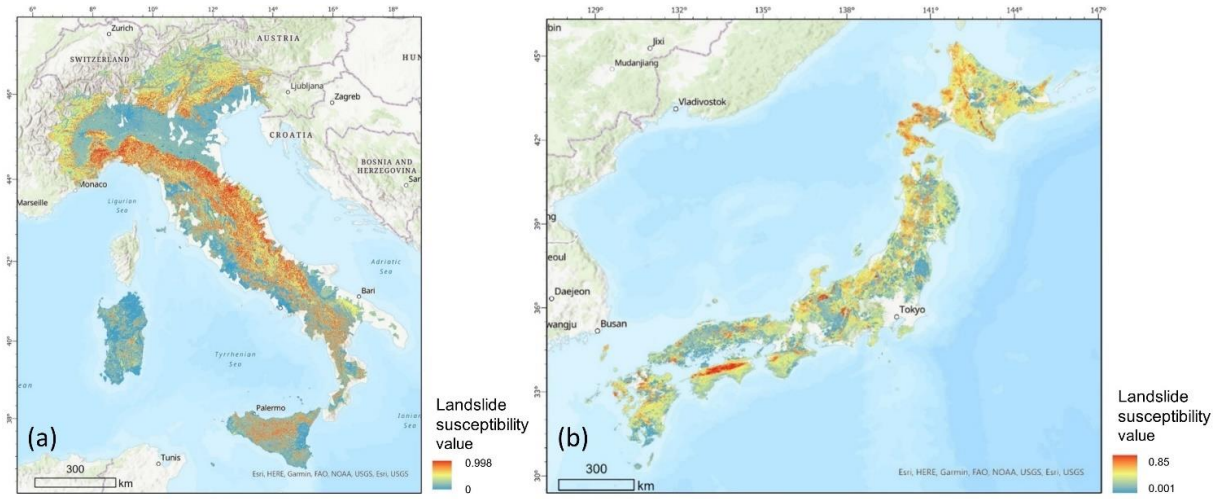

Figure 5-6 Landslide susceptibility evaluation result in Italy (a) and Japan (b)

The optimal LSI threshold in Italy is 0.53(Figure 5-7 (a)), while the threshold in Japan is 0.34 (Figure 5-7 (b)). The area with LSI values above these optimal thresholds was identified as the activated areas that have potential landslide occurrence.

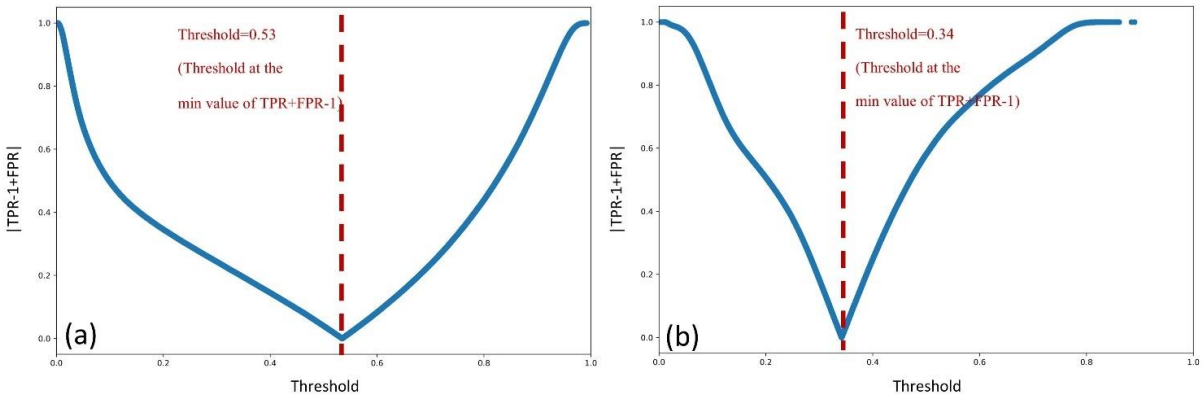

Figure 5-7 The optimal threshold for LSI result modelled in Italy (a) Japan (b)

5.4.2 Landslide Dam Formation Susceptibility Evaluation Results with Validations

The LDam formation index result of Italy is shown in Figure 5-8 (a). Approximately 39% of river reaches in Italy were identified with a null value of the LDam formation index due to a river width too large for LDam formation or due to the absence of the probability of landslide occurrence in the adjacent areas, these river reaches are mainly located in the plains. Likewise, Figure 5-8 (b) displays the LDam formation index results for Japan, indicating that around 31% of the river reaches have a null value. To provide more detail on the LDam formation index at smaller scales, two examples are presented along river longitudinal profiles in Figure 5-9. This confirms that the river reaches with LDam records have relatively high values of the LDam formation index, as would be expected.

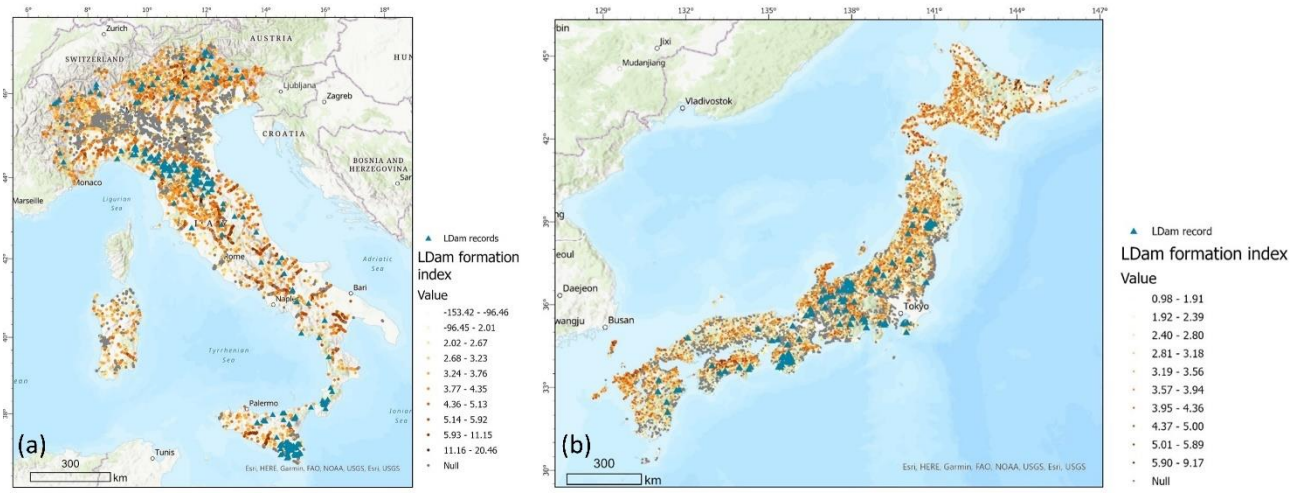

Figure 5-8 Landslide dam formation index result in Italy (a) and Japan (b)

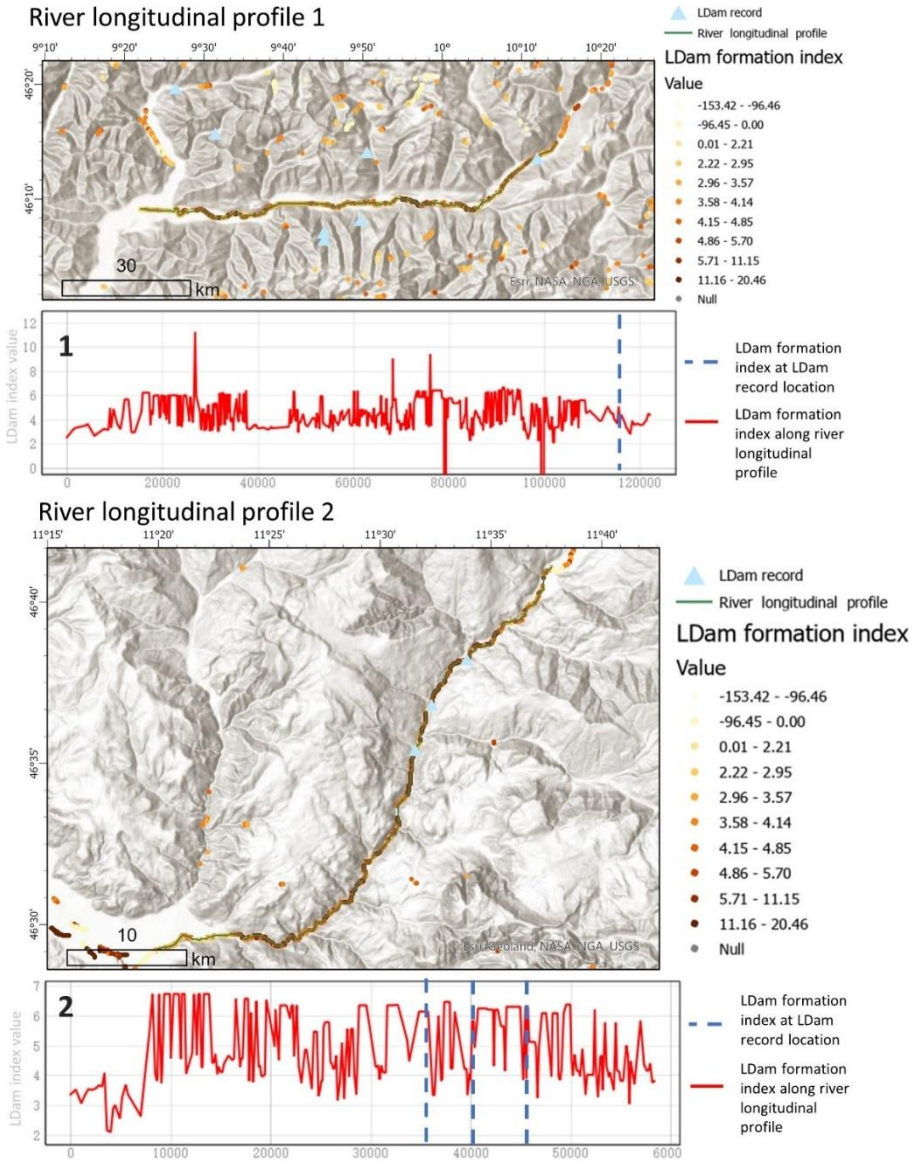

Figure 5-9 LDam formation index along the river longitudinal profiles (each dot with LDam formation index represented the centre of a river reach presented as 90m resolution grid in MERIT Hydro)

To validate the effectiveness of the LDam formation index, we conducted LDam formation index comparisons at all river reaches from global fluvial datasets and validated these indexes at the location of LDam records. Those LDam records that are located in lakes/reservoirs were excluded from the comparison as the LDam index would be low due to the lake presence, such as at inundation lakes or reservoirs behind old LDams. The LDam formation indexes for the reaches with LDam records in Italy ranged from 2.385

to 20.460, with a median value of 4.404 (Figure 5-10 (a)). Similarly, the LDam index for the reaches with LDam records in Japan ranged from 1.745 to 6.431, with a median value of 3.732 (Figure 5-10 (b)). The LDam records have a relatively higher value of the LDam formation index compared to those of all the river reaches with valid indexes. The sample size of LDam records with valid LDam formation index depends on the existence of river reaches represented in global fluvial datasets, especially those on the upstream catchment areas (Italy: 13%; Japan: 32% before excluding those LDam records currently located in the lakes).

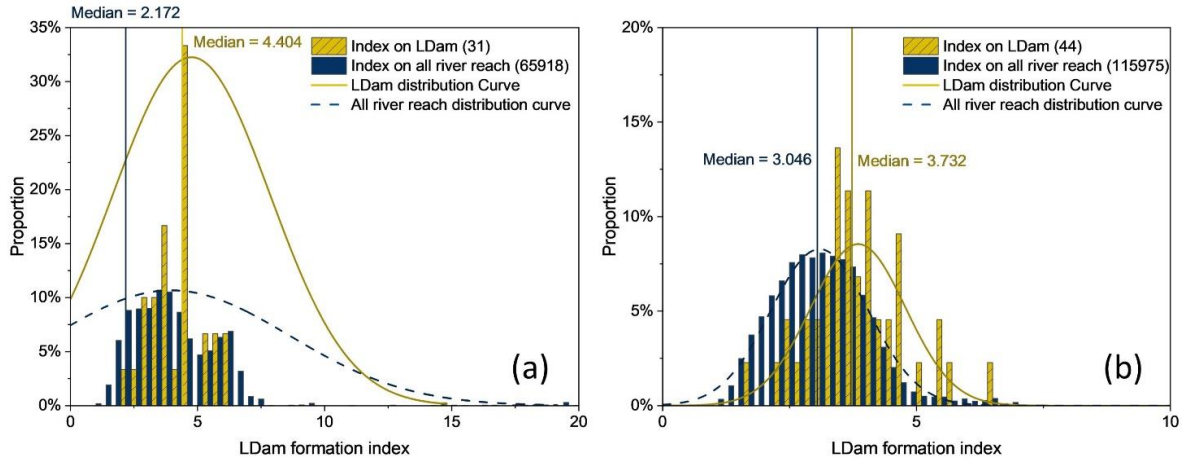

Figure 5-10 Validation of LDam index value at LDam records and all river reaches present in MERIT Hydro for the results in Italy (a) and Japan (b) (numbers are the sample size)

The logistic regression model was not only validated by the sense check using the ROC curve but also validated by the collated LDam records across the modelling areas. The LDam formation index proposed in this study has a relatively higher value compared to the index in all river reaches, which show the method is useful and a distinct improvement on the existing tools.

5.5 Discussion

5.5.1 Applicability of Framework

The proposed LDam formation framework can be directly applied to other areas. Most of the LDam and landslide datasets that applied in this study, as well as global fluvial datasets, are open access, which enables the application of this methodology to

other study areas using the same data sources. Another advantage of applying this framework is that it relied very little on information from empirical relationships, such as landslide volume estimation. With less dependence on site-specific empirical relationships, the pre-assessment of LDam formation on a large-scale could be immediately conducted without the involvement of comprehensive landslide databases.

The framework can also provide a preliminary result for more local-scale research. The performance of this framework in two large-scale study regions, Italy and Japan, showed its applicability to other large-scale studies for exploring LDam formation, as most of the LDam formation index values at the LDam records are relatively high compared with all the valid indexes on the river reaches. By comparing our LDam formation susceptibility evaluation result with another local-scale research on the Arno River basin (Figure 5-11), we found the river reaches with relatively high value of our LDam formation index shown in the main Arno River between Florence to Arezzo, which is consistent to the areas with high damming susceptibility of landslides. However, it should be noted that some tributaries were not represented in the global fluvial datasets in our analysis. Further smaller scale analysis could also use this framework with similar input data, if data resources on a local scale with more details and finer resolution are available.

This proposed framework is the first one to estimate the LDam formation on river reaches while most previous studies focus on the DFL formation on the adjacent slopes or the LDam formation probability of each landslide event. Therefore, the proposed LDam formation index cannot be directly compared to any previous geomorphological LDam formation index. The framework can be directly applied to any other study area around the world when reliable LSI products are available, as the study applied multiple global datasets to develop and identify the characteristics required that are applicable in a global framework.

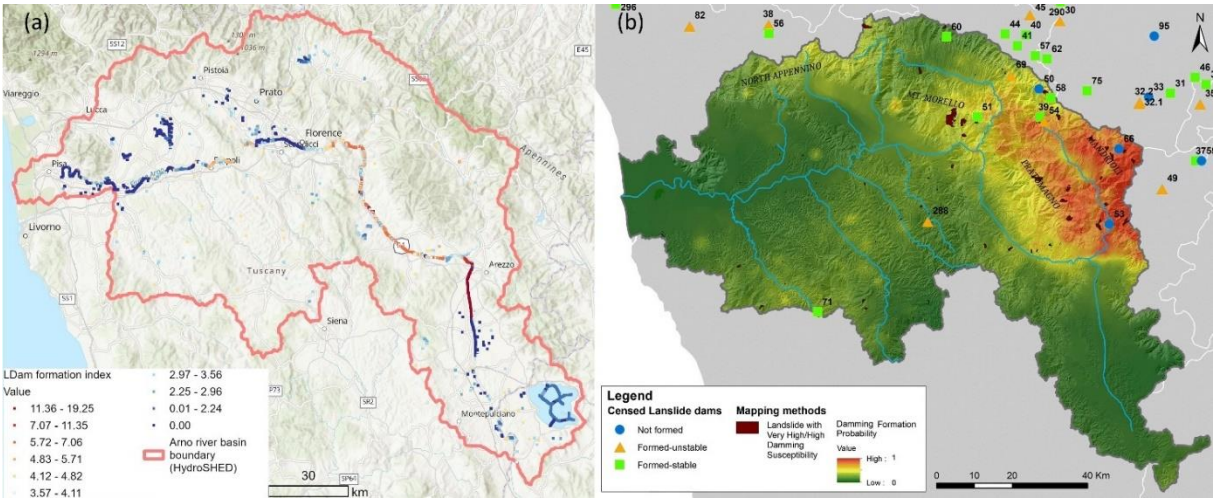

Figure 5-11 Comparison of LDam formation results in Arno River basin, Tuscany, Italy (~8,200 km^2): (a) LDam formation index on river reaches conducted by this study (each dot represented a 90m river reach on MERIT hydro); (b) Damming formation probability of landslides based on local-scale datasets (Tacconi Stefanelli et al. 2020)

5.5.2 Uncertainties

Three main uncertainties could affect the LDam formation evaluation framework according to the methods and results: 1) the diversity of landslide susceptibility result, 2) the focus of river channel representation and LDam record, and (3) their inconsistency.

Landslide susceptibility results were impacted by the data sources and modelling procedures. Limitations in large-scale landslide datasets, such as the data quality and comprehensiveness always become a large uncertainty source for data-driven models. Landslide types were undistinguished in this study as the detailed information was not available for most large-scale and open-access landslide datasets, but they crucially affected the landslide run-out distance, area and volume (Corominas 1996; Larsen et al. 2010; Fan et al. 2014). Even when using identical input variables and employing similar data processing procedures for landslide susceptibility evaluation, it is inevitable to encounter varying contributions of variables to the evaluation result. Moreover, uncertainties could rise due to the diversity of the types within specific categorized variables, such as the vegetation and lithology types. However, such uncertainty could have relatively little effect on the following LDam formation analysis because the landslide susceptibility result, derived from different methods, data, and scope, in a

specific area could still show largely similar results (Stanley and Kirschbaum 2017). Within the realm of such uncertainty, it is essential to acknowledge the ongoing deformations that affect the slopes involved in mass rock creep processes (Chigira and Kiho 1994), which can further evolve in rock avalanches. It is important to note that the occurrence of such rock avalanches is not primarily determined by force-driven failure mechanisms but rather by viscosity-driven processes. (Marmoni et al. 2023). The case of the Scanno rock avalanche in Italy which caused the damming of the homonymous lake along the Tasso River is a nice example to show this impact (Esposito et al. 2013). The event was dated with a back analysis by Della Seta et al. (2017), while the role of creep processes in providing ultimate scenarios of LDam formation was also demonstrated. Such a process is particularly efficient in high-mountain areas as in the case of the Zagros Mountain (Iran), where giant rock avalanches caused formed a LDam with enormous volume result in a lake-system evolution over thousands of years before the present (Delchiaro et al. 2019). However, such ongoing deformation could be underrepresented by the landslide susceptibility result given the relatively coarse resolution of the data source (Figure 5-12).

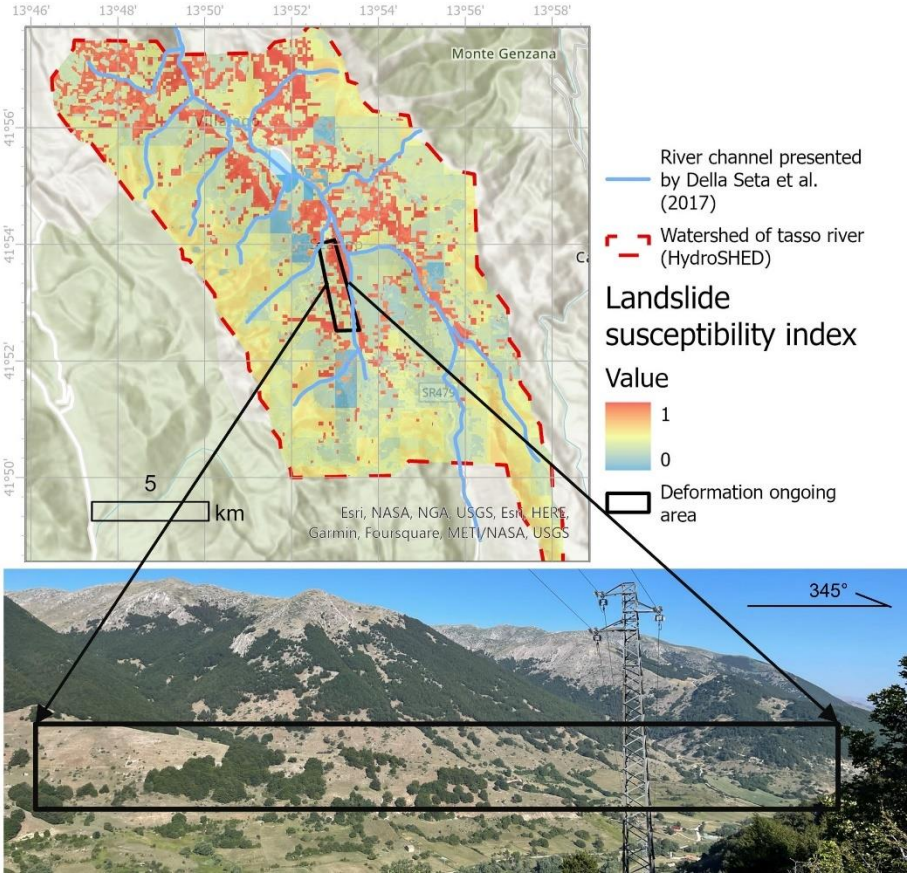

Figure 5-12 Landslide susceptibility evaluation result in Tasso River, Abruzzo, Italy and a deformation ongoing area seen from the field

The inconsistency in representing river channels and the focus on LDam records can result in the omission of numerous streams or upstream rivers that could have a large potential to be dammed in the result of LDam formation susceptibility assessment. More than 80% of LDam records are typically located on the upstream catchment with drainage areas less than 500 km^2 (Wu et al. 2022), where these have steeper hillslopes for drainage area delineation and thus can lead to a limited representation for upstream rivers. The catchments at this scale were classified as streams or small rivers according to Bernhofen et al. (2021)'s classification. For global fluvial datasets, the representation of river channels relies on the quality and resolution of input data, such as DEM and climate data (Dottori et al. 2016), and the computational efficiency of global flood models (Bernhofen et al. 2021). The different sizes of the threshold for river channel representation can lead to the flood exposure difference (Bernhofen et al. 2021) and can directly influence the output of the LDam formation index through the river width data. Currently, global fluvial

datasets may have more complete and accurate data for larger rivers compared with the upstream rivers where LDams are prone to occur as a good representation of smaller rivers remains to be resolved (Yamazaki et al. 2019). Figure 5-13 shows the representation of the LDam formation index at river reaches from MERIT Hydro in the Tasso River basin, Italy. The river reach crossing the Scanno Lake (Lago di Scanno) was represented well, while the other narrow river reaches didn't contain valid river width data or were not represented in the global fluvial dataset. We used a colour matrix presenting landslide susceptibility from the adjacent slope drainage units and LDam formation index on each river reach to show the contribution of landslide susceptibility result to the final LDam formation index. The comparison shows that the area around Scanno Lake is in a relatively stable stage given the fact that either landslide susceptibility or LDam formation index is low.

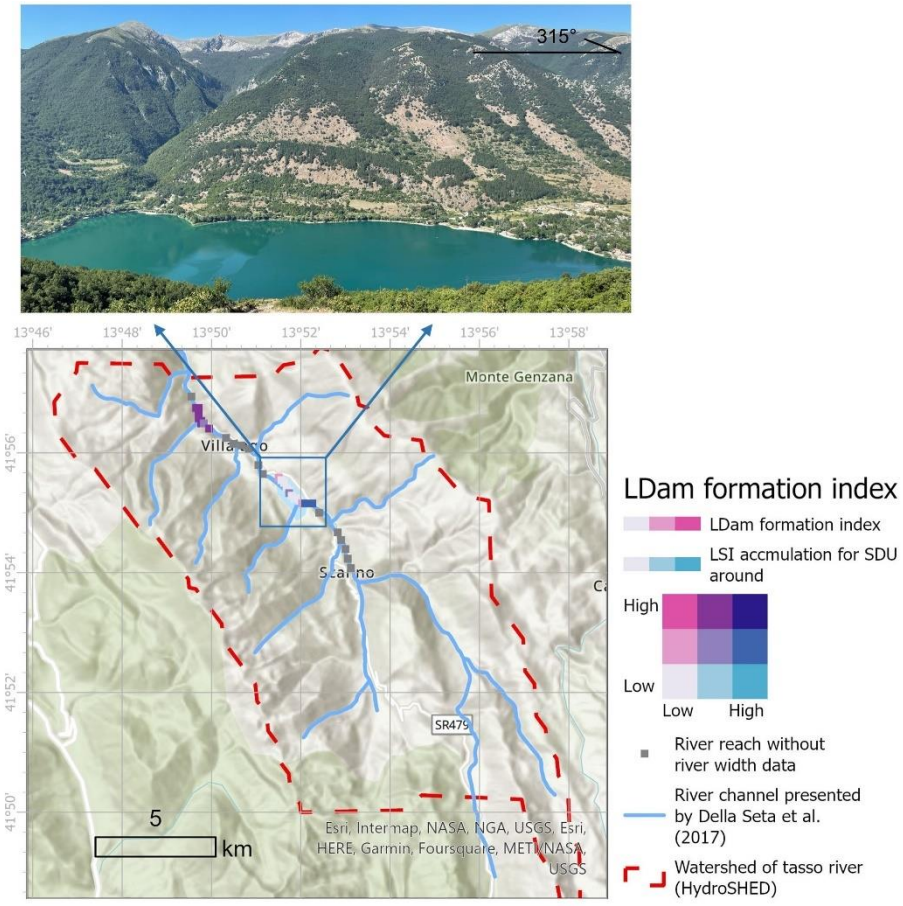

Figure 5-13 LDam formation susceptibility evaluation result in Tasso River, Abruzzo, Italy and the field picture of Scanno rock avalanche impounded lake (Lago di Scanno/Scanno Lake) (SDU: delineated slope drainage unit; LSI: Landslide

susceptibility index; the square represented the centre of a river reach shown as 90m resolution grid in MERIT Hydro)

5.6 Conclusions

Previous research has attempted to assess the probability of LDam formation; however, they relied heavily on the local-scale datasets, or the empirical relationships based on local data and focused more on one side of the physical LDam formation processes, the occurrence of landslides of sufficient magnitude to obstruct river (Damming formation probability of landslides). The LDam formation susceptibility evaluation framework was developed by combining landslide susceptibility evaluation and global fluvial datasets to estimate the LDam formation susceptibility on river reaches. Most of the input data, including the landslide datasets that were collected globally, global fluvial datasets and input data for landslide susceptibility are openly accessible.

The framework was built based on the unit of the delineated slope drainage and tested in Italy and Japan with all the results being validated against the data of LDam records. The logistic regression model employed for landslide susceptibility evaluation in Italy demonstrated excellent performance, achieving an AUC value of 0.89. In Japan, the logistic model achieved an AUC value of 0.74, which is considered an acceptable model performance. The LDam formation index results demonstrated the effectiveness of such an index to present the probability of LDam formation at specific river reaches because the data distribution of the LDam formation index for reaches with LDam records show higher values compared to other river reaches. Moreover, the locations of relatively high LDam index are consistent with the LDam record positions along the river longitudinal profiles and the areas with relatively high damming formation probability of landslides. These results indicate the framework's capability to assess LDam formation susceptibility at river reaches in different large-scale regions.

Overall, the developed framework offers a valuable tool for assessing LDam formation susceptibility at river reaches globally. Its reliance on open access data, including landslide datasets and global fluvial datasets, enhances its accessibility and applicability across various regions, even though such large-scale datasets introduce

certain uncertainties for the final result. The framework's performance in Italy and Japan, along with the demonstrated effectiveness of the LDam formation index, further support its potential for widespread implementation and utilization.

The LDam formation susceptibility results obtained from this framework can be utilized by international or national institutions as a preliminary exploration and hazard prevention of LDam formation prior to actual landslides occurring. This will allow preventative measures, such as improving land use planning, applying early warning systems on adjacent slopes or rivers, and undertaking targeted infrastructure projects to reduce the risk of slope failure, can be implemented to mitigate the risk of a LDam event. Continued research and collaboration, especially the smaller scale research, can further refine the framework, expand its applicability, and strengthen its contributions to global efforts in managing and mitigating LDam-related risks.

5.7 References

Allen GH, Pavelsky TM (2018) Global extent of rivers and streams. Science 361(6402):585–588

Alkhasawneh M, Ngah UK, Tay LT, Mat Isa, NA, Al-batah MS (2013). Determination of important topographic factors for landslide mapping analysis using MLP network. Sci World J 2013:415023.

Alvioli M, Guzzetti F, Marchesini I (2020) Parameter-free delineation of slope units and terrain subdivision of Italy. Geomorphology 358:107124

Ayalew L, Yamagishi H (2005) The application of GIS-based logistic regression for landslide susceptibility mapping in the Kakuda-Yahiko Mountains, Central Japan. Geomorphology, 65(1-2):15-31

Bernhofen MV, Trigg MA, Sleigh PA, Sampson CC, Smith AM (2021) Global flood exposure from different sized rivers. Nat Hazards Earth Syst Sci 21(9):2829-2847

Borrelli P, Ballabio C, Yang JE, Robinson DA, Panagos P (2022) GloSEM: High-resolution global estimates of present and future soil displacement in croplands by water erosion. Sci Data 9(1):406

Budimir MEA, Atkinson PM, Lewis HG (2015) A systematic review of landslide probability mapping using logistic regression. Landslides 12(3):419-436

Calvello M, Pecoraro G (2018) FraneItalia: a catalog of recent Italian landslides. Geoenviron Disasters 5(13):1-16

Cantarino I, Carrion MA, Goerlich F, Martinez Ibañez V (2018) A ROC analysis-based classification method for landslide susceptibility maps. Landslides 16(2):265-282

Canuti P, Casagli N, Ermini L (1998) Inventory of landslide dams in the Northern Apennine as a model for induced flood hazard forecasting. In: Andah, K. (Ed.), Managing Hydro-geological Disasters in a Vulnerate Environment. CNR-GNDCI Publication 1900. CNR-GNDCI-UNESCO (IHP), Perugia, pp 189–202

Casagli N, Ermini L (1999) Geomorphic analysis of landslide dams in the Northern Apennine. Trans Jpn Geomorphol 20 (3):219–249

Cencetti C, De Rosa P, Fredduzzi A (2020) Characterization of landslide dams in a sector of the central-northern Apennines (Central Italy). Heliyon, 6(6): e03799.

Chen CY, Chang JM (2016) Landslide dam formation susceptibility analysis based on geomorphic features. Landslides, 13(5):1019-1033

Chigira M, Kiho K (1994) Deep-seated rockslide-avalanches preceded by mass rock creep of sedimentary rocks in the Corominas Akaishi Mountains, central Japan. Eng Geol 38(3-4):221-230

Costa JE, Schuster RL (1988) The formation and failure of natural dams. Geol Soc Am Bull 100(7):1054–1068

Delchiaro M, Della Seta M, Martino S, Dehbozorgi Nozaem MR, Nozaem R (2019). Reconstruction of River valley Evolution before and after the Emplacement of the Giant Seymareh Rock Avalanche (Zagros Mts., Iran). Earth Surf Dynam 7:929–947

Della Seta M, Esposito C, Marmoni GM, Martino S, Scarascia Mugnozza G, Troiani F (2017) Morpho-structural evolution of the valley-slope systems and related implications on slope-scale gravitational processes: New results from the Mt. Genzana case history

(Central Apennines, Italy). Geomorphology 289:60-77

Dikshit A, Sarkar R, Pradhan B, Acharya S, Dorji K (2019) Estimating rainfall thresholds for landslide occurrence in the Bhutan Himalayas. Water 11(8):1616

Domènech G, Alvioli M, Corominas J (2019) Preparing first-time slope failures hazard maps: from pixel-based to slope unit-based. Landslides 17(2):249-265

Dottori F, Salamon P, Bianchi A, Alfieri L, Hirpa FA, Feyen L (2016) Development and evaluation of a framework for global flood hazard mapping. Adv Water Resour 94: 87-102

Dou J, Tien Bui D, Yunus AP, Jia K, Song X, Revhaug I, Xia H, Zhu Z (2015) Optimization of Causative Factors for Landslide Susceptibility Evaluation Using Remote Sensing and GIS Data in Parts of Niigata, Japan. PLoS One 10(7): e0133262.

Dufresne A, Ostermann M, Preusser F (2018) River-damming, late-Quaternary rockslides in the Ötz Valley region (Tyrol, Austria). Geomorphology 310:153-167

Dufresne A, Siebert L, Bernard B (2021) Distribution and geometric parameters of volcanic debris avalanches. In: Roverato M, Dufresne A, Procter J (eds) Volcanic Debris Avalanches - From Collapse to Hazards. Advances in Volcanology, Springer Heidelberg, pp75-90

Eilander D (2020) PyFlwdir: Fast methods to work with hydro- and topography data in pure Python, Zenodo [code], https://doi.org/10.5281/zenodo.4287338, 2020.

Erener A, Düzgün HSB (2011) Landslide susceptibility assessment: what are the effects of mapping unit and mapping method. Environ Earth Sci. 66(3):859-877

Ermini L, Casagli N (2003) Prediction of the behaviour of landslide dams using a geomorphological dimensionless index. Earth Surf Processes Landforms 28(1):31-47

Esposito G, Matano F (2021) CAmpi Flegrei LAndslide Geodatabase (CAFLAG). 4TU.ResearchData. Dataset. https://doi.org/10.4121/14440757.v2. Accessed 20 Feb 2022

Fan X, Dufresne A, Siva Subramanian S, Strom A, Hermanns R, Tacconi Stefanelli C,

Hewitt K, Yunus AP, Dunning S, Capra L, Geertsema M, Miller B, Casagli N, Jansen JD, Xu Q (2020). The formation and impact of landslide dams – State of the art. Earth-Sci Rev 203

Fan XM, Rossiter DG, van Westen CJ, Xu Q, Gorum T (2014) Empirical prediction of coseismic landslide dam formation. Earth Surf Proc Land 39(14):1913–1926

Fan X, van Westen CJ, Xu Q, Gorum T, Dai F (2012) Analysis of landslide dams induced by the 2008 Wenchuan earthquake. J. Asian Earth Sci 57:25-37

Feng D, Gleason CJ, Yang X, Allen GH, Pavelsky TM (2022) How Have Global River Widths Changed Over Time? Water Resour Res 58(8): e2021WR031712

Fick SE, Hijmans RJ (2017) WorldClim 2: new 1km spatial resolution climate surfaces for global land areas. Int J Climatol 37(12): 4302-4315

Frasson RPD, Pavelsky TM, Fonstad MA, Durand MT, Allen GH, Schumann G, Lion C, Beighley RE, Yang X (2019) Global relationships between river width, slope, catchment area, meander wavelength, sinuosity, and discharge. Geophys Res Lett 46(6):3252–3262

Gong P, Wang J, Yu L, Zhao Y, Zhao Y, Liang L, Niu Z, Huang X, Fu H, Liu S, Li C, Li X, Fu W, Liu C, Xu Y, Wang X, Cheng Q, Hu L, Yao W, Zhang H, Zhu P, Zhao Z, Zhang H, Zheng Y, Ji L, Zhang Y, Chen H, Yan A, Guo J, Yu L, Wang L, Liu X, Shi T, Zhu M, Chen Y, Yang G, Tang P, Xu B, Giri C, Clinton N, Zhu Z, Chen J, Chen J (2013) Finer resolution observation and monitoring of global land cover: first mapping results with Landsat TM and ETM+ data. Int J Remote Sens 34(7):2607-2654

Günther A, Van Den Eeckhaut M, Malet JP, Reichenbach P, Hervás J (2014) Climate-physiographically differentiated Pan-European landslide susceptibility assessment using spatial multi-criteria evaluation and transnational landslide information. Geomorphology 224:69-85

Guzzetti F, Ardizzone F, Cardinali M, Rossi M, Valigi D (2009) Landslide volumes and landslide mobilization rates in Umbria, central Italy. Earth Planet Sci Lett 279(3–4):222–229

Guzzetti F, Reichenbach P, Cardinali M, Galli M, Ardizzone F (2005) Probabilistic

landslide hazard assessment at the basin scale. Geomorphology 72(1):272-299

Hartmann J, Moosdorf N (2012) The new global lithological map database GLiM: A representation of rock properties at the Earth surface. Geochem Geophys Geosyst 13(12)

Hawker L, Uhe P, Paulo L, Sosa J, Savage J, Sampson C, Neal J (2022) A 30 m global map of elevation with forests and buildings removed. Environ Res Lett 17(2): 024016

Hengl T, de Jesus JM, MacMillan RA, Batjes NH, Heuvelink GB, Ribeiro E, Samuel-Rosa A, Kempen B, Leenaars JG, Walsh MG, Gonzalez MR. (2014) SoilGrids1km — Global Soil Information Based on Automated Mapping. PLoS ONE 9(8): e105992.

Hengl T, Walsh MG, Sanderman J, Wheeler I, Harrison SP, Prentice I.C (2018) Global mapping of potential natural vegetation: an assessment of machine learning algorithms for estimating land potential. PeerJ 6: e5457

Hovius N, Stark CP, Allen PA (1997). Sediment flux from a mountain belt derived by landslide mapping. Geology 25(3): 231-234

Jacobs L, Kervyn M, Reichenbach P, Rossi M, Marchesini I, Alvioli M, Dewitte O (2020) Regional susceptibility assessments with heterogeneous landslide information: Slope unit- vs. pixel-based approach. Geomorphology, 356: 107084

Jibson RW, Harp EL (2012). Extraordinary Distance Limits of Landslides Triggered by the 2011 Mineral, Virginia, Earthquake. Bull Seismol Soc Am 102(6):2368-2377

Jones ES, Mirus BB, Schmitt RG, Baum RL, Burns WJ, Crawford M, Godt JW, Kirschbaum DB, Lancaster JT, Lindsey KO, McCoy KE, Slaughter S, Stanley TA (2019) Summary Metadata – Landslide Inventories across the United States, U.S. Geological Survey data release, https://doi.org/10.5066/P9E2A37P. Accessed 20 Feb 2022

Kirschbaum DB (2019) High Mountain Asia Landslide Catalog, Version 1. Boulder, Colorado USA. NASA National Snow and Ice Data Center Distributed Active Archive Center. https://doi.org/10.5067/5ST0TZCD9RQ3. Accessed 23 Feb 2022

Kirschbaum DB, Stanley T, Zhou Y (2015) Spatial and Temporal Analysis of a Global Landslide Catalog. Geomorphology. doi:10.1016/j.geomorph.2015.03.016.

Kornejady A, Ownegh M, Bahremand A (2017) Landslide susceptibility assessment using maximum entropy model with two different data sampling methods. Catena 152:144-162

Korup O (2002) Recent research on landslide dams - a literature review with special attention to New Zealand. Prog Phys Geog 26(2):206–235

Korup O (2004) Geomorphometric characteristics of New Zealand landslide dams. Eng Geol 73(1):13–35

Larsen IJ, Montgomery DR, Korup O (2010) Landslide erosion controlled by hillslope material. Nat Geosci 3(4):247–251

Lehner B, Grill G (2013) Global river hydrography and network routing: baseline data and new approaches to study the world's large river systems. Hydrol Processes 27(15):2171-2186

Lin L, Lin Q, Wang Y (2017) Landslide susceptibility mapping on a global scale using the method of logistic regression. Nat Hazards Earth Syst Sci Discuss 17(8):1411-1424

Linke S, Lehner B, Ouellet Dallaire C, Ariwi J, Grill G, Anand M, Beames P, Burchard-Levine V, Maxwell S, Moidu H, Tan F, Thieme M (2019) Global hydro-environmental sub-basin and river reach characteristics at high spatial resolution. Sci Data 6(1): 1-15

Marmoni GM, Martino S, Censi M, Menichetti M, Piacentini D, Mugnozza GS, Torre D, Troiani F (2023) Transition from rock mass creep to progressive failure for rockslide initiation at Mt. Conero (Italy). Geomorphology. 108750.

Martinello C, Cappadonia C, Conoscenti C, Agnesi V, Rotigliano E (2020) Optimal slope units partitioning in landslide susceptibility mapping. J Maps 17(3):152-162

Martinello C, Cappadonia C, Conoscenti C, Rotigliano E (2022) Landform classification: a high-performing mapping unit partitioning tool for landslide susceptibility assessment—a test in the Imera River basin (northern Sicily, Italy). Landslides 19(3):539-553

Martino S, Caprari P, Fiorucci M, Marmoni GM (2022) Italian Catalogue of Earthquake-

Induced Ground Failures (CEDIT), University of Rome Sapienza, https://gdb.ceri.uniroma1.it/index.php/view/map/?repository=cedit&project=Cedit Accessed 08 Sept 2022

Melillo M, Brunetti MT, Peruccacci S, Gariano SL, Guzzetti F (2016) Rainfall thresholds for the possible landslide occurrence in Sicily (Southern Italy) based on the automatic reconstruction of rainfall events. Landslides 13:165-172

Nadim F, Kjekstad O, Peduzzi P, Herold C, Jaedicke C (2006) Global landslide and avalanche hotspots. Landslides 3(2): 159-173

National Research Institute for Earth Science and Disaster Prevention of Japan (2014) Digital Archive for Landslide Distribution Maps. National Research Institute for Earth Science and Disaster Prevention of Japan. https://dil-opac.bosai.go.jp/publication/nied_tech_note/landslidemap/index.html Accessed 23 Feb 2022 (in Japanese)

Palau RM, Hürlimann M, Berenguer M, Sempere-Torres D (2020) Influence of the mapping unit for regional landslide early warning systems: comparison between pixels and polygons in Catalonia (NE Spain). Landslides 17(9):2067-2083

Palladino MR, Viero A, Turconi L, Brunetti MT, Peruccacci S, Melillo M, Luino F, Deganutti AM, Guzzetti F (2018) Rainfall thresholds for the activation of shallow landslides in the Italian Alps: The role of environmental conditioning factors. Geomorphology 303: 53-67.

Paudel U, Oguchi T, Hayakawa Y (2016) Multi-Resolution Landslide Susceptibility Analysis Using a DEM and Random Forest. Int J Geosci 07(05):726-743

Pedregosa F, Varoquaux G, Gramfort A, Michel V, Thirion B, Grisel O, Blondel M, Prettenhofer P, Weiss R, Dubourg V, Vanderplas J (2011) Scikit-learn: Machine learning in Python. J Mach Learn Res 12:2825-2830

Raja NB, Çiçek I, Türkoğlu N, Aydin O, Kawasaki A (2016) Landslide susceptibility mapping of the Sera River Basin using logistic regression model. Nat Hazard 85(3):1323-1346

Rossi M, Guzzetti F, Reichenbach P, Mondini AC, Peruccacci S (2010) Optimal landslide susceptibility zonation based on multiple forecasts. Geomorphology 114(3):129-142

Saito H, Korup O, Uchida T, Hayashi S, Oguchi T (2014) Rainfall conditions, typhoon frequency, and contemporary landslide erosion in Japan. Geology 42(11):999-1002

Scarascia Mugnozza G, Bianchi Fasani G, Esposito C, Martino S, Saroli M, Di Luzio E, Evans SG. (2006) Rock avalanche and mountain slope deformation in a convex dip-slope: the case of the Maiella massif, Central Italy. In: Evans SG, Scarascia Mugnozza G, Strom A, Hermanns RL (eds) Landslide from Massive Rock Slope Failure, Springer

Schmitt RG, Tanyas H, Nowicki Jessee MA, Zhu J, Biegel KM, Allstadt KE, Jibson RW, Thompson EM, van Westen CJ, Sato HP, Wald DJ, Godt JW, Gorum T, Xu C, Rathje EM, Knudsen KL (2017). An open repository of earthquake-triggered ground-failure inventories. U.S. Geological Survey data release collection, https://doi.org/10.5066/F7H70DB4. Accessed 23 Feb 2022.

Shafieiganjeh R, Ostermann M, Schneider-Muntau B, Gems B (2022) Assessment of the landslide dams in Western Austria, Bavaria and Northern Italy (part of the Eastern Alps): Data inventory development and application of geomorphic indices. Geomorphology 415: 108403

Shao X, Ma S, Xu C, Zhou Q (2020) Effects of sampling intensity and non-slide/slide sample ratio on the occurrence probability of coseismic landslides. Geomorphology, 363: 107222

Simonett DS (1967) Landslide distribution and earthquakes in the Bewani and Torricelli Mountains, New Guinea, statistical analysis. In: Jennings JN, Mabbutt JA (eds), Landform Studies from Australia and New Guinea, Cambridge University Press, Cambridge, pp64-84

Stanley T, Kirschbaum DB (2017) A heuristic approach to global landslide susceptibility mapping. Nat Hazards (Dordr), 87(1):145-164

Strom A, Abdrakhmatov K (2018). Rockslides and Rock Avalanches of Central Asia - Distribution, Morphology, and Internal Structure. Elsevier.

Struble WT, Roering JJ, Burns WJ, Calhoun NC, Wetherell LR, Black BA (2021) The Preservation of Climate-Driven Landslide Dams in Western Oregon. J Geophys Res.: Earth Surf 126(4): e2020JF005908.

Swanson FJ, Oyagi N, Tominaga M (1986) Landslide dams in Japan. In: Schuster RL(ed), Landslide Dams: Processes, Risk, and Mitigation. ASCE pp131–145

Tacconi Stefanelli C, Casagli N, Catani F (2020) Landslide damming hazard susceptibility maps: a new GIS-based procedure for risk management. Landslides 17(7):1635-1648

Tacconi Stefanelli C, Segoni S, Casagli N, Catani F (2016) Geomorphic indexing of landslide dams evolution. Eng Geol 208:1–10

Tacconi Stefanelli C, Vilímek V, Emmer A, Catani F (2018) Morphological analysis and features of the landslide dams in the Cordillera Blanca. Peru Landslides 15(3):507–521

Trigila A, Iadanza C, Spizzichino D (2010) Quality assessment of the Italian Landslide Inventory using GIS processing. Landslides 7:455–470

Trigg MA, Dehghani MS, Kesete YY, Carr AB, Trigg SG, Zekkos D, Lopez D, Pertierra M, van Westen CJ, Jetten V, Ogden FL (2023) Realities of bridge resilience in Small Island Developing States. Mitigation Adapt Strategies Global Change, 28(1)

van Westen CJ, Van den Bout B, Lombardo L, Jetten V (2020) Reducing Debris and Water Flow Risks from landslides for Infrastructure Resilience of the Commonwealth of Dominica, Report to the World Bank by Faculty of Geo-Information Science and Earth Observation (ITC) University of Twente, Enschede, the Netherlands. (Unpublished report)

van Westen C J, Zhang J (2018). Landslides and floods triggered by Huricane Maria (18 September, 2017) in Dominica. Digital or Visual Products, UNITAR-UNOSAT. http://www.unitar.org/unosat/node/44/2762 Accessed 23 May 2021

Vakhshoori V, Zare M (2018) Is the ROC curve a reliable tool to compare the validity of landslide susceptibility maps? Geomatics, Nat Hazards Risk 9(1):249-266

Verdin KL, Verdin JP (1999) A topological system for delineation and codification of the

Earth's river basins. J Hydrol 218(1-2):1-12

Wu H, Trigg MA, Murphy W, Fuentes R (2022) A new global landslide dam database (RAGLAD) and analysis utilizing auxiliary global fluvial datasets. Landslides, 19(3):555-572

Yamazaki D, Ikeshima D, Sosa J, Bates PD, Allen GH, Pavelsky TM (2019) MERIT Hydro: A High-Resolution Global Hydrography Map Based on Latest Topography Dataset. Water Resour Res 55(6): 5053-5073

Chapter 6. Synthesis and Conclusions

This thesis aims to establish a comprehensive framework for assessing the impact of LDam as a multi-hazard phenomenon on a global scale. The primary focus lies in presenting the distribution and characteristics of LDams, while also showing a universally adaptable approach for evaluating the susceptibility of LDam formation on a global scale. Chapter 2 provided a literature review for current LDam studies with a summary of the current research gap, mainly in the biased integration from various natural systems related to LDam, and the limited large-scale applicability due to the constraints posed by localised datasets and the empirical relationships derived solely from them. To address these two gaps, Chapters 3 to 5 integrated landslides with GFDs and provided some new insights respectively from the perspectives of data, relationships, and spatial probability estimation. In Chapter 3, by integrating auxiliary GFDs as a supplementary data source for the fluvial-related parameters of the LDam dataset, such as drainage area and river width, a new global-scale geolocated LDam dataset was established with a further analysis using collating LDam records from multiple sources. Chapter 4 utilised data derived from the LDam records collected in Chapter 3 and compared their morphometric and spatial characteristics to the landslides more generally, which were collated from multiple landslide inventories, mainly from regional-scale to global-scale. Based on the theory derived from Chapter 4 and the collected LDam and landslide records, Chapter 5 proposed a global-scale applicable LDam formation assessment framework by combining landslide susceptibility evaluation and the identification of LDam formation prone areas using geomorphology-based delineated slope drainage units. The proposed framework was validated by application to two large-scale study regions, Italy and Japan, which had national-scale landslide inventories and more complete LDam records when compared to other regions.

This chapter aims to synthesis the key findings and outcomes from the previous chapters and includes a discussion of the limitations of these outcomes. To address these limitations, some future works or opportunities based on this study are also proposed.

6.1 Key Findings and Outcomes

6.1.1 Development of LDam-related Datasets (Data Sources)

The thesis provides a literature review of the recent development of LDam-related datasets, including large-scale landslide datasets, GFDs and LDam datasets, as shown in the sections of **Chapter 1 and 2**. The LDam presents itself as a complex amalgamation of multi-hazards that interlink hillslope and fluvial systems. Within this muti-hazard system, the potential for floods and landslides to act as triggers, setting off cascading events that amplify the impacts of LDam, is evident. The data sources for LDam studies are always the first step to conducting any further analysis, especially for data-driven modelling. The currently available LDam dataset development was introduced and summarized in **Chapter 2**, with a more specific literature review presented in **Chapters 3 to 5**. One of the challenges behind the existing LDam datasets is that the data sources mainly rely on landslide datasets. This means they are missing many fluvial system elements which means that the comprehensiveness and quality of LDam records are actually strongly biased towards the landslide system rather than all attributes related to LDams. The other related datasets to LDam formation that are utilized in this thesis, such as landslide inventories and GFDs, were introduced in **Chapter 1**. Such datasets were either applied as direct input datasets for expanding the attribute comprehensiveness of the LDam records (**Chapter 3**), comparing the spatial and morphometric characteristics of DFLs and landslides more generally (**Chapter 4**), or spatial data sources for prefiltering and identifying geomorphological-based LDam potential formation zones in the LDam formation susceptible framework (**Chapter 5**). The spatial distribution and scale of these datasets, mainly the regional-scale and global-scale ones, were introduced through the literature review.

6.1.2 A Comprehensive Global Scale Geolocated LDam Dataset is Required

Hazard inventories play a key role in susceptibility evaluation modelling and impact the quality and precision of modelling input data (Cascini 2008). Based on the literature review of LDam dataset development in **Chapter 2**, **Chapter 3** illustrates the establishment of a new global-scale geolocated LDam dataset named RAGLAD, containing 779 records, which was mainly compiled from literature, in multiple languages,

with enhanced geospatial accuracy and the supplement fluvial data from GFDs. The dataset is already in use and was used as evidence to guide the LDam dataset development and triggers of LDam occurrence in Cencetti and Di Matteo (2022). Subsequently in this thesis, RAGLAD has been incorporated as a data source for the subsequent comparative analysis and assessment of LDam formation susceptibility, respectively presented in **Chapters 4 and 5**. Similar to the result of previous global-scale LDam datasets (Costa and Schuster 1988; Fan et al. 2020), the study's results indicate that LDam records from around the world tend to concentrate in mountainous regions, aligning with areas prone to landslide occurrences. A potential threshold of LDam formation was identified based on the relationship between landslide volume and river width, which could aid in estimating LDam formation risk when landslides occur in proximity to rivers. The LDam dataset not only provides a comprehensive data source for further analysis but also provides the validation data for testing the capabilities of the landslide susceptibility framework without the direct input of LDam records, which are less available for directly driving a data-driven model. However, given the situation that the landslide dimension may be controlled by landslide types, occurrence location etc. (Korup 2002; Jibson and Harp 2012; Tacconi Stefanelli et al. 2018), comprehensive LDam inventories with more records are always required to cover more area with different landscapes and environmental settings.

6.1.3 Factors Affecting the Location of LDam Formation

A comprehensive overview of our current understanding of the multiple factors influencing LDam formation is provided in **Chapter 2**. In **Chapter 3**, the establishment of the RAGLAD dataset reveals new and distinct morphometric data and relationships when compared to landslides more generally. **Chapter 4** further analyses the reasons behind these differences to explore which factors impact the relationships more by the inclusion of landslide datasets. Specifically, whether it is the morphometric characteristics or spatial distribution of the locations themselves that lead to some areas being more prone to LDam occurrence is explored. This investigation draws upon multiple LDam and landslide datasets. The results showed that the LDams form at the locations that have higher SPI value in relatively upstream areas, where hillslope areas are more confined to develop long-runout landslides. These outcomes, combined with an exploration of spatial

relationships among LDam formation, landslide occurrences, and proximity to rivers, explain the differences in morphometric characteristics, including landslide volume and H/L ratio, between DFLs and landslides more generally. These insights also serve as the foundational basis for quantifying a credible geomorphology-based buffer zone for river reaches prone to damming, a process applied in **Chapter 5** to delineate LDam formation susceptibility along river reaches.

6.1.4 A New Global-scale Applicable Framework for LDam Formation That Relies Less on Datasets

The applicability of the LDam formation index has been extensively discussed in previous studies, revealing its limitations that tie it to the local-scale context and its limited potential to be adapted to diverse study areas or different spatial scales (Dufresne et al. 2018; Tacconi Stefanelli et al. 2018; Cencetti et al. 2020; Argentin et al. 2021; Struble et al. 2021). The use of LDam formation susceptibility evaluation methods, by mapping the probability of DFL occurrence based on the empirical relationship to estimate the landslide run-out distance and volume estimate LDam formation probability in data scarce area is possible (Fan et al. 2014; Tacconi Stefanelli et al. 2020). Despite the creation of a new global-scale LDam dataset in **Chapter 3**, the number of records remain significantly fewer than actual LDam occurrences, and their spatial distribution remains concentrated in tectonically active regions that have received more research attention.

Rather than relying on LDam records as input data for data-driven susceptibility evaluation models, this study introduces a novel globally applicable framework to map the LDam formation probability on river reaches from GFDs in **Chapter 5**. This framework was accomplished by combining landslide susceptibility evaluation and LDam formation prone area identification based on the findings from **Chapter 4**, along with the LDam records obtained from **Chapter 3** for validation.

The outcomes were further validated through more detailed-scale research within the same basin (Tacconi Stefanelli et al. 2020), confirming the reliability of extrapolating results from large-scale research to smaller scales. The work is the first globally applicable framework for estimating LDam formation susceptibility, offering preliminary

LDam formation insights that can be valuable for early warnings, particularly in regions with insufficient LDam records.

6.2 Contributions to Science

6.2.1 Extension of Data Collection Method for LDam Dataset Establishment

Instead of mainly relying on LDam and landslide datasets or empirical relationships for data collection, this research introduces a fresh perspective by including the GFDs as reliable data sources to supply and enhance the inclusiveness of fluvial-related attributes, such as drainage area and river width. Remarkably, this study marks the first instance of GFDs being utilized to bolster the establishment of the LDam dataset and demonstrates their superior reliability compared to data derived from empirical relationships. This improvement was supported by the findings of Frasson et al. (2019), who indicated weak correlations within a unified empirical relationship between fluvial parameters. The integration of GFDs not only enhances the precision of data but also establishes a more robust foundation for LDam research, which will allow researchers to discover a wealth of fluvial information that contributes to a deeper understanding of LDam formation. The utilization of GFDs underscores the significance of embracing multiple data sources from different disciplines to enhance the progress of multi-hazard assessment and management practices.

6.2.2 A New Perspective for LDam Formation Probability Mapping

Previous LDam formation probability mapping focused on estimating the probability of DFL occurrence, which relied on the comprehensive landslide and LDam inventories on a local scale and thus the applicability to other study areas was constrained. This thesis takes a shift, changing the attention from the DFL occurrence (primarily landslide focused) to instead explore a river reaches susceptible to LDam formation. The transition was achieved through a modification of the procedures from landslide volume or run-out calculations based on empirical relationship establishment to quantification of LDam formation probability, which takes into account both fluvial characteristics and the probability of landslide occurrences within areas prone to LDam formation. Instead of providing a limited uniform distance threshold from specific locations on hillslopes to

rivers to quantify the probability of DFL reached the river, the new LDam formation susceptibility framework incorporates a geomorphological-based buffer zone based on the slope drainage delineation and spatial proximities. The framework utilized landslide susceptibility evaluation in a new way, a well-studied aspect that can be efficiently updated when new landslide susceptibility or GFDs are available.

6.2.3 Integration of Multiple Data Sources for LDam Studies

As highlighted in **Chapter 1**, the diversity of spatial distribution and comprehensiveness can hamper the seamless integration of datasets from multiple aspects into LDam muti-hazard risk modelling. This thesis provides insights to address this challenge by incorporating the landslide datasets and GFDs as the data source to quantify the LDam formation prone areas, which further contributed to the final LDam formation probability on the river reaches. This methodology offers the opportunity to lessen dependence on patchy LDam records and their associated empirical relationships, which might be underrepresented in regions where actual LDam occurrences have taken place, but not been recorded. Additionally, it enhances the comprehensiveness of attributes within LDam datasets. To increase the involvement from the fluvial side to better present the LDam-related processes and to reduce the data reliance on the landslide side, GFDs were extensively employed throughout the whole thesis as a data source for supplying fluvial attributes in the LDam dataset (**Chapter 3**), supplying the comparison of the characteristics between DFL and landslides more generally (**Chapter 4**), supplying LDam formation susceptibility evaluation and validating the results (**Chapter 5**). This integration underscores the potential of GFDs in mitigating record based data reliance on the landslide side and in enhancing the understanding of the complex multidiscipline dynamics underlying LDam formation.

6.3 Limitations and Future Works

6.3.1 Limitations of This Research

Even though a new LDam dataset was established with the supplement of GFDs, the number and quality of LDam records remains inadequately represented, especially for those areas in regions with limited R&D investment, despite their substantial potential for

landslide occurrences, such as the Rift valley in Sub-Saharan Africa or much of Asia and South America (Emberson et al. 2020). The challenges arising from the underrepresentation of LDam records are, in part, inherited from the complexities associated with landslides. The complexity encompassing factors like types, triggers, and locations, contribute to the variation in recorded final run-out distances and landslide volumes. Unlike large-scale hazardous events such as earthquakes or floods, the creation of landslide inventory maps and databases entails a meticulous process, involving the individual mapping and description of landslides, each with potentially distinctive characteristics (van Western et al. 2006).

The assumption for establishment of most empirical relationships is that the past is the key to the future. However, the non-stational effects, such as climate changes, which impact the landslide occurrence frequency and size as well as fluvial geomorphology, and land use changes, which have rapidly increased in recent decades, oversimplify the reality and thus can result in more uncertainties. Korup et al. (2012) found that according to their size and scaling analysis, the climatic changes could be one of the factors that affected the landslide distribution, and magnitude, but it is still challenging to isolate the landslide inventories from climatic (or other environmental) changes. Reichenbach et al. (2014) explored the impact of multiple land use scenarios on landslide susceptibility evaluation results and found an increasing number of unstable slope units as the forest area decreased. East and Sankey (2020) found that climate-driven changes have become evident, especially reflected by slope stability, when exploring the geomorphic and sedimentary response to ongoing anthropogenic warming in recent decades. Besides, they also mentioned the fluvial geomorphic changes in recent years may not be mainly triggered by hydroclimate factors, while plenty of uncertainties remain given the limited data availability. As a multi-hazard connecting fluvial and hillslope system, it would be more challenging for the LDam database establishment to consider such effects and apply it for LDam formation probability modelling. Climactic factors can directly influence the triggering processes of LDam formation and can further result in the unexpected failure of a LDam, but such factors were still not included in the modelling processes (Fan et al. 2020).

Moreover, while there are global-scale datasets available for specific types of

landslides, such as earthquake-triggered landslides (Schmitt et al. 2017), rainfall-triggered landslides (Kirschbaum et al. 2015), and fatal landslides (Petley 2012; Froude and Petley 2018), they are assembled using varying standards. These challenges continue to be relevant today, as the establishment of a unified standard for landslide inventories remains unclear (Guzzeti 2021), despite efforts made during the 1990s to standardize classification and nomenclature, as well as parameters like activity, causes, rates of movement, and remedial measures for landslides (IAEG Commission on Landslides 1990; IUGS-Working group on Landslides 1995). Consequently, this poses a significant challenge in terms of integrating and managing data to develop comprehensive global-scale landslide datasets that encompass all types of landslides. A similar challenge is encountered at the national scale in the compilation of landslide datasets. For the USA national-scale landslide dataset establishment, Mirus et al. (2020) selected a few attributes that are commonly found across datasets of different scales and sources, in addition to geolocation, including identification, date, fatalities, confidence, source, link, and notes. Notably, landslide types and detailed morphometric attributes were largely absent from datasets of such substantial scale, with only 2 out of 11 landslide datasets including both landslide types and detailed morphometric attributes, as illustrated in Figure 4-1 in Chapter 4. Moreover, the open-access landslide inventories of precise spatial coordinates and comprehensiveness are largely inconsistent.

For LDam research, the uncertainties and inconsistencies stemming from the engagement of multiple, differently formatted, data sources impede seamless data integration and the effective presentation of final results, as illustrated in Chapters 3 to 5). Namely: 1) The establishment of the LDam dataset is hindered by this lack of coherence, resulting in misrepresentation of location and inaccurate compilation outcomes; 2) for characteristic comparison, the limitation constraint on the data comprehensiveness of the fluvial system relates to the underrepresentation of smaller river reaches in upstream catchments; and 3) for LDam formation susceptibility evaluation, constraints directly curtail the accurate presentation of final results and amplify uncertainties in outcomes, particularly within confined deep river channels.

6.3.2 Future Works

Gathering a more extensive collection of LDam records is imperative to explore the characteristics more precisely, particularly in regions where a substantial number of LDam events are presently underrepresented. This endeavour would serve as an extension of the work discussed in Chapter 4, aiming to provide a more robust data source for analysis and validation and provide a more robust data source for analysis and validation as the RAGLAD dataset which sets an example by combining those necessary attributes summarized from previous LDam datasets. It would be more efficient to record the LDam records directly from comprehensive landslide inventories, especially for those collected within a single triggering event, such as an earthquake, intensive precipitation or floods.

Given the fact that landslide susceptibility evaluation constitutes as one of the key elements for the proposed LDam formation, it is necessary to enhance the performance of landslide susceptibility evaluation for enhancing LDam formation susceptibility in future studies. Guzzeti et al. (2012) underscored that the uncertainties and the absence of comprehensive landslide risk maps directly linked to the challenges and uncertainties inherent in compiling landslide inventories. Crucially, the inclusion of landslide types in these inventories is essential, as they directly influence the mechanisms of movement. Loche et al. (2022) set a precedent by demonstrating the mapping of landslide susceptibility in Italy based on eight distinct landslide types. Their work highlighted variations among these types, revealing that inventories may have been compiled with varying levels of detail.

Another direction for potentially enhancing the performance of the proposed LDam formation susceptibility evaluation framework lies in its application with more detailed data input. This would enable the framework's performance to be validated across diverse areas and spatial scales. Applying this global framework to the other study regions will be a crucial next step in the framework development. It will allow the assimilation of valuable local insights and research into our broader global understanding of this critical multi-hazard field. Through these combined efforts, the framework's accuracy and applicability could be substantially fortified.

The LDam formation framework could enhance the current global flood modelling framework. The development of a global dataset, numerical algorithms,

development of large-scale modelling frameworks have all contributed to the research shift of flood models from a local scale to a global scale (Smith et al. 2019; Bernhofen et al. 2022). Therefore, the Global flood model (GFM) has been advanced in recent years and have been applied to map the flood inundation area, regardless of data availability in certain local area (Schumann et al. 2018). Current research on GFM has been expanding scope to cover multi-hazard processes that link to flood, such as river-coastal surge risk (Eilander et al. 2020) and human-made dams' effects (Zajac et al. 2017), however, it has not yet been expanded to include LDam effects. However, the current LDam stability understanding relies heavily on the materials/components and geometry of LDams (Fan et al. 2020), which is currently very hard to achieve from 2-D mapping products over large-scale study areas. Therefore, for further integration of LDam effects on GFM, this issue is required to be addressed first.

6.4 Final Conclusions

LDams have been receiving interest for several decades, particularly since the 1980s, as they constitute a natural multi-hazard phenomenon that links fluvial and hillslope systems. To assess the risk posed by this hazard, researchers have concentrated on collecting LDam records to establish datasets, analysing the characteristics of LDam formation, proposing indices for determining the potential for LDam formation, and mapping the probabilities of DFL occurrence. This thesis underscores and addresses LDams as a global-scale multi-hazard in three primary ways: first, by creating a new global LDam dataset linking GFDs as a data supplement; second, by showing the quantified disparities in spatial distribution and morphometric characteristics, when compared to landslides more generally; and third, by introducing a new framework capable of estimating the likelihood of LDam formation along river reaches that can be applied to the global scale. Throughout the whole thesis, landslide datasets and GFDs were applied as two key components, aiming to mitigate reliance solely on the limited LDam datasets and associated empirical relationships, as the available LDam records still inadequately represent their actual occurrence within a single triggering event. These findings not only provide insights for various stakeholders but also provide a new entry point for combining multiple natural systems to solve the risk assessment issues for multi-

hazards, within a consistent framework even with multiple data constraints.

6.5 References

Argentin AL, Robl J, Prasicek G, Hergarten S, Hölbling D, Abad L, Dabiri Z (2021) Controls on the formation and size of potential landslide dams and dammed lakes in the Austrian Alps. Nat Hazards Earth Syst Sci 21(5):1615-1637

Bernhofen MV, Cooper S, Trigg M, Mdee A, Carr A, Bhave A, Solano-Correa YT, Pencue-Fierro EL, Teferi E, Haile AT, Yusop Z. (2022) The role of global data sets for riverine flood risk management at national scales. Water Resour Res. 58(4):e2021WR031555.

Cascini L. Applicability of landslide susceptibility and hazard zoning at different scales. Engineering Geology. 2008 Dec 1;102(3-4):164-77.

Cencetti C, De Rosa P, Fredduzzi A (2020) Characterization of landslide dams in a sector of the central-northern Apennines (Central Italy). Heliyon 6(6):e03799

Costa JE, Schuster RL (1988) The Formation and Failure of Natural Dams. Geol Soc Am Bull 100(7): 1054-1068

Dufresne A, Ostermann M, Preusser F (2018) River-damming, late-Quaternary rockslides in the Ötz Valley region (Tyrol, Austria). Geomorphology 310:153-167

East AE, Sankey JB. (2020) Geomorphic and sedimentary effects of modern climate change: current and anticipated future conditions in the western United States. Rev Geophys

Eilander D, Couasnon A, Ikeuchi H, Muis S, Yamazaki D, Winsemius HC, Ward PJ (2020) The effect of surge on riverine flood hazard and impact in deltas globally. Environ Res Lett. 15(10):104007

Emberson R, Kirschbaum D, Stanley T. (2020) New global characterisation of landslide exposure. Nat Hazards Earth Syst Sci 20(12):3413-3424

Fan X, Dufresne A, Siva Subramanian S, Strom A, Hermanns R, Tacconi Stefanelli C, Hewitt K, Yunus AP, Dunning S, Capra L, Geertsema M, Miller B, Casagli N, Jansen JD,

Xu Q (2020). The formation and impact of landslide dams – State of the art. Earth-Sci Rev 203

Fan XM, Rossiter DG, van Westen CJ, Xu Q, Gorum T (2014) Empirical prediction of coseismic landslide dam formation. Earth Surf Proc Land 39(14):1913–1926

Frasson RPD, Pavelsky TM, Fonstad MA, Durand MT, Allen GH, Schumann G, Lion C, Beighley RE, Yang X (2019) Global relationships between river width, slope, catchment area, meander wavelength, sinuosity, and discharge. Geophys Res Lett 46(6):3252–3262

IAEG-Commission on Landslides (1990). Suggested nomenclature for landslides. Bull Int Assoc Eng Geol. 41:13-16

IUGS-Working group on landslide (1995). A suggested method for describing the rate of movement of a landslide. Bull Int Assoc Eng Geol. 52:75-78

Jibson RW, Harp EL (2012). Extraordinary Distance Limits of Landslides Triggered by the 2011 Mineral, Virginia, Earthquake. Bull Seismol Soc Am 102(6):2368-2377

Kirschbaum DB, Stanley T, Zhou Y (2015) Spatial and Temporal Analysis of a Global Landslide Catalog. Geomorphology. doi:10.1016/j.geomorph.2015.03.016.

Korup O (2002) Recent research on landslide dams - a literature review with special attention to New Zealand. Prog Phys Geog 26(2):206–235

Korup O, Görüm T, Hayakawa Y. (2012) Without power? Landslide inventories in the face of climate change. Earth Surf Processes Landforms. 37(1):92-99

Loche M, Alvioli M, Marchesini I, Bakka H, Lombardo L (2022) Landslide susceptibility maps of Italy: Lesson learnt from dealing with multiple landslide types and the uneven spatial distribution of the national inventory. Earth Sci Rev. 18:104125

Mirus BB, Jones ES, Baum RL, Godt JW, Slaughter S, Crawford MM, Lancaster J, Stanley T, Kirschbaum DB, Burns WJ, Schmitt RG. (2020) Landslides across the USA: occurrence, susceptibility, and data limitations. Landslides. 17:2271-2285

Petley D (2012) Global patterns of loss of life from landslides. Geology 40(10):927-930

Reichenbach P, Busca C, Mondini AC, Rossi M (2014) The influence of land use change

on landslide susceptibility zonation: the Briga catchment test site (Messina, Italy). Environ Manage 54:1372-1384

Schmitt RG, Tanyas H, Nowicki Jessee MA, Zhu J, Biegel KM, Allstadt KE, Jibson RW, Thompson EM, van Westen CJ, Sato HP, Wald DJ, Godt JW, Gorum T, Xu C, Rathje EM, Knudsen KL (2017). An open repository of earthquake-triggered ground-failure inventories. U.S. Geological Survey data release collection, https://doi.org/10.5066/F7H70DB4. Accessed 23 Feb 2022

Schumann G, Bates PD, Apel H, Aronica GT (2018) Global flood hazard mapping, modeling, and forecasting: Challenges and perspectives. Global Flood Hazard: Applications in Modeling, Mapping, and Forecasting. 239-244

Smith A, Bates PD, Wing O, Sampson C, Quinn N, Neal J. (2019) New estimates of flood exposure in developing countries using high-resolution population data. Nat Commun.10(1):1814

Struble WT, Roering JJ, Burns WJ, Calhoun NC, Wetherell LR, Black BA (2021) The Preservation of Climate-Driven Landslide Dams in Western Oregon. J Geophys Res.: Earth Surf 126(4): e2020JF005908.

Tacconi Stefanelli C, Vilímek V, Emmer A, Catani F (2018) Morphological analysis and features of the landslide dams in the Cordillera Blanca. Peru. Landslides 15(3):507–521

Tacconi Stefanelli C, Casagli N, Catani F (2020) Landslide damming hazard susceptibility maps: a new GIS-based procedure for risk management. Landslides 17(7):1635-1648

Zajac Z, Revilla-Romero B, Salamon P, Burek P, Hirpa FA, Beck H. (2017) The impact of lake and reservoir parameterization on global streamflow simulation. J Hydrol 548:552-568

Appendix A. Supplement Materials for Chapter 3

Appendix A1. Reference of Landslide Dam Records

The RAGLAD dataset can be accessed at: https://doi.org/10.5518/1477.
The reference order of LDam record followed the order of LDam index in RAGLAD.

[1-2]. Kuo, Y.-S., Tsang, Y.-C., Chen, K.-T., Shieh, C.-L., 2011. Analysis of landslide dam geometries. Journal of Mountain Science, 8(4), 544-550.

[3]. Cui, P., Zhou, G.G.D., Zhu, X.H., Zhang, J.Q., 2013. Scale amplification of natural debris flows caused by cascading landslide dam failures. Geomorphology, 182, 173-189.

[4]. James, A., De Graff, J.V., 2012. The draining of Matthieu landslide-dam lake, Dominica, West Indies. Landslides, 9(4), 529-537.

[5-6]. DeGraff, J.V., Rogers, C.T., 2003. An unusual landslide-dam event in Dominica, West Indies, Landslide News, pp. 8-11.

[7]. Chai, H.L., Hanchao; Zhang, Zhuoyuen, 1995. The catalog of Chinese landslide dam events. Hournal of Geological hazards and Environment Preservation, 4. (in Chinese, with English title and abstract)

Costa, J.E., Schuster, R.L., 1987. The Formation and Failure of Natural Dams. Geological Society of America Bulletin, 100(7), 1054-1068.

Li, T.C., Schuster, R.L., Wu, J.S., 1986. Landslide dams in south-central China. In: Schuster R (ed) Landslide dams: processes, risk and mitigation. Geotechnical Special Publication No. 3, ASCE, 146–162

[8]. Li, M.H., Hsu, M.H., Hsieh, L.S., Teng, W.H., 2002. Inundation potentials analysis for Tsao-Ling landslide lake formed by Chi-Chi earthquake in Taiwan. Natural Hazards, 25(3), 289-303.

Evans, S.G., Delaney, K.B., Hermanns, R.L., Strom, A., Scarascia-Mugnozza, G., 2011. The Formation and Behaviour of Natural and Artificial Rockslide Dams; Implications for Engineering Performance and Hazard Management. Natural and artificial rockslide dams, 133. Springer Science & Business Media.

[9]. Li, M.H., Hsu, M.H., Hsieh, L.S., Teng, W.H., 2002. Inundation potentials analysis for Tsao-Ling landslide lake formed by Chi-Chi earthquake in Taiwan. Natural

Hazards, 25(3), 289-303.

[10]. Costa, J.E., Schuster, R.L., 1987. The Formation and Failure of Natural Dams. Geological Society of America Bulletin, 100(7), 1054-1068.

Li, T.C., 1994. Landslide Disasters and Human Responses in China. Mountain Research and Development, 14(4), 341-346.

Li, M.H., Hsu, M.H., Hsieh, L.S., Teng, W.H., 2002. Inundation potentials analysis for Tsao-Ling landslide lake formed by Chi-Chi earthquake in Taiwan. Natural Hazards, 25(3), 289-303.

Evans, S.G., Delaney, K.B., Hermanns, R.L., Strom, A., Scarascia-Mugnozza, G., 2011. The Formation and Behaviour of Natural and Artificial Rockslide Dams; Implications for Engineering Performance and Hazard Management. Natural and artificial rockslide dams, 133. Springer Science & Business Media.

[11]. Li, M.H., Hsu, M.H., Hsieh, L.S., Teng, W.H., 2002. Inundation potentials analysis for Tsao-Ling landslide lake formed by Chi-Chi earthquake in Taiwan. Natural Hazards, 25(3), 289-303.

[12]. 范建容, 田兵伟, 程根伟, 陶和平, 张建强, 严冬, 苏凤环, 刘斌涛, 2008. 基于多源遥感数据的 5· 12 汶川地震诱发堰塞体信息提取 山地学报, 26(3), 257-262. (In Chinese, with English title and abstract)

Yin, Y., Wang, F., Sun, P., 2009. Landslide hazards triggered by the 2008 Wenchuan earthquake, Sichuan, China. Landslides, 6(2), 139-152.

[13]. 殷跃平, 2008. 汶川八级地震地质灾害研究. 工程地质学报, 16(4), 433-444. (In Chinese, with English title and abstract)

Yin, Y., Wang, F., Sun, P., 2009. Landslide hazards triggered by the 2008 Wenchuan earthquake, Sichuan, China. Landslides, 6(2), 139-152.

[14]. 范建容, 田兵伟, 程根伟, 陶和平, 张建强, 严冬, 苏凤环, 刘斌涛, 2008. 基于多源遥感数据的 5· 12 汶川地震诱发堰塞体信息提取 山地学报, 26(3), 257-262. (In Chinese, with English title and abstract)

殷跃平, 2008. 汶川八级地震地质灾害研究. 工程地质学报, 16(4), 433-444. (In Chinese, with English title and abstract)

Yin, Y., Wang, F., Sun, P., 2009. Landslide hazards triggered by the 2008

Wenchuan earthquake, Sichuan, China. Landslides, 6(2), 139-152.

Xu, Q., Fan, X.-M., Huang, R.-Q., Westen, C.V., 2009. Landslide dams triggered by the Wenchuan Earthquake, Sichuan Province, south west China. Bulletin of Engineering Geology and the Environment, 68(3), 373-386.

[15-23]. 殷跃平, 2008. 汶川八级地震地质灾害研究. 工程地质学报, 16(4), 433-444. (In Chinese, with English title and abstract)

Yin, Y., Wang, F., Sun, P., 2009. Landslide hazards triggered by the 2008 Wenchuan earthquake, Sichuan, China. Landslides, 6(2), 139-152.

Xu, Q., Fan, X.-M., Huang, R.-Q., Westen, C.V., 2009. Landslide dams triggered by the Wenchuan Earthquake, Sichuan Province, south west China. Bulletin of Engineering Geology and the Environment, 68(3), 373-386.

[24]. 常东升, 张徐耀, & 黄润秋, 2009. 红石河堰塞湖漫顶溃坝风险评估. 工程地质学报, 17(1), 50-55. (In Chinese, with English title and abstract)

殷跃平, 2008. 汶川八级地震地质灾害研究. 工程地质学报, 16(4), 433-444. (In Chinese, with English title and abstract)

Yin, Y., Wang, F., Sun, P., 2009. Landslide hazards triggered by the 2008 Wenchuan earthquake, Sichuan, China. Landslides, 6(2), 139-152.

Xu, Q., Fan, X.-M., Huang, R.-Q., Westen, C.V., 2009. Landslide dams triggered by the Wenchuan Earthquake, Sichuan Province, south west China. Bulletin of Engineering Geology and the Environment, 68(3), 373-386.

[25]. 殷跃平, 2008. 汶川八级地震地质灾害研究. 工程地质学报, 16(4), 433-444. (In Chinese, with English title and abstract)

何秉顺, 丁留谦, 王玉杰, 徐文杰, 赵宇飞, 2009. 四川安县肖家桥堰塞湖稳定性初步评估. 岩石力学与工程学报, 28(S2), 3626-3630. (In Chinese, with English title and abstract)

Yin, Y., Wang, F., Sun, P., 2009. Landslide hazards triggered by the 2008 Wenchuan earthquake, Sichuan, China. Landslides, 6(2), 139-152.

[26]. 殷跃平, 2008. 汶川八级地震地质灾害研究. 工程地质学报, 16(4), 433-444. (In Chinese, with English title and abstract)

Yin, Y., Wang, F., Sun, P., 2009. Landslide hazards triggered by the 2008

Wenchuan earthquake, Sichuan, China. Landslides, 6(2), 139-152.

Xu, Q., Fan, X.-M., Huang, R.-Q., Westen, C.V., 2009. Landslide dams triggered by the Wenchuan Earthquake, Sichuan Province, south west China. Bulletin of Engineering Geology and the Environment, 68(3), 373-386.

[27]. 殷跃平, 2008. 汶川八级地震地质灾害研究. 工程地质学报, 16(4), 433-444. (In Chinese, with English title and abstract)

Yin, Y., Wang, F., Sun, P., 2009. Landslide hazards triggered by the 2008 Wenchuan earthquake, Sichuan, China. Landslides, 6(2), 139-152.

Xu, C., Shyu, J.B.H., Xu, X., 2014. Landslides triggered by the 12 January 2010 Port-au-Prince, Haiti, Mw= 7.0 earthquake: visual interpretation, inventory compiling, and spatial distribution statistical analysis. Natural Hazards and Earth System Sciences, 14(7), 1789-1818.

[28-40]. 殷跃平, 2008. 汶川八级地震地质灾害研究. 工程地质学报, 16(4), 433-444. (In Chinese, with English title and abstract)

Yin, Y., Wang, F., Sun, P., 2009. Landslide hazards triggered by the 2008 Wenchuan earthquake, Sichuan, China. Landslides, 6(2), 139-152.

Xu, Q., Fan, X.-M., Huang, R.-Q., Westen, C.V., 2009. Landslide dams triggered by the Wenchuan Earthquake, Sichuan Province, south west China. Bulletin of Engineering Geology and the Environment, 68(3), 373-386.

[41]. 殷跃平, 2008. 汶川八级地震地质灾害研究. 工程地质学报, 16(4), 433-444. (In Chinese, with English title and abstract)

Yin, Y., Wang, F., Sun, P., 2009. Landslide hazards triggered by the 2008 Wenchuan earthquake, Sichuan, China. Landslides, 6(2), 139-152.

徐梦珍, 王兆印, 漆力健, 2012. 汶川地震引发的次生灾害链. 山地学报, 30(4), 502-512. (In Chinese, with English title and abstract)

[42-44]. 殷跃平, 2008. 汶川八级地震地质灾害研究. 工程地质学报, 16(4), 433-444. (In Chinese, with English title and abstract)

Yin, Y., Wang, F., Sun, P., 2009. Landslide hazards triggered by the 2008 Wenchuan earthquake, Sichuan, China. Landslides, 6(2), 139-152.

[45]. Butt, M.J., Umar, M., Qamar, R., 2012. Landslide dam and subsequent dam-break

flood estimation using HEC-RAS model in Northern Pakistan. Natural Hazards, 65(1), 241-254.

Evans, S.G., Delaney, K.B., Hermanns, R.L., Strom, A., Scarascia-Mugnozza, G., 2011. The Formation and Behaviour of Natural and Artificial Rockslide Dams; Implications for Engineering Performance and Hazard Management. Natural and artificial rockslide dams, 133. Springer Science & Business Media.

Chen, X., Cui, P., You, Y., Cheng, Z., Khan, A., Ye, C., Zhang, S., 2017. Dam-break risk analysis of the Attabad landslide dam in Pakistan and emergency countermeasures. Landslides, 14(2), 675-683.

[46]. Konagai, K., Sattar, A., 2011. Partial breaching of Hattian Bala Landslide Dam formed in the 8th October 2005 Kashmir Earthquake, Pakistan. Landslides, 9(1), 1-11.

Sattar, A., Konagai, K., Kiyota, T., Ikeda, T., Johansson, J., 2010. Measurement of debris mass changes and assessment of the dam-break flood potential of earthquake-triggered Hattian landslide dam. Landslides, 8(2), 171-182.

[47]. Shi, Z.M., Xiong, X., Peng, M., Zhang, L.M., Xiong, Y.F., Chen, H.X., Zhu, Y., 2016. Risk assessment and mitigation for the Hongshiyan landslide dam triggered by the 2014 Ludian earthquake in Yunnan, China. Landslides, 14(1), 269-285.

Zhang, S., Xie, X., Wei, F., Chernomorets, S., Petrakov, D., Pavlova, I., Tellez, R.D., 2015. A seismically triggered landslide dam in Honshiyan, Yunnan, China: from emergency management to hydropower potential. Landslides, 12(6), 1147-1157.

[48]. Micu, M., Jurchescu, M., Micu, D., Zarea, R., Zumpano, V., Bălteanu, D., 2014. A morphogenetic insight into a multi-hazard analysis: Bâsca Mare landslide dam. Landslides, 11(6), 1131-1139.

[49]. Acharya, T.D., Mainali, S.C., Yang, I.T., Lee, D.H., 2016. Analysis of Jure Landslide Dam, Sindhupalchowk Using Gis and Remote Sensing. ISPRS - International Archives of the Photogrammetry, Remote Sensing and Spatial Information Sciences, XLI-B6, 201-203.

Pokharel, J.R., Regmi, S.B., Bhattarai, D.R., 2014. A report on study of Sunkoshi landslide dam in Jure, Sindhupalchowk, Nepal Engineers' Association.

Shrestha, B.B., Nakagawa, H., 2016. Hazard assessment of the formation and failure of the Sunkoshi landslide dam in Nepal. Natural Hazards, 82(3), 2029-2049.

[50-77]. Chen, C.-Y., Chang, J.-M., 2015. Landslide dam formation susceptibility analysis based on geomorphic features. Landslides, 13(5), 1019-1033.

[78]. Nibigira, L., Havenith, H.B., Archambeau, P., Dewals, B., 2017. Formation, breaching and flood consequences of a landslide dam near Bujumbura, Burundi. Natural Hazards and Earth System Sciences, 18(7), 1867-1890.

[79]. Xu, C., Shyu, J.B.H., Xu, X., 2014. Landslides triggered by the 12 January 2010 Port-au-Prince, Haiti, Mw= 7.0 earthquake: visual interpretation, inventory compiling, and spatial distribution statistical analysis. Natural Hazards and Earth System Sciences, 14(7), 1789-1818.

[80]. Shroder, J.F., Weihs, B.J., 2010. Geomorphology of the lake shewa landslide dam, badakhshan, afghanistan, using remote sensing data. Geografiska Annaler: Series A, Physical Geography, 92(4), 469-483.

[81]. Tsou, C.-Y., Feng, Z.-Y., Chigira, M., 2011. Catastrophic landslide induced by Typhoon Morakot, Shiaolin, Taiwan. Geomorphology, 127(3-4), 166-178.

Wu, C.-H., Chen, S.-C., Feng, Z.-Y., 2013. Formation, failure, and consequences of the Xiaolin landslide dam, triggered by extreme rainfall from Typhoon Morakot, Taiwan. Landslides, 11(3), 357-367.

[82]. Dong, J.-J., Lai, P.-J., Chang, C.-P., Yang, S.-H., Yeh, K.-C., Liao, J.-J., Pan, Y.-W., 2013. Deriving landslide dam geometry from remote sensing images for the rapid assessment of critical parameters related to dam-breach hazards. Landslides, 11(1), 93-105.

[83]. Ishizuka, T., Kaji, A., Morita, K., Mori, T., Chiba, M., KashiwabarA, Y., Yoshino, K., Uchida, T., Mizuyama, T., 2017. Analysis for a Landslide Dam Outburst Flood in Ambon Island, Indonesia.

Yakti, B.P., Adityawan, M.B., Farid, M., Suryadi, Y., Nugroho, J., Hadihardaja, I.K., Pribadi, K., Sugeng, B., Hadihardaja, I.K., 2018. 2D Modeling of Flood Propagation due to the Failure of Way Ela Natural Dam. MATEC Web of Conferences, 147.

[84]. Bricker, J.D., Schwanghart, W., Adhikari, B.R., Moriguchi, S., Roeber, V., Giri, S., 2017. Performance of Models for Flash Flood Warning and Hazard Assessment: The 2015 Kali Gandaki Landslide Dam Breach in Nepal. Mountain Research and Development, 37(1), 5-15.

[85]. Nash, T., Bell, D., Davies, T., Nathan, S., 2008. Analysis of the formation and failure of Ram Creek landslide dam, South Island, New Zealand. New Zealand Journal of Geology and Geophysics, 51(3), 187-193.

Harrison, L.M., Dunning, S.A., Woodward, J., Davies, T.R.H., 2015. Post-rock-avalanche dam outburst flood sedimentation in Ram Creek, Southern Alps, New Zealand. Geomorphology, 241, 135-144.

[86]. Duman, T.Y., 2009. The largest landslide dam in Turkey: Tortum landslide. Engineering Geology, 104(1-2), 66-79.

[87]. Dai, F.C., Lee, C.F., Deng, J.H., Tham, L.G., 2005. The 1786 earthquake-triggered landslide dam and subsequent dam-break flood on the Dadu River, southwestern China. Geomorphology, 65(3-4), 205-221.

[88]. Chen, Y.J., Zhou, F., Feng, Y., Xia, Y.C., 1992. Breach of a Naturally Embanked Dam on Yalong River. Can J Civil Eng, 19(5), 811-818.

Chen, Y.J., Zhou, F., Feng, Y., Xia, Y.C., 1994. Breach of a naturally embanked dam on Yalong River. Canadian Journal of Civil Engineering, 19(5), 811-818.

Costa, J.E., Schuster, R.L., 1987. The Formation and Failure of Natural Dams. Geological Society of America Bulletin, 100(7), 1054-1068.

Evans, S.G., Delaney, K.B., Hermanns, R.L., Strom, A., Scarascia-Mugnozza, G., 2011. The Formation and Behaviour of Natural and Artificial Rockslide Dams; Implications for Engineering Performance and Hazard Management. Natural and artificial rockslide dams, 133. Springer Science & Business Media.

[89]. Hancox, G.T., McSaveney, M.J., Manville, V.R., Davies, T.R., 2005. The October 1999 Mt Adams rock avalanche and subsequent landslide dam-break flood and effects in Poerua river, Westland, New Zealand. New Zealand Journal of Geology and Geophysics, 48(4), 683-705.

Harrison, L.M., Dunning, S.A., Woodward, J., Davies, T.R.H., 2015. Post-rock-avalanche dam outburst flood sedimentation in Ram Creek, Southern Alps, New Zealand. Geomorphology, 241, 135-144.

[90]. Alford, D., Schuster, R.M., 2000. Usoi landslide dam and Lake Sarez–an assessment of hazard and risk in the Pamir Mountains, Tajikistan, United Nations, New York and Geneva.

Costa, J.E., Schuster, R.L., 1987. The Formation and Failure of Natural Dams. Geological Society of America Bulletin, 100(7), 1054-1068.

Evans, S.G., Delaney, K.B., Hermanns, R.L., Strom, A., Scarascia-Mugnozza, G., 2011. The Formation and Behaviour of Natural and Artificial Rockslide Dams; Implications for Engineering Performance and Hazard Management. Natural and artificial rockslide dams, 133. Springer Science & Business Media.

Strom, A., 2010. Landslide dams in Central Asia region. Journal of the Japan Landslide Society, 47(6), 309-324.

[91]. Wang, G., Huang, R., Kamai, T., Zhang, F., 2013. The internal structure of a rockslide dam induced by the 2008 Wenchuan (Mw7.9) earthquake, China. Engineering Geology, 156, 28-36.

[92-93]. Shoaei, Z., 2014. Mechanism of the giant Seimareh Landslide, Iran, and the longevity of its landslide dams. Environmental Earth Sciences, 72(7), 2411-2422.

[94]. Paliaga, G., Faccini, F., Luino, F., Turconi, L., Bobrowsky, P., 2019. Geomorphic processes and risk related to a large landslide dam in a highly urbanized Mediterranean catchment (Genova, Italy). Geomorphology, 327, 48-61.

[95]. Kim, T.H., Cruden, D.M., Martin, C.D., Froese, C.R., 2009. The 2007 Fox Creek landslide, Peace River Lowland, Alberta, Canada. Landslides, 7(1), 89-98.

Miller, B., Dufresne, A., Geertsema, M., Atkinson, N., Evensen, H., Cruden, D., 2018. Longevity of dams from landslides with sub-channel rupture surfaces, Peace River region, Canada. Geoenvironmental Disasters, 5(1).

[96]. Catane, S.G., Abon, C.C., Saturay, R.M., Mendoza, E.P.P., Futalan, K.M., 2012. Landslide-amplified flash floods—The June 2008 Panay Island flooding, Philippines. Geomorphology, 169-170, 55-63.

[97]. Cruden, D.M., Keegan, T.R., Thomson, S., 1993. The landslide dam on the Saddle River near Rycroft, Alberta. Can Geotech J, 30(6), 1003-1015.

[98]. Uzuoka, R., Sento, N., Mori, T., Kazama, M., 2011. Geotechnical Properties of Yunokura Landslide Dam Induced by 2008 Iwate-Miyagi Nairiku Earthquake. Journal of Japan Association for Earthquake Engineering, 11(5), 80-93. (In Japanese, with English title and abstract)

[99]. 森俊勇, 坂口哲夫, 井上公夫, 2011. 日本の天然ダムと対応策. 古今書院. (In

Japanese)

[100]. Delaney, K.B., Evans, S.G., 2015. The 2000 Yigong landslide (Tibetan Plateau), rockslide-dammed lake and outburst flood: Review, remote sensing analysis, and process modelling. Geomorphology, 246, 377-393.

Evans, S.G., Delaney, K.B., Hermanns, R.L., Strom, A., Scarascia-Mugnozza, G., 2011. The Formation and Behaviour of Natural and Artificial Rockslide Dams; Implications for Engineering Performance and Hazard Management. Natural and artificial rockslide dams, 133. Springer Science & Business Media.

李志威, 汤韬, 袁昕亚, 余国安, 2019. 堰塞体堵江对雅鲁藏布大峡谷地区河流地貌的影响. 长江科学院院报, 37(8), 16-21. (In Chinese, with English title and abstract)

殷跃平, 2000. 西藏波密易贡高速巨型滑坡特征及减灾研究. 水文地质工程地质(4), 8-11.(In Chinese, with English abstract)

[101]. Penna, I.M., Derron, M.-H., Volpi, M., Jaboyedoff, M., 2013. Analysis of past and future dam formation and failure in the Santa Cruz River (San Juan province, Argentina). Geomorphology, 186, 28-38.

Perucca, L.P., Esper Angillieri, M.Y., 2009. Evolution of a debris-rock slide causing a natural dam: the flash flood of Río Santa Cruz, Province of San Juan—November 12, 2005. Natural Hazards, 50(2), 305-320.

[102-162]. Hermanns, R.L., Folguera, A., Penna, I., Fauqué, L., Niedermann, S., 2011. Landslide Dams in the Central Andes of Argentina (Northern Patagonia and the Argentine Northwest), Natural and Artificial Rockslide Dams. Lecture Notes in Earth Sciences, pp. 147-176.

[163]. King, J., Loveday, I., chuster, R.L., 1989. The 1985 Bairaman landslide dam and resulting debris flow, Papua New Guinea. Quarterly Journal of Engineering Geology and Hydrogeology, 22(4), 257-270.

[164]. Sakals, M.E., Geertsema, M., Schwab, J.W., Foord, V.N., 2011. The Todagin Creek landslide of October 3, 2006, Northwest British Columbia, Canada. Landslides, 9(1), 107-165. Dal Sasso, S.F., Sole, A., Bateman Pinzón, A., Medina, V., Mirauda, D., Volpe Plantamura, A., Giosa, L., Guariglia, A., 2016. Analysis of river bed dynamic evolution following a landslide dam. La Houille Blanche(6), 88-95.

[165]. Dal Sasso, S.F., Sole, A., Pascale, S., Sdao, F., Bateman Pinzòn, A., Medina, V.,

2014. Assessment methodology for the prediction of landslide dam hazard. Natural Hazards and Earth System Sciences, 14(3), 557-567.

[166-168]. Wei, R., Zeng, Q., Davies, T., Yuan, G., Wang, K., Xue, X., Yin, Q., 2018. Geohazard cascade and mechanism of large debris flows in Tianmo gully, SE Tibetan Plateau and implications to hazard monitoring. Engineering Geology, 233, 172-182.

[169]. Clague, J.J. and Evans, S.G., 1994. Formation and failure of natural dams in the Canadian Cordillera., Geological Survey of Canada.

[170-190]. Clague, J.J. and Evans, S.G., 1994. Formation and failure of natural dams in the Canadian Cordillera., Geological Survey of Canada.

[191]. Costa, J.E., Schuster, R.L., 1987. The Formation and Failure of Natural Dams. Geological Society of America Bulletin, 100(7), 1054-1068.

Evans, S.G., Delaney, K.B., Hermanns, R.L., Strom, A., Scarascia-Mugnozza, G., 2011. The Formation and Behaviour of Natural and Artificial Rockslide Dams; Implications for Engineering Performance and Hazard Management. Natural and artificial rockslide dams, 133. Springer Science & Business Media.

Kojan, E., Hutchison, J.N., 1978. Mayunmarca Rockslide and Debris Flow, Peru. Developments in Geotechnical Engineering, 14. Elsevier.

[192-193]. Costa, J.E., Schuster, R.L., 1987. The Formation and Failure of Natural Dams. Geological Society of America Bulletin, 100(7), 1054-1068.

[194]. Costa, J.E., Schuster, R.L., 1987. The Formation and Failure of Natural Dams. Geological Society of America Bulletin, 100(7), 1054-1068.

Evans, S.G., Delaney, K.B., Hermanns, R.L., Strom, A., Scarascia-Mugnozza, G., 2011. The Formation and Behaviour of Natural and Artificial Rockslide Dams; Implications for Engineering Performance and Hazard Management. Natural and artificial rockslide dams, 133. Springer Science & Business Media.

[195]. Costa, J.E., Schuster, R.L., 1987. The Formation and Failure of Natural Dams. Geological Society of America Bulletin, 100(7), 1054-1068.

Hadley, J.B., 1978. Madison Canyon Rockslide, Montana, U.S.A. Developments in Geotechnical Engineering, 14.

[196-200]. Costa, J.E., Schuster, R.L., 1987. The Formation and Failure of Natural Dams. Geological Society of America Bulletin, 100(7), 1054-1068.

[201-205]. Evans, S.G., Delaney, K.B., Hermanns, R.L., Strom, A., Scarascia-Mugnozza, G., 2011. The Formation and Behaviour of Natural and Artificial Rockslide Dams; Implications for Engineering Performance and Hazard Management. Natural and artificial rockslide dams, 133. Springer Science & Business Media.

[205-387]. Stefanelli, T. C., Catani, F., Casagli, N., 2015. Geomorphological investigations on landslide dams. Geoenvironmental Disasters, 2(1).

[388]. Stefanelli, T. C., Catani, F., Casagli, N., 2015. Geomorphological investigations on landslide dams. Geoenvironmental Disasters, 2(1).

Pappalardo, G., Mineo, S., Angrisani, A.C., Di Martire, D., Calcaterra, D., 2018. Combining field data with infrared thermography and DInSAR surveys to evaluate the activity of landslides: the case study of Randazzo Landslide (NE Sicily). Landslides, 15(11), 2173-2193.

[389-463]. Stefanelli, T.C., Catani, F., Casagli, N., 2015. Geomorphological investigations on landslide dams. Geoenvironmental Disasters, 2(1).

[464-514]. Stefanelli, T.C., Vilímek, V., Emmer, A., Catani, F., 2018. Morphological analysis and features of the landslide dams in the Cordillera Blanca, Peru. Landslides, 15(3), 507-521.

[515]. Kumar, V., Gupta, V., Jamir, I., Chattoraj, S.L., 2019. Evaluation of potential landslide damming: Case study of Urni landslide, Kinnaur, Satluj valley, India. Geoscience Frontiers, 10(2), 753-767.

[516-517]. 森俊勇, 坂口哲夫, 井上公夫, 2011. 日本の天然ダムと対応策. 古今書院.(In Japanese)

遠江地震と池口くずれ, https://www.cbr.mlit.go.jp/tenjyo/symposium/data/sympo-densyo05.pdf. (In Japanese)

[518-522]. 森俊勇, 坂口哲夫, 井上公夫, 2011. 日本の天然ダムと対応策. 古今書院.(In Japanese)

[523]. 森俊勇, 坂口哲夫, 井上公夫, 2011. 日本の天然ダムと対応策. 古今書院.(In Japanese)

コラム 15： 1502 年の姫川流域・真那板山の大崩壊と天然ダム, https://isabou.net/knowhow/colum-rekishi/colum15.asp. (In Japanese)

[524-527]. 森俊勇, 坂口哲夫, 井上公夫, 2011. 日本の天然ダムと対応策. 古今書院.(In Japanese)

[528]. 森俊勇, 坂口哲夫, 井上公夫, 2011. 日本の天然ダムと対応策. 古今書院.(In Japanese)

野崎保, 井上裕治, 2005. 天正地震 (1586) による前山地すべりの発生機構. 日本地すべり学会誌, 42(2), 115-120. (In Japanese)

[529]. 森俊勇, 坂口哲夫, 井上公夫, 2011. 日本の天然ダムと対応策. 古今書院.(In Japanese)

[530]. 森俊勇, 坂口哲夫, 井上公夫, 2011. 日本の天然ダムと対応策. 古今書院.(In Japanese)

栗本享宥, 苅谷愛彦, 目代邦康, 2019. 岐阜県郡上市明宝の水沢上地すべりと 1586 年天正地震, 2019 年度日本地理学会春季学術大会. 公益社団法人 日本地理学会, 神奈川県川崎市多摩区, pp. 69. (In Japanese, with English title)

[531-532]. 森俊勇, 坂口哲夫, 井上公夫, 2011. 日本の天然ダムと対応策. 古今書院.(In Japanese)

[533]. 森俊勇, 坂口哲夫, 井上公夫, 2011. 日本の天然ダムと対応策. 古今書院.(In Japanese)

コラム 4：寛文二年（1662）の近江・若狭地震と町居崩れ. https://isabou.net/knowhow/colum-rekishi/colum04.asp

[534]. 森俊勇, 坂口哲夫, 井上公夫, 2011. 日本の天然ダムと対応策. 古今書院.(In Japanese)

[535-537]. 森俊勇, 坂口哲夫, 井上公夫, 2011. 日本の天然ダムと対応策. 古今書院.(In Japanese)

小山内信智, 井上公夫, 2014. 地震と土砂災害, 報告書（1707 宝永地震）災害教訓の継承に関する専門調査会報告書, 内閣府. (In Japanese)

[538]. 森俊勇, 坂口哲夫, 井上公夫, 2011. 日本の天然ダムと対応策. 古今書院.(In Japanese)

田中収, 1982. 東海地震による富士川河岸白鳥山崩壊の危険性: 応用地質, 日本地質学会学術大会講演要旨 第 89 年学術大会 (1982 新潟). 一般社団法人 日本地質学会, pp. 478. (In Japanese)

[539]. 森俊勇, 坂口哲夫, 井上公夫, 2011. 日本の天然ダムと対応策. 古今書院.(In Japanese)

[540]. 森俊勇, 坂口哲夫, 井上公夫, 2011. 日本の天然ダムと対応策. 古今書院.(In Japanese)

コラム 12 ：1707 年の宝永地震による仁淀川中流・舞ヶ鼻の天然ダム, https://isabou.net/knowhow/colum-rekishi/colum12.asp. (In Japanese)

[541]. 森俊勇, 坂口哲夫, 井上公夫, 2011. 日本の天然ダムと対応策. 古今書院.(In Japanese)

コラム 16 ：1714 年の信州小谷地震による姫川・岩戸山の天然ダム, https://www.isabou.net/knowhow/colum-rekishi/colum16.asp. (In Japanese)

[542-544]. 森俊勇, 坂口哲夫, 井上公夫, 2011. 日本の天然ダムと対応策. 古今書院.(In Japanese)

[545]. 森俊勇, 坂口哲夫, 井上公夫, 2011. 日本の天然ダムと対応策. 古今書院.(In Japanese)

コラム 17 ：豪雨（1757）による梓川上流・トバタ崩れと天然ダム, https://isabou.net/knowhow/colum-rekishi/colum17.asp.

[546-548]. 森俊勇, 坂口哲夫, 井上公夫, 2011. 日本の天然ダムと対応策. 古今書院.(In Japanese)

[549]. 森俊勇, 坂口哲夫, 井上公夫, 2011. 日本の天然ダムと対応策. 古今書院.(In Japanese)

天明 8 年の山崩れ. 2013. https://www.shikoku-saigai.com/archives/9626?preurl=&query_pref=%E9%AB%98%E7%9F%A5%E7%9C%8C&query_city=%E9%A6%99%E7%BE%8E%E5%B8%82%EF%BC%88%E7%89%A9%E9%83%A8%E6%9D%91%EF%BC%89&query_dis_kind=%E5%9C%9F%E7

%A0%82%E7%81%BD%E5%AE%B3.

[550]. 森俊勇, 坂口哲夫, 井上公夫, 2011. 日本の天然ダムと対応策. 古今書院.(In Japanese)

[551]. コラム 30 寛政西津軽地震（1793）による追良瀬(おいらせ)川上流の天然ダム, https://isabou.net/knowhow/colum-rekishi/colum30.asp.

森俊勇, 坂口哲夫, 井上公夫, 2011. 日本の天然ダムと対応策. 古今書院.(In Japanese)

[552-557]. 森俊勇, 坂口哲夫, 井上公夫, 2011. 日本の天然ダムと対応策. 古今書院.(In Japanese)

[558]. 森俊勇, 坂口哲夫, 井上公夫, 2011. 日本の天然ダムと対応策. 古今書院.(In Japanese)

1854 安政東海地震・安政南海地震, http://www.bousai.go.jp/kohou/kouhoubousai/h24/68/past.html. (In Japanese)

[559]. 森俊勇, 坂口哲夫, 井上公夫, 2011. 日本の天然ダムと対応策. 古今書院.(In Japanese)

田中収, 1982. 東海地震による富士川河岸白鳥山崩壊の危険性: 応用地質, 日本地質学会学術大会講演要旨 第 89 年学術大会 (1982 新潟). 一般社団法人 日本地質学会, pp. 478. (In Japanese)

[560]. コラム 22 飛越地震（1858）による土砂災害, https://isabou.net/knowhow/colum-rekishi/colum22.asp. (In Japanese)

森俊勇, 坂口哲夫, 井上公夫, 2011. 日本の天然ダムと対応策. 古今書院.(In Japanese)

[561-564]. 森俊勇, 坂口哲夫, 井上公夫, 2011. 日本の天然ダムと対応策. 古今書院.(In Japanese)

[565]. 森俊勇, 坂口哲夫, 井上公夫, 2011. 日本の天然ダムと対応策. 古今書院.(In Japanese)

井上公夫, 藤井昭二, 2008. 大規模土砂災害. 災害教訓の継承に関する専門

調査会報告書　平成 20 年 3 月, 69-91. (In Japanese)

[566-570]. 森俊勇, 坂口哲夫, 井上公夫, 2011. 日本の天然ダムと対応策. 古今書院.(In Japanese)

[571-599]. コラム 28 明治 22 年（1889）紀伊半島豪雨による土砂災害, https://isabou.net/knowhow/colum-rekishi/colum28.asp. (In Japanese)

森俊勇, 坂口哲夫, 井上公夫, 2011. 日本の天然ダムと対応策. 古今書院.(In Japanese)

井上公夫, 土志田正二, 2012. 紀伊半島の 1889 年と 2011 年の災害分布の比較. 砂防学会誌 65(3), 42-46. (In Japanese, with English title and abstract)

Inoue, K., Doshida, S., Inoue, M., 2012. Formation and Outburst of Landslide Dams in 1889 along Totsu River, Central Kii Peninsula. (In Japanese, with English title and abstract)

[600-601]. コラム 57 大規模土砂災害と防災施設の現地見学会① －和歌山県田辺市奇絶峡付近の風穴と巨石積堰堤を歩く-, https://isabou.net/knowhow/colum-rekishi/colum57.asp.

森俊勇, 坂口哲夫, 井上公夫, 2011. 日本の天然ダムと対応策. 古今書院.(In Japanese)

Inoue, K., Doshida, S., Inoue, M., 2012. Formation and Outburst of Landslide Dams in 1889 along Totsu River, Central Kii Peninsula. (In Japanese, with English title and abstract)

[602-603]. 森俊勇, 坂口哲夫, 井上公夫, 2011. 日本の天然ダムと対応策. 古今書院.(In Japanese)

Inoue, K., Doshida, S., Inoue, M., 2012. Formation and Outburst of Landslide Dams in 1889 along Totsu River, Central Kii Peninsula. (In Japanese, with English title and abstract)

[604-606]. 森俊勇, 坂口哲夫, 井上公夫, 2011. 日本の天然ダムと対応策. 古今書院.(In Japanese)

[607]. 2013. 明治 25 年の高磯山崩壊, https://www.shikoku-

saigai.com/archives/10957.

森俊勇, 坂口哲夫, 井上公夫, 2011. 日本の天然ダムと対応策. 古今書院.(In Japanese)

[608]. 森俊勇, 坂口哲夫, 井上公夫, 2011. 日本の天然ダムと対応策. 古今書院.(In Japanese)

[609]. Abe, S., Takahashi, A., 1997. Landslide Processes during Earthquakes in the "Green Tuff" Area in the Tohoku District. The Rikuu Earthquake and Senboku Earthquake in Akita Prefecture. Journal of the Japan Society of Engineering Geology, 38(5), 265-279. (In Japanese, with English title and abstract)

森俊勇, 坂口哲夫, 井上公夫, 2011. 日本の天然ダムと対応策. 古今書院.(In Japanese)

[610]. コラム 34 富士川支流・大柳川における天然ダムの形成と災害対策, https://isabou.net/knowhow/colum-rekishi/colum34.asp. (In Japanese)

森俊勇, 坂口哲夫, 井上公夫, 2011. 日本の天然ダムと対応策. 古今書院.(In Japanese)

[611-614]. 森俊勇, 坂口哲夫, 井上公夫, 2011. 日本の天然ダムと対応策. 古今書院.(In Japanese)

[615]. 森俊勇, 坂口哲夫, 井上公夫, 2011. 日本の天然ダムと対応策. 古今書院.(In Japanese)

井上公夫, 蒲原潤一, 本橋和志, 渡部康弘, 2008. 安倍川中流・蕨野地区の西側山腹崩壊で生じた河道閉塞と 1914 年の水害. 砂防学会誌, 61(2), 30-35. (In Japanese, with English title and abstract)

[616-627]. 森俊勇, 坂口哲夫, 井上公夫, 2011. 日本の天然ダムと対応策. 古今書院.(In Japanese)

[628]. 森俊勇, 坂口哲夫, 井上公夫, 2011. 日本の天然ダムと対応策. 古今書院.(In Japanese)

昭和 14 年 4 月風張山大崩壊. Nagano Prefecture, https://www.pref.nagano.lg.jp/himesabo/jimusho/documents/s14.pdf. (In Japanese)

[629-631]. 森俊勇, 坂口哲夫, 井上公夫, 2011. 日本の天然ダムと対応策. 古今書院.(In Japanese)

[632]. 森俊勇, 坂口哲夫, 井上公夫, 2011. 日本の天然ダムと対応策. 古今書院.(In Japanese)

河南良男, 吉村元吾, 今森直紀, 田中健貴, 千東圭央, 井上公夫, 永田雅一, 中根和彦, 今村隆正, 2017. 有田川上流域における昭和 28 年災害の土砂災害分布について. In: 平. 年度（公社）砂防学会定時総会並びに研究発表会実行委員会 (Ed.), 平成 29 年度砂防学会研究発表会. 公益社団法人 砂防学会, 奈良春日野国際フォーラム　甍　I・RA・KA. (In Japanese)

[633-640]. 森俊勇, 坂口哲夫, 井上公夫, 2011. 日本の天然ダムと対応策. 古今書院.(In Japanese)

[641]. 森俊勇, 坂口哲夫, 井上公夫, 2011. 日本の天然ダムと対応策. 古今書院.(In Japanese)

井良沢道也, 1986. 大西山の大崩壊. 砂防学会誌, 39(1), 30-32. (In Japanese)

[642]. 森俊勇, 坂口哲夫, 井上公夫, 2011. 日本の天然ダムと対応策. 古今書院.(In Japanese)

第２回里山探検隊, 2015. 大災害から５０年が経過した徳山白谷（旧徳山村）の見学会を実施しました. (In Japanese)

[643-644]. 森俊勇, 坂口哲夫, 井上公夫, 2011. 日本の天然ダムと対応策. 古今書院.(In Japanese)

[645]. 森俊勇, 坂口哲夫, 井上公夫, 2011. 日本の天然ダムと対応策. 古今書院.(In Japanese)

姫川流域の地すべり, 1978.地すべりの学会新潟分部,土質工学会 北陸支部. (In Japanese)

[646]. 森俊勇, 坂口哲夫, 井上公夫, 2011. 日本の天然ダムと対応策. 古今書院.(In Japanese)

望月巧一, 1971. 小土山地すべりについて. 地すべり, 8(2), 44-45. (In

Japanese)

[647]. 森俊勇, 坂口哲夫, 井上公夫, 2011. 日本の天然ダムと対応策. 古今書院.(In Japanese)

[648]. 科学技術庁国立防災科学技術センター, 1977. 1976 年台風第 17 号による兵庫県一宮町福知抜山地すべり，および香川県小豆島の災害調査報告. (In Japanese)

森俊勇, 坂口哲夫, 井上公夫, 2011. 日本の天然ダムと対応策. 古今書院.(In Japanese)

[649]. 森俊勇, 坂口哲夫, 井上公夫, 2011. 日本の天然ダムと対応策. 古今書院.(In Japanese)

[650]. 森俊勇, 坂口哲夫, 井上公夫, 2011. 日本の天然ダムと対応策. 古今書院.(In Japanese)

[651-655]. コラム 45 長野県西部地震（1984）による御岳崩れと土石流. (In Japanese)

森俊勇, 坂口哲夫, 井上公夫, 2011. 日本の天然ダムと対応策. 古今書院.(In Japanese)

[656]. 国土交通省東北地方整備局新庄河川事務所, 2011. 立谷沢川支川濁沢川で土砂崩壊が発生. 山形県東田川郡庄内町大字立谷沢地内. (In Japanese)

森俊勇, 坂口哲夫, 井上公夫, 2011. 日本の天然ダムと対応策. 古今書院.(In Japanese)

[657-658]. 森俊勇, 坂口哲夫, 井上公夫, 2011. 日本の天然ダムと対応策. 古今書院.(In Japanese)

[659]. 森俊勇, 坂口哲夫, 井上公夫, 2011. 日本の天然ダムと対応策. 古今書院.(In Japanese)

高村舜介, 1973. 舟形町の地すべりについて. 地すべり, 10(1), 35-35.

[660]. 森俊勇, 坂口哲夫, 井上公夫, 2011. 日本の天然ダムと対応策. 古今書院.(In Japanese)

[661-662]. 森俊勇, 坂口哲夫, 井上公夫, 2011. 日本の天然ダムと対応策. 古今書

院.(In Japanese)

(社)砂防学会研究開発部会, 2005. 新潟県中越地震土砂災害調査研究委員会報告. 砂防学会誌, 57(6), 80-81. (In Japanese)

[663]. 森俊勇, 坂口哲夫, 井上公夫, 2011. 日本の天然ダムと対応策. 古今書院.(In Japanese)

国土交通省所管楢木地すべり, https://www.jasdim.or.jp/gijutsu/kobetsu/chiiki/niigata/naraki/naraki.htm. (In Japanese)

[664]. 丸井英明, 吉松弘行, 若井明彦, 渡部直喜, 石井靖雄, 2014. 「芋川地区直轄地すべり防止工事完了判定委員会」の開催について. (In Japanese)

森俊勇, 坂口哲夫, 井上公夫, 2011. 日本の天然ダムと対応策. 古今書院.(In Japanese)

[665]. 河道閉塞箇所の特性について, http://www.hrr.mlit.go.jp/yuzawa/sabo/chuetsu/taisaku/iinkai_2nd/tokusei.pdf. (In Japanese)

森俊勇, 坂口哲夫, 井上公夫, 2011. 日本の天然ダムと対応策. 古今書院.(In Japanese)

[666]. 里深好文, 吉., 水山高久, 小川紀一朗, 内川龍男, & 森俊勇., 2007. 天然ダムの決壊に伴う洪水流出の予測手法に 関する研究. 水工学論文集, 51, 901-906. (In Japanese, with English title and abstract)

森俊勇, 坂口哲夫, 井上公夫, 2011. 日本の天然ダムと対応策. 古今書院.(In Japanese)

[667]. 西本晴男, 2009. 岩手・宮城内陸地震における河道閉塞 （天然ダム）対応について, 国総研講演会. 国土技術政策総合研究所, 東京都千代田区. (In Japanese)

森俊勇, 坂口哲夫, 井上公夫, 2011. 日本の天然ダムと対応策. 古今書院.(In Japanese)

[668]. 常田賢一, 渦岡良介, 細矢卓志, 2010. 天然ダムと河道閉塞, 平成20年（2008年）岩手・宮城内陸地震災害調査報告書,地盤工学会. (In Japanese)

森俊勇, 坂口哲夫, 井上公夫, 2011. 日本の天然ダムと対応策. 古今書院.(In Japanese)

[669-680]. 森俊勇, 坂口哲夫, 井上公夫, 2011. 日本の天然ダムと対応策. 古今書院.(In Japanese)

[681-682]. Butler, D.R., Malanson, G.P., Oelfke, J.G., 1991. Potential catastrophic flooding from landslide-dammed lakes, Glacier National Park, Montana, USA. Zeitschrift für Geomorphologie Supplementband, 83, 195-209.

Costa, J.E., Schuster, R.L., 1987. The formation and failure of natural dams. 87-392.

[683-688]. Strom, A., 2010. Landslide dams in Central Asia region. Journal of the Japan Landslide Society, 47(6), 309-324.

[689-714]. Nash, T., 2003. Engineering Geological Assessment of Selected Landslide Dams Formed from the 1929 Murchison and 1968 Inangahua Earthquakes. Master, University of Canterbury.

[715]. Casagli, N., Cigna, F., Bianchini, S., Hölbling, D., Füreder, P., Righini, G., Del Conte, S., Friedl, B., Schneiderbauer, S., Iasio, C., Vlcko, J., Greif, V., Proske, H., Granica, K., Falco, S., Lozzi, S., Mora, O., Arnaud, A., Novali, F., Bianchi, M., 2016. Landslide mapping and monitoring by using radar and optical remote sensing: Examples from the EC-FP7 project SAFER. Remote Sensing Applications: Society and Environment, 4, 92-108.

Greif, V., Vlcko, J., 2011. Monitoring of post-failure landslide deformation by the PS-InSAR technique at Lubietova in Central Slovakia. Environmental Earth Sciences, 66(6), 1585-1595.

[716]. Wartman, J., Montgomery, D.R., Anderson, S.A., Keaton, J.R., Benoît, J., dela Chapelle, J., Gilbert, R., 2016. The 22 March 2014 Oso landslide, Washington, USA. Geomorphology, 253, 275-288.

[717]. Evans, S.G., Delaney, K.B., Hermanns, R.L., Strom, A., Scarascia-Mugnozza, G., 2011. The Formation and Behaviour of Natural and Artificial Rockslide Dams; Implications for Engineering Performance and Hazard Management. Natural and artificial rockslide dams, 133. Springer Science & Business Media.

[718]. Li, M.H., Hsu, M.H., Hsieh, L.S., Teng, W.H., 2002. Inundation potentials

analysis for Tsao-Ling landslide lake formed by Chi-Chi earthquake in Taiwan. Natural Hazards, 25(3), 289-303.

Evans, S.G., Delaney, K.B., Hermanns, R.L., Strom, A., Scarascia-Mugnozza, G., 2011. The Formation and Behaviour of Natural and Artificial Rockslide Dams; Implications for Engineering Performance and Hazard Management. Natural and artificial rockslide dams, 133. Springer Science & Business Media.

[719-720]. Fan, X., Xu, Q., Alonso-Rodriguez, A., Subramanian, S.S., Li, W., Zheng, G., Dong, X., Huang, R., 2019. Successive landsliding and damming of the Jinsha River in eastern Tibet, China: prime investigation, early warning, and emergency response. Landslides, 16(5), 1003-1020.

[721]. Greicius, T. 2015, https://www.nasa.gov/jpl/hazardous-landslide-dammed-lake-pisang-annapurna-region-nepal

[722]. Guthrie, R.H., Friele, P., Allstadt, K., Roberts, N., Evans, S.G., Delaney, K.B., Roche, D., Clague, J.J., Jakob, M., 2012. The 6 August 2010 Mount Meager rock slide-debris flow, Coast Mountains, British Columbia: characteristics, dynamics, and implications for hazard and risk assessment. Natural Hazards and Earth System Sciences, 12(5), 1277-1294.

[723-724]. 田中収, 1982. 東海地震による富士川河岸白鳥山崩壊の危険性: 応用地質, 日本地質学会学術大会講演要旨 第 89 年学術大会 (1982 新潟). 一般社団法人 日本地質学会, pp. 478. (In Japanese)

[725]. 游勇, 陈兴长, 柳金峰, 2011. 四川绵竹清平乡文家沟“8·13”特大泥石流灾害. 灾害学, 26(4), 68-72. (In Chinese, with English title and abstract)

[726-733]. 范建容, 田兵伟, 程根伟, 陶和平, 张建强, 严冬, 苏凤环, 刘斌涛, 2008. 基于多源遥感数据的 5· 12 汶川地震诱发堰塞体信息提取 山地学报, 26(3), 257-262. (In Chinese, with English title and abstract)

[734-742]. 李志威, 汤韬, 袁昕亚, 余国安, 2020. 堰塞体堵江对雅鲁藏布大峡谷地区河流地貌的影响. 长江科学院院报, 37(8), 16-21. (In Chinese, with English title and abstract)

[743-744]. Massey, C., Townsend, D., Rathje, E., Allstadt, K.E., Lukovic, B., Kaneko, Y., Bradley, B., Wartman, J., Jibson, R.W., Petley, D.N., Horspool, N., Hamling, I., Carey,

J., Cox, S., Davidson, J., Dellow, S., Godt, J.W., Holden, C., Jones, K., Kaiser, A., Little, M., Lyndsell, B., McColl, S., Morgenstern, R., Rengers, F.K., Rhoades, D., Rosser, B., Strong, D., Singeisen, C., Villeneuve, M., 2018. Landslides Triggered by the 14 November 2016 Mw 7.8 Kaikōura Earthquake, New Zealand. Bulletin of the Seismological Society of America, 108(3B), 1630-1648.

[745-754]. Chai, H.L., Hanchao; Zhang, Zhuoyuen, 1995. The catalog of Chinese landslide dam events. Hournal of Geological hazards and Environment Preservation, 4. (In Chinese, with English title and abstract)

[755]. 王永兴, 1995. 滑坡导致的溃坝型洪水研究. 中国地质灾害与防治学报, 6(1), 15-23. (In Chinese, with English title and abstract)

[756]. Jacobs, L., Dewitte, O., Poesen, J., Delvaux, D., Thiery, W., Kervyn, M., 2015. The Rwenzori Mountains, a landslide-prone region? Landslides, 13(3), 519-536.

[757]. Geertsema, M., Clague, J.J., Schwab, J.W., Evans, S.G., 2006. An overview of recent large catastrophic landslides in northern British Columbia, Canada. Engineering Geology, 83(1-3), 120-143.

McDougall, S., Boultbee, N., Hungr, O., Stead, D., Schwab, J.W., 2006. The Zymoetz River landslide, British Columbia, Canada: description and dynamic analysis of a rock slide–debris flow. Landslides, 3(3), 195-204.

[758]. Bovis, M.J., Jakob, M., 2000. The July 29, 1998, debris flow and landslide dam at Capricorn Creek, Mount Meager Volcanic Complex, southern Coast Mountains, British Columbia. Canadian Journal of Earth Sciences, 37(10), 1321-1334.

[759]. Wang, F.-W., Zhang, Y.-M., Huo, Z.-T., Matsumoto, T., Huang, B.-L., 2004. The July 14, 2003 Qianjiangping landslide, Three Gorges Reservoir, China. Landslides, 1(2).

[760]. Mulas, M., Ciccarese, G., Ronchetti, F., Truffelli, G., Corsini, A., 2018. Slope dynamics and streambed uplift during the Pergalla landslide reactivation in March 2016 and discussion of concurrent causes (Northern Apennines, Italy). Landslides, 15(9), 1881-1887.

[761]. Dang, K., Sassa, K., Fukuoka, H., Sakai, N., Sato, Y., Takara, K., Quang, L.H., Loi, D.H., Van Tien, P., Ha, N.D., 2016. Mechanism of two rapid and long-runout landslides in the 16 April 2016 Kumamoto earthquake using a ring-shear apparatus and computer simulation (LS-RAPID). Landslides, 13(6), 1525-1534.

野村真一, 石濱茂崇, 中出剛, 片山政弘, 2017. 平成 28 年熊本地震による阿蘇大橋地区斜面防災対策 「砂防災害関連緊急事業 (直轄)」 の取り組み. 砂防学会誌, 70(3), 58-65. (In Japanese, with English title and abstract)

[762]. Yamada, M., Matsushi, Y., Chigira, M., Mori, J., 2012. Seismic recordings of landslides caused by Typhoon Talas (2011), Japan. Geophysical Research Letters, 39(13)

[763]. Jevremovic, D., Kostic, S., Andrejev, K., 2015. Landslide dam in river bed of Leva reka near Kraljevo due to cyclone,, Tamara' in May 2014. Tehnika, 70(4), 609-615. (In Serbian, with English title and abstract)

Krušić, J., Samardžić-Petrović, M., Marjanović, M., Abolmasov, B., Miljković, S., 2018. Preliminary results of numerical modelling of debris flow - case study Leva reka, Serbia. ce/papers, 2(2-3), 707-712.

[764]. Catane, S.G., Cabria, H.B., Tomarong, C.P., Saturay, R.M., Zarco, M.A.H., Pioquinto, W.C., 2006. Catastrophic rockslide-debris avalanche at St. Bernard, Southern Leyte, Philippines. Landslides, 4(1), 85-90.

[765]. Tien, P.V., Sassa, K., Takara, K., Fukuoka, H., Dang, K., Shibasaki, T., Ha, N.D., Setiawan, H., Loi, D.H., 2018. Formation process of two massive dams following rainfall-induced deep-seated rapid landslide failures in the Kii Peninsula of Japan. Landslides, 15(9), 1761-1778.

[766]. Hernández-Madrigal, V.M., Mora-Chaparro, J.C., Garduño-Monroy, V.H., 2010. Large block slide at San Juan Grijalva, Northwest Chiapas, Mexico. Landslides, 8(1), 109-115.

[767]. Fan, X., Xu, Q., Scaringi, G., Dai, L., Li, W., Dong, X., Zhu, X., Pei, X., Dai, K., Havenith, H.-B., 2017. Failure mechanism and kinematics of the deadly June 24th 2017 Xinmo landslide, Maoxian, Sichuan, China. Landslides, 14(6), 2129-2146.

[768]. Ehteshami-Moinabadi, M., 2007. Valasht Lake, a landslide dam triggered by historical earthquake, Alborz Mountains Belt, North Iran.

[769]. Ehteshami-Moinabadi, M., Nasiri, S., 2017. Geometrical and structural setting of landslide dams of the Central Alborz: a link between earthquakes and landslide damming. Bulletin of Engineering Geology and the Environment, 78(1), 69-88.

[770]. Drechsleret, M., Ripper, I., Warren, E., 1989. The Kaiapit Landslide, Papua New Guinea, The international conference on engineering geology on tropical terrains, Bangi,

Malaysia.

Peart, M., 1991. The Kaiapit Landslide - Events and Mechanisms. Q J Eng Geol, 24(4), 399-411.

[771]. Dunning, S.A., Rosser, N.J., Petley, D.N., Massey, C.R., 2006. Formation and failure of the Tsatichhu landslide dam, Bhutan. Landslides, 3(2), 107-113.

[772]. Evans, S.G., Tutubalina, O.V., Drobyshev, V.N., Chernomorets, S.S., McDougall, S., Petrakov, D.A., Hungr, O., 2009. Catastrophic detachment and high-velocity long-runout flow of Kolka Glacier, Caucasus Mountains, Russia in 2002. Geomorphology, 105(3-4), 314-321.

Huggel, C., Zgraggen-Oswald, S., Haeberli, W., Kääb, A., Polkvoj, A., Galushkin, I., Evans, S.G., 2005. The 2002 rock/ice avalanche at Kolka/Karmadon, Russian Caucasus: assessment of extraordinary avalanche formation and mobility, and application ofQuickBird satellite imagery. Natural Hazards and Earth System Sciences, 5(2), 173–187.

[773]. 何秉顺, 丁留谦, 王玉杰, 徐文杰, 赵宇飞, 2009. 四川安县肖家桥堰塞湖稳定性初步评估. 岩石力学与工程学报, 28(S2), 3626-3630. (In Chinese, with English title and abstract)

黄润秋, 王运生, 董秀军, 2009. 2009 年 8·6 四川汉源猴子岩崩滑的现场应急调查及危岩处理. 工程地质学报, 17(4), 445-448. (In Chinese, with English title and abstract)

[774]. Evans, S.G., Tutubalina, O.V., Drobyshev, V.N., Chernomorets, S.S., McDougall, S., Petrakov, D.A., Hungr, O., 2009. Catastrophic detachment and high-velocity long-runout flow of Kolka Glacier, Caucasus Mountains, Russia in 2002. Geomorphology, 105(3-4), 314-321.

[775-776]. Jibson, R.W., Crone, A.J., Harp, E.L., Baum, R.L., Major, J.J., Pullinger, C.R., Escobar, C.D., Martínez, M., Smith, M.E., 2004. Landslides triggered by the 13 January and 13 February 2001 earthquakes in El Salvador, Natural Hazards in El Salvador.

[777-778]. Xu, C., Shyu, J.B.H., Xu, X., 2014. Landslides triggered by the 12 January 2010 Port-au-Prince, Haiti, Mw= 7.0 earthquake: visual interpretation, inventory compiling, and spatial distribution statistical analysis. Natural Hazards and Earth System Sciences, 14(7), 1789-1818.

[779]. Macías, J.L., Capra, L., Scott, K.M., Espíndola, J.M., García-Palomo, A., Costa,

J.E., 2004. The 26 May 1982 breakout flows derived from failure of a volcanic dam at El Chichón, Chiapas, Mexico. Geological Society of America Bulletin, 116(1).

Appendix A2. Processes of Precise Geolocating for Landslide Dam records

The original spatial information from landslide dam (LDam) record is not always precisely recorded. Additionally, given the fact that some LDam records were only accessible in local reports, the coordination that applied in the LDam record could be recorded with local spatial reference and thus required coordination transformation when applying to global scale studies. The transformation can further result in the imprecision and inaccuracy of spatial information caused by datum differences. At Figure A2-1(a), it is clearly presented the difference of Yuhama LDam location before and after precise geolocating.

The processes of precise geolocating LDam records can be described as three steps: 1) noting and remarking the spatial information from LDam records, including spatial coordinates, administrative divisions where the event occurred, and location description with landmarks nearby, as well as the time of LDam occurrence; 2) exploring relative information of the LDam records from various data source, such as blogs, local government reports, news articles, press release or other relevant academic publications for gathering images and descriptions for the event (Figure A2-1(b)); 3) matching the information with the relative landmarks of LDam including landslide features(scarps, toes, etc.), the extreme colour difference on the surface, hazard mitigation infrastructures and existing LDam bodies and impounded lakes presented google earth and geolocated the event(Figure A2-1(c)). All of the geolocating processes were operated on Google Earth Pro, which is a free app for users and contains a large amount of historical satellite images, which can be applied as the data sources for the landslide and LDam reignition by manual image interpretation.

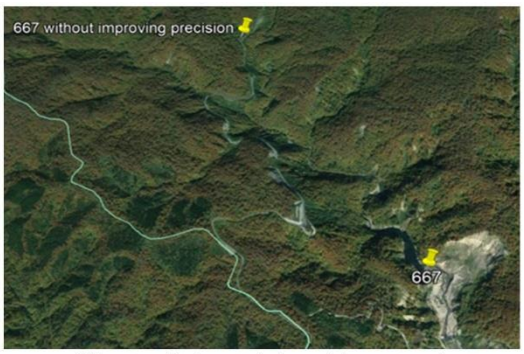

(a) locations of Yuhama LSD before and after precise geolocating

(b) aerial photo taken by Tohokuchihoseibi Bureau after 2008 Iwate–Miyagi Nairiku earthquake happened

(c) Geolocated Yuhama LSD location on google earth

Figure A2-1 Example of LDam location with the improvement on its spatial precision

When we know the time of specific LDam event occurrence, it is easier to capture the precise location of that record. The global surface water explorer provides a reliable data source of the location and temporal distribution of water surfaces at the global scale since 1984 (Pekel et al. 2016). Figure A2-2 presented an example for exploring the location and time information of Sunkoshi/Jure LDam record (Index 49 in RAGLAD): the large difference of monthly water presented before and after LDam formation presented the impounded lake existence while the increment of water occurrence intensity in specific channel segment and the decrement on the downstream area can also indicate the formation of impounded lake in this period.

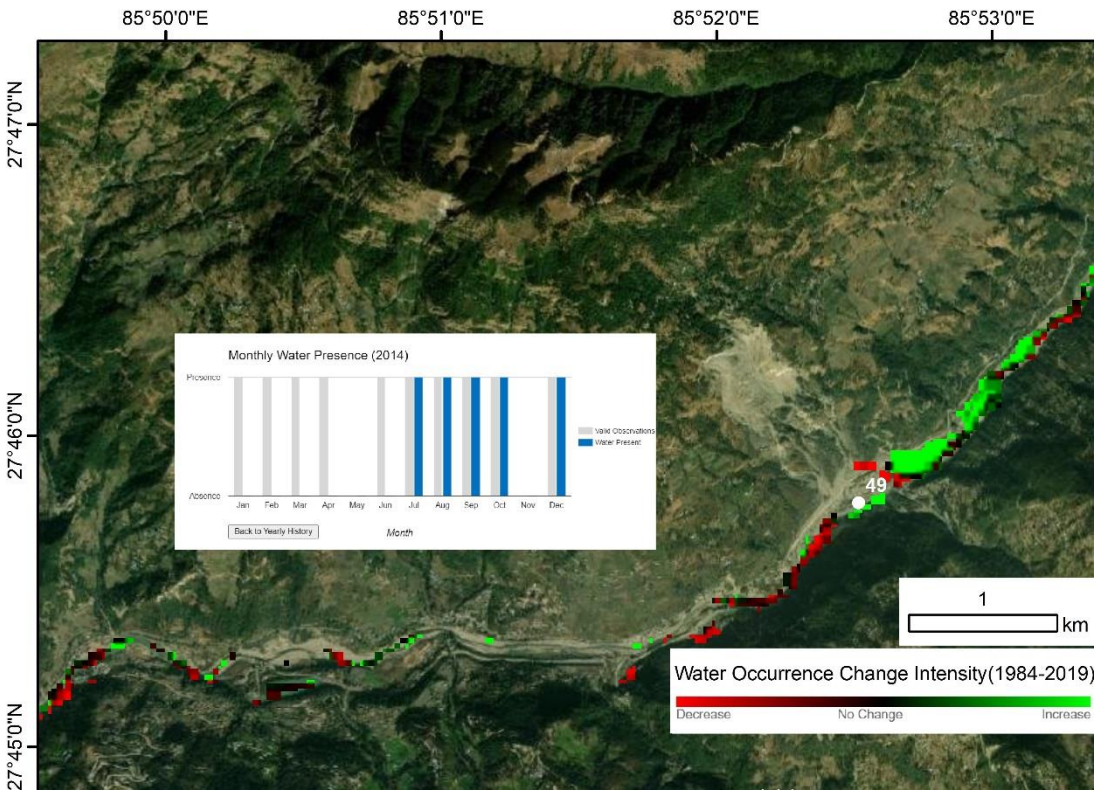

Figure A2-2 Exploration of location and time information of LDam record based on global surface water explorer

Reference

Pekel, J.F., Cottam, A., Gorelick, N., Belward, A.S., 2016. High-resolution mapping of global surface water and its long-term changes. Nature, 540(7633), 418-422.

Appendix A3. Attributes in RAGLAD_LDam_record_GFD.shp

RAGLAD_LDam_record_GFD.shp, a shapefile stored the LDam records from RAGLAD, can be downloaded at: https://static-content.springer.com/esm/art%3A10.1007%2Fs10346-021-01817-z/MediaObjects/10346_2021_1817_MOESM1_ESM.rar

Index: Geolocated landslide dam record index in RAGLAD

Drainage_a: Drainage area data from RAGLAD

River_widt: River width data from RAGLAD

GFD: River width data from global fluvial dataset

DA_GFD: River width data from global fluvial dataset

Appendix A4. Data Entry Quality of Parameters in RAGLAD

Table A4-1 Data entry quality of parameters in RAGLAD

Parameters	%Complete	%Complete after geolocating and adding GFD
Index	100	- (No changes before and after geolocating)
Name	47.1	-
Number of Hazard	100	-
y(latitude)	68.1	85.5
x(longitude)	68.1	85.5
Location	89.6	-
Country/region	100	-
Location (text)	89.6	-
Formation time	73.1	-
LDam status	35.2	-
Dam failure time	30.3	-
Failure mechanism	13.9	-
Overflow/flood Time	9.0	-
Duration from formation to flood (lake life)	26.7	-
Landslide Subcategories	76.7	-
Type of landslide movement	76.7	-
Drainage area	71.7	85.5
River width	38.3	85.5
Landslide area	39.0	-
Landslide-elevation difference	52.4	-
Landslide length	56.7	-
H/L Ratio	51.0	-
Landslide volume	70.3	-
LDam-type	54.0	-
Dam materials	67.3	-
Reported cause	65.1	-
Interpreted cause	65.1	-
Dam height	68.7	-
Dam length	63.3	-
Dam width	63.4	-
Impounded lake length	19.6	-
Impounded lake volume	38.0	-
Mean flow velocity	2.4	-
Peak flow velocity	4.1	-

Causalities	8.2	-
Economic loss	18.9	-
References	100	-
More details	40.4	-

Appendix B. Supplement materials for Chapter 5

Appendix B1. Visualisation of LDam Formation Susceptibility Evaluation Framework

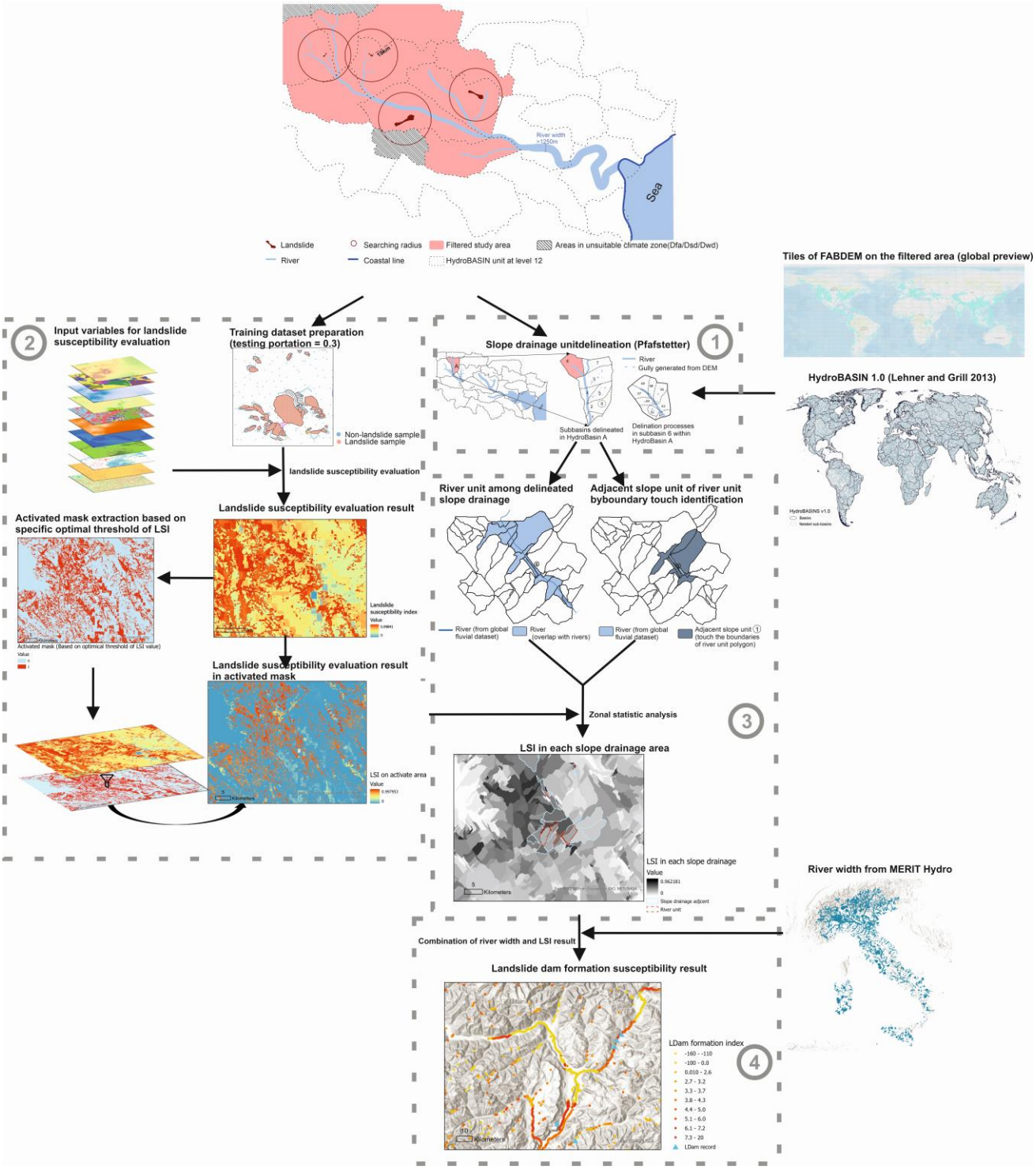

Figure B1-1 Visualisation of LDam formation susceptibility evaluation framework (4 steps were coherent to the four step descriptions in the beginning of method section; Full size jpg was also attached at the supplements)

Appendix B2. Details of Initial Study Area Prefiltering for LDam Formation

Mainly five steps were applied for initial study area prefiltering for LDam formation based on collected landslides and landslide dam records, as not all the areas contained suitable conditions for LDam formation:

1) The subbasins at the most detailed level (level 12) of HydroBASINS were chosen as the basic unit for initial prefiltering the study area for LDam formation. This decision was made based on the recent updates to HydroBASINS, which involve manually assigning different stream orders to different watersheds and resolving subbasin coding issues in various locations compared with other global scale subbasin products or methods (Linke et al. 2019).

2). To ensure that the prefiltered study area adequately reflects the collected landslide characteristics, we removed all the HydroBASIN level 12 subbasins with no landslides located nearby from the filtered study areas for this study by excluding the overlap subbasins within the buffer zone of 19km of all collected landslide and LDam records, which came from the landslide and LDam datasets collected globally. The buffer searching radius threshold of 19 km was selected based on the longest travel distance of landslides that blocked the river from the global-scale LDam dataset RAGLAD (Wu et al. 2022).

3). The subbasins in which the river width exceeded 1250m were excluded from further analysis, as the river reaches larger than at such width were unlikely to be blocked by landslide mass according to Wu et al. (2022).

4). Remove all subbasins adjacent to continental shorelines, including the banks of lakes, but retain those containing LDams because many of river reaches near continental coastline can be classified as depositional areas within river systems, or the mass of landslides occurring on coasts could potentially fall into the ocean and trigger

tsunamis.

5). Exclude all of the climate zones with few landslides (<0.07% of total, ~500 landslides), mainly those climate types are located in subarctic or extremely high altitude areas, including dfa (Hot-summer humid continental climate), dsd (Mediterranean-influenced extremely cold subarctic climate), and dwd (Monsoon-influenced extremely cold subarctic climate), according to the Köppen-Geiger climate classification (Beck et al. 2018).

The results of the prefiltered study area for LDam formation based on the collected datasets were shown in Figure B2- 1. There were a total of 14,130 level-12 HydroBASIN subbasins in the initial filtered study areas. The final prefiltered study area for LDam formation covered an area of 2,220,379 km^2, equal to ~0.4% of the total land surface area of the Earth. Most of them were distributed in the countries with a lot of landslides and LDams recorded, such as Italy and Japan.

Figure B2- 1 Final prefiltered study areas for LDam formation based on the collected datasets

Appendix B3. Processes and Information of Delineating Slope Drainage unit

The digital elevation model (DEM) that was used for slope drainage unit delineation is FABDEM (Forest And Buildings removed Copernicus DEM)), a global scale DEM with correction of vegetation and buildings, with 30 m spatial resolution (Hawker et al. 2022). To handle the global-scale data pre-processing, it is efficient to separate and mosaic tiles from global-scale raster dataset for restructuring the data storage and management based on the basic calculation unit. The DEM tiles that were located within initial filtered study area for LDam formation were selected from FABDEM to reduce the computing time of data processing (Figure B3-1). The slope drainage delineation was proceeded within each HydroBASIN unit by Pfafstetter method (Verdin and Verdin, 1999). Figure B3-2 and Figure B3-3 show an example of merging of multiple DEM tiles from FABDEM into a new DEM raster for slope drainage unit delineation. After these processes, the data size decreased from 406.32 GB to 17 GB, while the calculation time decreased from more than a week to couple of hours.

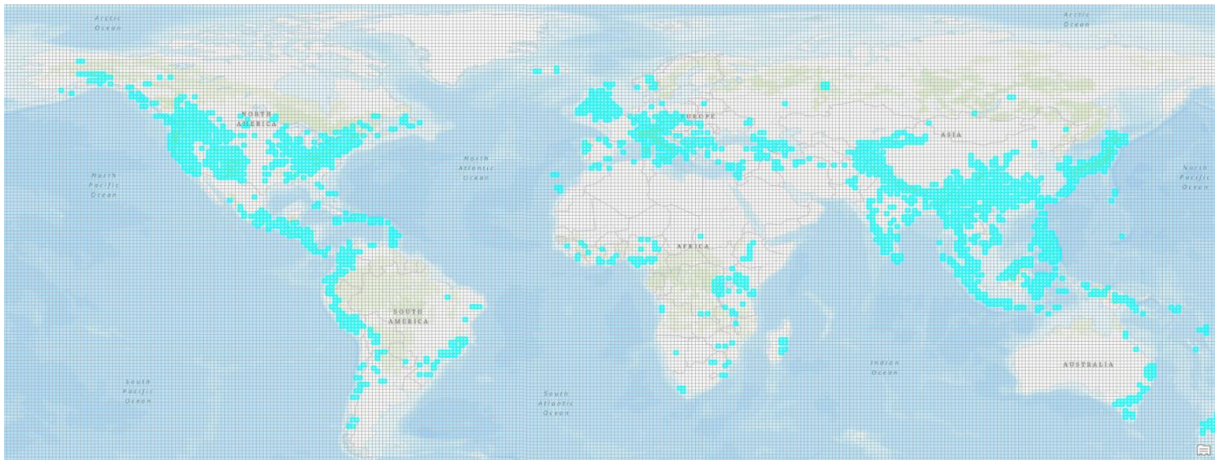

Figure B3-1 Selected tiles that located in prefiltered study area for LDam formation from FABDEM (stored in 1degree ×1 degree tiles)

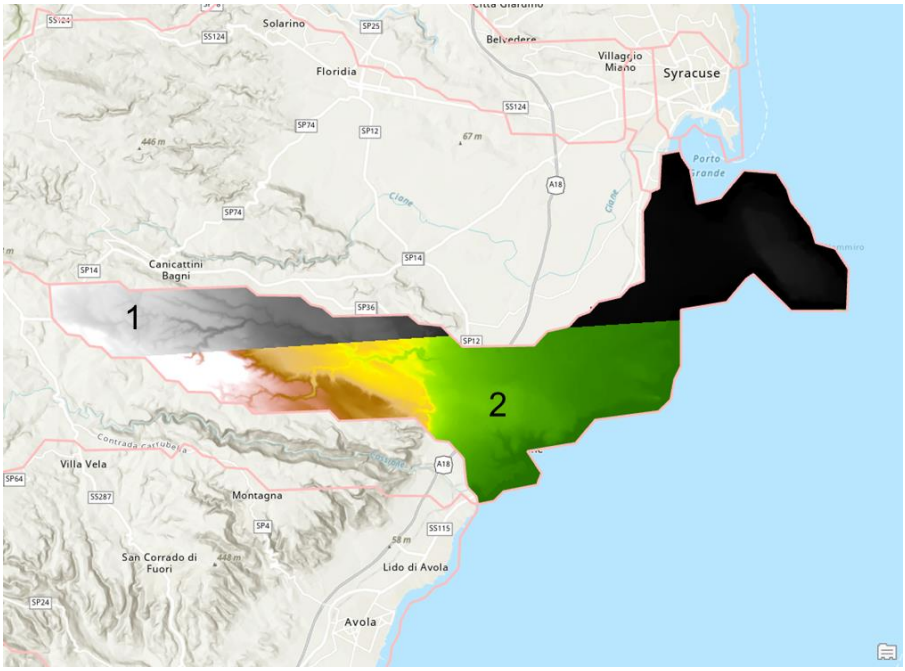

Figure B3-2 Two clipped FABDEM tiles for a level-12 HydroBASIN unit (ID: N36_2120046520_1963)

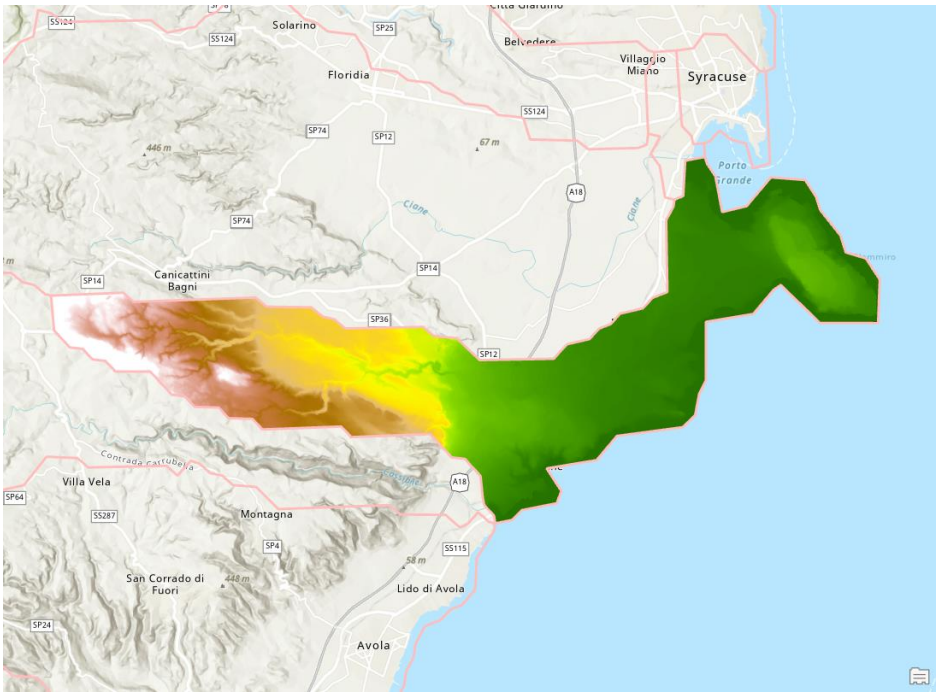

Figure B3-3 The merged DEM raster of a level-12 HydroBASIN unit for further slope drainage unit delineation (ID: N36_2120046520_1963)

The dataset of the delineated slope drainage unit is stored at https://doi.org/10.5518/1346.

Cite as: Wu H, Trigg M, Murphy W, Fuentes R (2023) Global slope drainage units for landslide dam formation. University of Leeds. [Dataset] https://doi.org/10.5518/1346

Appendix B4. References of Supplementary Documents

Beck H, Zimmermann N, McVicar T, Vergopolan N, Berg A, Wood EF (2018) Present and future Köppen-Geiger climate classification maps at 1-km resolution. Sci Data 5:180214

Linke S, Lehner B, Ouellet Dallaire C, Ariwi J, Grill G, Anand M, Beames P, Burchard-Levine V, Maxwell S, Moidu H, Tan F, Thieme M, 2019. Global hydro-environmental sub-basin and river reach characteristics at high spatial resolution. Sci Data, 6(1):1-15

Verdin KL, Verdin JP (1999) A topological system for delineation and codification of the Earth's river basins. J Hydrol 218(1-2):1-12

Wu H, Trigg MA, Murphy W, Fuentes R (2022) A new global landslide dam database (RAGLAD) and analysis utilizing auxiliary global fluvial datasets. Landslides 19(3):555-572